Effects of malnutrition on epithelia-microbe interactions in the intestinal tract of *Drosophila melanogaster*

Dissertation

zur Erlangung des Doktorgrades

der Mathematisch-Naturwissenschaftlichen Fakultät

der Christian-Albrechts-Universität zu Kiel

vorgelegt von

Jakob von Frieling

Kiel, 2020

Erstgutachter: Prof. Dr. Thomas Roeder

Zweitgutachter: Prof. Dr. Holger Heine

Tag der Disputation: 11.05.2020

Table of contents

Abbreviations

AA	amino acid
AMP	antimicrobial peptide
Akt	v-akt murine thymoma viral oncogene
AMPK	AMP-activated protein kinase
AM	anterior midgut
ATG13	autophagy-related gene 13
BCA	branched-chained amino acids
BCFA	branched-chain fatty acid
Bsk	basket
CAZymes	carbohydrate-active enzymes
CD	control diet
CR	caloric restriction
d	day
DAPI	4,6-diamidine-2-phenylindole dihydrochloride
Dip	diptericin
Def	defensin
DR	dietary restriction
Dros	drosocin
Drsm	drosomycin
Dome	domeless
DSS	dextran sulfate sodium
EB	enteroblast
EC	enterocyte
EEC	enteroendocrine cell
EGFR	epidermal growth factor receptor
Erk	extracellular-regulated kinase
Esg	escargot
Fig	figure
FoxO	forkhead box O
GF	germ-free
GFP	green fluorescent protein
h	hour
HD	holidic diet
HFD	high fat diet
IGF-1	insulin/insulin-like growth factor
IR	insulin receptor
IRS1	insulin receptor 1
ISC	intestinal stem cell
JAK/Stat	Janus kinase-signal transducers and activators of transcription
JNK	Jun N-terminal kinase
FFA	free fatty acids
Hep	hemipterous
MEK	mitogen-activated kinase
min	minute

Mtk	metchnikowin
mTor	mechanistic target of rapamycin
mTorC1/2	mechanistic Tor complex C1/2
ns	not significant
OHD	optimized holidic diet
OEMHD	optimized exom-matched holidic diet
PEM	protein-energy malnutrition
pH3	phospho histone 3
PI3K	phosphoinositide 3 kinase
PIP_3	phosphatidylinositol-(3,4,5)-triphosphate
PCoA	principal coordinate analysis
pJNK	phospho-JNK
PM	posterior midgut
Raf	rapidly accelerated fibrosarcoma
Ras	rat sarcoma
RC	recolonized
RFP	red fluorescent protein
Rheb	ras homolog enriched in brain
SCFA	short-chain fatty acid
Sesn	sestrin
SREBP1	sterol regulatory element binding protein 1
Su(H)GBE	suppressor-of-hairless
S6K1	P70-S6 kinase 1
SY	sugar yeast
TAG	triacylglycerol
Trp	L-tryptophan
TSC1/2	tuberous sclerosis complex ½
UAS	upstream activated sequence
ULK1	unc-51-like kinase
Upd	unpaired
Wg	wingless
4EBP	eIF4E binding protein

Summary

Malnutrition is defined by an imbalance between the supply of nutrients and energy and the body's demand to ensure optimal growth, maintenance and specific bodily functions. The term malnutrition covers 2 broad groups of conditions. One is undernutrition, which includes wasting, stunting and insufficiencies in mineral or vitamins, whereas the other group comprises overweight and obesity. Today's major health challenges in both developing and in more economically developed countries arise from excessive intake of high-energy dense food and/or the lack of dietary protein and calories, leading to overweight, obesity and protein-energy malnutrition (PEM), respectively. On the other hand, dietary restriction (DR), which is a reduction of particular nutrient intake without causing malnutrition, is believed to mediate positive effects of a plethora of health-associated parameters. The intestine is in close contact to dietary components and is a central mediator between the microbial community and the host. Maintaining the intestinal epithelial homeostasis requires an equilibrium between the microbial community and the intestinal epithelium and dietary interventions are believed to have an impact on this equilibrium. In my research, I focused on the effect of nutritional stressors, such as high-fat dieting (HFD), PEM and DR on epithelia-microbe interactions in the intestine of *Drosophila melanogaster*. I revealed that high fat dieting led to an increased hyperproliferation of intestinal stem cells and to an elevated number of enteroendocrine cells. The HFD-induced activation of stem cells depended on JNK pathway-mediated secretion of the cytokine Upd3 in enterocytes. Upd3 in turn activated JAK/Stat signaling in stem cells and enteroblasts. The increased stem cell activity upon high fat dieting critically depended on the presence of the indigenous microbiota as the observed hyperproliferation of stem cells was completely repressed in germ-free flies. I showed that a HFD led to a changed microbial composition and increased bacterial abundancy. Microbiota transplantation experiments failed to recapitulate the HFD-associated hyperproliferation phenotype suggesting that the increased abundance of bacteria is responsible for the activation of intestinal stem cells. For the purpose of standardization and reproducibility of PEM and DR experiments, I used a chemically well-defined holidic diet. However, existing holidic diet protocols were not able to support the development of conventional and germ-free flies. Therefore, I optimized holidic diet protocols that now allows development of conventional and germ-free flies comparable to standard complex *Drosophila* diets. I used this diet to investigate the effect of DR and PEM on the host-microbiota interaction in the intestinal ecosystem. PEM and DR led to changes of the intestinal structure, stem cell activity, enterocyte size and cellular composition, whereas some of these observations were depended on the indigenous microbiota. DR and PEM induced an increased

susceptibility to pathogenic *S. marcescens* infection and genotoxic chemicals. To study how host genetics contributes to DR and PEM-mediated intestinal phenotypes, I focused on the Tor pathway, which is a central mediator of amino acid and energy sensing in the cell. The DR and PEM induced changes in the intestinal structure were absent in Tor deficient flies. Moreover, Tor deficient flies revealed a decreased infection susceptibility. I showed that DR and PEM induced substantial changes in the transcriptional profile of the intestine. The impact of the indigenous microbiota on the intestinal transcriptome increased with lower amino acid contents in the diet. Furthermore, I analyzed the intestinal transcriptional profile of flies that lived for 14 days on the control diet after a 7 days period of PEM. Thereby, I revealed that a short-term intervention of PEM led to long-lasting memory effects in the transcriptome.

Zusammenfassung

Eine Mangelernährung ist definiert durch ein Ungleichgewicht zwischen Nährstoffaufnahme und Nährstoffbedarf, die für das Wachstum und die Aufrechterhaltung von Körperfunktionen benötigt werden. Die Bezeichnung Mangelernährung umfasst zwei Kategorien. Eine Kategorie der Mangelernährung wird als Unterernährung bezeichnet und beinhaltet Magerkeit („wasting“), Längenwachstumstörungen („stunting“) und ein Mineral/Vitamin-Insuffizienz. Demgegenüber umfasst die zweite Kategorie der Mangelernährung die Ausprägungen Übergewicht und Fettleibigkeit. Die heutigen gesundheitlichen Herausforderungen in Industrie- und Entwicklungsländern entstehen häufig durch den übermäßigen Konsum von Lebensmitteln mit hoher Energiedichte oder durch eine unzureichende Zufuhr von Proteinen und Kalorien, welche zu Übergewicht und Fettleibigkeit beziehungsweise einer Protein-Energie-Mangelernährung (PEM) führen können. Diätetische Restriktion (DR) bezeichnet hingegen die Reduktion von Nahrung beziehungsweise die Reduktion von bestimmten Makro-/Mikronährstoffen, ohne dass sich dabei eine Unterernährung einstellt. Im Gegensatz zu Übergewicht, Fettleibigkeit und PEM ist DR mit einer Reihe gesundheitsfördernder Effekte assoziiert. Der Darm steht in Kontakt mit der aufgenommenen Nahrung und ist ein wichtiger Mediator zwischen der mikrobiellen Gemeinschaft und dem Wirtsorganismus. Die Aufrechterhaltung der intestinalen Epithelhomöostase benötigt ein Equilibrium zwischen der mikrobiellen Gemeinschaft und dem intestinalen Epithel, wobei vermutet wird das diätische Interventionen einen Einfluss auf dieses Equilibrium haben. In meiner Studie habe ich die Auswirkungen einer Hochfett-Diät (HFD), DR und PEM auf Epithel-Mikroben Interaktionen im Darm von *Drosophila melanogaster* untersucht. Ich habe herausgefunden, dass die Zufuhr einer HFD zu einer Hyperproliferation von intestinalen Stammzellen und zu einer erhöhten Anzahl von Enteroendokrinen Zellen führte. Die HFD-induzierte Aktivierung der intestinalen Stammzellen wurde durch den JNK Signalweg in den Enterozyten vermittelt. Die Aktivierung des JNK Signalweges führte zu einer Sezernierung des Zytokins Upd3 aus den Enterozyten, welches wiederum den JAK/Stat Signalweg in intestinalen Stammzellen und Enteroblasten aktivierte. Zudem konnte ich zeigen, dass die durch die HFD hervorgerufene erhöhte Stammzellaktivität abhängig von der Anwesenheit der intestinalen Mikrobiota war, da die Verfütterung einer HFD an keimfreie Fliegen nicht zu der zuvor beobachteten Hyperproliferation führte. Zudem führte die Aufnahme einer HFD zu einer veränderten mikrobiellen Zusammensetzung, sowie zu einer erhöhten Menge an Bakterien. Da eine Mikrobiota-Transplantation nicht den gleichen HFD-assoziierten Phänotyp rekapitulieren konnte, vermute ich das die erhöhte Menge an Bakterien zu einer Aktivierung der intestinalen

Stammzellen führte. Um reproduzierbare und standardisierte DR und PEM Diäten herzustellen, habe ich eine definierte holidische Diät benutzt. Vorhandene holidische Diäten für *Drosophila* fördern jedoch nicht ausreichend die Entwicklung von konventionellen und keimfreien Fliegen. Aufgrund dessen habe ich eine holidische Diät entwickelt, welche nun die Entwicklung von konventionellen und keimfreien Fliegen erlaubt. Ich habe diese Diät benutzt, um den Effekt einer DR oder einer PEM auf Wirts-Mikrobiota Interaktionen im intestinalen Ökosystem zu untersuchen. DR als auch PEM führten zu einer Veränderung der intestinalen Struktur, der Stammzellaktivität, der Größe der Enterozyten und der zellulären Zusammensetzung. Einige der beobachteten strukturellen und zellulären Phänotypen waren abhängig von der Anwesenheit der intestinalen Mikrobiota. Mit DR und PEM ernährte Fliegen wiesen eine erhöhte Anfälligkeit gegenüber genotoxischen Chemikalien und einer Infektion mit *S. marcescens* auf. Um zu untersuchen welchen Einfluss der Genotyp des Wirts auf den DR- oder PEM-vermittelten intestinalen Phänotypen hat, habe ich mich auf den Tor Signalweg fokussiert. Der Tor Signalweg ist ein zentraler intrazellulärer Mediator für den Aminosäure- und Energiestatus. Die durch DR und PEM induzierten strukturellen Veränderungen des Darms waren in Tor-defiziente Fliegen nicht mehr zu detektieren. Zudem wiesen Tor-defiziente Fliegen eine geringere Anfälligkeit gegenüber einer *S. marcescens* Infektion auf. Darüber hinaus habe ich in einem weiteren Experiment gezeigt, dass eine DR und eine PEM zu erheblichen Veränderungen im transkriptionellen Profil der Därme führte. Der Einfluss der Mikrobiota auf die intestinale Transkription wurde größer, je niedriger der Aminosäuregehalt war. Zudem habe ich das intestinale transkriptionelle Profil von Fliegen analysiert, welche für 7 Tage mit einer PEM gefüttert wurden und anschließend für 14 weitere Tage mit einer Kontrolldiät. Mit diesem Versuch konnte ich zeigen, dass eine kurzzeitige Intervention mit einer PEM zu langanhaltenden Effekten im intestinalen Transkriptom führte.

1 Introduction

1.1 Impact of nutrition in health and disease

Nutrition is one of the most important contributors to human health. Nutrition is a fundamental factor to support growth, development and body functionality but also for the prevention and treatment of several diseases. Over 2 billion people worldwide are malnourished and this malnutrition can be found in developing countries and in more economically developed countries. Malnutrition is an excess, deficiency or imbalance of energy and/or nutrients, which can lead to adverse consequences on the body composition and physiological function. The term malnutrition includes several conditions like undernutrition, overweight, obesity and micronutrient-related malnutrition.

1.1.1 Obesity

The World Health Organization (WHO) defines overweight and obesity as excessive fat accumulation and is diagnosed at a body mass index (BMI) $\geq$ 25 kg/m^2 or $\geq$ 30 kg/m^2, respectively. In 2016, 13 % of the world's adult population were obese and 39 % were overweight (1). Whereas overweight and obesity were considered as a high-income country problem, it is also on the rises in low- and middle-income countries (2,3). It is expected that the obesity rates will increase further (4). The main cause of obesity and overweight is an imbalance between increased intake of highly processed energy-dense foods and low physical activity (5,6). The so-called western-diet is high-energy dense food characterized by high contents of fats, sugars and refined grains and at the same time by low dietary fibers, vitamins and minerals (7). Overweight and obesity can lead to several diseases, such as diabetes mellitus (8), several types of cancer (9), non-alcoholic fatty liver disease (10), cardiovascular disease (11), musculoskeletal disorders (12) and poor mental health (13). An excessive intake of high-energy dense food can also lead to the metabolic syndrome, which is characterize by visceral obesity, hypertension, insulin resistance, elevated fasting and postprandial serum triglycerides and low serum high-density lipoproteins (14). Therefore, the life expectancy of obese people, but not of overweight people, is reduced compared to normal weight people (15,16). Plasma levels of free fatty acids (FFA) are mostly elevated in obese people (17). Plasma FFA mainly derive from intracellular lipolysis of triacylglycerols (TAG) in adipose tissues or from lipolysis of TAG-rich lipoproteins within the circulation. The plasma FFA levels in obese people are elevated

because enlarged adipose tissue releases more FFAs and reduces clearance of circulating FFAs (18). It was shown that increased plasma FFA levels induce insulin resistance, whereas decreased plasma FFAs are associated with an improved insulin response (19,20,21,22). When the insulin resistance is not compensated by an enhanced secretion of insulin, as observed in pre-diabetic individuals, it may development into type 2 diabetes (23). Moreover, increased plasma FFAs impair the anti-lipolytic effect of insulin, which in turn further increases the release of FFAs into the circulation (24). Increased FFA availability leads to intracellular accumulation of TAGs in skeletal muscles and abdominal fat and are associated with pro-inflammatory conditions in healthy and obese individuals (25,26,27,28). Fatty acids differ by the length of their aliphatic chain and whether or not this chain is saturated or unsaturated. The major saturated fatty acids in most diets are myristic acid and palmitic acid. Saturated fatty acids are associated with a variety of pathophysiological effects as they can cause an increase of blood cholesterol or of pro-inflammatory cytokine expression in adipose tissue (29,30). The impact of mono- or polyunsaturated fatty acids on inflammation in literature is inconsistent. Arachidonic acid, which is particularly obtained from meat products is able to stimulate the synthesis of pro-inflammatory cytokines (31,32). On the other hand, eicosepantenoic acid, mainly obtained from fish, has anti-inflammatory properties (31,33). It is also suggested that obesity is inheritable and genetic and epigenetic factors can cause a disregulated energy homeostasis (34,35). Therefore, it is in discussion if obesity is a disease or a behavioral abnormality. It was shown that gene deficiencies targeting leptin, leptin receptor, proopiomelanocortin, melanoncortin 4 receptor 4 or single-minded homolog 1 are associated with obesity (36,37,38,39,40). However, these genetic deficiencies have stronger effects in individuals with a sedentary lifestyle or in those living in more obesogenic environments (41). From an evolutionary perspective, 10.000 years ago people were adopted to barely processed diets that were low in fat and high in fiber. As in many organisms, storing energy as fat when food is abundant was a fitness advantage in times of periodic hunger. The diets have changed dramatically through the agricultural- and industrial revolution in most parts of the world and the time was maybe insufficient for genetic adaptions for the modern food environment (42,43). However, obesity is a preventable disease. There are several strategies to prevent obesity such as a dietary adjustment, physical activity, pharmacotherapy or individual behavior therapy.

1.1.2 Protein-energy malnutrition

Factors that cause undernutrition comprise reduced food intake, impaired absorption, excess nutrient losses, increased energy expenditure or intake of food deficient in macro- and/or micronutrients. These factors can contribute to deficiencies in macronutrients (protein, carbohydrates and fat), which in turn can lead to a primary or secondary protein-energy malnutrition (PEM, 44). Nearly 11 % of the world's population are undernourished with most living in developing countries (45). In 2011, undernutrition was the cause of 45 % of all child deaths worldwide (46). There are 3 physiological measures of undernutrition in children: stunting (low height-for-age), wasting (low weight-for-height) and underweight (low weight-for-age). Stunting indicates chronic weight loss, whereas wasting results from recent weight loss (47). Undernutrition can lead to muscle wasting, fat depletion, impaired cardiac function, diarrhea as well as impaired immune function and wound healing (48). Severe forms of PEM in children are Marasmus and Kwashiorkor. Marasmus results from an inadequate energy and protein intake and is characterized by muscle wasting, depletion of subcutaneous fat and absence of edema. Kwashiorkor results from an inadequate intake of proteins with reasonable energy intake and leads to edema, large protuberant belly, fatty liver and an inability to grow or gain weight. However, there are also children suffering from marasmic kwashiorkor with pathological features of marasmus and kwashiorkor (49,44). Children who suffer from kwashiorkor normally have a higher mortality rate and are more difficult to treat than those suffering from marasmus (50). This is due to the more complex physiological and pathologic changes in kwashiorkor in comparison to marasmus. Kwashiorkor is associated with lower concentrations of ß-carotene, vitamin E and glutathione compared to marasmus, which in turn is associated with higher oxidative damage (51,52,53). The whole-body breakdown of proteins occurs at a slower rate in children suffering from kwashiorkor than in those with marasmus, which limits the supply of amino acids (54). Furthermore, the lipolysis is much slower in children with kwashiorkor than in children with marasmus, which indicates an insufficient mobilization and utilization of lipids (55). Notably, undernourished children have an increased risk to die of an infection disease (56). PEM is associated with an atrophy of the thymus and the bone narrow. This atrophy causes anemia, leucopenia as well as changes in the B- and T-cell repertoire. (57,58). PEM also affect the acute phase response, as elevated C-reactive protein levels were found in malnourished children with and without infections. At the same time, the negative acute phase proteins pre-albumin or fibronectin are reduced in malnourished children (59,60,61,62). PEM also leads to structural changes of the epithelial barrier of the skin and the intestine providing a potential entry for pathogens (63,64,65). Even when the treatment is

difficult, some symptoms of kwashiorkor and marasmus are reversible. Children who suffered from kwashiorkor or marasmus for a certain time can physically recover in height and weight (66). However, chronic PEM in childhood can impair cognitive processes such as learning, memory and coordination in later life (67,68). Even though mostly children suffer from PEM, also elderly people are at risk for a compromised nutritional status. The prevalence of PEM in elderly patients ranges from 5-40 % and is associated with a highly increased mortality (69,70,71).

1.1.3 **Dietary restriction**

In contrast to PEM or overnutrition, dietary restriction (DR) is associated with a plethora of health promoting effects (72). The term DR is often equated with caloric restriction (CR), even though they represent different interventions. CR describes a 20-40 % reduction of total caloric intake, without malnutrition. DR represent a broader range of nutritional interventions that differ from conventional diets in restriction of at least one specific macro- or micronutrient. Moreover, the term DR is associated with a several feeding pattern such as time restricted feeding or intermittent fasting (73). Studies in several animals models, including *Saccharomyces cerevisiae*, *Caenorhabditis elegans*, *Drosophila melanogaster* and mice showed that DR increases overall lifespan and healthy lifespan in short lived organisms (74). These data lead to the assumption that lifespan extension underlies evolutionary conserved mechanisms. Proteins seems to have the greatest impact on DR associated effects among the macronutrients. It was show that lowering the dietary protein content increases the lifespan of a variety of organisms reproducibly (75,76,77). Besides the DR effects on lifespan extension, DR protects against a variety of pathophysiological conditions such as obesity, cardiovascular disease, cancer, neurodegeneration, diabetes, and loss of motor and immune functions in non-human primates and rodents (78,79,80,81,82). Important molecular mechanism that mediate the effects of DR are the nutrient-sensing mechanistic target of rapamycin (mTor) and insulin/insulin-like growth factor (IGF-1) pathways (83). The impact of the IGF-1 signaling network and the mTor pathway on regulating lifespan was established in a variety of model organisms, where a negative modulation of either pathway leads to an increased lifespan (84,85,86). mTor senses energetic stress, oxygen, hormones, growth factors as well as amino acids (87). Thus, positive effects on lifespan and body function can also be potentially achieved by reduction of specific amino acids. It was shown that a restriction of single amino acids such as glutamate, tryptophan or methionine is sufficient to extend the lifespan of *Drosophila*

melanogaster, *Saccharomyces cerevisiae* and mice (88,89,90). It is hypothesized that the organism reallocates resources from reproduction to somatic maintenance in order to survive times of resource limitations (91). Therefore, DR is often associated with a reduced fecundity (90,92). Interestingly, the fecundity can be fully restored by adding only methionine without decreasing the lifespan in a DR model of *Drosophila melanogaster* (93). Proteins from different sources can have different impacts on aging and body function. Plant-derived proteins from soy or wheat seems to have health promoting effects, whereas proteins derived from milk or casein are associated with pathophysiological effects. Soy and wheat proteins are low in methionine and tryptophan. They reduce IGF-1 signaling, insulin sensitivity as well as adiposity and increase lifespan. On the other hand, milk and casein are high in methionine or tryptophan and increases IGF-1 signaling (94,95,96,97). Interestingly, the reduction in IGF-1 signaling upon feeding a low protein diet is associated with a reduced mortality and cancer prevalence in younger but not older populations. Conversely, a high-protein intake reduces the cancer and mortality rate in older people (98). It was also shown that a high-carbohydrate low-protein diet lead to a caloric intake-independent increased lifespan and improved cardiometabolic function in mice (99,100). A beneficial effect on lifespan of high-carbohydrate low-protein diets was also shown in invertebrates such as *Drosophila* with an optimal protein:carbohydrate ratio of 1:16 (101,102). These data highlight the importance of an optimized nutritional geometry and of a balanced amino acid composition to achieve an increased and healthy lifespan. Times-restricted feeding, as a type of DR, is characterized by a reduction in overall caloric intake or by a restriction of specific macronutrients over a period of time. Intermittent fasting, as a type of time-restricted feeding, involves periods of fasting and feeding. The 16:8 diet, in which feeding is limited to an 8 hour period daily, attenuates a variety of metabolic diseases in mice and human (103,104,105). Intermittent fasting also leads to an increased lifespan in mice independent from caloric intake or diet composition (106). A repetitive starvation period of 24 hours followed by 24 hours of *ad libitum* feeding, the so-called every-other-day feeding, cause lifespan extension in mice and a delayed onset of neoplastic disorders (107). However, these effects seem to be dependent on the age at onset of the dietary intervention. The initiation of every-other-day feeding in young mice is accompanied by lifespan extension, whereas the initiation in older mice lead to a decreased lifespan (108). On the other hand, late life stage onset of DR causes a lifespan extension in *Drosophila* (109). As periods of fasting are not feasible for most people, it was shown that even periodically recurrent phases of DR are sufficient to benefit from the advantages of DR (110). All these data suggest that the underlying molecular changes caused by DR to extent lifespan must occur within a short time frame.

1.2 Nutrition and the microbiome

The microbiome refers to the collection of genomes of all microorganisms in a specific environment, whereas the microbiota is the community of microorganisms themselves including bacteria, viruses and fungi. Bacteria exists in many parts of the human body but primarily on internal and external surfaces such as the skin, saliva, oral mucosa or the gastrointestinal tract. The human body contains approximately $3x10^{13}$ cells, where an estimate stated that $4x10^{14}$ bacteria live in association with the human body. Thus, the bacteria in the human body outnumber the human cells at a ratio of 1.3 bacterial cells for every human cell (111). Most of the bacteria live in the intestine with about 10^{11} cells and an estimated number of 1000 bacterial species. All these species contain approximately 2000000 genes, which is 100 times more than the estimated 20.000 human genes (112). Bacteria can function within a host as mutualists, communalists or pathogens, which could result in beneficial or detrimental consequences for host health. There are diverse host-endogenous and host-exogenous factors that have an impact on the composition and function of the microbial community. Each individual has a unique microbial composition, however, close relatives often have more similar microbial communities than unrelated individuals (113,114). Although host genetics can shape the human microbiota, host genetics are outweighed by environmental factors (115, 116). Host nutrition emerges as a crucial determinant in influencing microbial function and composition. Nutrition can have a direct influence on the intestinal microbial population, as nutrients are able to promote or inhibit growth kinetics (117). Diet-induced alterations in the intestinal microbiota occur also during seasonal changes in traditional hunter-gatherer communities. The Hadza community in Tanzania consume a plant-based diet during the wet season and an animal-based diet during the dry season and the intestinal microbiota follows a cyclic succession of species that correspond with enrichment of seasonally associated functions (118). Plant-based diets or diets that are high in protein are associated with high bacterial diversity, while high-fat, high-sugar western diets are associated with a low bacterial diversity (119,120,121). Low bacterial diversity was observed in people with obesity, inflammatory bowel disease, Crohn's disease as well as type 1 and type 2 diabetes (113,122,123,124). On the other hand, higher bacterial diversity is associated with improved metabolic health (125,126). Dietary modulation of the microbiota also alters its metabolic capacities, which can have influences on the host physiology. The fermentation of dietary fibers by bacterial-derived carbohydrate-active enzymes (CAZymes) is the most dominant function. Resistant starch, inulin, cellulose and fructo-oligosaccharide reach the intestine in their undigested form, because the human genome encodes a limited number of CAZymes (127). The end products of bacterial dietary fiber

fermentation are short-chain fatty acids (SCFA) such as acetate, propionate and butyrate (127,128). Butyrate is the main energy source for human colonocytes and has an important role in prevention of carcinogenesis and in maintaining intestinal immune homeostasis, epithelial barrier function as well as oxygen homeostasis (129,130,131,132). Propionate is able to regulate intestinal hormones and gluconeogenesis in the liver (133,132). Acetate is the most abundant SCFA and an essential metabolite for other bacteria as well as a bacterial growth regulator (134,135). Besides the SCFA production, bacteria are able to contribute to vitamin synthesis of vitamin K and family members of B vitamins (136). The intestinal microbiota also has a strong proteolytic capability and play a pivotal role in the catabolism of nitrogen compounds such as amino acids. Essential as well as nonessential amino acids are utilized by the microbiota. The end products of amino acid metabolism and fermentation are SCFA, ammonia, nitric oxide, biogenic amines, hydrogen sulfide, polyamines, branched-chain fatty acids (BCFA), thiols phenolic and indolic compounds (137). Microbiota-mediated amino acid catabolism is negatively connotated as many of the metabolites, such as indole, phenol, hydrogen sulfide and ammonia can be toxic to the host (138,139,140,141,142). However, polyamines such as putrescine, spermidine and spermine are known to improve the intestinal integrity and have anti-inflammatory properties (143,144,145). Bacteria are able to synthesize up to 20 kinds of amino acids *de novo* by using several substrates like ammonia (146,147). The contribution of the *de novo* synthesis of amino acids in the intestine of mono-gastric animals appears to be a crucial regulator in maintaining amino acid balance in the host (148). Moreover, it is estimated that bacterially synthesized L-lysine accounts for approximately 10 % to the daily L-lysine requirements in pigs (149). The microbial-derived L-lysine in the ileum of humans account for 44 % of the total volume of lysine in the plasma (150). All these data support the hologenome theory of evolution, which posits that the holobiont acts as a unit of selection in evolutionary change. Suggesting microbes play an important role in both adaption and evolution of the host to its environment, while the beneficial effect is transferred from one generation to the other (151,152).

1.3 Energy and nutrient sensing

The mTor, insulin and IGF-1 signaling network are important mediators of the cellular energy homeostasis and coordinate cell growth, protein synthesis, autophagy, mRNA translation, lipid and nucleotide synthesis (153,154). mTor is a highly conserved serine/threonine protein kinase in a variety of animals that forms 2 distinct multiprotein complexes, known as mTor complex

1 (mTorC1) and mTor complex 2 (mTorC2,155). mTorC1 consists of 5 components: mTor, regulatory-associated protein of mTor (Raptor), mammalian lethal with Sec13 protein 8 (mLST8), prolin-rich AKT substrate 40 kDa (PRAS40) and DEP-domain-containing mTor-interacting protein (Deptor). mTorC2 is defined by 6 components: mTor, rapamycin-insensitive companion of mTor (Rictor), mammalian stress-activated protein kinase interaction protein (mSIN1), protein observed with Rictor-1 (Protor-1), mLST8 and Deptor (156). The bacterial macrolide rapamycin is known to inhibit mTorC1 functions by binding to FK506-binding protein of 12 kDa (FKBP12) and interaction with the FKBP12-rapamycin binding domain (FRB) of mTor. In contrast to mTorC1, the mTorC2 complex is insensitive to rapamycin treatment (157). mTorC1 positively regulates the protein synthesis mainly through the phosphorylation of p70-S6 kinase 1 (S6K1) and eIF4E binding protein (4EBP). S6K1 activation lead to translation of ribosomal proteins, mRNA biogenesis and an cap-dependent translation as well as elongation (158,159). The phosphorylation of 4EBP prevents the binding to eIF4E, which enables mRNA translation (160). mTorC1 also represses autophagy via autophagy-related gene 13 (ATG13) and unc-51-like kinase (ULK1) phosphorylation (161). mTorC1positively regulates lipid and nucleotide synthesis by the activation of the sterol regulatory element binding protein 1 (SREBP1) or by inducing the expression of MTHFD2, respectively (162,163). The mTorC1 induced anabolism only occurs in case of sufficient amino acid, oxygen, energy or pro-growth factor availability. The amino acids leucine, arginine and glutamine are known to directly stimulate mTORC1 activity (164,165). Proteins of the Rag family, which are related to small GTPases, are known to interact with mTorC1 in an amino acid-sensitive manner. Cellular amino acid availability stimulates the Rag proteins to bind Raptor and recruit mTorC1 to lysosomal surfaces where the small Ras-related GTPase Ras homolog enriched in brain (Rheb) is present. Rheb directly interacts with mTorC1 and stimulates its activity (166). However, glutamine activates mTorC1 in a Rag-independent pathway (167). Intracellular adenosine triphosphate (ATP) levels are sensed via the AMP-activated protein kinase (AMPK). Low levels of ATP activate AMPK, which in turn phosphorylates the tuberous sclerosis complex 2 (TSC2) or Raptor. Phosphorylation of TSC2 or Raptor lead to an inactivation of mTorC1(168,169). Growth factors stimulate mTorC1 via the IGF-1 or rat sarcoma (Ras) signaling pathway. Both pathways integrate growth factor signals and inhibit the tuberous sclerosis complex (TSC), a negative regulator of mTorC1. TSC is a heterodimer comprising TSC1 and TSC2 and functions as a GTPase-activating protein and converts Rheb in its inactive form (170). Ras activates the rapidly accelerated fibrosarcoma (Raf)/mitogen-activated kinase (MEK)/extracellular signal-regulated kinase (Erk) signaling

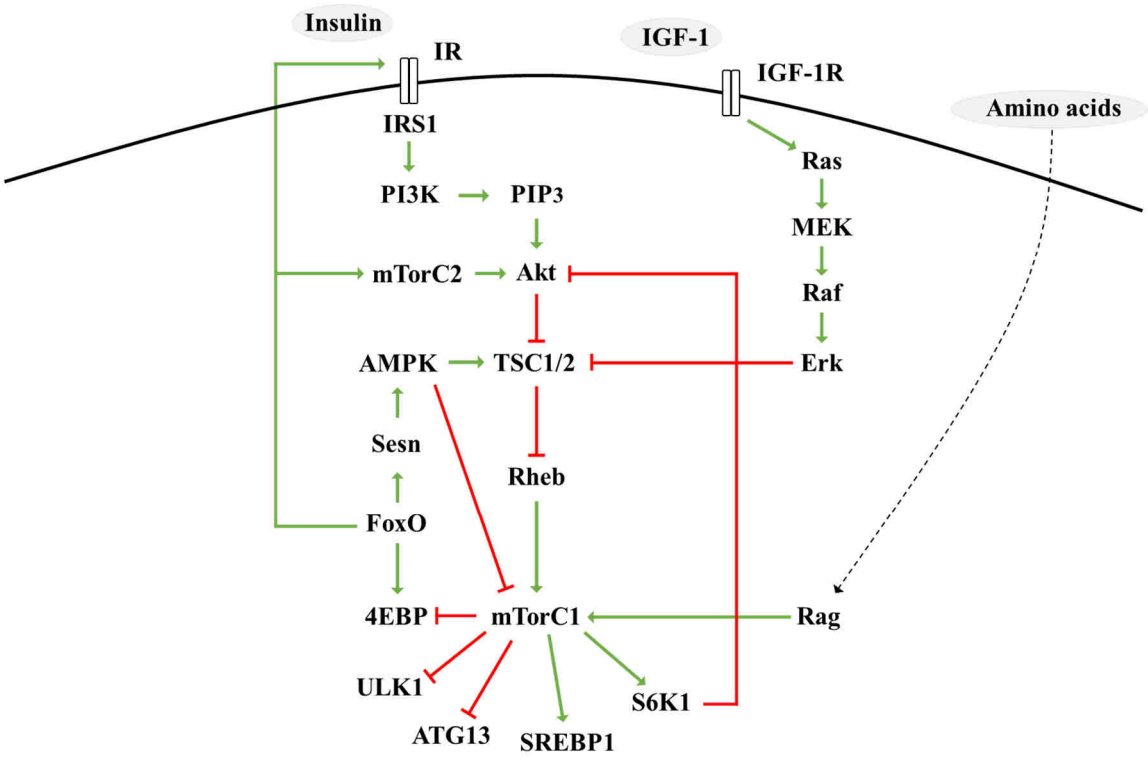

Fig. 1: Scheme of the mTor, insulin and IGF-1 signaling network. The mTor, insulin and IGF-1 signaling network are important sensors of the amino acid and energy level of the cell. These pathways mediate the cellular energy homeostasis and coordinate cell growth, protein synthesis, autophagy, mRNA translation, lipid and nucleotide synthesis. A positive regulation is illustrated by green arrows, whereas a negative regulation is shown as red inhibitory arrows. IR: insulin receptor, IRS1: insulin receptor 1, PI3K: phosphoinositide 3 kinase, PIP_3: phosphatidylinositol-(3,4,5)-triphosphate, Akt: v-akt murine thymoma viral oncogene, mTorC1: mechanistic Tor complex C1, mTorC2: mechanistic Tor complex C2, TSC1/2: tuberous sclerosis complex 1/2, AMPK: AMP-activated protein kinase, Sesn: Sestrin, FoxO: forkhead box O, 4EBP: eIF4E binding protein, Rheb: ras homolog enriched in brain, IGF-1: insulin like growth factor-1, ras: rat sarcoma, MEK: mitogen-activated kinase, Raf: rapidly accelerated fibrosarcoma, Erk: extracellular-regulated kinase, ULK1: unc-51-like kinase, ATG13: autophagy-related gene 13, SREBP1: sterol regulatory element binding protein 1, S6K1: p70-S6 Kinase 1.

cascade leading to phosphorylation of TSC2 by Erk and subsequent inactivation of the TSC complex (171). Binding of insulin to the insulin receptor (IR) activates its tyrosine kinase causing phosphorylation of IR and of IR substrates (IRS). Phosphorylated IRS recruits phosphoinositide 3-kinase (PI3K), which stimulates the production of phosphatidylinositol-(3,4,5)-triphosphate (PIP_3) at the plasma membrane causing an activation of the serine/threonine protein kinase v-akt murine thymoma viral oncogene (Akt). Akt phosphorylates several substrates such as TSC2, glycogen synthase kinase 3ß (GSK3ß) or forkhead family box O (FoxO,172). However, Akt can also be activated though phosphorylation by mTorC2 (173). FoxO proteins are highly conserved in invertebrates and mammals; 1 FoxO gene exists in invertebrates while mammals have 4 FoxO genes, namely FoxO1, FoxO3, FoxO4 and FoxO6 (174,175). FoxO transcription factors are involved in the regulation of longevity in several organisms (176,177,178). FoxO proteins are negatively regulated by Akt and regulate numerous cellular functions such as proliferation, differentiation,

apoptosis, autophagy, oxidative stress modulation, DNA repair and immunity (179,180,181,182,183,184). There are a variety of regulatory circuits that mediates interplays between FoxO and mTor. The activation of FoxO leads to a stimulation of 4EBP and therewith counteracts mTorC1 activity (185). FoxO is able to indirectly inhibit mTorC1 activity by stimulating AMPK via Sestrin (Sesn)-expression regulation, which in turn activates TSC2 (186). FoxO has the potential to elevate the expression of the IR, which in turn stimulate IR downstream molecules and thereby limits FoxO activation (187,188). When sufficient growth factors are present, mTorC1can initiate a negative feedback loop via S6K1 to inhibit Akt (189). The inhibition of Akt leads to an activation of FoxO, whereby FoxO elevates the transcriptional regulation of Sesn and Rictor. Elevated levels of Rictor increases mTorC2 activity, which subsequently activates Akt. Thereby, the homeostatic balance between mTor and Akt activities is balanced (190).

1.4 *Drosophila* as a model organism

For nearly 100 years, *Drosophila melanogaster* is one of the most studied multi-cellular, eukaryotic organisms in biology and offers several advantages for the investigation of molecular and cellular mechanisms underlying behavior, development and many other processes. A short generation time, a large number of offspring, cheap and easy stock breeding are characteristics of *Drosophila* as a model organism. The fly genome was completely sequenced in 2000 and contains approximately 13.600 genes on only four chromosomes, allowing the research community to reveal homologs in human or other vertebrates (191). Over 75 % of known human disease-associated genes have a homolog in the *Drosophila* genome (192). With regards to the parallels between the genome of humans and *Drosophila,* the fly is an important model organism for the study of human diseases as well as for development and behavior. An advance in genetic manipulation in *Drosophila* was the development of the GAL4/UAS system (193). The system utilizes the GAL4 transcription factor from yeast, a transactivator that specifically binds a downstream upstream activating sequence (UAS)-element. The main advantage of the GAL4/UAS system in *Drosophila* is the separation of the responder from the transactivator in two distinct transgenic fly lines. Therefore, a construct with an enhancer or a promotor region of interest, driving the expression of the GAL4 gene, is used to create a transgenic fly. This fly line is called driver line. A second fly strain is made containing construct with a target gene downstream of a UAS-element, namely the responder line. Target genes are used to express reporter genes, downregulate (RNAi element) or to

overexpress a specific gene. In absence of the GAL4 transcription factor, no expression of the target gene is induced. By crossing the transgenic fly lines, the target gene is exclusively expressed in a specific cell or tissue and temporal pattern defined by the gene specific promotor upstream of the GAL4.

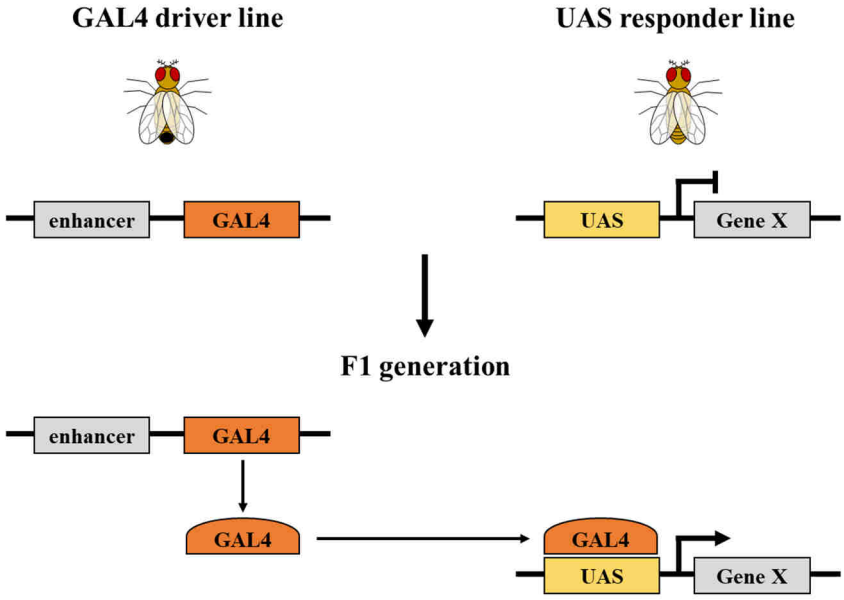

Fig. 2: The GAL4/UAS-system in *Drosophila melanogaster*. The binary expression system GAL4/UAS in *Drosophila* comprises a GAL4 driver line and UAS responder line. GAL4 and UAS are fused to an enhancer of interest and a gene of interest, respectively. The F1 generation expresses both constructs, thus, the gene of interest is expressed in a spatio-temporal manner. UAS: upstream activated sequence.

1.4.1 The intestinal tract of flies and humans

The intestinal tract is the central organ for digestion and absorption of essential dietary nutrients. The intestinal tract is a mediator of the metabolic status as is regulates food intake and nutrient storage through bidirectional neuronal and endocrine signaling to the brain or other peripheral organs (194). The intestinal tract is in continuous contact with a diverse and dynamic array of mutualistic and symbiotic microorganisms. Moreover, it serves as the largest epithelial barrier against a variety of ingested pathogens and toxins. Thus, the intestine is increasingly acknowledged for its importance in promoting health. The empirical knowledge and the progress in intestinal research relied heavily on the extensive use of model organisms. With regard to human diseases, a model organism should reflect the biology of humans while reducing the complexity of the human disease of interest. The structure and function of the intestinal tract is broadly conserved among metazoan (195). In the last decades, the fruit fly *Drosophila melanogaster* has become a model for intestinal research as it shares many features with the human intestinal structure, homeostasis and physiology (196,197). The gastrointestinal

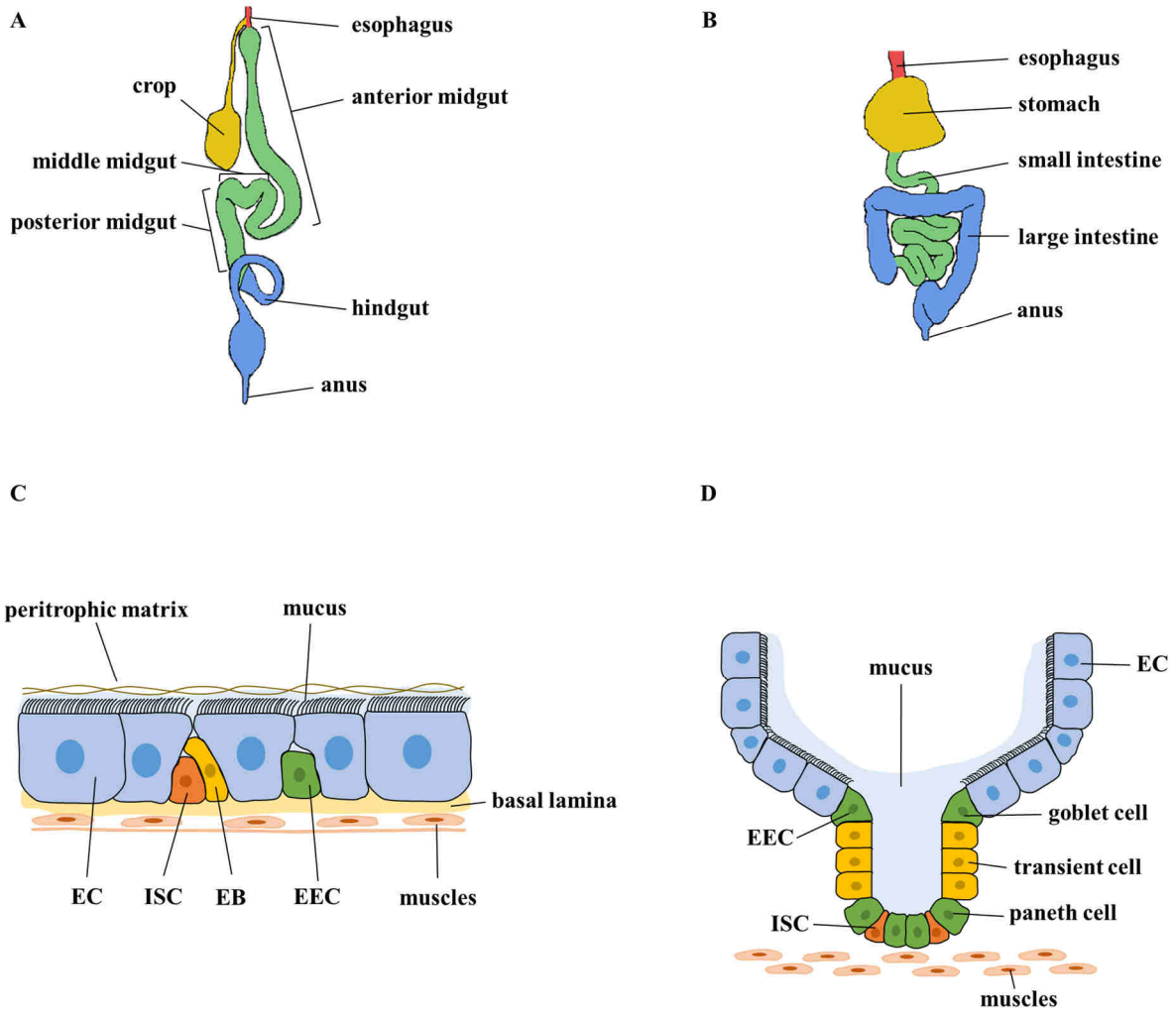

Fig. 3: The gastrointestinal tract of *Drosophila melanogaster* and humans. (A) The gastrointestinal tract of *Drosophila* melanogaster is subdivided into crop, esophagus, anterior midgut, middle midgut, posterior midgut, hindgut and anus. (B) The gastrointestinal tract of humans is subdivided into esophagus, stomach, small intestine, large intestine and anus. The colored compartments illustrate functional similarities between the gastrointestinal tract of *Drosophila* and humans. (C) The epithelial monolayer of the *Drosophila* intestine consists of pluripotent ISCs, EBs, secretory EECs and absorptive ECs. The monolayer is protected by a chitinous peritrophic matrix and mucus on the luminal side and is surrounded by two layers of visceral muscles towards the body cavity. (D) The epithelial monolayer of crypts in the human intestine consists of ISCs, EECs, ECs, paneth cells, transient cells and goblet cells. ISC: intestinal stem cell, EB: enteroblast, EEC: enteroendocrine cell, EC: enterocyte.

tract of *Drosophila* is subdivided into distinct compartments: the foregut with its crop, anterior midgut, middle midgut, posterior midgut, hindgut and anus (198,197). In *Drosophila*, the midgut is further subdivided into 10-14 morphologically and molecularly distinct regions, each with specific histological, cellular, physical or gene expression properties (198, 199). The human gastrointestinal tract is subdivided in esophagus, stomach, small intestine, large intestine, rectum and anus. There are similarities between the foregut and the esophagus as well as the crop and the stomach. Ingested food passes through the foregut into the crop in *Drosophila* or through the esophagus into the stomach in humans, respectively. The crop as well as the stomach are responsible for early digestion and food storage (200–202). In

Drosophila the food passages through the anterior midgut, middle midgut and posterior midgut where nutrients absorption takes place. Afterwards, it passes the hindgut where water and electrolyte resorption may occur and finally reaches the anus for excretion (203,204). In humans, the food moves to the small and large intestine for nutrient, water and electrolyte absorption and finally reaches the rectum for excretion (200). The *Drosophila* gut consists of a tubular epithelium surrounded by a basal lamina, nerves, visceral muscles and trachea (205,206). The *Drosophila* midgut originates from the mesoderm and a mucus layer as well as a semipermeable chitinous layer, the peritrophic matrix, lines the luminal side. Besides the protection against physical damage, the peritrophic matrix serves as a physical barrier to pathogenic microorganisms (207). The foregut and the hindgut are of ectodermal origin and are protected by an impermeable cuticle on the distal side. The intestine of *Drosophila* is composed of a monolayer of cells consisting of 4 cell types: intestinal stem cells (ISC), enteroblasts (EB), enterocytes (EC) and enteroendocrine cells (EEC). The ECs are large polyploid cells with nutrient absorptive and digestive enzymes secretion properties, whereas the EECs are small secretory cells (197). The human intestine is also an epithelial monolayer consisting pluripotent ISCs, ECs, and EECs. Other types of secretory cell types in the human intestine are antimicrobial peptide (AMP)- producing Paneth cells and mucus-producing goblet cells. In contrast to *Drosophila,* the human intestinal epithelium exhibit indentations to maximize the surface area, the so-called crypts. Both *Drosophila* and human ECs develop brush borders on their apical side to increase the cellular surface area (208). In *Drosophila*, ISCs undergo symmetric or asymmetric division. In asymmetric divisions, one ISC remains mitotically active, whereas the other daughter cell becomes an EB. The EB further differentiate into an EC or an EEC. (209,210,211). In human, asymmetric division gives rise to transient amplifying (TA) cells that moves up the crypt and undergo differentiation into either ECs, EECs, goblet or Paneth cells (212).

1.4.2 **Intestinal plasticity in *Drosophila***

Drosophila belongs to the group of holometabolic insects, therefore, the intestine undergoes complete metamorphosis. The gastrointestinal tract of *Drosophila* is replaced during development. The larval intestine and the pupal intestine degenerate during metamorphosis and are replaced by the adult intestine (213). Under steady-state conditions, the adult *Drosophila* intestine is renewed within 1 to 2 weeks (210). The renewal is achieved by ISCs, which undergo symmetric or asymmetric division. During asymmetric division ISCs produces an ISC and an

EB, whereas the EB is devoid of mitotic capability. The EBs differentiates terminally into either ECs or EECs, controlled by Delta-Notch signaling. The Delta (Dl) ligand is predominantly expressed in ISCs and activates Notch receptors on EBs. A strong Notch signal induces the fate of an EB to the EC, whereas a weak Notch signal directs the EB to an EEC (214). Both, ISCs and EBs express the marker gene *escargot* (esg). ISCs can be specifically identified by the expression of Dl, whereas EBs can be detected by the expression of the Notch signal reporter *suppressor-of-hairless* Su(H)GBE (215,216). ECs specifically express *myo1A* whereas EECs are Prospero-positive (211,216). However, a recent study showed that only ECs are generated through Su(H)GBE$^+$ cells, whereas EECs are generated through a distinct progenitor pre-EEC (217). ISCs are highly responsive to signals from neighboring cells, to environmental factors and to the metabolic state of the host. Intestinal tissue damage by pathogenic bacteria, corrosive agents, such as dextran sodium sulfate (DSS), bleomycin or paraquat, or other stressors leads to an increase of ISC mitotic activity (218,219). ISC proliferation and differentiation ensure tissue integrity by replacing lost cells. However, EBs are also produced by ISCs in the absence of an epithelial stressors or local turnover. EBs pause their differentiation as long as demand for new ECs is lacking, which in turn leads to a significantly faster replacement of lost cell (220). The nutritional state of the fly as well as the direct contact with nutrients influences the ISC homeostasis. It was shown that intestinal tissue growth was promoted via insulin signaling, when food was abundant. Moreover, insulin signaling directs ISC into symmetric or asymmetric division (221,222). Even single amino acids such as methionine affect ISC division (223). Many aspects of the intestinal regenerative response are associated with the presence of the microbiota. The absence of an intestinal microbiota in *Drosophila* lead to a reduced proliferation as well as an altered cell composition and intestinal morphology (224,225). Aged intestines show ISC hyperproliferation, incorrect cell lineage differentiation and a disturbed intestinal epithelial integrity as well as immune homeostasis (226,227). Interestingly, aged flies reveal an increased intestinal bacterial load in comparison to young flies. Extinction of the indigenous microbiota leads to a decreased ISC proliferation rate, increased intestinal integrity and a reduced immune system activity (224,228). The intestinal homeostasis is coordinated by conserved signaling pathways, namely the Janus kinase-signal transducers and activators of transcription (JAK/Stat), Jun N-terminal kinase (JNK), epidermal growth factor receptor (EGFR), Hippo and Wingless (Wg) pathways (229,230,227,231,232,233). The JNK pathway is an upstream sensor of tissue damage in the *Drosophila* intestine. In injured ECs, the JNK pathway induces Unpaired (Upd), Unpaired 2 (Upd2) and Unpaired 3 (Upd3) cytokine expression via a kinase cascade mediated by Hemipterous (Hep, JNKK) and Basket (Bsk, JNK).

Upd3, a ligand for the receptor Domeless (Dome) induces JAK/Stat signaling in ISC and EBs, which in turn promotes proliferation and differentiation to replace damaged cells. The Jun kinase phosphatase Puckered, a JNK feedback inhibitor, is required to restrain upd3 expression in healthy animals to maintain normal intestinal homeostasis (229,234). Overexpression of Dome, Hopscotch (*Drosophila* JAK), or Stat92E (*Drosophila* Stat) in ISCs leads to massive hyperproliferation, whereas depletion of one of these pathway components impairs regeneration ability and infection resistance of the fly's intestine (229,224). Upd3 also acts in visceral muscles to induce the EGF ligand expression of Vein, which in turn activates EGFR/Ras/MAPK signaling in ISCs. Reciprocally, vein also acts in ECs to induce Upd expression to direct a positive feedback loop (234,231). EGFR signaling in ISCs is required for maintaining the growth and proliferative capacity, but has little or no influence on cell fate specification (235,236). The JNK pathway in ECs also mediates Wg expression in EBs upon cellular damage and leads to Myc-dependent ISC proliferation (233). Moreover, overexpression of Wg in ISCs induces the production of the EGF ligand Spitz in ISCs and an expression of Upd3 in ECs (237).

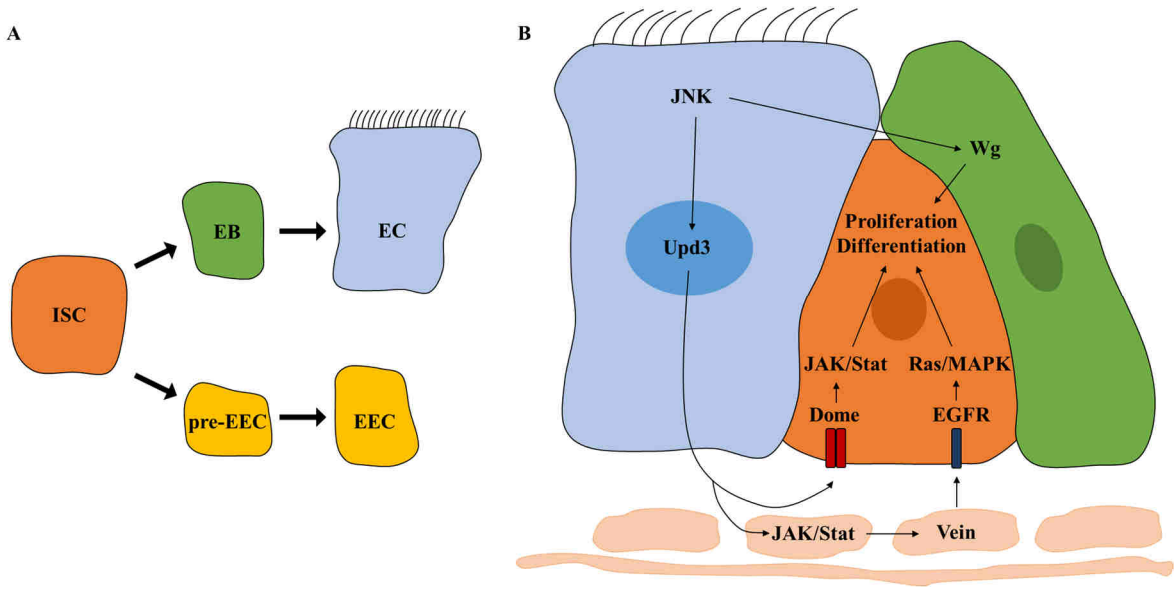

Fig. 4: Cell lineage and proliferation mechanism of intestinal stem cells in *Drosophila melanogaster*. (A) ISCs undergo symmetric or asymmetric divisions. Under asymmetric division, the ISC divide into an EB or a pre-EEC, whereas the ISC remain mitotically active. The EB further differentiate into an EC and the pre-EEC mature into an EEC. (B) Activation of the JNK pathway induces Upd3 secretion from ECs, which in turn activates JAK/Stat signaling by binding the receptor Dome in ISCs or in the surrounding muscles. An activated JAK/Stat pathway in muscles leads to a release of Vein, which induces the EGFR/Ras/MAPK signaling cascade in ISCs. Activation of JAK/Stat and/or EGFR/Ras/MAPK pathways in ISCs promote proliferation and differentiation. The JNK pathway also mediates Wg expression in EBs, which stimulates ISC proliferation. ISC: intestinal stem cell, EB: enteroblast, EEC: enteroendocrine cell, EC: enterocyte, JNK: Jun N-terminal kinase, Upd3: unpaired 3, JAK/Stat: Janus kinase-signal transducers and activators of transcription, Dome: Domeless, EGFR: epidermal growth factor receptor, Ras: rat sarcoma, MAPK: mitogen-activated protein kinase, Wg: wingless.

1.4.3 *Drosophila* to study host-microbe interactions

Drosophila melanogaster is a well-established model organism to study host-microbe interactions in a nutrition-dependent context. The gut lumen of *Drosophila* is associated with a relatively low bacterial diversity (1-30 taxa; 238,239), in contrast to the more complex diversity of vertebrates (> 500 taxa;240,241,242). The genetic tractability, the lower complexity of the microbiota as well as the ease in raising germ-free flies highlight the potential of this model organism to study the interactions between the host and its microbial flora. The composition of the bacterial community of *Drosophila* is highly influenced by the host's diet. In the wild, the food niches vary within the *Drosophilids* including rotting fruits, flowers, mushrooms and cacti. In wild type flies, up to 30 different bacterial taxa were found, whereas laboratory flies harbor only up to 8 taxa. However, only a three bacterial clades are associated with both natural and laboratory *Drosophila* populations: *Enterobacteriaceae*, *Acetobacteraceae* and the order *Lactobacillales* (238). The most prevalent bacterial species in flies are members of the genera *Lactobacillus* and *Acetobacter*, whereas the specific bacterial composition depends on the fly's diet suggesting the bacterial microbiome is environmentally acquired. Although the bacterial composition of the fly's food niche is highly complex, the fly represents only a subset of this composition. This data suggest that the fly has control properties to filter its bacterial community (238,239). It is unknown if *Drosophila* harbors a resident bacterial community and most researchers assume a transient microbiota. It was shown that *Drosophila* establishes and maintains its microbiome by frequently consuming bacteria. Flies that are transferred to fresh, sterile food daily harbor less bacterial populations than those that are not transferred (243). However, a recent study revealed bacterial species that stably associate with wild-type *Drosophila* independently from continuous inoculation. The intestine of lab *Drosophila* could be stable inoculated with 2 *Acetobacter* species, namely *Acetobacter thailandicus* and *Acetobacter cibinongensis*. Moreover, they were able to proliferate in the intestine and in addition, *Acetobacter thailandicus* exhibited mutualistic effects (244). The *Drosophila* embryo is sterile, whereas the chorion is contaminated with bacteria from the substratum niche as well as from the feces of adult flies. After hatching, the larvae acquire the bacteria through ingestion of the chorion and of the substratum (245). These data highlight the contribution of external inputs to sustaining the microbiome and that *Drosophila* inoculates its own substratum niche. Since *Drosophila* inoculates its own food niche, bacteria that are able to colonize the environment have the greatest chance to colonize the gut (243,246,247). Flies that were raised on either starch medium or molasses medium for several generations harbor different bacterial communities, thus, changes in the diet result in changes in the microbiota. Furthermore, flies

exhibit a mating preference for partners reared on the same medium suggesting that the microbiota influences the flies' behavior, e.g. by altering the level of sex pheromones (246). In the wild, this microbiota-induced mating preference would reduce interbreeding of *Drosophila* populations, and thus favor speciation. Besides the impact of the microbiota on behavior, there is also a link between intestinal microbiota and energy metabolism. The ability to raise germ-free flies indicates that the microbiota is dispensable for growth under optimal nutrient conditions, whereas it is required under restricted dietary conditions. Germ-free *Drosophila* larvae exhibit a delayed developmental time under poor diet conditions which can be fully restored by reintroduction of *Lactobacillus plantarum*. It is suggested that *Lactobacillus plantarum* affects the TOR pathway, the key sensor of the nutritional status of the cell (248). Another study showed, that *Acetobacter pomorum* can fully rescue developmental and size defects under protein-poor diet conditions by modulating insulin signaling (249). The *Drosophila* microbiota provides B vitamins on yeast-deprived diets, promotes protein nutrition and suppresses lipid/carbohydrate storage on high sugar diets (250). All these studies demonstrate that the microbiota has multiple impacts on *Drosophila's* metabolism in a nutrient-dependent context. *Drosophila*, with its less complex microbiota, can be utilized to investigate the influence of nutrition on the microbial community as well as the accompanied microbiota-associated metabolic effects to the host. Together with the possibility of genetic manipulations, *Drosophila* is a suitable model to discover the complex host-microbe-nutrition tripartite interaction network.

1.5 Aims of the study

Globally, over 2 billion people suffer from malnutrition, which is I defined by the World Health Organization as an excess, deficiency or imbalance in a person's intake of energy and/or nutrients. Malnutrition is an important risk factor for the burden of diseases in developing countries as well as in economically more developed countries. Tackling malnutrition in its all forms is one of the greatest global health challenges. On the other hand, dietary restriction is suspected to have a plethora of health-promoting effects including life span. The intestine is particularly predisposed to nutritional interventions because it is in close contact with dietary components. Maintaining the intestinal epithelial homeostasis requires an equilibrium between the microbial community and the intestinal epithelium and dietary interventions are believed to have an impact on this equilibrium. In my study, I am interested to examine the complex tripartite interplay between the intestinal epithelium, microbial community and nutritional stressors such as high-fat dieting, protein-energy malnutrition and dietary restriction in the versatile model *Drosophila melanogaster*.

The major aims of the study were:

1) to elucidate the effects and underlying mechanisms of high-fat dieting on the interplay between intestinal cellular homeostasis and the microbial community

2) to optimize holidic diet protocols, which allows optimal development of flies harboring an indigenous microbial community and germ-free flies

3) to examine the impact of protein-energy malnutrition and dietary restriction on host-microbiota interactions in the intestinal ecosystem

2 Material

2.1 Chemicals

Chemicals that were used for experimental approaches are shown in table 1.

Table 1: Chemicals.

Chemical	Source of supply
Agar-agar	Carl Roth
Agarose	Biozym
Bacto™ yeast extract	Becton, Dickinson and Company
Brewer's yeast	Leiber GmbH
Isopropanol	Carl Roth
$MgCl_2$	Thermofisher Scientific
dNTPs	Thermofissher Scientific
Chloroform	Carl Roth
Coconut fat	Palmin
Corn meal	Davert GmbH
D-glucose monohydrate	Carl Roth
D-fructose	Sigma-Adrich
D-sucrose	Carl Roth
Molasses	Biohof Heidelicht
Nipagin	Carl Roth
Normal goat serum	Sigma-Aldrich
Paraformaldehyde powder EM grade	Polysciences Inc.
Propionic acid	Carl Roth
Sugar beet syrup	Kanne Brottrunk GmbH
Tween-20	Carl Roth
Triton X-100	Carl Roth
Trioleate	Sigma-Aldrich
Mowiol	Carl Roth
Ethanol	Carl Roth
KCl	Merck
NaCl	Carl Roth
KH_2HPO_4	Carl Roth

Difco™ MRS	Fisher scientific
Brilliant Blue FCF food dye E133	Ruth

2.2 Kits and reagents

Kits and reagents that were used for experimental approaches are shown in table 2.

Table 2: Kit and reagents.

Kit/Reagent	Source of supply
DNeasy Blood and Tissue kit	Qiagen
Masterpure DNA purification kit	Epicentre
Ambion Purelink RNA mini kit	Thermofisher Scientific
Qubit dsDNA HS assay kit	Thermofisher Scientific
Qubit RNA HS assay kit	Thermofisher Scientific
RNA magic	Bio Budget
qPCRBIO SyGreen	PCR Bioystems
Amplex™ Red Uric Acid/Uricase assay kit	Thermofisher Scientific
BODIPY™ 493/503	Thermofisher Scientific
Infinity triglyceride solution	Thermofisher Scientific
Pierce™ BCA Protein assay kit	Thermofisher Scientific
DreamTaq polymerase	Thermofisher Scientific
ONE-Glo Luciferase Assay System	Promega
Phusion Hot Start Flex 2x Master Mix	NEB
SequalPrep Normalization Plate Kit	Thermofisher Scientific

2.3 Ingredients for holidic diet

The ingredients that were used for preparing the holidic diets are shown in table 3.

Table 3: Ingredients for holidic diets.

Ingredient	Source of supply
Cholesterol	Sigma-Aldrich (C8667)
Ergosterol	Sigma-Aldrich (45480)
KH_2PO_4	Carl Roth (P018.2)
$NaHCO_3$	Sigma-Aldrich (S5761)
Glacial acid	Carl Roth (3738.2)

Agar-agar	Carl Roth (5210.2)
L-alanine	Sigma-Aldrich (A7627)
L-aspartic acid	Sigma-Aldrich (A6683)
L-asparagin	Sigma-Aldrich (A0884)
Glycin	Carl Roth (0079.1)
L-prolin	Carl Roth (T205.2)
L-glutamin	Carl Roth (3772.2)
L-serin	Carl Roth (1714.2)
L-cystein HCl	Carl Roth (3468.2)
L-arginine monohydrochloride	Sigma-Aldrich (A5131)
L-threonin	Carl Roth (T206.2)
L-methionine	Carl Roth (9359.1)
L-tryptophan	Carl Roth (4858.2)
L-phenylalanine	Carl Roth (4491.1)
L-histidine	Carl Roth (3852.3)
L-lysin HCl	Carl Roth (9357.1)
L-valin	Carl Roth (4879.4)
L-isoleucine	Carl Roth (3922.2)
L-leucine	Carl Roth (3984.3)
L-tyrosine	Carl Roth (T207.2)
Cholin chloride	Sigma-Aldrich (C1879)
Myo-inositol	Sigma-Aldrich (I7508)
Inosine	Carl Roth (6770.1)
Uridine	Carl Roth (0714.3)
Folic acid	Carl Roth (T912.1)
Riboflavin	Carl Roth (9607.1)
D(+)-biotin	Carl Roth (3822.1)
Nicotinic acid	Carl Roth (3815.2)
Calcium-D(+)-pantothenat	Carl Roth (3812.2)
Thiamine	Sigma-Aldrich (T4625)
Pyridoxine HCl	Carl Roth (T914.1)
L-glutamic acid monosodium salt hydrate	Sigma-Aldrich (G5889)
Copper(II) sulfate pentahydrate	Sigma-Aldrich (C7631)
Zinc sulfate • $5H_2O$	Sigma-Aldrich (Z0251)

Iron(II) sulfate • $5H_2O$	Sigma-Aldrich (F7002)
Manganese(II) chlorid • $4H_2O$	Sigma-Aldrich (M3634)
CaCl • $6H_2O$	Carl Roth (5239.2)
$MgSO_4$ • $4H_2O$	Carl Roth (P027.2)
Ribonucleic acid from torula yeast	Sigma-Aldrich (R6625)
Cobalamin	Sigma-Aldrich (V6629)
Molybdenum	Carl Roth (0274.1)
Cobalt	Sigma-Aldrich (CDS004010)

2.4 Buffers and solutions

Table 4 shows buffers and solutions that were used for experimental approaches.

Table 4: Solutions and buffers.

Solution/Buffer	Ingredients
10x phosphate-buffered saline (PBS)	80 g/l NaCl, 2 g/l KCl, 17.8 g/l NaH_2PO_4, 2.4 g/l KH_2PO_4 (pH = 7.4)
PBS containing 0.1 % Triton X-100 (0.1 % PBT)	0.1 % (v/v) Triton X-100 in 1x PBS
Blocking solution	5 % (v/v) normal goat serum in 0.1 % PBT
10 % nipagin	10 % (w/v) in 70 % EtOH
10 % propionic acid	10 % (v/v) propionic acid in dH_2O
4 % paraformaldehyde	4 % (w/v) paraformaldehyde in 1x PBS
Enzymatic lysis buffer	20 mM Tris Cl (pH = 8.0), 2 mM sodium EDTA, 1.2 % Triton X-100

2.5 Oligonucleotides

Primers and oligonucleotides that were used in this study are shown in table 5.

Table 5: Primers and oligonucleotides.

Primer	Sequence
8FM	F: AGAGTTTGATCMTGGCTCAG
Bact515R	R: TTACCGCGGCKGCTGGCAC
Upd3	F: GAGAACACCTGCAATCTGAA
	R: AGAGTCTTGGTGCTCACTGT

Drsm	F: ACCAAGCTCCGTGAGAACCTT R: TTGTATCTTCCGGACAGGCAG
Def	F: TCTTCGTTCTCGTGGCTATC R: TTCCAGTTCCACTTGGAGAG
Dros	F: GCGAATTCATTCCAATCGATCGGTATC R: CTGACAGGCCATTGCGAAG
Mtk	F: CCACCGAGCTAAGATGCAA R: AATAAATTGGACCCGGTCTTG
Rpl32	F: CCGCTTCAAGGGACAGTATC R: GACAATCTCCTTGCGCTTCT
Oligo dT	GAGAGAGGATCCAATACTAATACGACTCACTA TAGGGAGATTTTTTTTTTTTTTTTTTTTTTTT
341F	GTGCCAGCMGCCGCGGTAA
806R	GGACTACHVGGGTWTCTAAT

2.6 Antibodies

Primary and secondary antibodies that were used for immunohistochemistry are listed in table 6.

Table 6: Primary and secondary antibodies.

Antibody	Dilution	Source of supply
anti-GFP from mouse	1:300	Developmental Studies Hybridoma Bank
anti-GFP from rabbit	1:300	Sigma-Aldrich
anti-pH3 from rabbit	1:100	Cell Signaling Technology
anti-phospho JNK	1:100	Promega
anti-prospero	1:200	Developmental Studies Hybridoma Bank
anti-spectrin from mouse	1:100	Developmental Studies Hybridoma Bank

anti-coracle from mouse	1:100	Developmental Studies Hybridoma Bank
anti-mouse AlexaFluor 555	1:300	Cell Signaling Technology
anti-mouse Cy3	1:300	Jackson ImmunoResearch
Anti-rabbit AlexaFluor 488	1:300	Jackson ImmunoResearch

2.7 Culture media

2.7.1 Standard *Drosophila* culture medium

The standard *Drosophila* culture medium was used for all stocking flies. The following recipe is for 500 ml medium:

31.25 g corn meal

31.25 g brewer's yeast

5 g agar-agar

10 g D-glucose monohydrate

15 g molasses

15 sugar beet syrup

Add 500 ml dH_20 and mix well. Bring to a boil and simmer for 15 min, autoclave and let cool down to 65 °C. Add 3 % propionic acid (10 % propionic acid in dH_2O) and 1 % nipagin (10 % nipagin in 70 % in EtOH). Pour the medium into *Drosophila* culture vials and let it dry. The medium was stored at 8 °C until use.

2.7.2 High fat diet

The high fat diet consists of 20 % coconut fat and is based on a corn meal diet. The following recipe is for 500 ml high fat diet:

43 g corn meal

25 g yeast extract

5 g agar-agar

25 g D-glucose monohydrate

Add dH_2O ad 400 ml and mix well. Bring to boil and simmer for 15 min, autoclave and let cool down to 65 °C. Melt 100 g coconut fat at 50 °C and mix it fastly with the corn meal medium. Add 3 % propionic acid (10 % propionic acid in dH_2O) and 1 % nipagin (10 % nipagin in 70 % in EtOH). Pour the medium into *Drosophila* culture vials and let it dry. The medium was stored at 8 °C until use. The proper control medium was mixed with 100 ml dH_2O instead of coconut fat.

2.7.3 **Sugar-yeast diet**

The following recipe is for 500 ml sugar-yeast (SY) diet:

4g corn meal

50 g brewer's yeast

1 g agar-agar

2.5 g sucrose

Add 500 ml dH_20 and mix well. Bring to a boil and simmer for 15 min, autoclave and let cool down to 65 °C. Add 3 % propionic acid (10 % propionic acid in dH_2O) and 1 % nipagin (10 % nipagin in 70 % in EtOH). Pour the medium into *Drosophila* culture vials and let it dry. The medium was stored at 8 °C until use

2.7.4 **Optimized holidic diet**

The optimized holidic diet was prepared according to Piper *et al.*(251) with some modifications. The ingredients and stock solutions are listed in table 7.

Table 7: Components and stock solutions of the optimized holidic diet.

	Ingredient	**Stock**	**Amount per liter**
Gelling agent	Agar		20 g
Base	Buffer	10x: 30 m/l glacial acetic acid 30 g/l KH_2PO_4	100 ml

		10 g/l $NaHCO_3$	
Sugar	Glucose		75 g
Amino acids	L-isoleucine		3.64 g
	L-leucine		2.42 g
	L-tyrosine		0.84 g
Metal ions	$CaCl_2 \cdot 6H_2O$	1000x: 250 g/l	1 ml
	$CuSO_4 \cdot 5H_2O$	1000x: 2.5 g/l	1 ml
	$FeSO_4 \cdot 7H_2O$	1000x: 25 g/l	1 ml
	$MgSO_4$ (anhydrous)	1000x: 250 g/l	1 ml
	$MnCl_2 \cdot 4H_2O$	1000x: 1 g/l	1 ml
	$ZnSO_4 \cdot 7H_2O$	1000x: 25 g/l	1 ml
	Water (Milli-Q)	1 l minus combined volume to be added after autoclaving	458.3 ml

Autoclave for 15 min at 120 °C. The base buffer should be autoclaved separately.

Cholesterol	Cholesterol	20 mg/ml in EtOH	15 ml
Amino acids	Essential amino acid stock solution	8 g/l L-arginine 10 g/l L-histidine 19 g/l L-lysine (HCl) 8 g/l L-methionine 13 g/l L-phenylalanine 20 g/l L-threonine 5 g/l L-tryptophan 28 g/l L-valin	121.02 ml
	Nonessential amino acid stock solution	35 g/l L-alanine 17 g/l L-asparagine 17 g/l L-aspartic acid 1 g/l L-cysteine HCl 25 g/l L-glutamine 32 g/l glycine 15 g/ L-prolin 19 g/l L-serine	121.02 ml

	Sodium glutamate stock solution	100 g/l sodium glutamate	30.26 ml
Vitamins	Vitamin stock solution	100x: 0.2 g/l thiamine (aneurin) 1.33 g/l riboflavin 1.6 g/l nicotinic acid 2.1 g/l Ca pantothenate 0.33 g/l pyridoxine (HCl) 0.026 g/l biotin	10 ml
Other nutrients	Sodium folate	100x: 2.9 g/l 125x: 6.25 g/l choline chloride 0.63 g/l myo-inositol 8.13 g/l inosine 7.5 g/l uridine	10 ml 24 ml
Preservatives	Propionic acid	100 ml/l propionic acid in dH_2O	6 ml
	Nipagin	100 g/l methyl-4-hydroxybenzoate in 70 % EtOH	15 ml

Unless otherwise stated, all ingredients were dissolved in dH_2O. All stock solutions, except the sterols and preservatives, were sterile filtrated. All stock solutions were stored at -20 °C until used. The essential and the nonessential amino acid stock solution were adjusted to pH 4.5. The base buffer was adjusted to pH = 4.0 and stored at 8 °C.

2.7.5 Optimized exom-matched holidic diet

The optimized exom-matched holidic diet is based on the exom-matched holidic diet from Piper *et al.*(252) with some modifications. The ingredients and stock solutions are listed in table 8.

Table 8: Components and stock solutions of the optimized exom-matched holidic diet.

	Ingredient	**Stock**	**Amount per liter**
Gelling agent	Agar		20 g

Base	Buffer	10x: 30 m/l glacial acetic acid 30 g/l KH_2PO_4 10 g/l $NaHCO_3$	100 ml
Sugar	Sucrose		17.2 g
Amino acids	L-isoleucine		1.11 g
	L-leucine		2.01 g
	L-tyrosine		0.66 g
Metal ions	$CaCl_2 \cdot 6H_2O$	1000x: 250 g/l	1 ml
	$CuSO_4 \cdot 5H_2O$	1000x: 2.5 g/l	1 ml
	$FeSO_4 \cdot 7H_2O$	1000x: 25 g/l	1 ml
	$MgSO_4$ (anhydrous)	1000x: 250 g/l	1 ml
	$MnCl_2 \cdot 4H_2O$	1000x: 1 g/l	1 ml
	$ZnSO_4 \cdot 7H_2O$	1000x: 25 g/l	1 ml
	Water (Milli-Q)	1 l minus combined volume to be added after autoclaving	564.56 ml

Autoclave for 15 min at 120 °C. The base buffer should be autoclaved separately.

Sterols	Cholesterol	20 mg/ml in EtOH	7.5 ml
	Ergosterol	80 mg/ml in chloroform	7.5 ml
Cobalamin		50 mg/l	1 ml
Cobalt		1 g/l	1 ml
Molybdenum	$Na_2MoO_4 \cdot 2H_2O$	100 mg/l	1 ml
Ribonucleotides			2 g
Amino acids	Essential amino acid stock solution	10 g/l L-arginine 4.5 g/l L-histidine 10 g/l L-lysine (HCl) 4.3 g/l L-methionine 6.5 g/l L-phenylalanine 10 g/l L-threonine 1.7 g/l L-tryptophan 11 g/l L-valin	121.02 ml

	Nonessential amino acid stock solution	13.2 g/l L-alanine 8.3 g/l L-asparagine 9.4 g/l L-aspartic acid 8.2 g/l L-glutamine 10.9 g/l glycine 9.1 g/ L-prolin 14 g/l L-serine	121.02 ml
	Cysteine stock solution	74 g/l L-cysteine	
	Sodium glutamate stock solution	100 g/l sodium glutamate	13.4 ml
Vitamins	Vitamin stock solution	125x: 0.1 g/l thiamine (aneurin) 0.05 g/l riboflavin 0.6 g/l nicotinic acid 0.775 g/l Ca pantothenate 0.125 g/l pyridoxine (HCl) 0.01 g/l biotin	21 ml
Other nutrients	Sodium folate	1000x: 0.5 g/l 125x: 6.25 g/l choline chloride 0.63 g/l myo-inositol 8.13 g/l inosine 7.5 g/l uridine	1 ml 8 ml
Preservatives	Propionic acid	100 ml/l propionic acid in dH_2O	6 ml
	Nipagin	100 g/l methyl-4-hydroxybenzoate in 70 % EtOH	15 ml

Unless otherwise stated, all ingredients were dissolved in dH_2O. All stock solutions, except the sterols and preservatives, were sterile filtrated. All stock solutions were stored at -20 °C until used. The essential and the nonessential amino acid stock solution were adjusted to pH 4.5. The base buffer was adjusted to pH = 4.0 and stored at 8 °C.

2.8 *Drosophila* lines

Table 9 shows all Drosophila melanogaster lines that were used for experimental approaches.

Table 9: Used fly lines.

Name	Genotype	Source
yw	y[1]w[1118]	Bloomington Stock Center: 6598
w^{1118}	w[1118]	Bloomington Stock Center: 5905
esg>GFP	y[1]w[1118];esg-Gal4,UAS-GFP/CyO	
NP1-Gal4	w[1118]; NP1-Gal4	gift from D. Ferrandon, Strasbourg
hsNP1-Gal4	w[1118]; NP1-Gal4; tub-Gal80ts	gift from D. Ferrandon, Strasbourg
su(H)GBE-Gal4	w[1118];su(H)GBE-Gal4/Cyo	gift from S. Hou, Maryland
Tor^{k17004}	y[1]w[67c23]; P{w[+mC]=lacW} Tor[k17004] /CyOP{w[+mC]=lacW}Tor[k1700/CyO	Bloomington Stock Center: 11218
UAS-upd3 RNAi	y[1]sc[*]v[1];P{y[+t7.7] v[+t1.8]=TRiP.HMS00646}attP2	Bloomington Stock Center: 32859
UAS-luc	+;; p{UAS-Luciferase at attp2}/p{UAS-Luciferase at attp2}	gift from M. Markstein, Massachusetts
UAS-mCD8 GFP	w[1118]; P{w[+mC]=20XUAS-IVS-mCD8::GFP}attP2	Bloomington Stock Center: 32194
UAS-Dome DN	w[1118]; UAS-domeΔcyt2.1/UAS-domeΔcyt2.1	gift from N. Perrimon, Boston
UAS-GFP-mcherry-atg8a	y[1] w[1118]; P{w[+mC]=UASp-GFP-mCherry-Atg8a}2	Bloomington Stock Center: 37749

4EBP::RFP	;;4EBP::RFP	gift from J. Kang-Min, Seoul
Stat-GFP	w[1118];;10x STAT-GFP	gift from E. Bach, New York
Upd3-GFP	w[1118]; upd3-Gal4; UAS-GFP	gift from N. Perrimon, Boston
4xTRE-dsRed	TRE-dsRed attP40	gift from D. Bohmann, Rochester
Vkg-GFP	;Vkg-GFP	gift from U. Theopold, Stockholm

2.9 Devices and equipment

Devices and equipment that were used in this study are listed in table 10.

Table 10: Devices and equipment.

Device/equipment	Source of supply
Stereo light microscope Leica S6 E	Leica Microsystems
Stereo light microscope WILD M5A	Wild Heerbrugg
Fluorescence microscope Axio Imager Z1	Carl Zeiss
ApoTome	Carl Zeiss
Axiocam MRm camera	Carl Zeiss
Omni Bead Ruptor 24	Omni International
Thermomixer comfort	Eppendorf
Centrifuge 54515 D and 5417 R	Eppendorf
Drosophila activity monitor 2	TriKinetics Inc. Waltham
Vortex Genie 2	Scientific Industries
StepOne Real Time PCR System	Thermofisher Scientific
PCR cycler	Sensoquest
DeNoxiv DS-11 spectrometer	Biolabproducts GmbH
Qubit 3	Thermofisher Scientific
Micoplate reader Synergy H1	BioTek Instruments GmbH
Mediaclave 9	Integra Biosciences AG

GeneAmp PCR system 9700	Thermofisher Scientific
Cleanbench Labguard ES ClassII	Nuaire
MiSeq	Illumina
HiSeq4000	Illumina
Drosophila culture vials (50 ml)	Nerbe plus
Drosophila culture vials (175 ml)	Greiner Bio One
Drosophila culture vial cellulose plugs (30 mm)	Nerbe plus
Drosophila culture vial foam plugs (55 mm)	VWR
Forceps Dumont No. 9	Biolabproducts GmbH
Microscope slides	Carl Roth
Cover slips	Carl Roth
Ceramic beads (2.6 mm – 2.8 mm)	Biolabproducts GmbH

2.10 Software

Software that were used for this study are listed in table 11.

Table 11: Software.

Software	Source of supply
AxioVisionSE64 Rel.4.9	Carl Zeiss
ImageJ (FIJI)	
GraphPad Prism 8.0	GraphPad software Inc.
CLC Genomics workbench 9 and 12	Qiagen
CLC Microbial Genomic module	Qiagen
StepOne	Thermofisher Scientific
R	
Qiime2	
DAM FileScan software	Trikinetics Inc

3 Methods

3.1 Culturing of *Drosophila melanogaster*

Drosophila stock flies were kept in a climate chamber with a 12 h : 12 h light-dark cycle at 18 °C (day) : 16 °C (night) and a humidity of 65 %. The stock flies were transferred to fresh vial every 3 weeks on standard culture medium. If not otherwise noted, experimental flies were kept in a climate chamber with 12 h : 12 h light-dark cycle at 25 ° C (light) : 20 °C (dark) and a humidity of 65 %.

3.2 Drosophila crosses

For crossings the Gal4/UAS system was applied. In general, virgin UAS responder females or Gal4 driver females were crossed to either male Gal4 or UAS lines, respectively. For control genotypes, the driver and responder lines were backcrossed to the proper genetic background. The parental generation was removed after egg deposition. F1 progenies were used for experiments 3 -5 days after eclosion.

3.3 Dechorionisation

150 ml 2 % agar-agar in dH_2O was cooked and mixed with 150 ml apple-juice. The apple-juice agar was poured into 90 mm plastic petri dishes. For egg collection, respective fly lines were transferred into 150 ml *Drosophila* culture vials and the culture vial was plugged with the petri dish containing the apple-juice agar. The culture vial was sealed with tape and the flies were allowed to lay eggs for a maximal time of 16 h at 25 °C. Afterwards, the flies were removed from the vials. The eggs were washed off with 1x PBS and collected in baze basket. The following steps were prepared under sterile conditions in a laminar flow cabinet. The eggs were dechorionized in 6 % sodiumhypochlorid (in dH_2O) for 2 min followed by several washing steps with70 % EtOH and double autoclaved water. The gaze with the sterile embryos were transferred into culture vials with sterile fly food.

3.4 Bacterial recolonization

A mixture of the following bacterial species, which were cultured as previously described (253) was used to reconstitute the natural microbiota: *Acetobacter pomorum* (OD_{600} = 0.7), *Lactobacillus brevis*^{EW} (OD_{600} = 8), *Lactobacilles plantarum*^{WJL} (OD_{600} = 6), *Enterococcus faecalis* (OD_{600} = 0.8), and *Commensalibacter intestini*^{A911T} (OD_{600} = 1.5) (kindly provided by Carlos Ribeiro, Lisbon, Portugal). To prepare the stock solution for recolonization, the following volumes of each liquid culture were combined in a 15 ml falcon tube: 2 ml of *A. pomorum*, 0.02 ml of *L. brevis*^{EW}, 0.25 ml of *L. plantarum*^{WJL}, 2 ml of *E. faecalis*, and 1 ml of *C. intestini*^{A911T}. The bacterial mixture was centrifuged three times at 3000 rpm for 15 min and repeatedly resuspended in sterile phosphate-buffered saline (PBS). Finally, the mixture was centrifuged at 3000 rpm for 15 min and resuspended in 25% glycerol prepared in sterile PBS. Aliquots of 500 µl were stored at −20°C. A volume of 50 µl of the bacterial mixture was added to the surface of control or high-fat media and allowed to settle for 1 h at room temperature under sterile conditions. Thereafter, 3–5-day-old GF flies were transferred to the corresponding media.

3.5 Immunohistochemistry

Intestines were dissected in sterile 1x PBS and were immediately fixed in 4 % paraformaldehyde for 1 h at room temperature. Afterwards, the intestines were washed 3 times with 0.1 % PBT for 10 min each and blocked with 5 % blocking solution for 1 h at room temperature. After blocking, the intestines were incubated with the primary antibodies in blocking solution at 8 °C overnight. The intestines were washed with 0.1 % PBT 3 times for 10 min each, followed by an incubation with the secondary antibodies in blocking solution at 8 °C overnight. The secondary antibodies were removed and the intestines were incubated in a DAPI solution (1:2000 in 0.1 % PBT) for 10 min followed by 3 washing steps with 0.1 % PBT. The intestines were mounted on a microscope slide in Mowiol. Images were taken by an epifluorescent microscope Axio Imager Z1. For Z-projections the ApoTome was used and the intestines were stacked in 2 µm slices.

3.6 Fluorescence quantification

Images of fluorescent samples were taken by using the epifluorescent microscope AxiImager Z1. The exposure time and the slice thickness was fixed for every experimental group. The

fluorescence of single cells was quantified by using ImageJ. The cell of interest was selected with the drawing tool and the area, integrated density and the mean grey value was measured. A region next to the cell of interest without fluorescence was set as background control. To calculate the total fluorescence of a cell, the following equation was used: CTCF (corrected total fluorescence) = integrated density – (area of selected cell • mean fluorescence of backround reading).

3.7 Bodipy staining

Intestines were dissected in sterile 1x PBS and were immediately fixed in 4 % paraformaldehyde for 30 min at room temperature. Afterwards, the intestines were incubated with BODIPY^{TM} 493/503 at a concentration of 1:1000 in 1xPBS for 30 min in darkness. Subsequently, the intestines were washed 3 times with 0.1 % PBT for 10 min each. The intestines were mounted on a microscope slide with Mowiol. Images were taken by an epifluorescent microscope Axio Imager Z1. The ApoTome was used for processing Z-projections.

3.8 Triacylglyceride content quantification

The triacylglyceride content of whole flies was assessed by using a coupled colorimetric assay. 5 female flies were used per replicate. The flies were transferred into 2 ml screwcap tubes, weighted and homogenized in 500 µl 0.05 % Tween-20 (in dH_2O) by using a bead mill homogenizer at 3.25 m/s for 2 min. The homogenates were incubated at 70 °C for 5 min, followed by 3 min of centrifugation at 1000 x g. 500 µl supernatant was removed and stored at -20 °C until measurement. A standard curve (glycerol triolaeate: 100 µg/50µl – 3.12 µg/50µl) and 50 µl of the respective sample supernatants were pipetted into wells of a 96-well plate. The absorbance was determined at 562 nm (T_0). Afterwards, 200 µl of a prewarmed (37 °C) Thermo Infinity triglyceride solution was added into each. The absorbance was measured at 540 nm by using a Microplate Reader Synergy H1.

3.9 Uric acid content and uricase activity quantification

The uric acid content and uricase activity was quantified by using the Amplex Red Uric Acid/Uricase kit according to the manufacturer's protocol. In brief, 5 flies were homogenized

in 100 mM Tris (pH = 7.5) and debris were removed by centrifugation for 2 min at 3000 x g. For uric acid content quantification, uric acid standards (0 – 100 µM) were prepared from a 5 mM stock diluted in 1x reaction buffer. For uricase activity measurements, uricase standards (0 – 100 mU/ml) were prepared from a 100 U/ml stock diluted in 1x reaction buffer. Reactions were performed in 100 µl volume at 37 °C for 30 min protected from light. 20 mM H_2O_2 diluted in 1x reaction buffer served as a positive control. The fluorescence was measured at 590 nm by using a Microplate Reader Synergy H1.

3.10 Protein content quantification

The protein content of whole flies was quantified by using the Pierce™ BCA Protein assay kit. 5 female flies were used per replicate. The flies were transferred into 2 ml screwcap tubes, weighted and homogenized in 500 µl 0.05 % Tween-20 (in dH_2O) by using a bead mill homogenizer at 3.25 m/s for 2 min. The homogenate was centrifuged at 1000 x g for 3 min to pellet the debris and 500 µl was removed and stored at -20 °C until measurement. The Pierce™ BCA protein assay kit was used for the quantification of total protein amount in the supernatant. The assay was performed according to the manufacturer's protocol for the microplate procedure.

3.11 Excretion assay

A small piece of fly food supplemented with Brilliant Blue FCF food dye added at a concentration of 1 % (wt/vol) was transferred to the bottom of a vial. A coverslip was placed in the middle of the vial to split it into two halves. Individual flies were trapped in one half, together with the piece of food, and the vial was sealed with a foam plug. Flies were incubated at 20 °C for 24 h and the numbers of fecal spots on the coverslips were counted manually.

3.12 Determination of intestinal transit time

Each well of a 24-well plate was loaded with a small piece fly food supplemented with Brilliant Blue FCF food dye added at concentration of 1 % (wt/vol). Individual flies were starved for 24 h, transferred to the wells, and monitored every 15 min for 3 h. The appearance of the first dyed fecal spot determined the time from food ingestion to egestion in each individual fly, which was referred to as the transit time.

3.13 Fecal transplantation

Recolonized esg>GFP flies aged 3–5 days were cultured on high-fat or control media for 7 days. Subsequently, the intestines of five flies were homogenized in 300 µl of MRS medium using a bead mill homogenizer at 3.25 m/s for 2 min. Intestinal debris was removed by centrifugation, the supernatant was mixed with 5% sucrose, and 200 µl of the mixture was applied to sterile filter paper. GF esg>GFP flies were allowed to feed on the filter paper for 24 h and then transferred to control media for 5 or 7 days. Esg^+ cells in the anterior midgut region were counted.

3.14 Smurf assay

Flies were fed on either CD, DR or PEM for 14 days. Dyed medium was prepared by using the respective diet with Brilliant Blue FCF added at concentration of 1 % (wt/vol). After the dietary treatment, the flies were transferred onto the dyed medium for 24 h. A fly was counted as "smurf" when the blue dye could be observed not only inside the intestinal tract but also in the body cavity.

3.15 Locomotor activity

The *Drosophila* activity monitor (DAM) was used to determine the locomotor activity. Individual male flies were placed in glass tubes of 5 mm inner diameter, filled with the corresponding fly food at one end and plugged with a cotton plug at the other end. The glass tubes were placed into the DAM in an incubator with a 12 h : 12 h light-dark cycle at 25 °C and a humidity of 65 %. The activity of the flies was summarized in 2 minute bins. For data analysis Excel software and the DAMFileScan software of TriKinetics was used. The total number of beam breaks over 24 h of every single fly was summarized in intervals of 30 min. For sleep analysis, a 5 min bin of inactivity was considered as sleep phase.

3.16 Lifespan assay

Cohorts of 20 female flies were transferred into *Drosophila* culture vials with the respective fly flood. The flies were kept in a 12 h : 12 h light-dark cycle at 25 °C (light) : 20 °C (dark) and a

humidity of 65 %. Living flies were counted and transferred to fresh food vials every 3 days. In case of high fat dieting, the assay was performed at 20 °C.

3.17 Luciferase assay

The luciferase assay was performed as previously described (254) with minor modifications . The intestines of five adult flies per replicate were collected in 150 µl of ONE-Glo Lysis Buffer and homogenized using a bead mill homogenizer for 2 min at 3.25 m/s. The homogenate was transferred to a new reaction tube and stored at −20°C until further processing. For luciferase measurement, samples were thawed on ice and 50 µl was transferred to a white flat-bottom 96-well plate, with at least one empty well between treatments to minimize signal spill over Samples were mixed with the same amount of substrate provided by the ONE-Glo Luciferase Assay System immediately before signal detection. Luciferase signals were detected using a Microplate Reader Synergy H1. A mock control was included on each plate to normalize treatments across plates.

3.18 Infection assay with *Serratia marcescens*

Cohorts of 10 female flies were transferred for 7 days onto either CD, DR or PEM diets. Afterwards, the flies were transferred into *Drosophila* culture vials with a 2 % agar-agar base. A strip of filter paper was soaked with *S. marcescens* OD = 1 (in 5 % sucrose solution) and were placed onto the agar-agar base. For the control group the filter paper was soaked with a 5 % sucrose solution. The flies were orally infected daily.

3.19 DSS treatment

Cohorts of 10 female flies were transferred for 7 days onto either CD, DR or PEM diets. For the memory effect experiment, the flies were transferred onto either CD or PEM diet for 7 days. Afterwards, the flies were refed for 7 days on CD. After the dietary intervention, the flies were transferred into *Drosophila* culture vials with a 2 % agar-agar base.

3.20 DNA extraction

DNA was extracted by using the MasterPure DNA Purification kit. Dissected intestines were homogenized in 250 µl cell lysis solution by using a bead mill homogenizer for 2 min at 3.25 m/s. Afterwards, 1 µl proteinase K were added to the sample followed by an incubation at 54 °C for 15 min. The sample was cooled down to 37 °C and 1 µl of RNase A (5 µg/µl) was added. The sample was incubated at 37 °C for 30 min. To precipitate DNA, 175 µl of the protein precipitation reagent was added to the sample. Subsequently, the sample was vortexed for 10 s followed by centrifugation for 10 min at 14.000 g. The supernatant was transferred to a new reaction tube and 500 µl isopropanol was added. The sample was inverted 30 times followed by centrifugation for 10 min at 14.000 g for pelletisation. The supernatant was removed, and the DNA pellet was washed twice with 70 % ethanol. The pellet was resuspended in 30 µl TE buffer and stored at -20 °C until use.

For 16S analysis, 16S rDNA was extracted by using the Qiagen DNeasy Blood and Tissue kit. Before dissection, the flies were drowned for 10 s in 70 % EtOH to remove bacterial contamination from the animal's surface. The dissected intestines were homogenized in 200 µl sterile 1xPBS using a bead mill homogenizer at 3.25 m/s for 2 min. Afterwards, 180 µl ELB containing 20 mg/ml lysozyme was added to the sample and incubated at 37 °C for 30 min. 200 µl ATL buffer and 20 µl proteinase K was added to the sample and incubated at 56 °C for 30 min. 200 µl 100 % EtOH was added and vortexed. The mixture was pipetted into a DNeasy Mini spin column and centrifuged at 10.000 g for 1 min. The flow through was discarded and 500 µl AW1 buffer was added to the spin column followed by centrifugation at 10.000 g for 1 min. The flow trough was discarded and 500 µl AW2 buffer was added to the spin column followed by a centrifugation step at 20.000 g for 3 min. The flow through was discarded and the spin column was placed in a sterile 1.5 ml reaction tube. The DNA was eluted by adding 200 µl AE buffer to the spin column, incubated for 1 min and centrifuged a 10.000 g for 1 min. The extracted DNA was stored at -20 °C until use.

3.21 RNA extraction

The intestines were dissected in cold PBS and transferred to 500 µl RNA Magic. The intestines were homogenized in a bead mill homogenizer for 2 min at 3.25 m/s. Afterwards, 200 µl chloroform was added to the sample. The sample was inverted 20 times and incubated on ice for 5 min followed by a centrifugation for 15 min at 12.000 g and 4 °C. The upper aqueous phase was transferred to a new reaction tube and an equal volume of 70 % ethanol was added.

The sample was loaded onto an Ambion PureLink RNA Mini kit column. Further extraction was done by following the Ambion PureLink RNA Mini kit manufacturer's protocol. The total RNA was eluted in 30 µl RNase-free water and stored at -80 °C until use.

3.22 cDNA synthesis

The following mix was used to bind the oligo dT primer to RNA:

0.5 µl oligo dT primer (10 pM)

0.5 µl dNTPs (10 mM)

x µl RNA

ad 6.5 µl RNase free water.

The mix was incubated at 65 °C for 5 min and for 1 min on ice. The synthesis was performed by adding the following reagents to the mix:

µl 5x SSIV buffer

0.5 µl DTT (0.1 M)

0.5 µl Ribolock RNase Inhibitor (10 U)

0.5 µl Superscript IV reverse transcriptase (100 U)

The reaction mix was incubated at 25 °C for 5 min, followed by an incubation at 55 °C for 20 min. The reaction was stopped by incubating the mix at 80 °C for 10 min.

3.23 Polymerase chain reaction (PCR)

The following reaction mix was used for PCR:

0.5 µl reverse primer (10 µM)

0.5 µl forward primer (10 µM)

0.5 µl dNTPs (10 mM)

2.5 µl 10x AV buffer

25 ng DNA

1 µl DreamTaq polymerase

ad 25 µl DNase free water

The following cycling conditions were used (annealing and elongation times were adjusted individually):

95 °C	1:00 min
95 °C	0:30 min
55 °C	0:30 min (25 cycles)
72 °C	1:00 min
72 °C	5 min

3.24 Quantitative real-time PCR

Isolated RNA was transcribed to cDNA (see chapter 3.22) for quantitative analysis of the relative transcript levels. The following reaction mix was used for qRT-PCR:

5 µl qPCRBIO SyGreen

0.5 µl forward primer (5 µM)

0.5 µl reverse primer (5 µM)

4 µl sample (5 ng/µl)

The reaction was pipetted into well of a 48-well plate. The plate was subsequently sealed with adhesive film. The following cycle conditions were used:

95 °C	10:00 min
95 °C	0:15 min
60 °C	0:15 min (40 cycles)
72 °C	0:30 min
95 °C	00:15 min
60 °C	01:00 min
95 °C	00:15 min

The relative differential expression was calculated by using the ΔΔCP equation, whereby each gene was normalized to the house keeping gene *rpl32*:

ΔCP = CP target gene – CP reference gene

$\Delta\Delta CP = \Delta CP \text{ treatment} - \Delta CP \text{ control}$

$\text{Ratio} = 2^{-\Delta\Delta CP}$

3.25 RNA-seq analysis

RNA-seq analysis was performed by using the Qiagen CLC Genomics Workbench 9. Adapter sequences were trimmed and reads were normalized and mapped to the BDGP6 reference database by the RNA-Seq analysis tool. Differential expression was calculated by using the Differential Expression for RNA-Seq tool.

3.26 16s analysis

16s analysis for the high fat diet experiment were performed as follows: The V3-V4 region of the 16S gene was amplified using the dual barcoded primers 341F and 806R. Each primer contained additional sequences for a 12-base Golay barcode, an Illumina adaptor, and a linker sequence. PCR was performed using Phusion Hot Start Flex 2× Master Mix in a GeneAmp PCR system 9700 and the following program: 98°C for 3 min, 30 cycles of 98°C for 20 s, 55°C for 30 s, and 72°C for 45 s, followed by 72°C for 10 min and then 4°C hold. PCR was checked by agarose gel electrophoresis. Normalization was performed using a SequalPrep Normalization Plate Kit following the manufacturer's instructions. Equal volumes of normalized amplicons were pooled and sequenced on an Illumina MiSeq (2 × 300 nt). MiSeq sequence data were analyzed using MacQIIME v1.9.1. Briefly, all sequencing reads were trimmed to retain only nucleotides with a Phred quality score of at least 20, and then paired-end assembled and mapped onto the different samples using the barcode information. Rarefaction was performed at 34,000 reads per sample to normalize all samples against the minimum shared read count and to account for differential sequencing depth. Sequences were assigned to operational taxonomic units (OTUs) using UCLUST and the Greengenes reference database (gg_13_8 release) with 97% identity. Representative OTUs were picked and assigned to a taxonomy using UCLUST and the Greengenes database. Quality filtering was performed by removing chimeric sequences using ChimeraSlayer and by removing singletons and sequences that failed to align with PyNAST. The reference phylogenetic tree was constructed using FastTree 2. Relative abundance was calculated by dividing the number of reads for an OTU by the total number of sequences in the sample. Unweighted Unifrac beta diversity was calculated and visualized by generating principal coordinate plots. Differentially abundant taxa

were assessed using the nonparametric t test. p values were adjusted for multiple testing using the FDR correction. LEfSe was performed by using an online tool available at "http://huttenhower.sph.harvard.edu/galaxy". LDA denotes taxa based on their contribution to the overall observed differences between groups. 16s analysis for the protein-energy malnutrition experiment was performed as follows: The V1-V2 region of the 16s gene was amplified according to Rausch *et al*., 2019 (240). Amplicons were sequenced using Illumina MiSeq (2 x 300 nt). 16s analysis was performed by using the Qiagen CLC Genomics Workbench 20 Microbial Genomic module. Illumina sequencing adapters were trimmed from pair-end reads. OUT clustering was based on the 97 % Greengenes reference database (gg_13_8 release) with a similarity score of 80 % and best match finding option, using following settings: chimera cross over costs 3, Kmer size 6, mismatch costs 1, minimum score 40, gap costs 4, maximum unaligned end mismatches 5.

3.27 Statistics

Statistical analysis was performed by using the Graph Pad Prism software 8.3.1. The data was tested for distribution by using the Shapiro-Wilk normality test. Parametric data was analyzed with unpaired students t-test and non-parametric data with Mann-Whitney test. Life span data was analyzed with Log rank Mantel-Cox test.

4 Results

4.1 Effects of high fat dieting on epithelia-microbe interactions in the intestine of *Drosophila*

The *Drosophila* intestine has direct contact with the nutritional content, but little is known how dietary lipids affect the intestinal homeostasis. For this reason, I investigated the effect of a short-term intervention of 20 % coconut fat-based high fat diet (HFD) on the *Drosophila* intestine compared to the control diet (CD).

4.1.1 High fat dieting leads to hyperproliferation in the *Drosophila* midgut

Intestinal stem cells (ISCs) and enteroblasts (EBs) are marked by the expression of escargot (esg). I used the escargot reporter line (esg>GFP) fly line, which expresses membrane-bound GFP in ISCs and EBs, in order to examine the influence of a HFD on the stem cell proliferation. After 3 days of high fat dieting, I observed an increased number of esg$^+$ cells in the anterior (Fig. 5, B) as well as in the posterior midgut (Fig. 5, B') compared to the CD (Fig. 5, A and A'). To reveal how long this hyperproliferation persists in the midgut I used the aforementioned

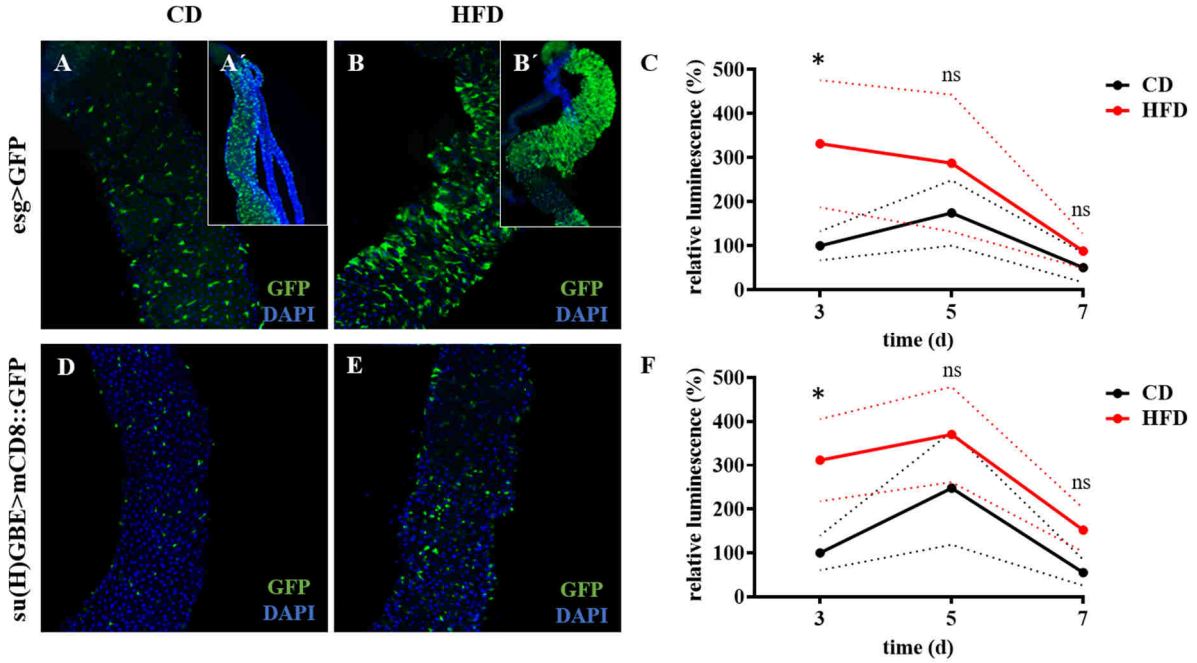

Fig. 5: High fat dieting leads to hyperproliferation of the *Drosophila* midgut. (A and B) esg>GFP flies fed for 3 days with HFD showed an increased number of esg$^+$ cells (GFP) compared to flies fed with CD. (A´ and B´) Representative images of esg$^+$ cells in the posterior midgut. (C) The amount of esg$^+$ cells was quantified in esg::GFP flies via co-expressed luciferase. The luminescence signal was significantly increased after 3 days of high fat dieting compared to flies fed with CD. (D and E) A higher number of EBs was observed in su(H)GBE>mCD8::GFP flies after 3 days of HFD feeding in comparison to flies fed a CD. (F) Expression of luciferase in EBs showed a significantly increased luminescence on day 3 in flies fed with HFD. HFD: high fat diet, CD: control diet, ISC: intestinal stem cell, EB: enteroblast, GFP: green fluorescent protein, esg: escargot, d: days, ns: not significant, *p < 0.05. n = 9-14.

esg>GFP fly lines with co-expressed luciferase, whereby the luciferase signal positively correlates with the number of ISCs and EBs. Flies fed with HFD showed a significant increase of ISCs and EBs on day 3 in comparison to flies fed a CD. No significant differences between flies fed the HFD and the CD could be observed on day 5 and 7 (Fig. 5, C). Specific expression of membrane-bound GFP in EBs by using the su(H)GBE-Gal4 driver revealed a higher number

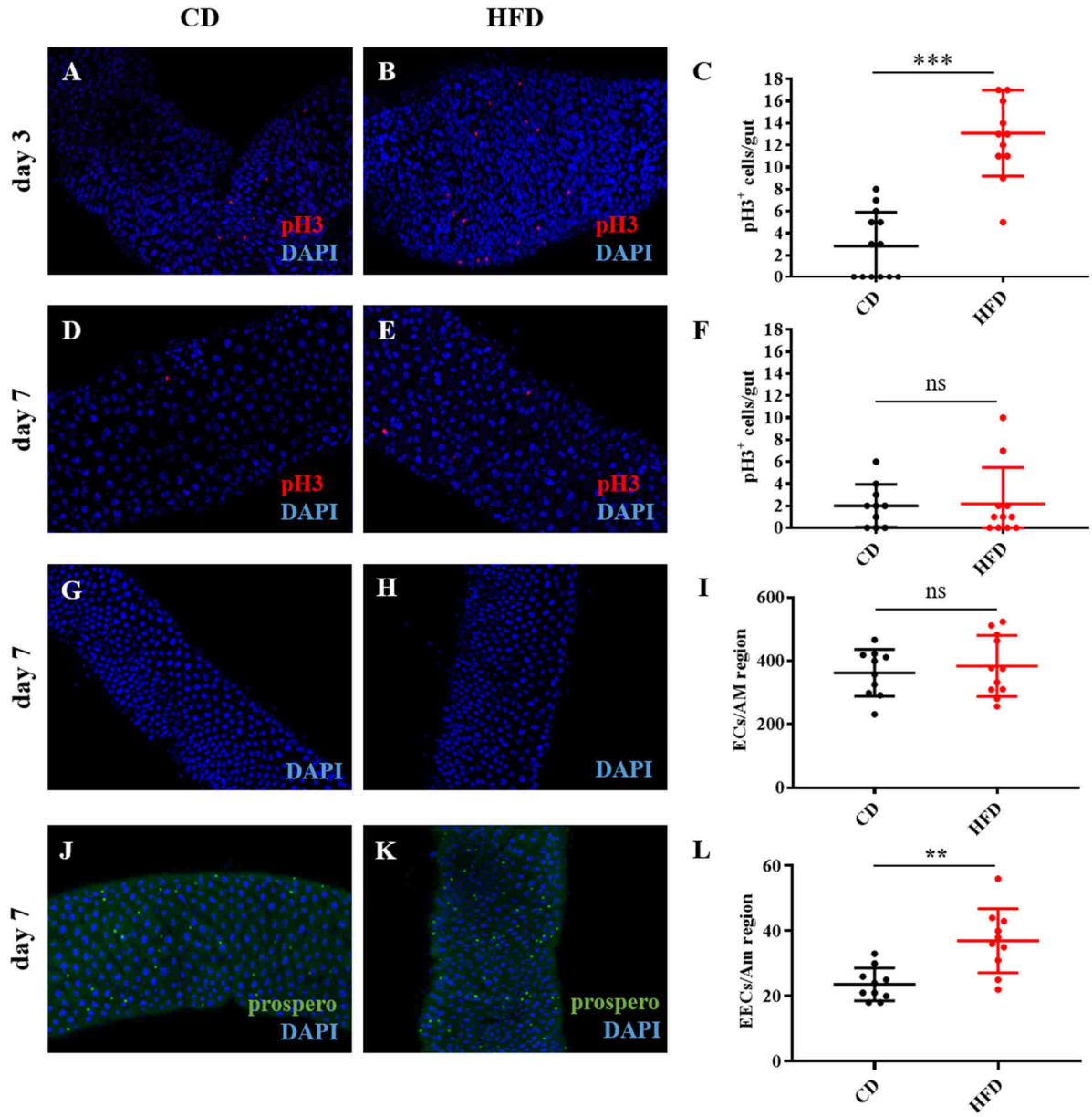

Fig. 6: **Impact of high fat dieting on the mitotic activity of intestinal stem cells and the intestinal cell composition.** (A-B) Representative images of anti-pH3 staining in the midgut of flies fed a HFD or CD for 3 days. (C) A significant increase of $pH3^+$ cells in the midgut was detectable after 3 days of high fat dieting compared to the corresponding control (n = 11-13). (D and E) Representative images of anti-pH3 staining of the midgut after a 7 days HFD or CD intervention. (F) Quantification of $pH3^+$ cells in the midgut of flies fed a HFD or CD for 7 days. (G-H) DAPI staining in the AM region of the intestines of flies after 7 days on a HFD or CD. Large, polyploid cells represent ECs. (I) No significant differences in the number of ECs were detected upon 7 days of high fat dieting in comparison to flies fed a CD (n = 10-11). (J-K) Representative images of anti-prospero staining, which specifically labels EECs, in the anterior midgut region of flies fed a HFD or CD for 7 days. (L) Quantitative analysis of the number of EECs of flies fed a HFD or CD (n = 10-11). HFD: high fat diet, CD: control diet, EC: enterocyte, EEC: enteroendocrine cell, pH3: phospho-histone 3, ns: not significant, $^{**}p < 0.01$, $^{***}p < 0.001$.

of EBs after 3 days on HFD in the anterior midgut (Fig. 5, E) compared to flies fed with CD (Fig. 5, D). Expression of luciferase in EBs led to a significant increased luminescence signal after 3 days of high fat dieting compared to the CD, whereas no differences could be detected on day 5 and day 7 (Fig. 5, F). The mitotic activity of ISCs was evaluated by using the phospho-histone 3 antibody (pH3), which specifically labels mitotic cells. The number of $pH3^+$ cells was increased after 3 days of HFD feeding (Fig. 6, B) in comparison to flies fed a CD (Fig. 6, A), which was further supported by a quantitative analysis of the number of $pH3^+$ cells of the complete midgut (Fig. 6, C). The number of $pH3^+$ declined after 7 days of high fat dieting (Fig. 6, E) and reached levels comparable to those of flies fed a CD (Fig. 6, D). The quantitative analysis of the number of $pH3^+$ cells of complete midguts after 7 days of high fat dieting revealed no significant differences compared to control dieting (Fig. 6, F), which correlates with the temporal pattern of the proliferation of esg^+ cells. To examine the effect of a HFD on the cellular composition, the number of enterocytes (ECs) and enteroendocrine cells (EECs) was counted, which are both descendants of EBs. A HFD intervention of 7 days had no effect on the number of enterocytes (Fig. 6, H) compared to flies fed a CD (Fig. 6, G). The number of enterocytes was evaluated by counting large polyploid DAPI-stained nuclei in the anterior midgut (Fig. 6, I). The effect of a HFD on the number of EECs was investigated by using an anti-prospero antibody, which specifically labels the EECs. In comparison to flies fed a CD for 7 days (Fig. 6, J and L), the number of EECs in the anterior midgut was increased in flies fed a HFD (Fig. 6, K and L).

4.1.2 **High fat dieting does not block differentiation of progenitor cells**

To further monitor the intestinal cell turnover upon high fat dieting, I used the ReDDM (repressible dual differential stability cell marker) tracing method (220). The ReDDM system combines the expression of the fluorescent proteins mCD8::GFP and H2B::RFP, which have short and long half-lives, respectively. The expression of these fluorescent proteins is under the control of an ubiquitous temperature-sensitive Gal4 repressor and a Gal4-promotor of choice. By using an esg-Gal4 driver, mCD8::GFP is expressed in progenitor cells (ISCs and EBs) but is not sustained in newly differentiated ECs and EECs. The stable H2B::RFP persist for several weeks and marks renewed ECs and EECs. Therefore, it is possible to evaluate a potential block of differentiation of progenitor cells. ReDMM flies fed a HFD for 3 days showed an increased number of marked progenitor cells (Fig. 7, A) compared to ReDMM flies fed a CD (Fig. 7, B). After 7 days of high fat dieting (Fig. 7, D), the number of marked progenitor cells was

comparable to that of flies fed a CD (Fig. 7, C). The quantitative analysis also revealed a significant increase of progenitor cells after 3 days of high fat dieting compared to the proper control, whereas no differences between the dietary interventions were detectable on day 7 (Fig. 7, E). The number of newly differentiated ECs and EECs, which are only marked by H2B:RFP, was not affected by a HFD on day 3 (Fig. 7, B) compared to flies fed a CD (Fig. 7, A). However, the number of renewed cells was increased in flies fed a HFD (Fig. 7, D) in comparison to control dieting flies (Fig. 7, C). The quantitative analysis showed a significant increase of newly differentiated cells after 7 days of high fat dieting and therefore an accelerated intestinal cell turnover, compared to flies fed a CD (Fig. 7, F).

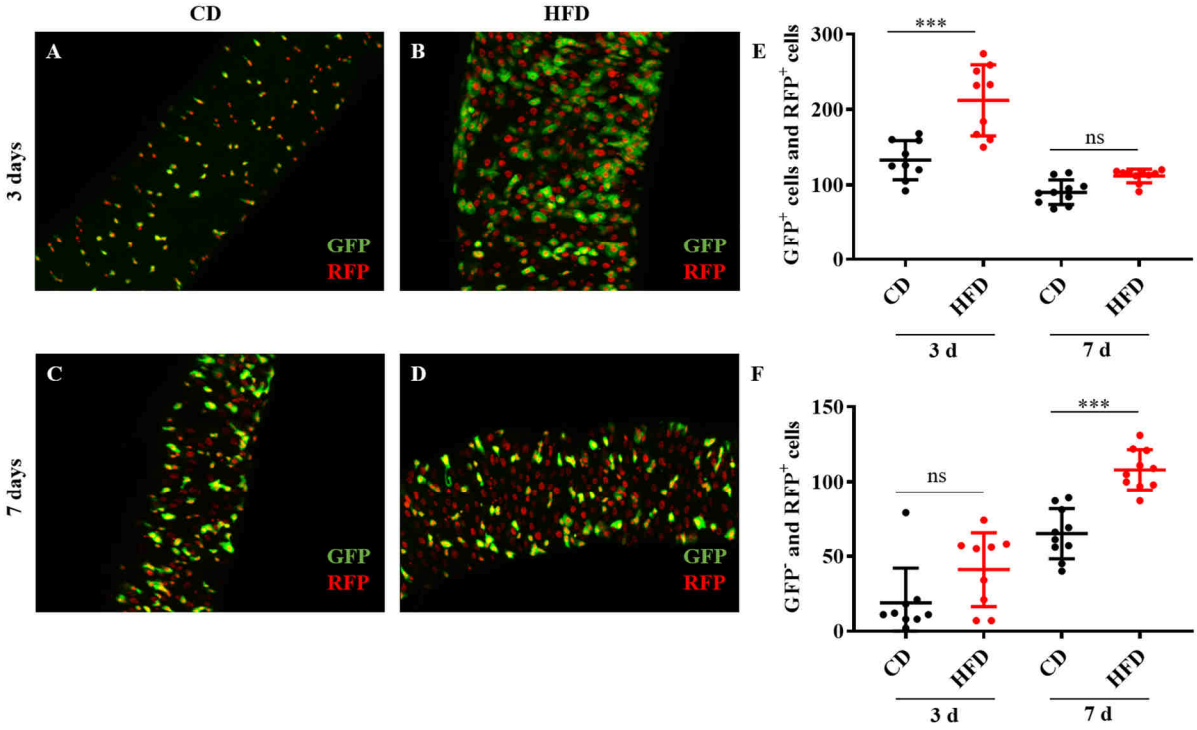

Fig. 7: High fat dieting lead to an accelerated turnover of intestinal cells and do not block differentiation. (A-B) The ReDMM tracing method was combined with an esg-Gal4 driver. Progenitor cells (ISCs and EBs) are marked with mCD8::GFP (GFP) and H2B::RFP (RFP), whereas renewed cells (ECs and EECs) are exclusively marked by H2B::RFP. The number of progenitor cells was increased after 3 days of high fat dieting compared to flies fed a CD. The number of newly differentiated cells was not affected. (C-D) The number of renewed cells was increased in flies fed a HFD after 7 days in comparison to control dieting flies. No differences in the number of progenitor cells was detectable between flies fed a HFD or CD. (E) Quantitative analysis of progenitor cells after 3 days and 7 days of high fat dieting compared to flies fed a CD (n = 9-10). (F) The quantitative analysis of newly differentiated cells in flies fed a HFD after 3 days and 7 days in comparison to control dieting flies (n = 9-10). HFD: high fat diet, CD: control diet, ISC: intestinal stem cell, EC: enterocyte, EEC: enteroendocrine cell, GFP: green fluorescent protein, RFP: red fluorescent protein, ReDMM: repressible dual differential stability cell marker, esg: escargot, ns: not significant, ***p < 0.001

4.1.3 Specific triglycerides phenocopy the HFD induced hyperproliferation

Coconut fat has a high content of saturated fatty acids (92 %) and consists mainly of medium-chain and long-chain triglycerides. The most abundant saturated fatty acids in coconut fat are

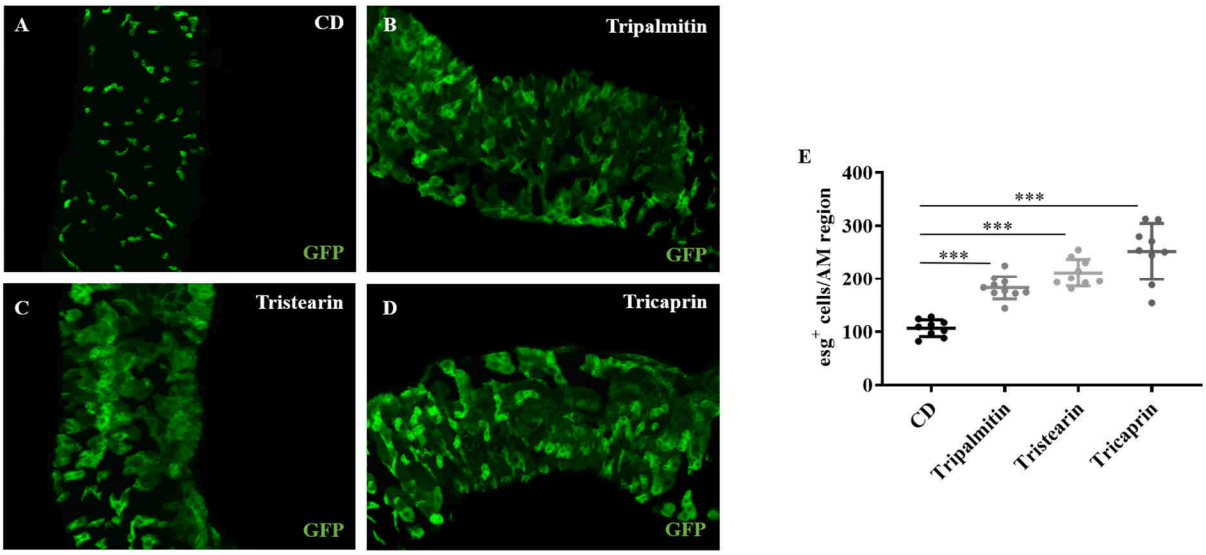

Fig. 8: Single triglycerides lead to hyperproliferation in the *Drosophila* intestine. (A-D) Esg>GFP flies were fed with a CD supplemented with 20 % tripalmitin, tristearin or tricaprin. A higher number of esg$^+$ cells (GFP) was observed in flies fed a tripalmitin-, tristearin- or tricaprin-based diet in comparison to flies fed a CD. (E) The quantitative analysis revealed a significant increase of esg$^+$ cells in the anterior midgut region of esg>GFP flies fed a triglyceride-supplemented diet compared to flies fed a CD (n = 9 -10). HFD: high fat diet, CD: control diet, GFP: green fluorescent protein, esg: escargot, AM: anterior midgut, ***p < 0.001.

lauric acid (47 %, 12 carbon atom chain), myristic acid (16.5 %, 14 carbon atom chain), caprylic acid (9 %, 8 carbon atom chain), palmitic acid (7.5 %, 16 carbon atom chain) and capric acid (7 %, 10 carbon atom chain (255). To examine if even single triglycerides can phenocopy the intestinal response observed in flies fed a 20 % coconut fat-based diet, I supplemented the CD with purified medium-chain or long-chain triglycerides. The following triglycerides were used with a concentration of 20 %: tripalmitin (16 carbon atom chain), tristearin (18 carbon atom chain) and tricaprin (10 carbon atom chain). Esg>GFP flies fed a tripalmitin-based diet (Fig. 8, B), a tristearin-based diet (Fig. 8, C) or a tricaprin-based diet (Fig. 8, D) showed a highly increased number of esg$^+$ cells compared to flies fed a CD (Fig. 8, A). The quantitative analysis revealed a significant increase of esg$^+$ cells in the anterior midgut region in flies fed a tripalmitin-, tristearin- or tricaprin-based diet in comparison to control dieting flies (Fig. 8, E). To evaluate the mitotic activity of ISCs upon feeding a triglyceride-supplemented diet, the intestines were stained with an anti-pH3 antibody. The number of pH3$^+$ cells was increased in flies fed a tripalmitin-based diet (Fig. 9, B), a tristearin-based diet (Fig. 9, C) or a tricaprin-based diet (Fig. 9, D) compared to flies fed a CD (Fig. 9, A). The quantitative analysis of pH3$^+$ in complete intestines revealed a significant increase of mitotically active cells upon feeding a diet supplemented with either tripalmitin, tristearin or tricaprin compared to control dieting flies (Fig. 9, E).

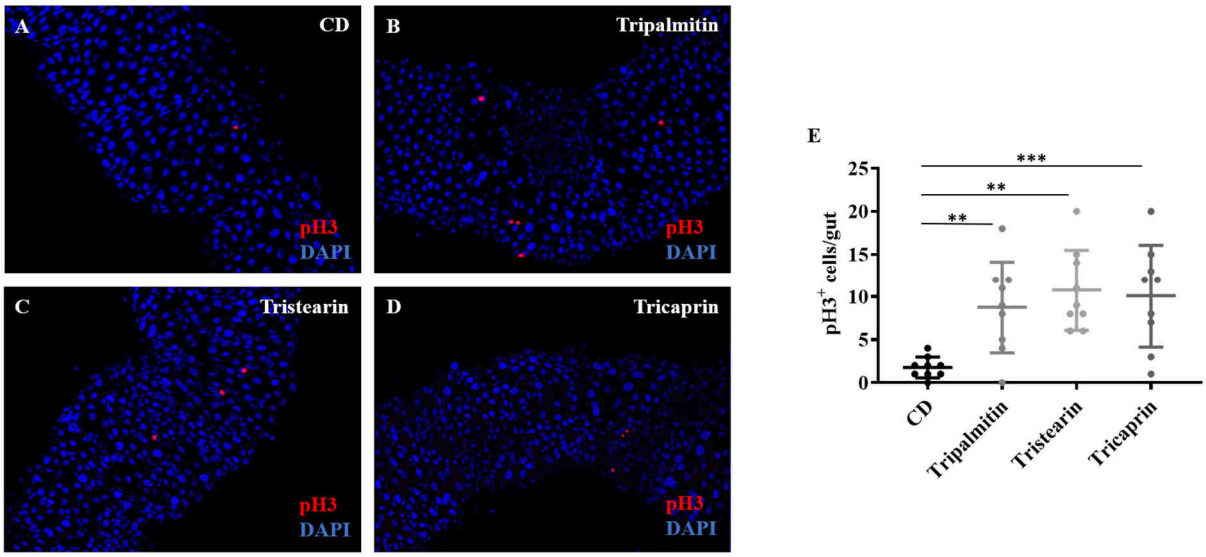

Fig. 9: A triglyceride-based diet leads an increased number of mitotically active ISCs in the fly's intestine. (A-D) Representative images of intestines of flies stained with an anti-pH3 (pH3) antibody after feeding on a tripalmitin-, tristearin-, or tricaprin-supplemented diet. The number of $pH3^+$ cells was increased in flies fed a triglyceride-based diet compared to flies fed a CD. (E) Quantitative analysis of the number of $pH3^+$ in complete intestines of flies upon feeding a triglyceride-based diet in comparison to control dieting flies (n = 9). HFD: high fat diet, CD: control diet, ISC: intestinal stem cell, pH3: phosphor-histone H3, **p < 0.01, ***p < 0.001.

4.1.4 JNK signaling is activated upon high fat dieting

The JNK (c-Jun NH_2-terminal kinase) signaling pathway is a major regulator that promotes cellular stress tolerance and is activated by a variety of environmental stressors (256) in the fly's intestine. To examine whether high fat dieting activates JNK signaling, I checked JNK phosphorylation by a specific anti-phospho-JNK antibody (pJNK). Flies fed a HFD showed an

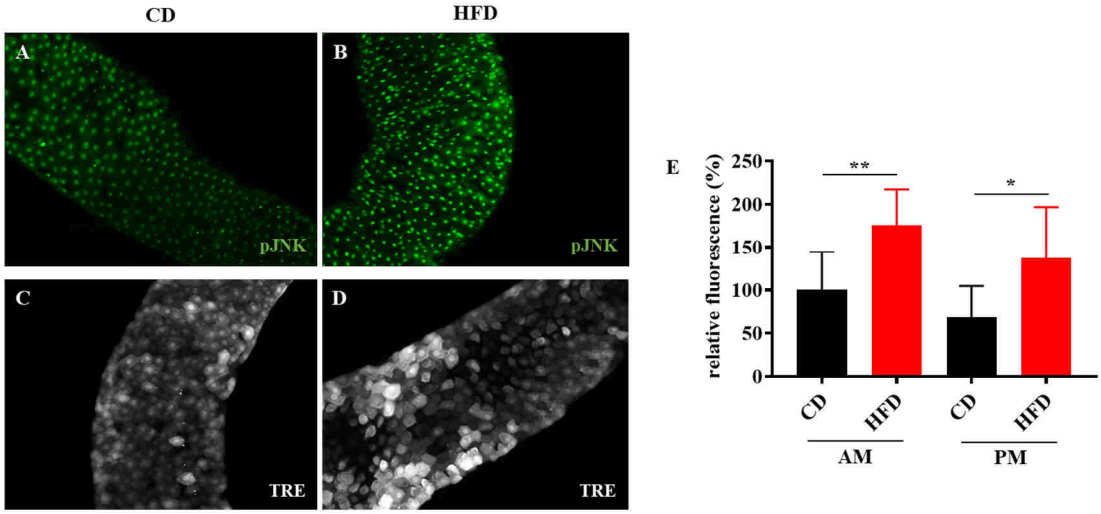

Fig. 10: High fat dieting induces JNK activation. (A-B) Staining with an anti-pJNK antibody in the anterior midgut of flies fed a HFD or a CD. HFD feeding leads to an increased pJNK fluorescence signal compared to flies fed a CD. (C-D) Representative images of the anterior midgut of the JNK reporter line 4xTRE-dsRed (E) Fluorescence quantification in the anterior midgut and posterior midgut of 4xTRE-dsRed flies after high fat dieting or control dieting (n = 8-10). HFD: high fat diet, CD: control diet, AM: anterior midgut, PM: posterior midgut, pJNK: phospho-JNK, ns: not significant, *p < 0.05, **p < 0.01.

increased level of pJNK (Fig. 10, B) in the antior midgut compared to CD fed flies (Fig. 10, A), which corresponds to activated JNK. To further support an activation of the JNK signaling pathway in the fly's intestine upon high fat dieting I used the JNK reporter line 4xTRE-dsRed (257). TREs (tetradecanoylphorbol) are binding sites for the AP-1 transcription factor c-Jun, which is regulated by JNK phosphorylation. High fat dieting leads to an increased TRE-dsRed fluorescence signal in the anterior midgut in comparison to flies fed a CD (Fig. 10, C-D). Quantification of the TRE-dsRed fluorescence revealed a significantly increased fluorescence in the anterior as well as in the posterior midgut compared to CD fed flies (Fig. 10, E).

4.1.5 High fat dieting induces upd3 signaling

The cytokine upd3 (unpaired 3) is a major target of the JNK pathway in ECs and is linked to activation of ISCs through paracrine signaling (229). Therefore, I used an upd3-GFP reporter line to study the effects of a HFD on upd3 signaling. The expression of upd3 was highly increased in flies fed a HFD (Fig. 11, B) compared to flies fed a CD (Fig. 11, A). qRT-PCR revealed that the relative transcript levels were significantly increased upon high fat dieting (Fig. 11, C). To evaluate, if the elevated upd3 expression in HFD fed flies is linked to the

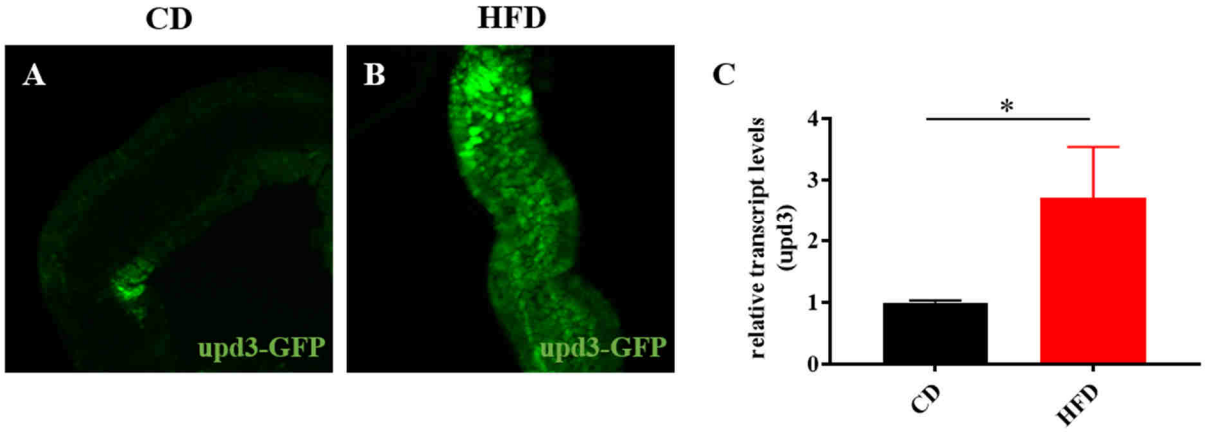

Fig. 11: Upd3 expression is increased upon high fat dieting. (A and B) A upd3-GFP reporter was used to monitor upd3 expression in the anterior midgut of flies fed a CD or a HFD. Flies fed a HFD showed an increased fluorescence signal compared to flies fed a CD. (C) qRT-PCR analysis revealed that HFD feeding lead to a significant increased relative level of upd3 in the intestine compared to flies fed a CD (n = 5). HFD: high fat diet, CD: control diet, GFP: green fluorescent protein, upd3: unpaired 3, *$p < 0.05$.

observed increase in mitotic activity in ISCs, I expressed upd3 RNAi in ECs. A lower number of $pH3^+$ was detectable in flies expressing upd3-RNAi in ECs (NP1>upd3 RNAi; Fig. 12, C) in comparison to the genotype controls (NP1>+, upd3 RNAi>+; Fig. 12, A and B) upon high fat dieting. This was further supported by the quantitative analysis of the number of $pH3^+$ cells

in the whole intestine. No significant differences were observed between the genotypes, which were fed a CD (Fig. 12, D).

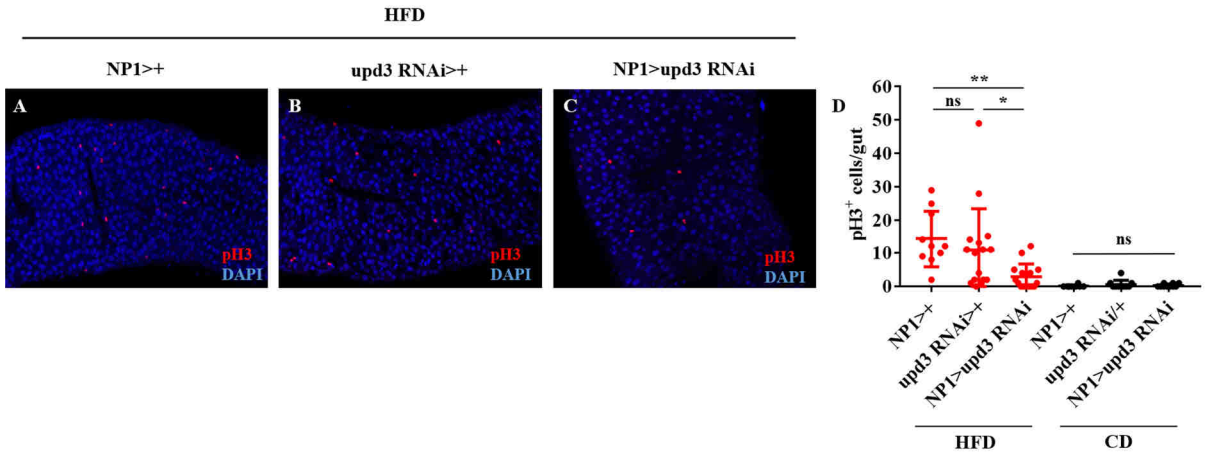

Fig. 12: HFD-induced mitotic activity in ISCs depends on upd3 expression in ECs. (A-C) Flies, which expressed upd3 RNAi in ECs (NP1>upd3 RNAi) were subjected to a HFD as well as the two genetic controls (NP1>+, upd3 RNAi>+). The number of pH3$^+$ cells in NP1>upd3 RNAi flies was lower compared to the genetic controls. (D) Quantitative analysis of the number of pH3$^+$ cells in the intestine. A significant lower number of pH3$^+$ cells was detectable in NP1>upd3 RNAi flies fed a HFD in comparison to the genetic controls on the same diet. No significant differences between the genotypes were observed in flies fed a CD (n = 8-16). HFD: high fat diet, CD: control diet, pH3: phospho-histone 3, upd3: unpaired 3, ns: not significant, *p < 0.05, **p < 0.01.

4.1.6 High fat diet response requires JAK/STAT signaling in progenitor cells

It is well known that the expression of upd3 in ECs triggers the proliferation of ISCs (229,258). In order to reveal activated JAK/STAT signaling as a response to HFD in the fly's intestine, I used a STAT-reporter (10xstat-GFP,259). Flies showed an increased fluorescence signal in progenitor cells upon high fat dieting (Fig. 13, B), whereas the signal in flies fed a CD was low (Fig. 13, A). Quantitative analysis of the fluorescence signal in the anterior midgut revealed a significantly stronger fluorescence signal in flies fed a HFD in comparison to corresponding control (Fig. 13, C). To confirm that JAK/STAT signaling in progenitor cells is required for the increased proliferation in flies fed a HFD, I ectopically overexpressed a dominant-negative

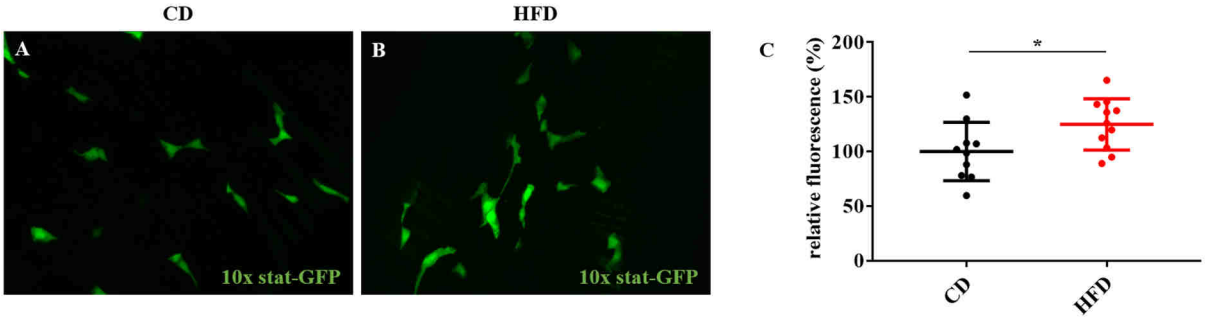

Fig. 13: High fat dieting leads to an increased STAT signaling in progenitor cells. (A-B) By using a STAT-reporter (10x stat-GFP), GFP was expressed in progenitor cells in the intestine. The fluorescence signal in progenitor cells was stronger in flies fed a HFD in comparison to CD fed flies. (C) Quantitative analysis of the relative fluorescence of 10x stat-GFP cells in the *Drosophila* intestine of flies fed a HFD or CD (n = 10-11). HFD: high fat diet, CD: control diet, *p < 0.05.

isoform of the JAK/STAT receptor domeless in progenitor cells (esg-GFP,Gal80>dome DN). In these animals, the number of pH3$^+$ cells was similar in HFD fed flies (Fig. 14, B) and in CD fed flies (Fig. 14, A). The quantitative analysis showed no significant increase in the number of pH3$^+$ upon high fat dieting compared the corresponding control (Fig. 14, C). This lack of response was also detectable, when esg$^+$ cells were analyzed (Fig. 14, D and E). No differences in the number of esg$^+$ cells were detectable in esg>dome DN flies fed a HFD or a CD (Fig. 14, F).

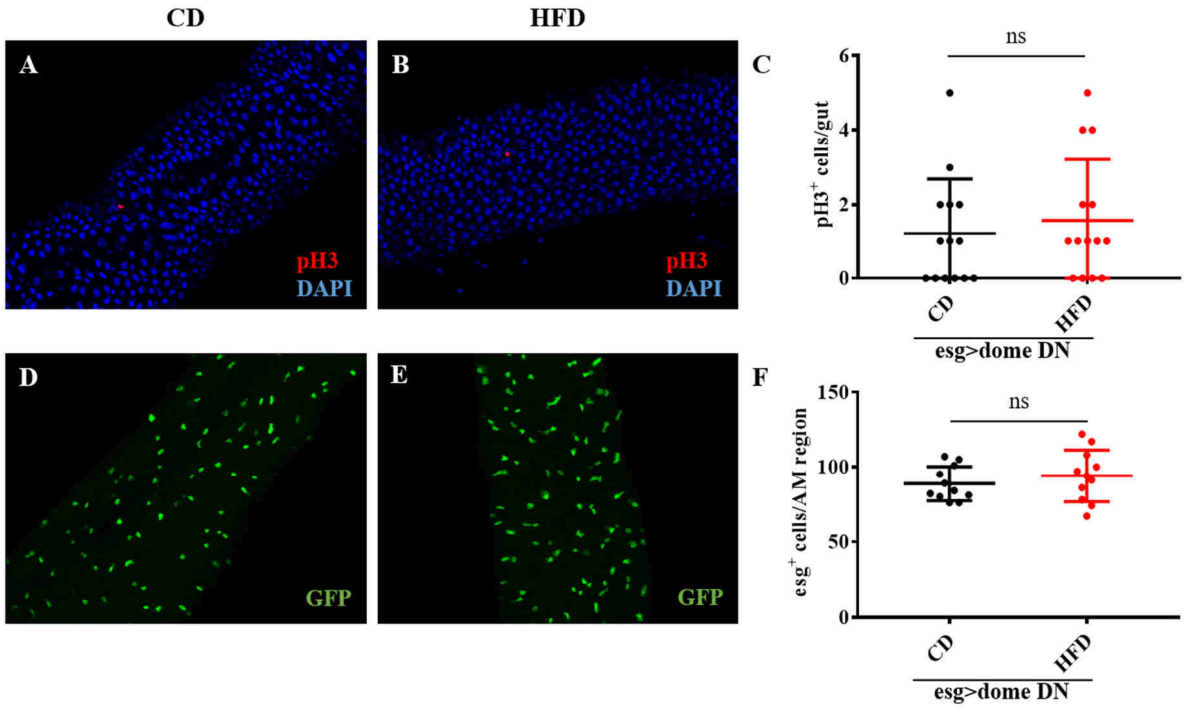

Fig. 14: The domeless receptor is required for the HFD mediated hyperproliferation in progenitor cells. (A-B) Representative images of an anti-pH3 staining in flies expressing a dominant-negative isoform of the domeless receptor (esg>dome DN) in progenitor cell. (C) Quantification of pH3$^+$ cells in the midgut of esg>dome DN flies fed a HFD or CD (n = 14). (D and E) The number of esg$^+$ cells in esg>dome DN flies fed a HFD was similar to flies fed a CD. (F) No significant differences in the number of esg$^+$ cells (GFP) were observed in esg>dome DN flies upon high fat dieting compared to the corresponding control (n = 10-11). HFD: high fat diet, CD: control diet, pH3: phospho-histone 3, esg: escargot, GFP: green fluorescent protein, esg: escargot, ns: not significant.

4.1.7 The high fat diet induced proliferation is microbiota dependent

It is well known, that dietary interventions can affect the intestinal microbiota. Therefore, I investigated the effect of the indigenous microbiota on the proliferation of ISCs in *Drosophila* by comparing germ-free (GF) flies to those that had been recolonized (RC) with a defined bacterial mix. To standardize all the experiments, all flies that were used in the following experiments were made GF by dechorionisation. Afterwards, the adult flies were recolonized with a bacterial mix, which comprised 5 different commensal bacterial species of *Drosophila melanogaster*: *Lactobacillus plantarum*, *Lactobacillus brevis*, *Acetobacter pomorum*,

Commensalibacter intestini and *Escherichia faecium*. As shown in chapter 4.1.1, high fat dieting leads to a significant increased number of esg$^+$ cells in the anterior midgut region of the intestine of RC esg>GFP flies (Fig. 15, A and F) compared to the CD fed control (Fig. 15, B and F). Interestingly, the HFD induced proliferation of esg$^+$ cells was not detectable in GF flies fed a HFD (Fig. 15, D) where the number of esg$^+$ cells was significantly decreased compared to RC flies upon high fat dieting (Fig. 15, F). Moreover, there were only a few esg$^+$ cells in GF flies fed a CD (Fig. 15, C) and the number of these cells was significantly decreased compared to RC flies on the same diet (Fig. 15, F).

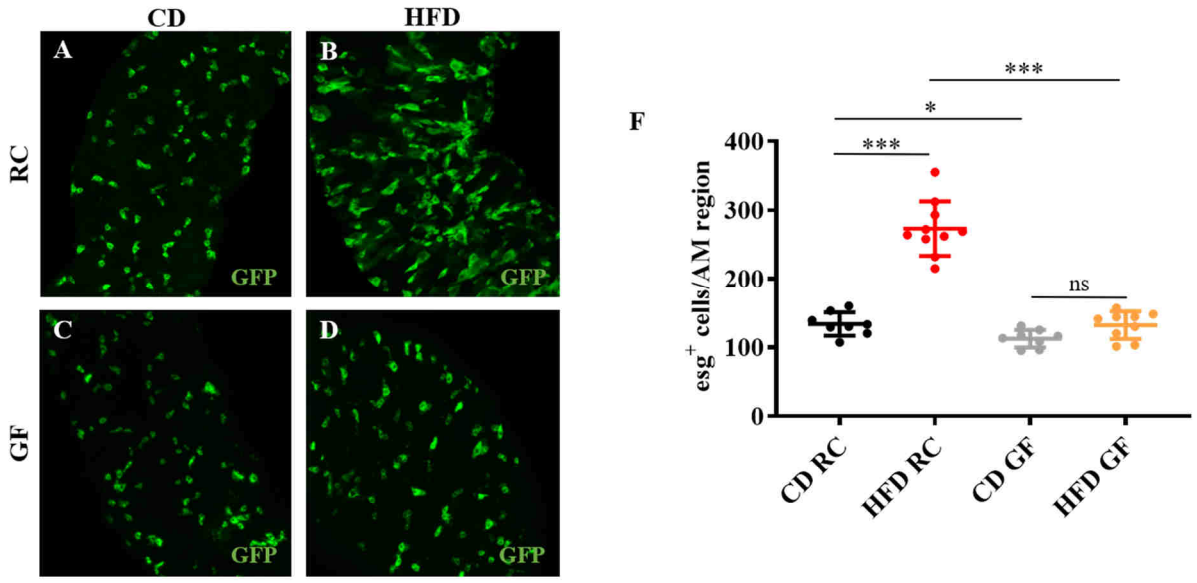

Fig. 15: HFD induced cell proliferation is dependent on the intestinal microbiota. (A-B) RC esg>GFP flies fed a high at diet showed an increased number of esg$^+$ cells (GFP) compared to RC flies fed a CD. (C-D) The HFD-triggered proliferation is not detectable in GF flies and the number of esg$^+$ cells is comparable to GF flies fed a CD (F) Quantitative analysis of esg$^+$ cells in the anterior midgut region of RC and GF upon high fat dieting or control dieting (n = 8-10). HFD: high fat diet, CD: control diet, RC: recolonized, GF: germ-free, GFP: green fluorescent protein, AM: anterior midgut, esg: escargot, ns: not significant, *p < 0.05, **p < 0.01, ***p < 0.001.

4.1.8 High fat diet associated upd3 signaling depends on the microbiota

As the HFD triggered cell proliferation in the intestine is highly microbiota dependent, I investigated if this lack of induction is also associated with upd3 signaling in ECs. Therefore, I used the upd3>GFP reporter line to study the compare the effects of a HFD in RC and GF animals. High fat dieting induced upd3 signaling in ECs in the intestine of RC flies (Fig. 16, A) compared to RC flies fed a CD (Fig. 16, B). The upd3 signal was low in GF fed a CD (Fig. 16, C). Interestingly, the HFD triggered upd3 signaling response was absent in GF flies upon high fat dieting (Fig. 16, D). This lack of response was also detectable by measuring the transcript levels of upd3 by using qRT-PCR. The transcript levels of upd3 in the intestine of GF flies fed a HFD were significantly lower compared to HFD fed flies, which harbors a

functional microbiota. Moreover, the upd3 transcript levels of GF flies fed a CD was even lower than the upd3 transcript levels of RC flies fed the similar diet (Fig. 16, E).

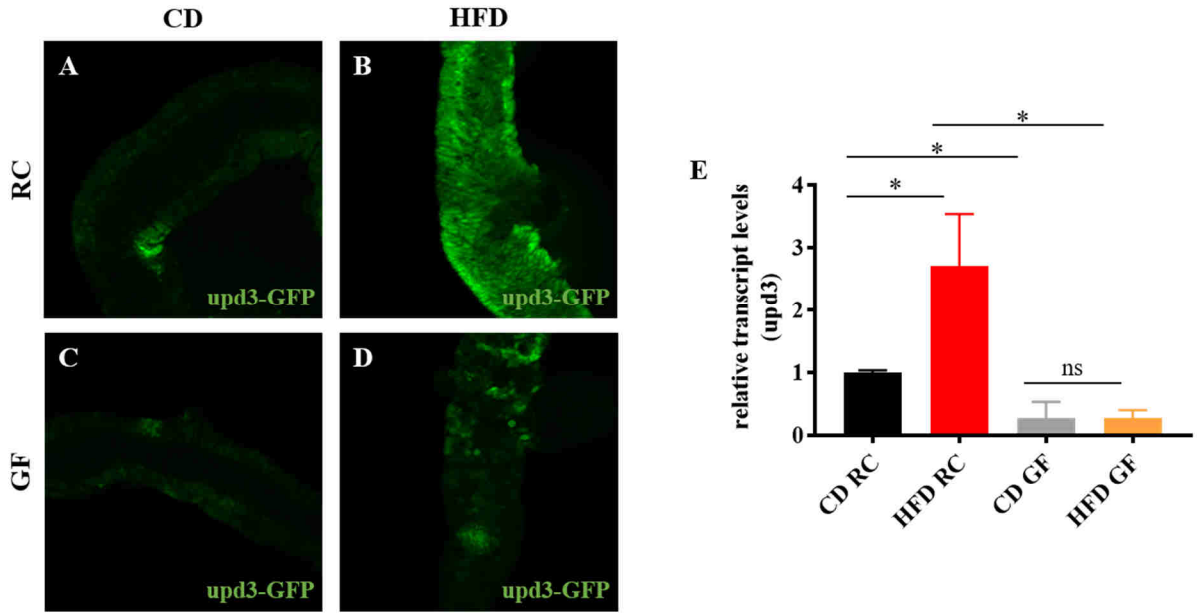

Fig. 16: HFD triggered upd3 signaling is absent in GF flies. (A-B) The upd3 expression in the anterior midgut of RC flies fed a CD or a HFD was examined by using a upd3-GFP reporter. RC flies fed a HFD showed an increased fluorescence signal compared to RC flies fed a CD. (C-D) The expression of upd3 in intestines of GF flies was low upon control dieting or high fat dieting. (E) qRT-PCR analysis of the upd3 transcript levels in the intestine in RC and GF flies fed a CD or HFD (n = 5). HFD: high fat diet, CD: control diet, RC: recolonized, GF: germ-free, upd3: unpaired-3, ns: not significant, *p < 0.05.

4.1.9 High fat dieting affects the intestinal microbial composition

To examine the effect of high fat dieting on the intestinal microbiota, I compared the microbial composition between flies fed a HFD and those fed a CD. High fat dieting lead to an altered microbial composition compared to flies fed a CD. The most abundant phyla on both diets were *Actinobacteria*, *Firmicutes*, *Bacteriodetes*, *Cyanobacteria*, and *Proteobacteria* (Fig. 17, A). The altered microbial community was also illustrated by the separation in beta diversity, which was evaluated by a principal coordinate analysis (PCoA) based on unweighted UNIFRAC. Each data point represents a single biological replicate (Fig. 17, B). Linear discriminant analysis effect size (LEfSe) revealed an enrichment of the order *Caulobacterales* with the family member *Caulobacteraceae*, *Enterobacteriales* and *Enterobacteriaceae*. *Caulobacterales* belong to the class of alpha-proteobacteria, whereas *Enterobacteriales* belongs to gamma-proteobacteria. High fat dieting also leads to an enrichment of 2 unknown species, which could not be identified by the Greengenes reference database. *Lactobacillacea* and the genus *Pedicoccus* where significantly enriched in flies fed a CD, which belong to the firmicutes phylum (Fig. 17, C).

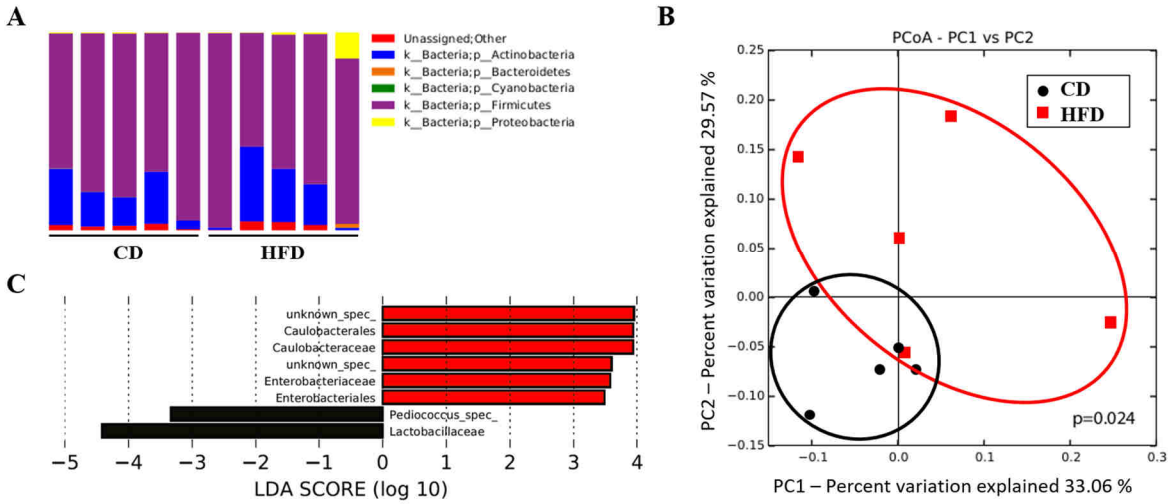

Fig. 17: High fat dieting alters the intestinal microbial composition in flies. (A) Abundance table of the microbial composition of flies fed a CD or HFD (n = 5). (B) Principal coordinate analysis revealed a significant shift in the microbial community upon high fat dieting compared to flies fed a CD (n = 5). (C) A linear discriminant analysis effect size showed significant enrichments of different bacterial orders, phyla or genera (n = 5). CD: control diet, HFD: high fat diet, PCoA: principal coordinate analysis.

4.1.10 **Altered microbial composition do not affect cell proliferation**

To examine if the altered microbiota is responsible for the observed increased cell proliferation observed in chapter 4.1.1, I performed a fecal transplantation experiment. Therefore, GF esg>GFP flies were recolonized with either the CD associated or with the HFD associated

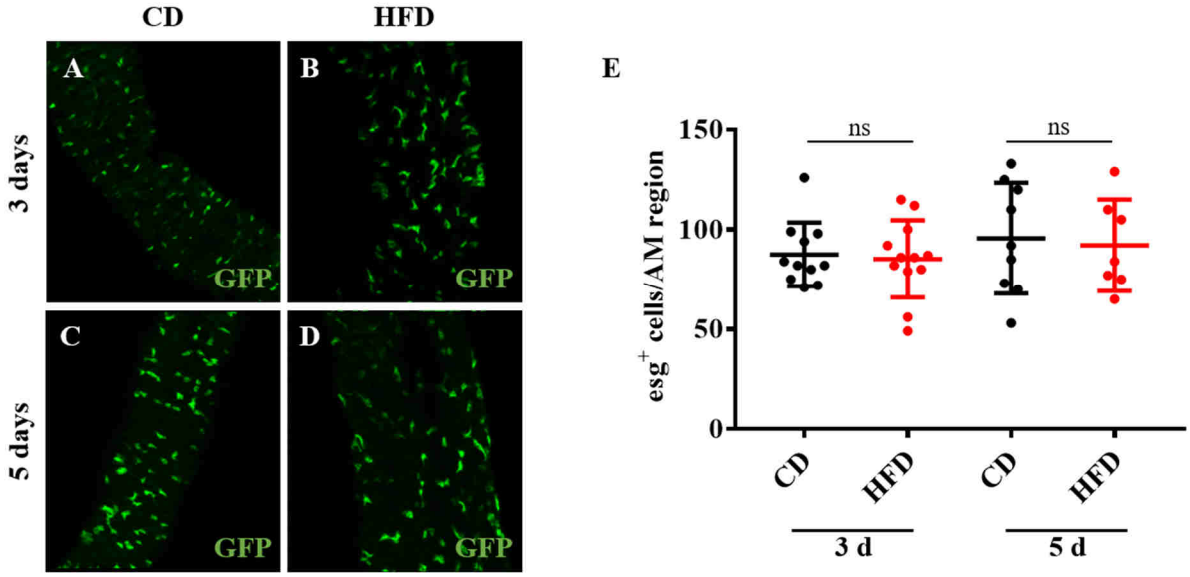

Fig. 18: Diet induced changes of the microbial composition has no impact on intestinal cell proliferation. (A-D) GF esg>GFP flies were recolonized with feces derived from flies fed a CD or HFD. The CD or HFD associated microbial community did not affect the number of esg$^+$ cells (GFP) in the intestine 3 days or 5 days after fecal transplantation. (E) Quantitative analysis of the number of esg$^+$ cells in the anterior midgut region 3 days or 5 days after recolonization with a CD or HFD associated microbial community (n = 7-12). HFD: high fat diet, CD: control diet, GF: germ-free, GFP: green fluorescent protein, AM: anterior midgut, esg: escargot, d: days, ns: not significant.

microbiota. Afterwards, all flies were kept on a CD for 3 or 5 days. No differences in the number esg$^+$ cells were observed 3 days or 5 days after recolonization between flies, which harbor a microbiota derived from flies fed a CD or HFD (Fig. 18, A-D). The quantitative analysis of the number of esg$^+$ cells also revealed no significant increased cell proliferation due to the transfer of a HFD associated microbial community (Fig. 18, E).

4.1.11 **High fat dieting slows down the egestion**

In order to elucidate if a HFD and the intestinal microbial community have an influence on the egestion functionality, I checked the number of fecal spots and the time necessary for a completed gut transit in RC and GF flies. Upon high fat dieting, RC flies showed a significantly lower number of fecal spots per fly over 24 hours compared to RC flies fed a CD (Fig. 19, A). No differences in the number of fecal spots were observed between GF flies fed a CD or HFD. Interestingly, the fecal spot production was significantly reduced in GF flies fed a CD compared to RC flies on the similar diet. This phenotype was not detectable in RC flies and GF flies fed a HFD (Fig. 19, A). High fat dieting in RC flies lead to a delay in fecal transit time in comparison to RC flies fed a CD, validated by measuring the completed gut transit time. The gut transit time is also significantly prolonged in GF flies fed a HFD compared to GF flies upon control dieting. No differences in gut transit time was observed between RC flies and GF flies, which were fed the same diet, respectively. (Fig. 19, B).

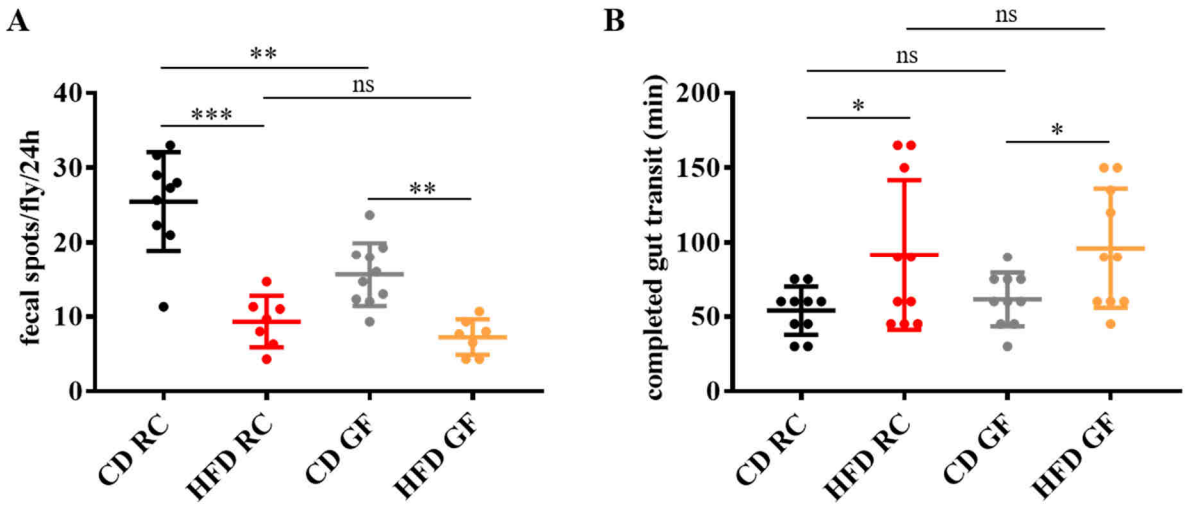

Fig. 19: High fat dieting affects the egestion. (A) Analysis of the fecal spot production per fly over 24 hours. High fat dieting highly reduced the number of fecal spots in RC flies and GF flies fed a HFD compared to the proper control dieting flies (n = 6-10). (B) RC flies and GF flies fed a HFD exhibited a prolonged complete gut transit time compared to the corresponding control flies fed a CD (n = 8-10). HFD: high fat diet, CD: control diet, RC: recolonized, GF: germ-free, ns: not significant, *p < 0.05, **p < 0.01, ***p < 0.001.

4.1.12 **A HFD affects intestinal diameter and the microbial abundance**

I measured the intestinal diameter of flies to investigate if the prolonged gut transit time lead to an increased pressure within the lumen. In fact, the intestinal diameter was increased in flies upon high fat dieting (Fig. 20, B) in comparison to flies fed a CD (Fig. 20, A). Quantitative analysis revealed that the intestine of flies fed a HFD are approximately 50 µm thicker than the intestines of control dieting flies, which may reflect an increased mass of food in the flies intestine (Fig. 20,C). Moreover, the reduced gut transit time and the increased intestinal thickness is associated with a higher intestinal bacterial abundance. The bacterial abundance was 2 fold higher in flies fed a HFD in comparison to flies fed a CD, verified by measuring the 16s rDNA copy number via qRT-PCR (Fig. 20, D).

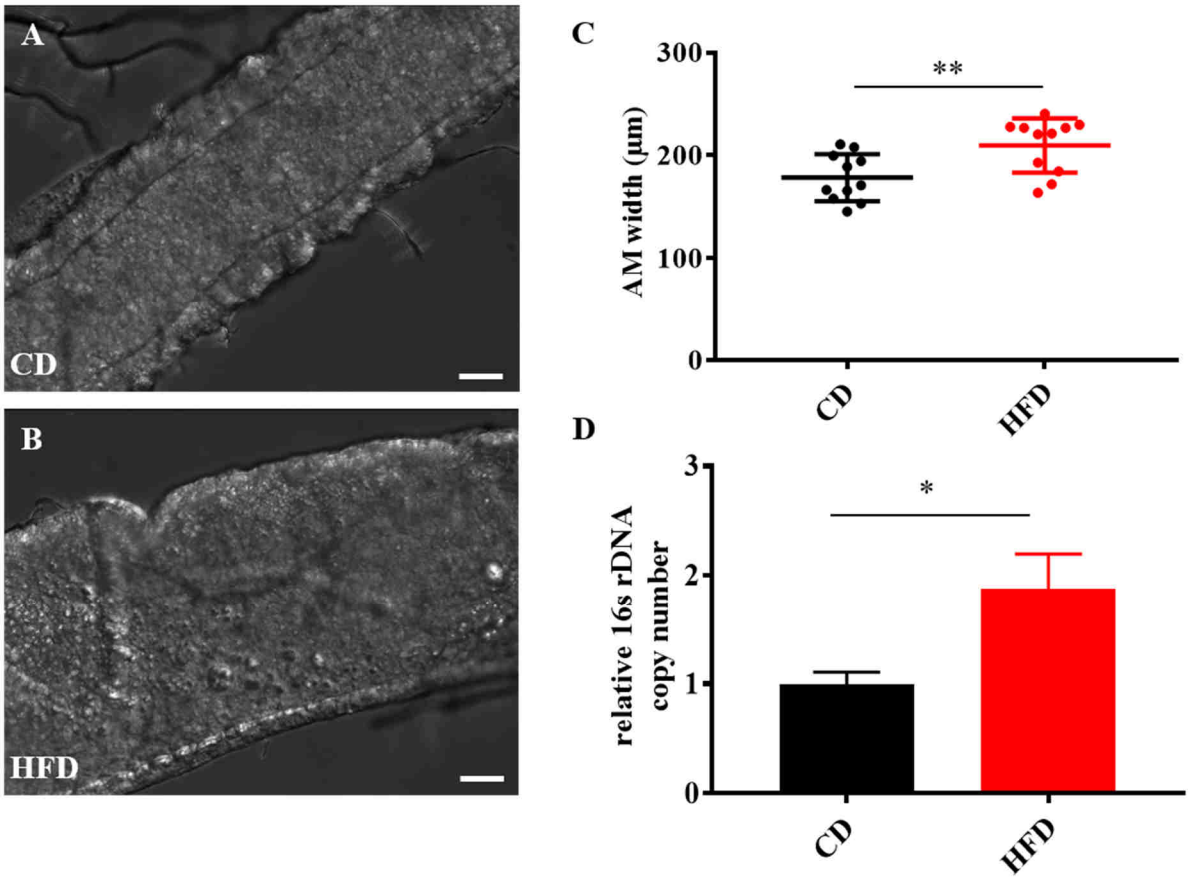

Fig. 20: Intestinal thickness and bacterial abundance of flies fed a HFD. (A-B) Representative images of intestines of flies fed a CD or HFD. Scale bar = 50 µm. (C) Quantification of the anterior midgut width of flies upon high fat dieting compared to flies fed a CD (n = 11). (D) The intestinal 16s rDNA copy number was analyzed by using universal 16s primers. The bacterial load was increased in flies fed a HFD in comparison to flies fed a CD (n = 5). HFD: high fat diet, CD: control diet, AM: anterior midgut, *p < 0.05, **p < 0.01.

4.1.13 **Triglyceride storage depends on the intestinal microbiota**

The lipid uptake in *Drosophila* is mainly regulated by ECs in the intestine, whereas ingested lipids are stored as triacylglycerols (TAG) in lipid droplets. I measured the TAG content of whole RC flies and GF flies, to investigate whether or not the dietary lipid is indeed ingested to the cells. RC flies fed a HFD had a significant increased TAG content compared to RC flies fed a CD. Interestingly, GF flies fed a CD had a higher TAG content than RC flies on the same diet. GF flies also stored significantly more TAGs upon high fat dieting than RC flies on the same diet. Moreover, upon high fat dieting GF flies revealed a higher TAG content than GF flies fed a CD (Fig. 21, A). The increased lipid uptake of RC flies fed a HFD or GF flies fed a CD did not affect the weight compared to RC flies upon control dieting. Surprisingly, the weight

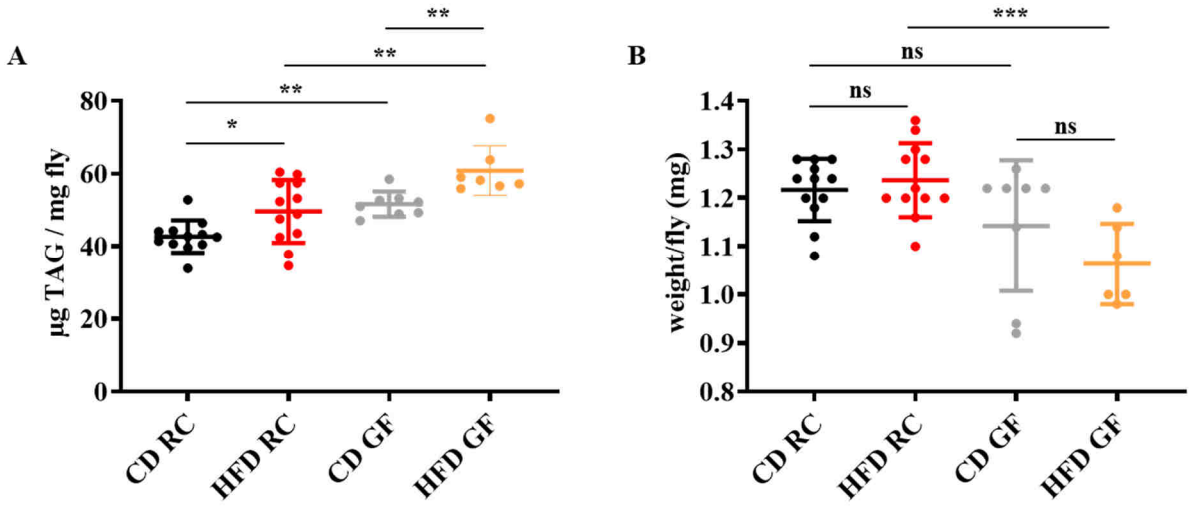

Fig. 21: High fat dieting leads to a microbiota-dependent increased TAG content. (A) The TAG content of RC flies and GF flies fed a HFD and CD. High fat dieting as well as the intestinal microbiota affects the TAG content in flies (n = 7-12). (B) The weight of RC flies and GF flies upon high fat dieting and control dieting (n = 7-12). HFD: high fat diet, CD: control diet, RC: recolonized, GF: germ-free, TAG: triacylglycerol, ns: not significant, *p < 0.05, **p < 0.01, ***p < 0.001.

of GF flies fed a HFD was significantly reduced in comparison to RC flies on the same diet (Fig. 21, B). The increased lipid uptake was also detectable in ECs in flies verified by BODIPY (boron-dipyrromethene) staining. Due to its nonpolar structure, BODIPY is able to stain neutral lipids, like TAGs in lipid droplets. The number of lipid droplets in anterior midgut ECs of RC flies fed a HFD (Fig. 22, B) was increased compared to RC flies fed a CD (Fig. 22, A). Furthermore, GF flies fed a CD (Fig. 22, C) revealed an increased number of lipid droplets in comparison to RC flies on the same diet. As already confirmed via TAG measurement, GF flies upon high fat dieting (Fig. 22, D) showed a highly increased lipid uptake in ECs compared to RC flies fed the same diet.

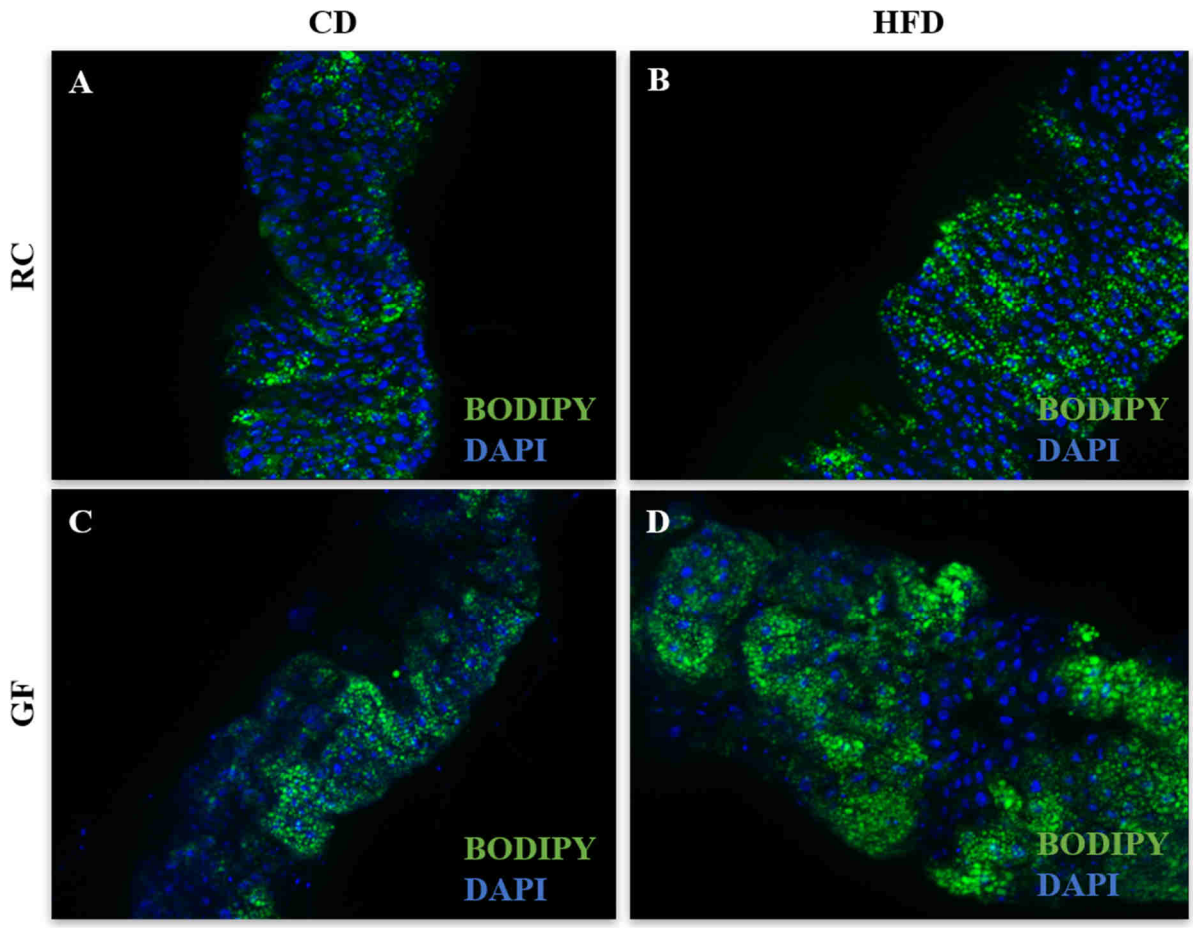

Fig. 22: Impact of a HFD and of the intestinal microbiota on the number of lipid droplets in ECs. (A-D) Dissected intestines of RC and GF flies upon high fat dieting or control dieting were stained with BODIPY to display lipid droplets in ECs. Representative images of the anterior midgut region are shown. CD: control diet, HFD: high fat diet, RC: recolonized, GF: germ-free, BODIPY: boron-dipyrromethene.

4.1.14 **High fat dieting affects the locomotor activity and time of sleep**

Next, I tested the influence of a HFD and of the intestinal microbial community on the physical activity of the fly. Therefore, I used a *Drosophila* activity monitor (DAM) which was placed in an incubator with a 12 h : 12 h light-dark cycle. High fat dieting rather affected the total activity than the circadian rhythm in flies compared to flies fed a CD. The period between of the morning and the evening peak in flies fed a HFD was similar to those fed a CD. The intestinal microbiota did not affect circadian rhythmicity as proofed by using GF animals (Fig. 23, A). The total activity over 24 hours was significantly reduced in RC flies fed a HFD in comparison to RC flies upon control dieting. The similar effect was detectable in GF flies fed a HFD or CD, whereas the microbiota had no impact on the total activity (Fig. 23, B). High fat dieting do not affect sleep rhythmicity in RC and GF flies compared to the proper control fed a CD (Fig. 23, C). However, the time of sleep was significantly increased in RC flies fed a HFD in comparison

to RC flies on the CD. The intestinal microbial community has no impact on the time of sleep as verified by comparing GF flies with RC flies (Fig. 23, D).

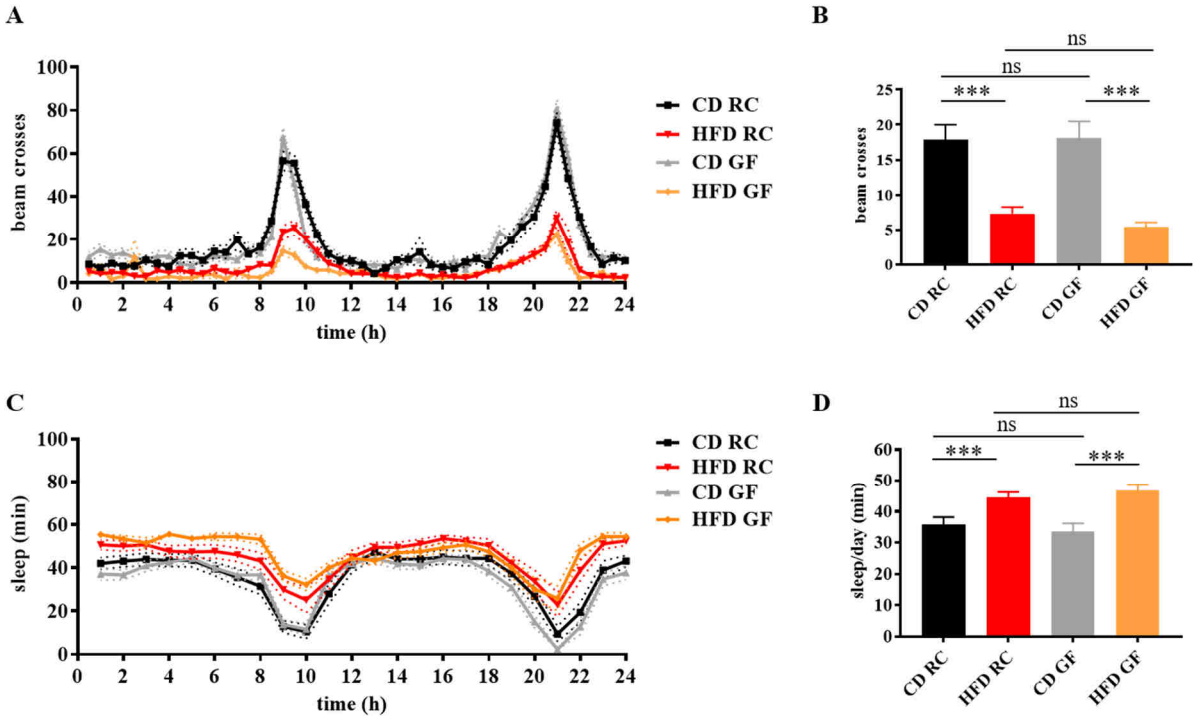

Fig. 23: A HFD affects the total locomotor activity as well as the time of sleep. (A) Monitored locomotor activity over 24 hours in RC flies and GF flies fed a HFD or CD. High fat dieting as well as the intestinal microbiota do not affect the circadian rhythmicity (n = 48). (B) Quantification of the number of beam crosses over 24 hours. A HFD significantly reduces the physical activity of RC flies and GF flies compared to the proper control (n = 48). (C) Monitored sleep rhythmicity over 24 hours in RC and GF flies fed a CD or a HFD (n = 48). (D) Quantification of the time of sleep over 24 hours (n = 48). Flies fed a HFD sleep significantly more than flies upon control dieting. The microbiota neither affect locomotor activity nor the time of sleep. HFD: high fat diet, CD: control diet, RC: recolonized, GF: germ-free, ns: not significant, ***p < 0.001.

4.1.15 **Effects of a HFD on lifespan and starvation resistance**

I further investigated the effect of a HFD on lifespan and starvation resistance. For lifespan analysis, I monitored 100 flies for each diet until they deceased. Flies that continuously fed a HFD showed a significantly decreased lifespan compared to flies fed a CD with a median lifespan of 42 days and 44 days, respectively. (Fig. 24, A). To test the starvation resistance, the flies were fed with either a HFD or a CD for 7 days. Afterwards, the flies were transferred to a 2 % agar medium. Although flies upon high fat dieting had an increased TAG content in comparison to CD fed flies (chapter 4.1.13), it surprisingly did not affect the starvation resistance (Fig. 24, B).

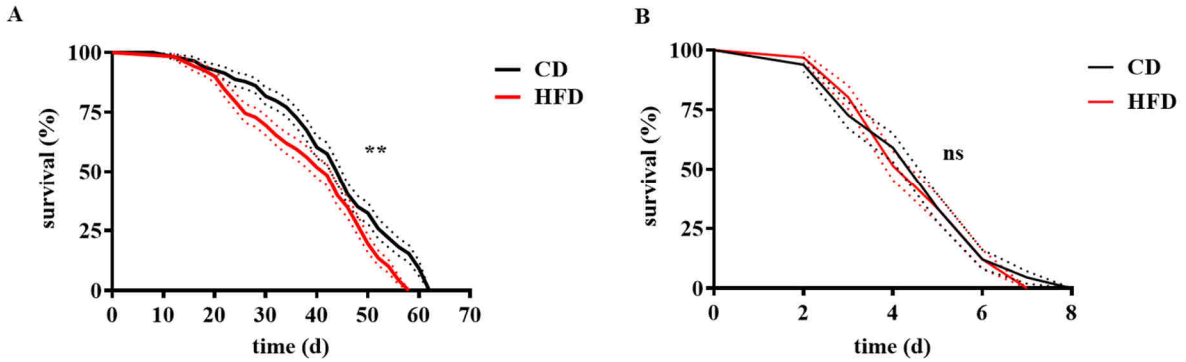

Fig. 24: **Effects of high fat dieting on lifespan, starvation resistance and metabolic rate.** (A) The lifespan of flies upon high fat dieting was significantly decreased compared to CD fed flies (n = 100, ~x_{HFD} = 42 days, ~x_{CD} = 44 days). (B) Starvation resistance assay of flies that were fed with either a HFD or CD for 7 days before starvation (n = 66). HFD: high fat diet, CD: control diet, ns: not significant, **p < 0.01.

4.1.16 **High fat dieting leads to increased JNK signaling in the brain.**

I wanted to find out, if long-term dietary interventions of high fat dieting also leads to stress signaling in the peripheral tissue. It is well known, that there is a bidirectional communication between the intestine and the brain via the gut-brain axis. Therefore, I stained brains with an anti-phospho-JNK (pJNK) antibody to reveal stress responses after 14 days or 21 days of high fat dieting. The brains were co-stained with an anti-bruchpilot (NC82) antibody to label presynaptic active zones in the fly's brain (Fig. 25, A and D). The presynaptic active zones are formed to neuropils, which represent different structures in the brain. Interestingly, 14 days of high fat dieting lead to an increased JNK signaling in the brain of HFD fed flies (Fig. 25, B) compared to CD fed flies (Fig. 25, E). The JNK signaling was mostly active in parts of the mushroom body (Fig. 25, C and D, marked as dashed lines). The quantification of the

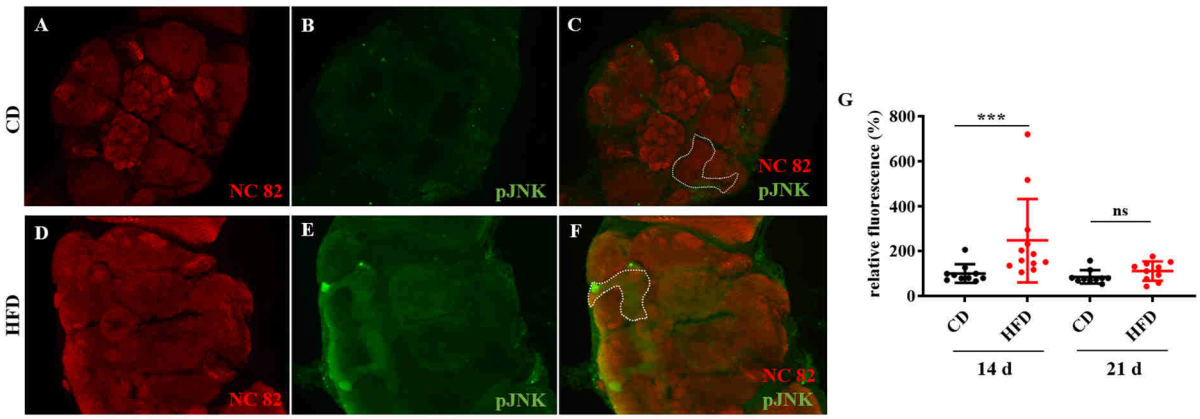

Fig. 25: A HFD triggers JNK signaling in the brain. (A-F) Fly brains were dissected 14 days after control dieting or high fat dieting. The neuropils were labeled with an anti-NC82 antibody and JNK signaling was revealed by using an anti-pJNK antibody. Parts of the mushroom bodies are marked by dashed lines. (G) Fluorescence quantification of the pJNK fluorescence signal in the mushroom body after 14 days and 21 days of control dieting or high fat dieting (n = 10-12). CD: control diet, HFD: high fat diet, NC82: bruchpilot, pJNK: phospho-JNK, ns: not significant, ***p < 0.001.

fluorescence signal of the mushroom body revealed a significant increase in JNK signaling after 14 days when fed a HFD compared to flies fed a CD. However, the JNK signaling decreased after 21 days of high fat dieting and the fluorescence signal was comparable to that of flies fed a CD (Fig. 25, G).

4.2 Development of an optimized holidic diet

Drosophila is an important model in nutrition research to study the response to dietary factors, diet-disease interactions or diet-host-microbiota interactions. Most of the *Drosophila* diets, the so-called complex diets, are based on corn meal, yeast, sucrose and agar (260). However, the experimental diets vary between studies and laboratories and the use of different diets can lead to high variances in the observed effects and to non-reproducible results. Therefore, a complete chemically defined diet (holidic diet) is required. There are currently only a few holidic diets available for *Drosophila* (251,252,261,262) but none of these diets sufficiently support the larval development.

4.2.1 Optimized holidic diet increases pupation and eclosion rate

Piper and colleagues created in 2014 a holidic diet (HD), which support adult fecundity, lifespan and development at reduced rate when compared to a standard complex *Drosophila* diet (251). A low protein to carbohydrate ratio was reported to decrease the developmental time and increases the egg-to-adult viability of *Drosophila* (263,264). Therefore, I changed the amount of essential as well as non-essential amino acids and the sugar in order to further support the developmental time and eclosion rate. I increased the sugar concentration from 17 g/l to 75 g/l and sucrose was replaced by glucose as glucose is the main hemolymph sugar of *Drosophila*. The total amount of amino acids was raised from 21.4 g/l to either 42.8 g/l (OHD 2xAA), which resulted in a protein:carbohydrate ratio of 1:1.75. I created a second diet, by increasing the total amount of amino acids from 21.4 g/l to 64.2 g/l (OHD 3xAA), to examine if a total increase of carbohydrates and amino acids improve the development. The vitamin concentrations were modified according to the synthetic diet published by Tânia Reis in 2016 (261). The developmental time, pupation rate and eclosion rate was compared to a complex diet (chapter 1.5.2), which serves as a control diet (CD). The developmental time from egg to pupa was comparable between larvae fed an OHD 2xAA, OHD 3xAA or HD. However, the

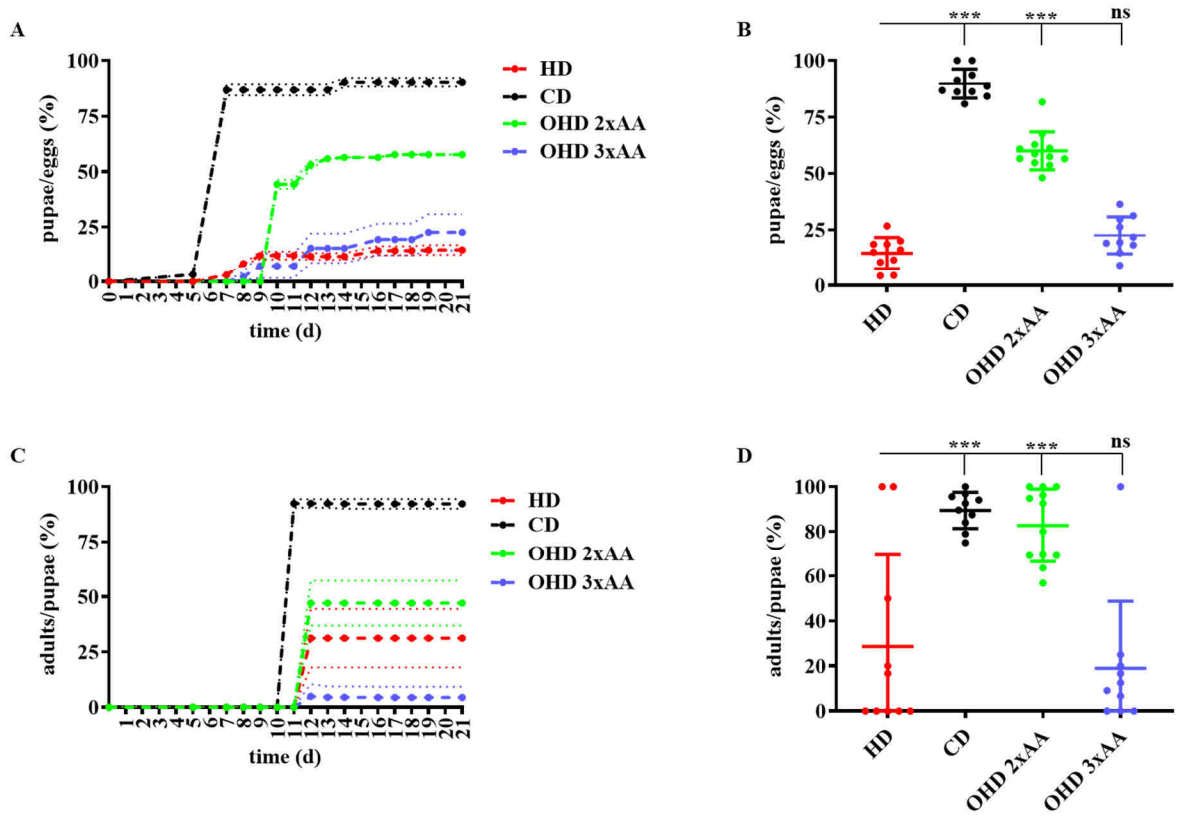

Fig. 26: Optimization of a holidic diet increased pupation and eclosion rate. (A) The developmental time from egg to pupa of larvae fed either a HD, a CD, an OHD 2xAA or an OHD 3x AA (n = 10). (B) Quantification of the pupation rate (n = 10-12). (C) The developmental time from egg to adult from larvae fed either a HD, a CD, an OHD 2xAA or an OHD 3xAA (n = 10). (D) Quantification of the eclosion rate (n = 10-12). CD: control diet, HD: holidic diet (Piper *et al*., 2014), OHD 2xAA: optimized holidic diet 2x amino acids, OHD 3xAA: optimized holidic diet 3x amino acids, ns: not significant, **p < 0.01, ***p < 0.001.

developmental time of larvae fed a CD was shorter compared to the HD, OHD 2xAA and OHD 3xAA (Fig. 26, A). The pupation rate was significantly increased in CD and OHD 2xAA fed larvae compared to larvae raised on a HD. Interestingly, the beneficial effect on the pupation rate by feeding the larvae with 42.8 g/l total amino acids is completely absent in larvae fed with 64.2 g/l total amino acids (Fig. 26, B). The developmental time from egg to adult was comparable between larvae fed a HD, OHD 2xAA and OHD 3xAA. Larvae fed a HD, an OHD 2xAA or an OHD 3xAA showed a longer developmental time from egg to adult than CD fed larvae (Fig. 26, C). The eclosion rate was significantly higher in larvae fed a CD or an OHD 2xAA compared to HD fed larvae. Again, the beneficial effect on the eclosion rate by feeding 42.8 g/l total amino acids was completely absent in larvae fed with 64.2 g/l total amino acids (Fig. 26, D). To examine the egg laying preference for the different diets, 100 mated female flies were transferred into cages with either a HD, a CD and an OHD 2xAA or a HD and an OHD 2xAA for 24 hours. In the presence of a HD, a CD and an OHD 2xAA, female flies laid significantly more eggs on the CD compared to the HD. No significant differences in the egg laying preference were observed between an OHD 2xAA and a HD (Fig. 27, A). When only a

HD and an OHD 2xAA are available for egg laying, the flies significantly preferred the OHD 2x AA (Fig. 27, B).

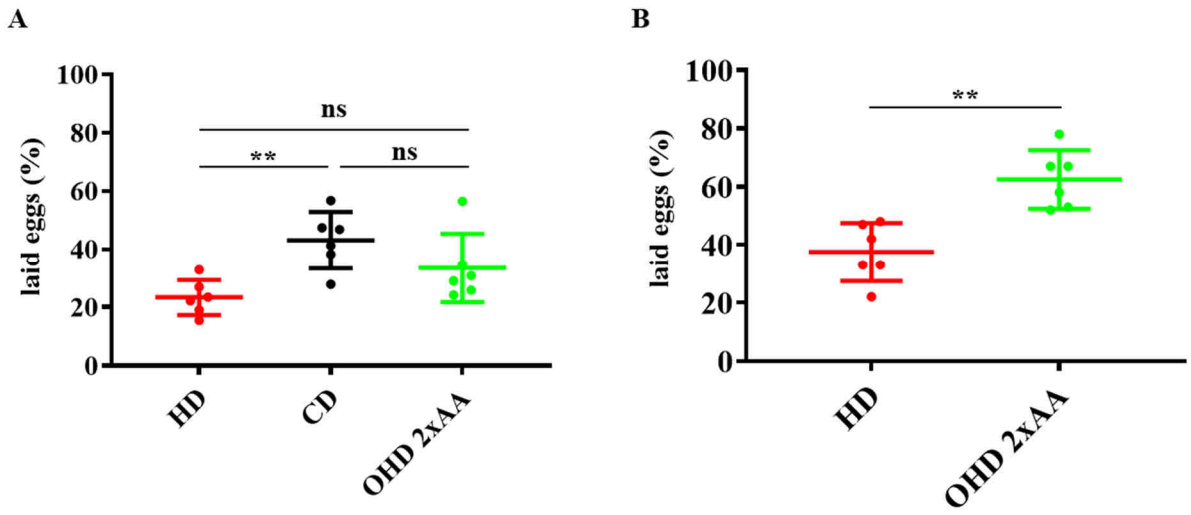

Fig. 27: Egg laying preference for HD, CD and OHD 2xAA. (A) 100 female flies were transferred into cages with plates filled with either a HD, a CD or an OHD 2xAA. The flies were allowed to lay eggs for 24 hours (n = 6). (B) Egg laying preference between a HD and an OHD 2xAA (n = 6). CD: control diet, HD: holidic diet (Piper *et al*., 2014), OHD 2xAA: optimized holidic diet 2x amino acids, ns: not significant, **p < 0.01.

4.2.2 Impact of fructose and ribonucleotides on the development

In collaboration with the Rimbach lab (University of Kiel) we discovered that the supplementation of the OHD 2xAA with cobalt, cobalamin, molybdenum and a cholesterol/ergosterol mixture (hereafter declared as OHD) further decreases the developmental time. Moreover, these supplements increased the pupation rate as well as the eclosion rate (data not shown). Based on this diet, I replaced glucose by fructose or by a fructose/glucose mixture to evaluate the optimal carbohydrate source, whereas the total amount of 75 g/l carbohydrates was equal in each diet. Besides this, I added 5 g/l ribonucleotides to the OHD as ribonucleotides are known to promote development, especially in rapid growth phases 265. With that, I examined if another carbohydrate source as well as ribonucleotides will further improve the diet regarding developmental time, pupation rate and eclosion rate. Interestingly, fructose as well as the fructose/glucose mixture had a negative influence on the developmental time from egg to pupa in comparison to the OHD. The supplementation of ribonucleotides improved the developmental time slightly (Fig. 28, A). The carbohydrate source or the ribonucleotides had no impact on the pupation rate (Fig. 28, B). Fructose and a fructose/glucose mixture increased the developmental time from egg to adult compared to the OHD. On the other hand, 5 g/l ribonucleotides had a positive influence on the developmental time from egg to adult (Fig. 28,

C). The eclosion rate was significantly decreased in animals fed a fructose diet compared to OHD fed animals. A fructose/glucose diet and a supplementation with ribonucleotides did not lead to significant differences in the eclosion rate in comparison to the OHD (Fig. 28, D).

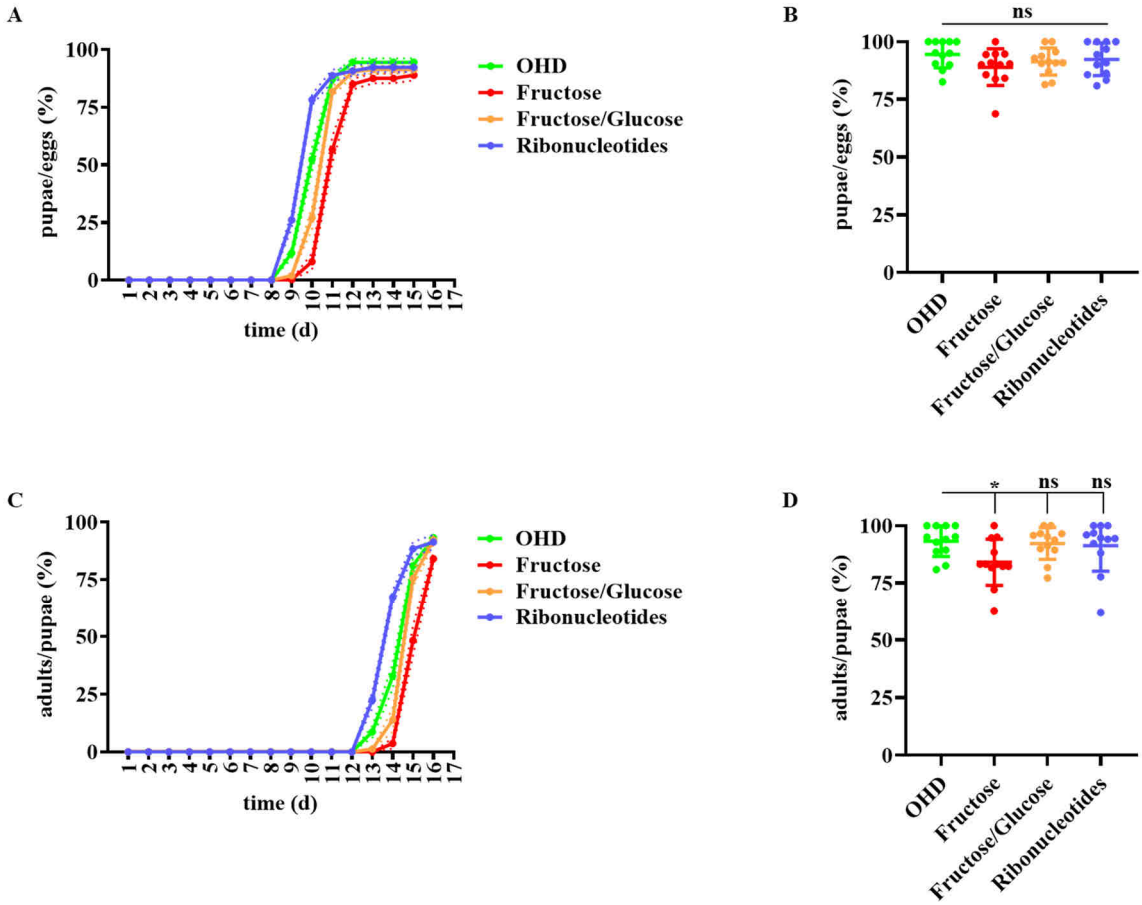

Fig. 28: Developmental time, pupation rate and eclosion rate in fructose and ribonucleotide supplemented diets. (A) Developmental time from egg to pupa of larvae fed either an OHD (containing glucose), a fructose/glucose or a fructose supplemented diet. The ribonucleotides were added to the glucose containing diet (n = 12). (B) Quantification of the pupation rate (n = 12). (C) Developmental time from egg to adult of larvae fed either a glucose, fructose/glucose, fructose or ribonucleotide supplemented diet (n = 12). (D) Quantification of the eclosion rate (n = 12). OHD: optimized holidic diet, ns: not significant, *p < 0.05.

4.2.3 The optimized holidic diet promotes germ-free development

In 2017, Piper *et al.* published an exom-matched holidic diet (EMHD) that uses genome information of *Drosophila* to define its amino acid requirements. The EMHD is based on the HD published by Piper et al. (2014) with a differed amino acid proportion. The EMHD enhanced growth and increased the reproduction capability compared to the HD (252). It is known that the developmental time of GF larvae is postponed on dietary restricted diets, whereas it is not impaired on complex diets (248). Therefore, I tested if the OHD, the HD and the EMHD are able to support GF development. The developmental time from egg to pupa from GF larvae fed an OHD was comparable to larvae harboring a normal microbiota (chapter 4.2.2), however, GF larvae on HD and EMHD did not develop (Fig. 29, A). Thus, the pupation rate of

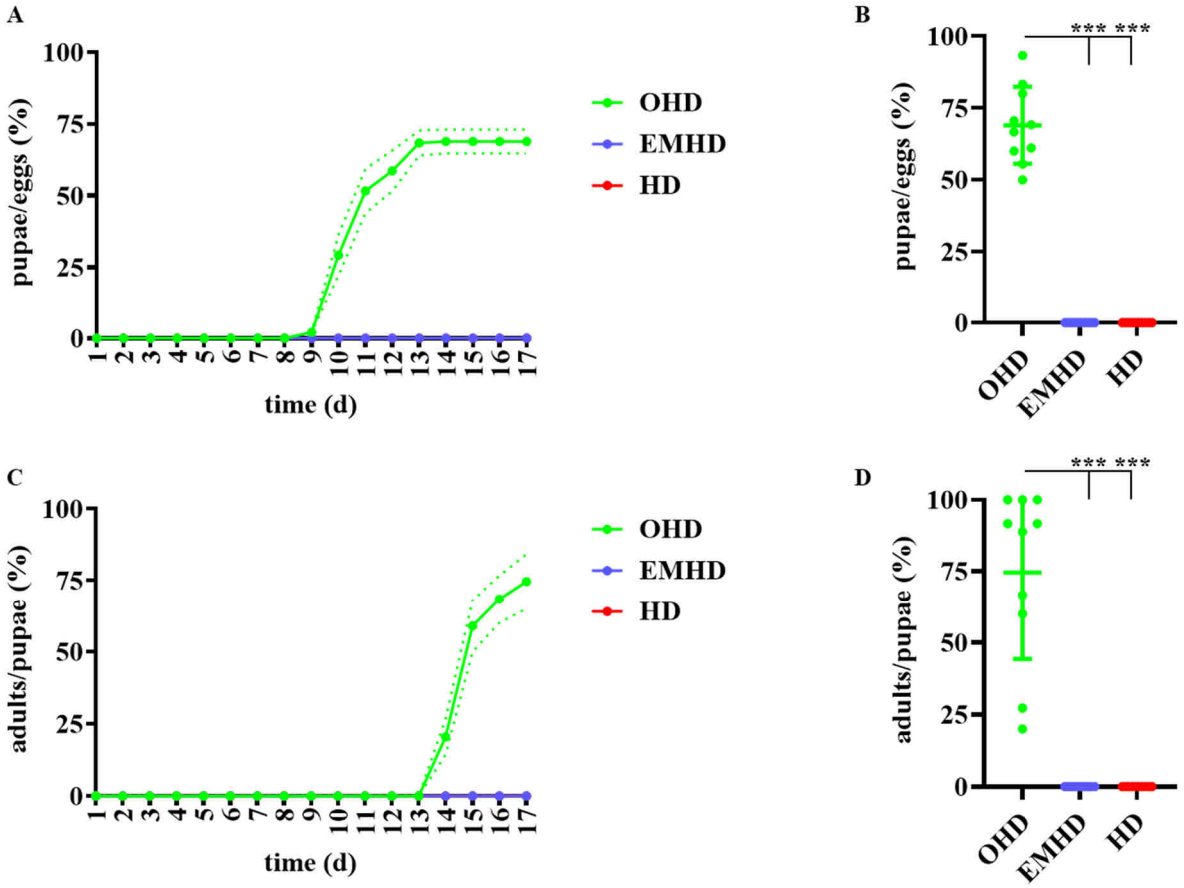

Fig. 29: **The OHD improves the development of GF flies.** (A) The developmental time from egg to pupa from GF larvae fed an OHD, EMHD or HD (n = 10). (B) Quantification of the pupation rate (n = 10). (C) The developmental time from egg to adult (n = 10). (D) Quantification of the eclosion rate (n = 10). OHD: optimized holidic diet, EMHD: exom-matched holidic diet, HD: holidic diet, GF: germ-free, ***p < 0.001.

OHD fed GF larvae was significantly increased compared to GF larvae fed an EMHD and HD (Fig. 29, B). The developmental time from egg to adult was highly improved by an OHD compared to an EMHD or a HD (Fig. 29, C). The eclosion rate was significantly increased in GF flies fed an OHD in comparison to EMHD and HD fed GF flies (Fig. 29, D). Taken together, the OHD improves the development of flies harboring a microbial community as well as of GF flies. Moreover, GF larvae fed a HD or an EMHD were smaller 7 days after oviposition

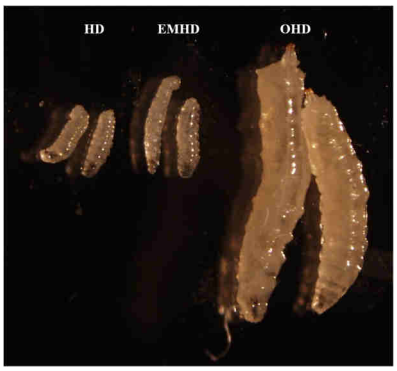

Fig. 30: Size comparison of GF larvae fed with either OHD, EMHD or HD. GF larvae fed a HD or an EMHD were smaller 7 days after egg laying in comparison to GF larvae fed an OHD. OHD: optimized holidic diet, EMHD: exom-matched holidic diet, HD: holidic diet, GF: germ-free.

compared to OHD fed GF larvae (Fig. 30). GF larvae fed an OHD reached L3 stage after 7 days, whereas GF larvae fed a HD or EMHD died.

4.2.4 Improvement of an exom-matched holidic diet

I created different diets based on the EMHD by manipulating ingredients such as ergosterol, cholesterol, cobalt, cobalamin, molybdenum, ribonucleotides and l-arginine to further improve the EMHD regarding developmental time, pupation rate and eclosion rate. The different diets and its manipulated ingredients are listed in table 12. The developmental time from egg to pupa was highly improved in larvae fed an optimized exom-matched holidic diet (OEMHD) in comparison to larvae fed diet 1-6 or EMHD (Fig. 31, A). The pupation rate of larvae fed an OEMHD was significantly increased compared to EMHD fed larvae. No differences in the pupation rate were observed between an OEMHD fed larvae and larvae that fed diet 1, diet 2, diet 3, diet 4, diet 5 or diet 6 (Fig. 31, B). Larvae fed an OEMHD examined a decreased developmental time from egg to adult in comparison to EMHD, diet 1, diet 2, diet 3, diet 4, diet 5 or diet 6 fed larvae (Fig. 31, C). The eclosion rate was significantly increased in flies fed an OEMHD compared to EMHD fed flies. The manipulated ingredients in diet 1, diet 2, diet 3,

Table 12: EMHD supplemented with combinations of ergosterol, cholesterol, sucrose, glucose, cobalt, cobalamin, molybdenum, ribonucleotides and l-arginine.

Abbreviation	Sugar	Sterols	Cobalt Cobalamine Molybdenum	Ribonucleotides	L-arginine
OEMHD	17.12 g/l sucrose	150 mg/l ergosterol 150 mg/ml cholesterol	+	5 g/l	-
EMHD	17.12 g/l sucrose	150 mg/ml cholesterol	-	-	-
Diet 1	17.12 g/l sucrose	300 mg/ml ergosterol	-	-	-
Diet 2	17.12 g/l sucrose	150 mg/l ergosterol 150 mg/ml cholesterol	-	-	-
Diet 3	17.12 g/l sucrose	300 mg/l cholesterol	+	5 g/l	-
Diet 4	75 g/l glucose	150 mg/l ergosterol 150 mg/ml cholesterol	+	2 g/l	-
Diet 5	75 g/l glucose	150 mg/l ergosterol 150 mg/ml cholesterol	+	5 g/l	2x
Diet 6	75 g/l glucose	150 mg/l ergosterol 150 mg/ml cholesterol	+	5 g/l	-

diet 4, diet 5 and diet 6 do not further support the eclosion rate in comparison to the OEMHD (Fig. 31, D). The pupae size was significantly increased in larvae that fed an OEMHD in comparison to EMHD and diet 1 fed larvae. The pupae size was comparable between OEMHD fed animals and animals fed a diet 2, diet 3, diet 4, diet 5, and diet 6 (Fig. 31, E). The adult weight was highly increased in flies fed an OEMHD in comparison to EMHD and diet 2 fed flies. The adult weight was not significantly affected in flies fed a diet 1, diet 3, diet 4, diet 5 or diet 6 compared to OEMHD fed flies (Fig. 31, F).

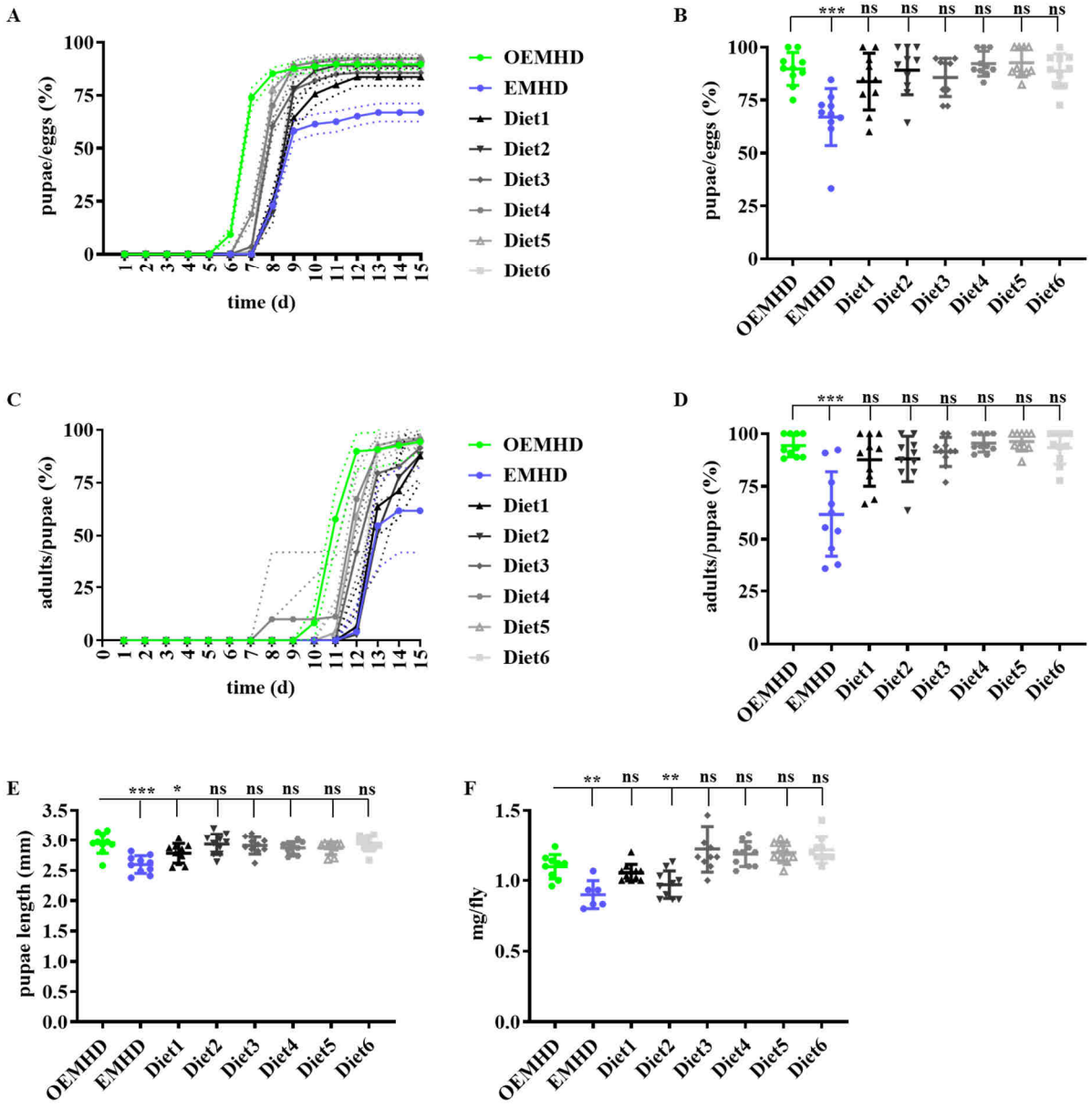

Fig. 31: An optimized exom-matched diet improves the development. (A) Developmental time from egg to adult of larvae that fed diets listed in table 3 (n = 10). (B) Quantification of the pupation rate (n = 10). (C) Developmental time from egg to adult of larvae that fed diets listed in table 3 (n = 3). (D) Quantification of the hatching rate (n = 10). (E) The pupae length of larvae fed a diet listed in table 3 (n = 10). The pupae size of flies fed an OEMHD was enhanced in comparison to EMHD fed flies. (F) The adult weight of flies 7 after hatching. The adult weight was increased in flies fed an OEMHD compared to EMHD fed flies. OEMHD: optimized exom-matched holidic diet, EMHD: exom-matched holidic diet, ns: not significant, *p < 0.05, **p < 0.01, ***p < 0.001.

4.2.5 Determination of the optimal carbohydrate source and concentration

Based on the OEMHD, I wanted to determine the optimal carbohydrate source and concentration. Therefore, different carbohydrate sources were added to the OEMHD such as sucrose, fructose and glucose with increasing concentrations of 10 g/l, 17.2 g/l, 35 g/l and 50 g/l. The OEMHD contained 17.2 g/l sucrose and served as control. The developmental time from egg to pupa was decreased in larvae fed a diet with 10 g/l or 17.2 g/l sucrose in comparison to larvae fed a diet with 35 g/l or 50 g/l sucrose (Fig. 32, A). Whereas, the developmental time from egg to pupa was comparable in larvae fed an OEMHD with 10 g/l, 17.2 g/l, 35 g/l and 50 g/l glucose (Fig. 32, B). No differences in the developmental time from egg to pupa were

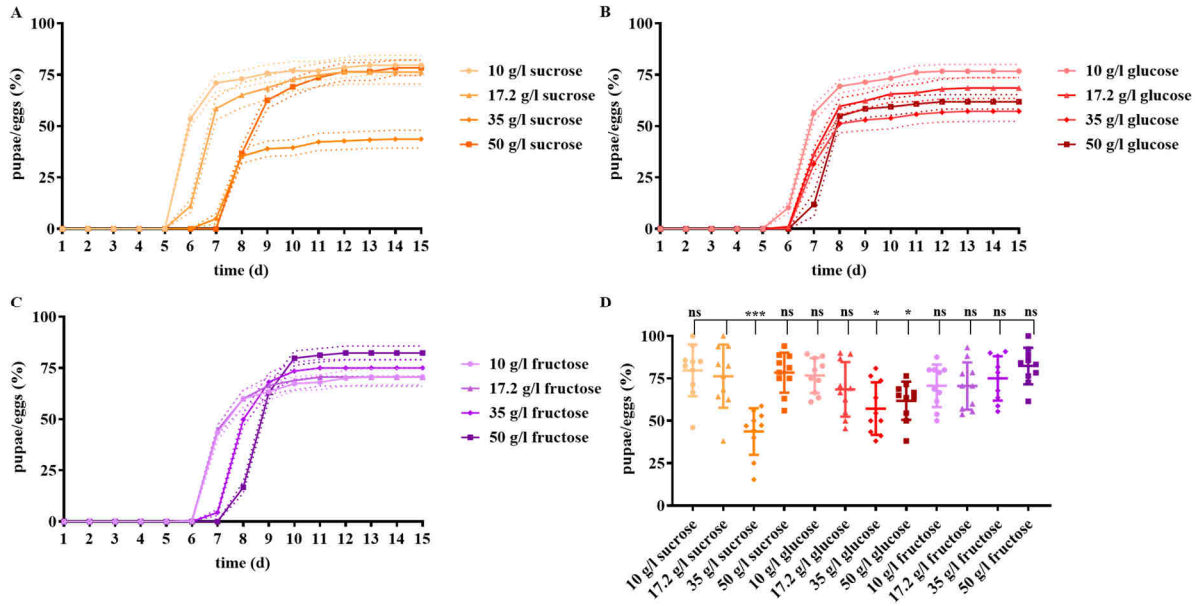

Fig. 32: Determination of the optimal sugar source and concentration in the OEMHD to improve the developmental time from egg to pupa. (A-C) Developmental time from egg to pupa of larvae fed an OEMHD with the indicated sugar source and concentration (n = 10). (D) Quantification of the pupation rate (n = 10). OEMHD: optimized exom-matched holidic diet, ns: not significant, *p < 0.05, ***p < 0.001.

observed in larvae fed a diet with 10 g/l, 17.2 g/l, 35 g/l or 50 g/l fructose (Fig. 32, C). The pupation rate of larvae fed a diet with 17.2 g/l sucrose was significantly increased in comparison to larvae fed a diet with either 35 g/l sucrose, 35 g/l glucose or 50 g/l glucose. The pupation rate of larvae fed a diet with either 10 g/l sucrose, 50 g/l sucrose, 10 g/l glucose, 17.2 g/l glucose, 10 g/l fructose, 17.2 g/l fructose, 35 g/l fructose or 50 g/l fructose was not affected in comparison to larvae fed an OEMHD with 17.2 g/l sucrose (Fig. 32, D). The developmental time from egg to adult of larvae fed a diet with 10 g/l sucrose or 17.2 g/l sucrose was decreased in comparison to larvae fed a diet with 35 g/l sucrose or 50 g/l sucrose (Fig. 33, A). Different concentration of glucose did not affect the developmental time of larvae (Fig. 33, B). The developmental time from egg to adult was increased in larvae fed a diet with 50 g/l fructose

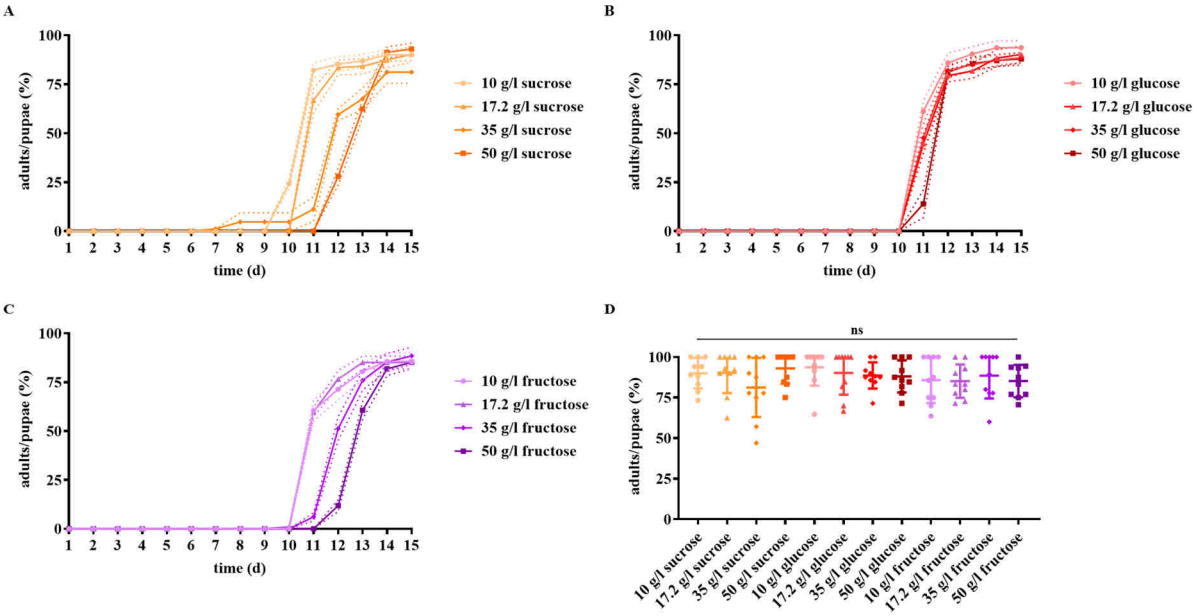

Fig. 33: Determination of the optimal sugar source and concentration in the OEMHD to improve the developmental time from egg to adult. (A-C) Developmental time from egg to adult of larvae fed an OEMHD with the indicated sugar source and concentration (n = 10). (D) Quantification of the eclosion rate (n = 10). OEMHD: optimized exom-matched holidic diet, ns: not significant.

compared to larvae fed a diet with either 10 g/l, 17.2 g/l or 35 g/l fructose (Fig. 33, C). No significant differences of the eclosion rate were observed of larvae fed diets with different concentrations of either sucrose, glucose or fructose (Fig. 33, D). The pupae size of larvae fed an OEMHD with 17.2 g/l sucrose was significantly increased in comparison to larvae fed a diet with 50 g/l sucrose, 10 g/l glucose, 35 g/l glucose or 17.2 g/l fructose. The size of the pupae were not affected in larvae fed a diet with either 10 g/l sucrose, 35 g/l sucrose, 17.2 g /l glucose, 50 g/l glucose, 10 g/l fructose, 35 g/l fructose or 50 g/l fructose compared to larvae fed a diet with 17.2 g/l sucrose (Fig. 34, A). The weight of adult flies was significantly decreased in flies fed a diet with 17.2 g/l fructose compared to flies fed a diet with 17.2 g/ sucrose. However, the weight of adult flies was not affected in the other diets compared to flies fed an OEMHD with 17.2 g/l sucrose (Fig. 34, B). The sugar source as well as the sugar concentration had no impact on the wing area of adult flies, which is an indicator for the body size of the fly (Fig. 34, C).

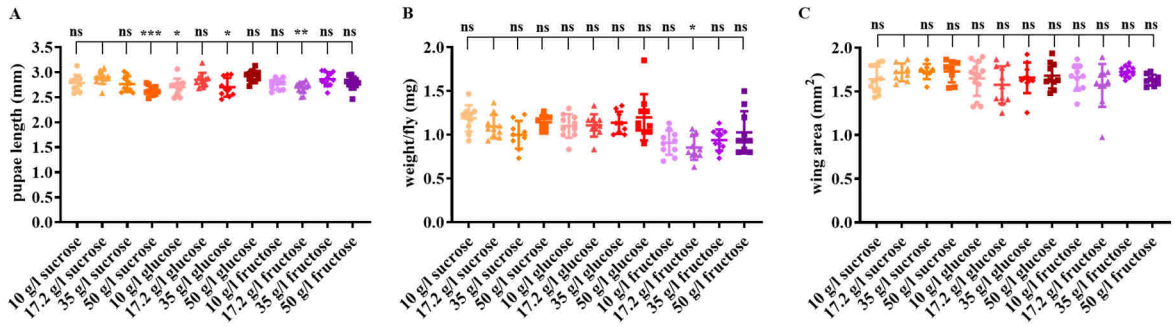

Fig. 34: Pupae length, weight and wing area of flies fed an OEMHD with different sugar sources and sugar concentrations. (A) Pupae length of larvae fed an OEMHD with either sucrose, glucose or fructose and increasing sugar concentrations (n = 10-12). (B) The weight of adult flies 7 days after fed one of the indicated diets (n = 9-10). Wing area of adult flies fed either a sucrose, glucose or fructose containing OEMHD (n = 8-12). OEMHD: optimized exom-matched holidic diet, ns: not significant, *p < 0.05, ***p < 0.001.

4.2.6 Cobalamin and cobalt did not improve GF development

In chapter 4.2.3 it was shown, that the OHD improves GF development and that an EMHD did not support the survival of GF larvae. Next, I tested if an OEMHD can support GF development as good as an OHD. Furthermore, cobalamin and its central atom cobalt were depleted from the OEMHD to examine if these components are important promoters for the GF development as it is known that cobalamin is synthesized by some bacteria and archaea but not by animals or plants (266). A complex diet served a positive control diet (CD, chapter 1.5.2). The developmental time from egg to pupa of GF larvae fed an OEMHD was increased in comparison to CD fed GF larvae. Cobalamin as well as cobalt did not improve the developmental time (Fig. 35, A). The pupation rate was significantly increased in GF larvae fed a CD compared to GF larvae fed an OEMHD. However, the depletion of cobalamin or cobalt or both from an OEMHD did not significantly decrease the pupation rate in GF larvae in comparison to GF larvae fed an OEMHD (Fig. 35, B). The developmental time from egg to adult of GF larvae fed a CD was decreased compared to GF larvae fed an OEMHD. The depletion of cobalamin or cobalt did not affect the developmental time of GF larvae in comparison to OEMHD fed GF larvae (Fig. 35, C). The eclosion rate was comparable between GF larvae fed an OEMHD, a cobalt depleted OEMHD, a cobalamin depleted OEMHD, a cobalt/cobalamin depleted OEMHD and a CD (Fig. 35, D). The pupae length was increased of GF larvae fed a CD compared to GF larvae fed an OEMHD. No significant differences of the pupae length was observed between a cobalt depleted OEMHD, a cobalamin depleted OEMHD, a cobalt/cobalamin depleted OEMHD and an OEMHD (Fig. 35, E). Interestingly, the wing area of adult flies was decreased in GF flies fed a cobalt/cobalamin depleted OEMHD in comparison to OEMHD fed GF flies, which indicates a smaller body size. On the other hand, the wing area

of GF flies fed a CD was significantly increased compared to GF flies fed an OEMHD (Fig. 35, F).

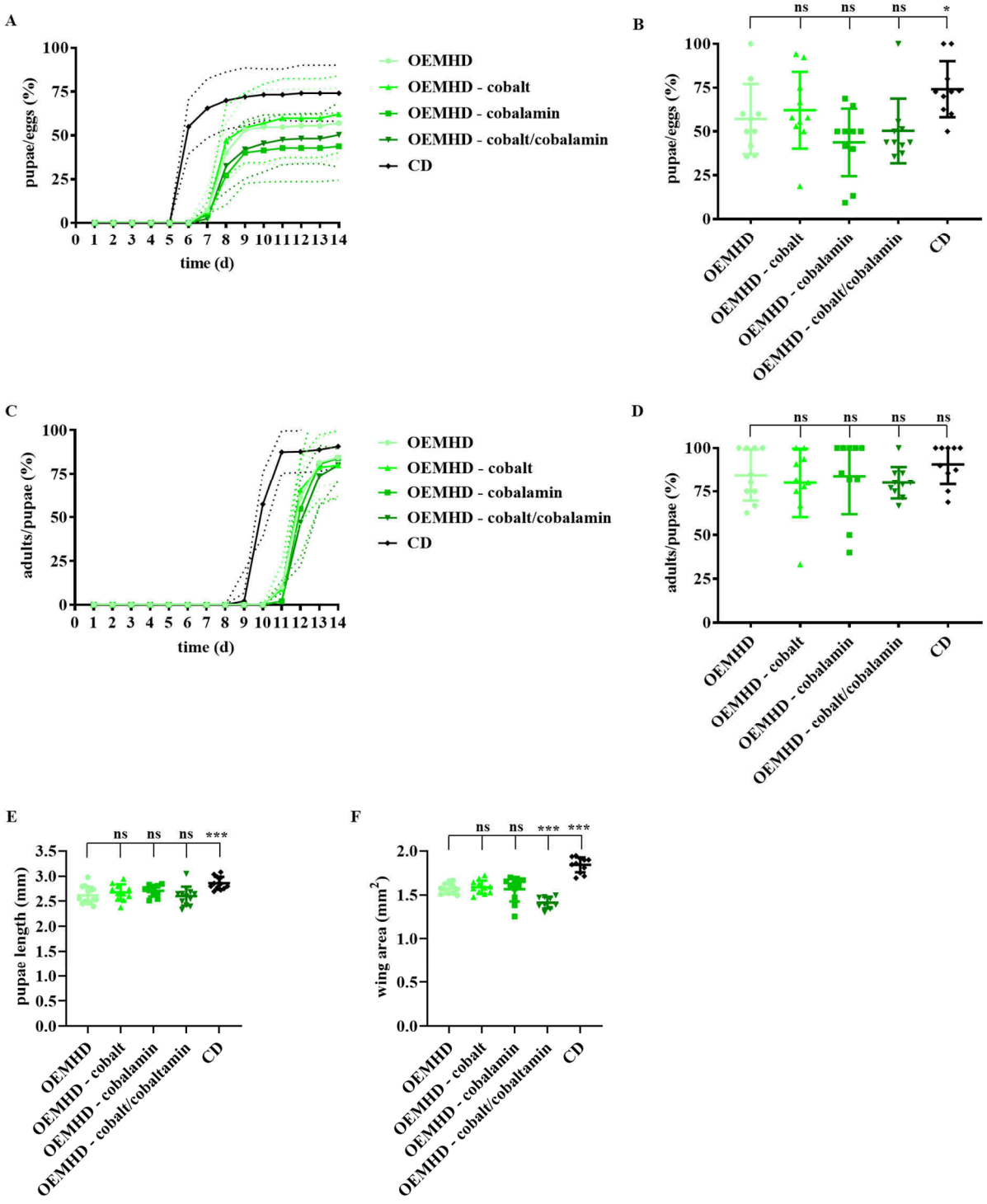

Fig. 35: Effect of cobalamin and cobalt on the development of OEMHD fed GF larvae. (A) Developmental time from egg to pupa of GF larvae fed an OEMHD or a complex diet, which served as a control diet (CD). Either Cobalt, Cobalamine or both were depleted from the OEMHD (n = 10). (B) Quantification of the pupation rate (n = 10). (C) Developmental time from egg to adult of GF larvae fed one of the indicated diets (n = 10). (D) Quantification of the eclosion rate (n = 10). (E) Quantification of the pupae length (n = 10). (F) Quantification of the wing area of adult GF flies (n = 9-11). OEMHD: optimized exom-matched holidic diet, CD: control diet, ns: not significant, *p < 0.05.

4.2.7 Fitness parameters of an OEMHD and an EMHD

I compared fitness parameters like, protein content, adult weight, metabolic rate, fecundity and locomotor activity between an OEMHD and an EMHD. The protein content, the adult weight and the metabolic rate of adult flies fed an OEMHD or an EMHD for 7 days were analyzed. The protein content as well as the adult weight was significantly increased in flies fed an OEMHD in comparison to flies fed an EMHD (Fig. 36, A and B). Furthermore, OEMHD fed flies revealed an increased metabolic rate compared to flies fed an EMHD (Fig. 36, C). The fecundity was determined on 8 days after 1 female fly was mated with 5 male flies on the respective diet. The number of laid eggs was comparable between OEMHD fed flies and flies fed an EMHD (Fig. 36, D). No differences in circadian rhythmic and the total locomotor activity were detectable between flies fed an OEMHD and EMHD fed flies (Fig. 36, E and F). However, when feeding on an OEMHD adult flies died within 30 minutes when cultured in a sealed container. It is suggested that chloroform, the solvent of ergosterol, induced the observed phenotype.

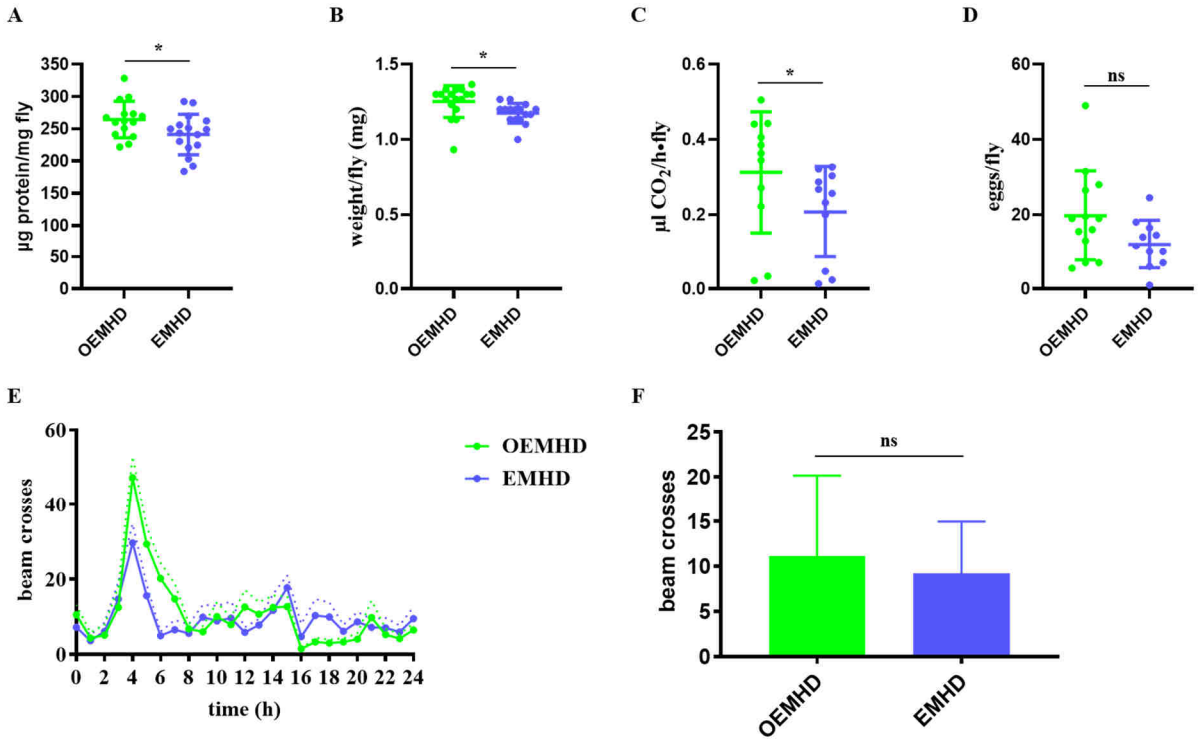

Fig. 36: **Fitness parameters of flies fed an OEMHD or an EMHD.** (A) Protein content of flies fed an OEMHD or an EMHD (n = 14-16). (B) The weight of adult OEMHD fed flies and EMHD fed flies (n = 14-16). (C) Metabolic rate of flies fed an OEMHD or an EMHD for 7 days (n = 11). (D) Number of laid eggs of female flies, 8 days after feeding an OEMHD or an EMHD (n = 11). (E) Circadian rhythm of flies fed on of the indicated diets (n = 24). (F) Total locomotor activity of adult flies fed an OEMHD or an EMHD (n = 24). OEMHD: optimized exom-matched holidic diet, EMHD: exom-matched holidic diet, ns: not significant, *p < 0.05.

4.2.8 Effect of ergosterol based diets on the development

It was shown that yeast-based complex *Drosophila* diets mainly contain ergosterol and only traces of cholesterol (267,268) Therefore, I examined if the supplementation of the EMHD with solely ergosterol is able to support the larval development. As chloroform lead to an increased the mortality of adult flies in sealed containers, I dissolved 80 mg/l ergosterol in 100 % butanol. Additionally, the ergosterol-based EMHD was supplemented with cobalt, cobalamin, molybdenum and ribonucleotides or combinations of them. The combinations and its associated abbreviations are listed in table 13. The developmental time from egg to pupa was increased in larvae fed an EMHD, an EMHD + E or an EMHD + EVM compared to flies fed an EMHD + EVMR. However, the developmental time of larvae fed an EMHD + EVMR was increased in comparison to larvae fed a sugar-yeast complex diet (SY, Fig. 37, A). The pupation rate of larvae fed an EMHD + EVMR was not significantly different compared to larvae fed an EMHD + EVM, an EMHD + E, an EMHD or a SY diet (Fig. 37, B). The developmental time from egg to adult was decreased in larvae fed an EMHD + EVMR in comparison to larvae fed an EMHD + E, an EMHD + EVM or an EMHD. Larvae fed a SY diet revealed an improved developmental time from egg to adult compared to larvae fed an EMHD, an EMHD + E, an EMHD +EVM or an EMHD + EVMR (Fig. 37, C). The eclosion rate was significantly increased in larvae fed an EMHD + EVMR compared to larvae fed and EMHD + E. No significant differences in the eclosion rate were observed between larvae fed an EMHD + EVMR and EMHD + EVM, EHMD or SY diet fed larvae (Fig. 37, D). The pupae length of larvae fed a SY diet was significantly increased in comparison to EMHD + EVMR fed larvae. The pupae length was comparable between EMHD + EVMR fed larvae and larvae fed an EMHD + E, an EMHD + EVM or an EMHD (Fig. 37, E). Interestingly, the wing area of adult flies was significantly smaller of flies fed an EMHD, EMHD + E or an EMHD +EVM in comparison to flies fed an

Table 13: EHMD supplemented with combinations of ergosterol, cobalt, cobalamin, molybdenum and ribonucleotides.

Abbreviation	Sterols	Cobalt Cobalamine Molybdenum	Ribonucleotides
EMHD	300 mg/l cholesterol	-	-
EMHD + E	300 mg/ml ergosterol	-	-
EMHD + EVM	300 mg/l ergosterol	+	-
EMHD + EVMR	300 mg/l ergosterol	+	2 g/l

EMHD +EVMR. The measurement of the wing area did not reveal significant differences between EMHD + EVMR fed flies and flies fed a SY diet (Fig. 37, F).

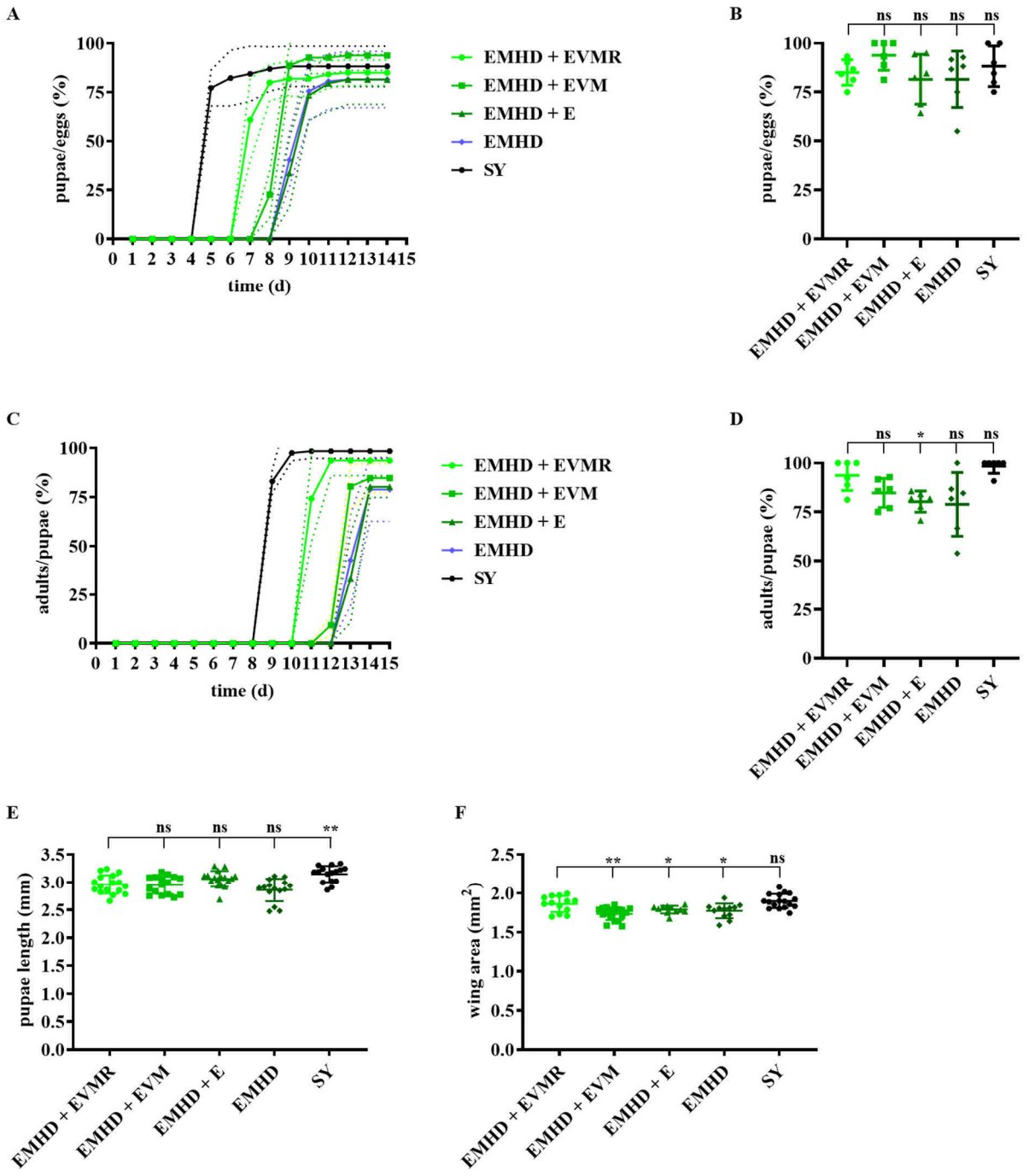

Fig. 37: Effect of ergosterol based diets on the developmental time, pupation rate, eclosion rate, pupae length and wing area. (A) Developmental time from egg to pupa of larvae fed an EMHD + EVMR, an EHMD + EVM, an EHMD + E, an EMHD or a SY diet (n = 6). (B) Quantification of the pupation rate (n =6). (C) Developmental time from egg to adult of larvae fed one of the indicated diets (n =6). (D) Quantification of the eclosion rate (n =6). (E) Pupae length of larvae fed an EMHD + EVMR, an EHMD + EVM, an EHMD + E, an EMHD or a SY diet (n = 15-16). (F) Quantification of the wing area of adult flies fed for 7 days on of the indicated diets (n = 11-18). SY: sugar-yeast, EMHD: exom-matched holidic diet, E: ergosterol, VM: vitamin mineral, R: ribonucleotides, ns: not significant, *p < 0.05, **p < 0.01.

4.3 Effect of DR and PEM on epithelia-microbe interactions in the intestine of *Drosophila*

Dietary restriction (DR) is linked with a plethora of health promoting effects (72,269), whereas protein-energy malnutrition (PEM) is associated to range of pathological conditions (44). However, little is known about the impact of DR or PEM on the cellular homeostasis as well as about the function of the intestinal microbiota under chronic protein shortage. Therefore, I used the OHD (chapter 5.2.1) as a basis to design diets with following protein:carbohydrate (PC) ratios: PC 1:75, PC 1:16 and PC 0:1. The OHD with a PC 1:2 ratio served as a control diet (CD), the OHD with a PC 1:16 represented a DR, whereas the OHD with a PC 0:1 ratio represented a PEM. These diets were used to examine the effect of a 14 days long-term intervention with amino acid-restricted diets on host-microbe interactions in the *Drosophila* intestine. Unless otherwise stated, yw flies were used for all the experiments.

4.3.1 Effect of DR and PEM on lifespan

DR is associated with a prolonged lifespan in *Drosophila*, whereas PEM is linked to increased mortality (102). I performed lifespan experiments to validate that the designed DR and PEM based on the OHD leads to its aforementioned phenotype in comparison to a CD. Indeed, the lifespan of flies fed a DR diet was increased compared to flies fed a CD with a median lifespan of 90 days and 65 days, respectively. On the other hand, the lifespan of PEM fed flies was significantly decreased compared to CD fed flies with a median lifespan of 48 days and 65 days, respectively (Fig. 38).

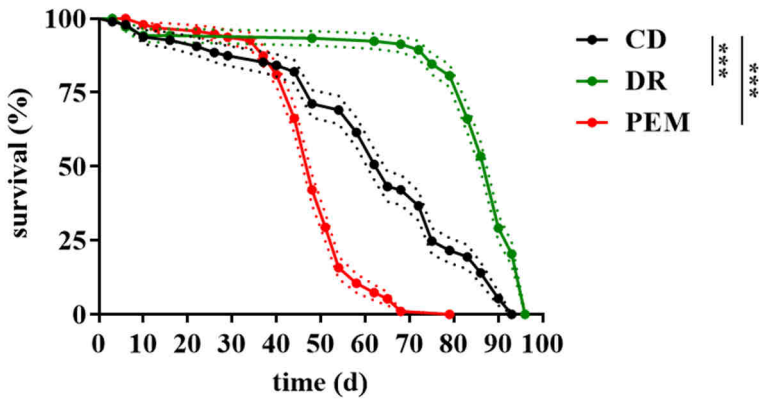

Fig. 38: Impact of a DR diet and a PEM on the lifespan. Lifespan of flies fed a CD, a DR diet or a PEM diet (~x_{CD} = 65 days, ~x_{DR} = 90 days, ~x_{PEM} = 48 days, n = 100). CD: control diet, DR: dietary restriction, PEM: protein-energy malnutrition, ***p < 0.001.

4.3.2 Impact of DR and PEM on the body composition of *Drosophila*

Next, I investigated the impact of DR and PEM on the fly's body compositions such as protein content, TGA content and weight. Flies fed a CD revealed a significant higher protein content than flies subjected to DR or PEM (Fig. 39, A). The TAG content of flies fed either a CD, DR diet or PEM diet was not affected (Fig. 39, B). Flies subjected to DR or PEM showed a significant decreased body weight compared to control dieting flies (Fig. 39, C).

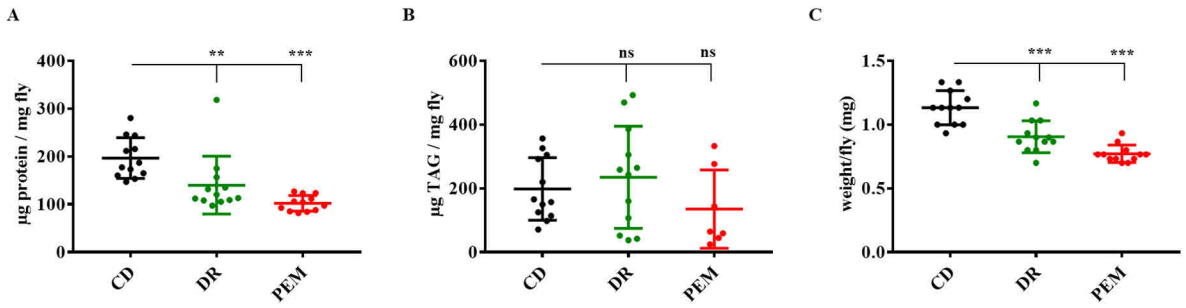

Fig. 39: Body composition of flies subjected to DR or PEM. (A) Protein content of flies fed either a CD, DR diet or PEM diet (n = 12). (B) TAG content of flies fed with the indicated diets (n = 8-12). (C) Weight of flies subjected to a CD, DR or PEM diet (n = 12). CD: control diet, DR: dietary restriction, PEM: protein-energy malnutrition, TAG: triacylglyceride, ns: not significant, **p < 0.01, ***p < 0.001.

4.3.3 Amino acid-restricted diets and the microbiota affects the intestinal morphology

The length as well as the width of the intestine was measured in order to examine the effect of an amino acid-restricted diet and of the microbiota on intestinal structure. The length of the gut was shortened in RC flies subjected to DR or PEM in comparison to RC flies fed a CD. Moreover, RC flies fed a CD or a DR diet revealed significantly longer guts compared to GF

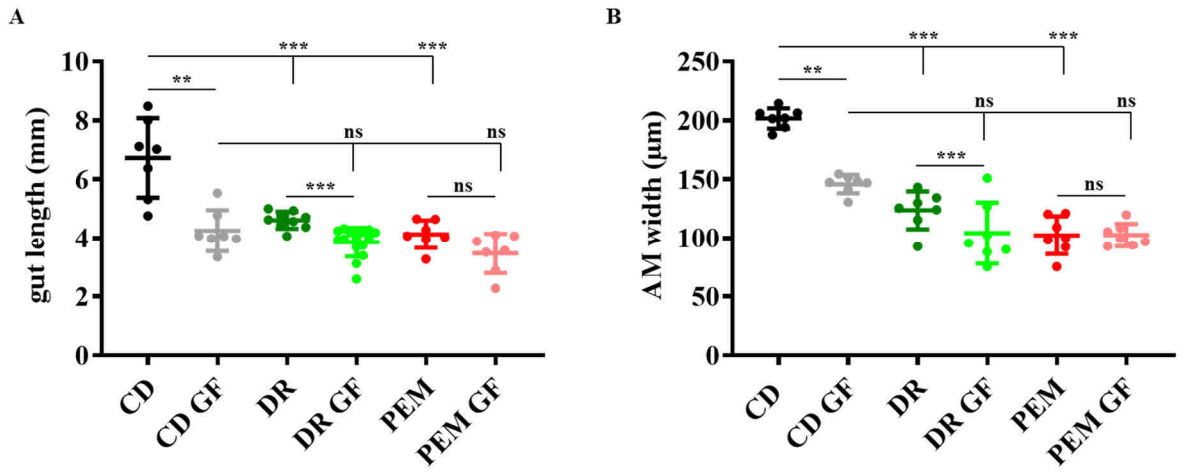

Fig. 40: The intestinal length and width of RC and GF flies fed a CD, DR diet or PEM diet. (A) The gut length of RC and GF flies fed a CD, DR diet or PEM diet (n = 7-15). (B) The anterior midgut width of RC and GF flies subjected to a CD, DR or PEM (n = 7). RC: reconstituted, GF: germ-free, CD: control diet, DR: dietary restriction, PEM: protein-energy malnutrition, AM: anterior midgut, ns: not significant, **p < 0.01, ***p < 0.001.

flies fed the respective diet. No significant differences in the length of the intestine were observed between GF flies subjected to PEM and RC flies fed the equivalent diet. The length of the intestine between GF flies treated with CD, DR or PEM was comparable (Fig. 40, A). The width of the anterior midgut was significantly thicker in flies fed a CD compared to DR or PEM treated flies. GF flies fed a CD or a DR diet examined thinner anterior midguts in comparison to RC flies subjected to a CD or DR, respectively. The anterior midgut width was comparable between RC and GF PEM treated flies. No significant differences in the gut width were detectable between GF flies fed a CD, DR diet or PEM diet (Fig. 40, B).

4.3.4 Impact of the microbiota and dietary amino acid-restriction on the intestinal proliferation

The esg>GFP reporter line was used to examine the influence of a amino acid-restricted diet on the intestinal proliferation. Furthermore, RC and GF esg>GFP flies were compared to reveal the impact of the intestinal microbial community on the ISC proliferation on amino acid restricted diets. The number of esg$^+$ cells in the anterior midgut of RC esg>GFP flies decreases

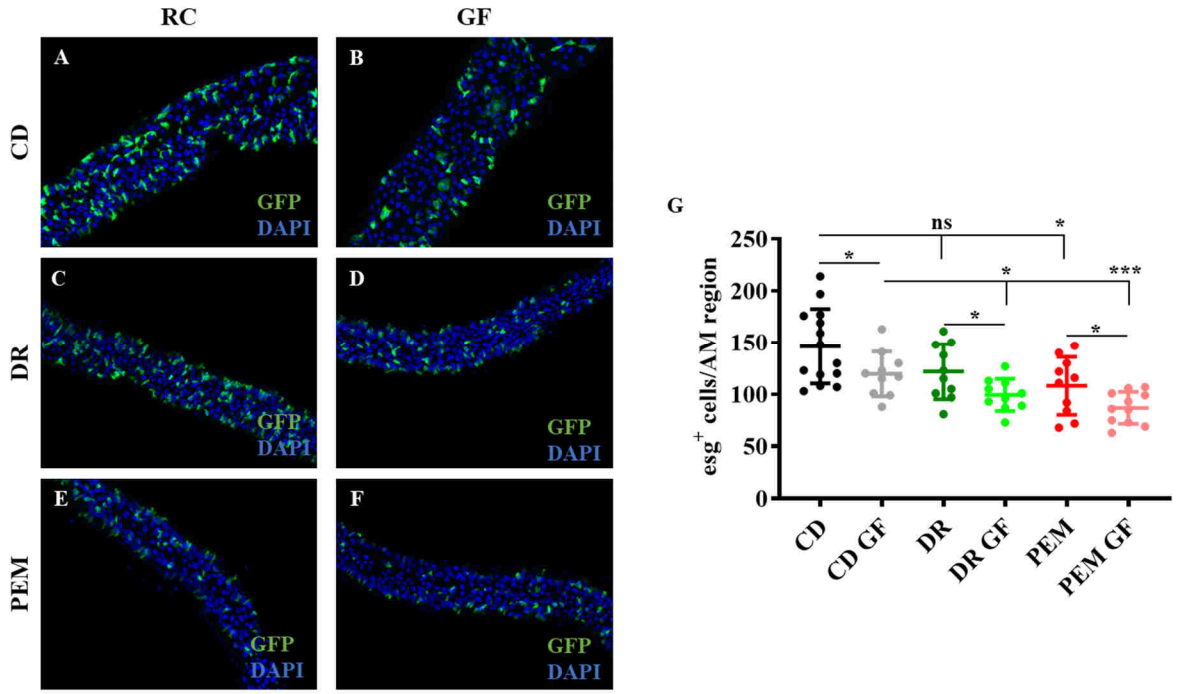

Fig. 41: Impact of amino acid-restricted diets and of the microbiota on the intestinal proliferation. (A-F) Representative images of anterior midgut regions of RC and GF esg>GFP flies either fed a CD, DR or a PEM. The number of esg$^+$ cells (GFP) decreases with lowering the amino acid content in the diet in RC and GF esg>GFP flies. GF esg>GFP flies fed a CD, DR or a PEM revealed lower proliferation of esg$^+$ cells compared to RC esg>GFP flies fed the respective diet. (G) Quantitative analysis of the number of esg$^+$ cells in RC and GF esg>GFP flies fed a CD, DR diet or PEM diet (n = 10-14). RC: reconstituted, GF: germ-free, CD: control diet, DR: dietary restriction, PEM: protein-energy malnutrition, esg: escargot, GFP: green fluorescent protein, AM: anterior midgut, ns: not significant, *p < 0.05, ***p < 0.001.

with lowering the amino acid content in the diet (Fig. 41, A, C and E). GF esg>GFP flies fed a CD, DR diet or PEM diet revealed a lower number of esg$^+$ cells in comparison to RC esg>GFP flies fed the equivalent diet (Fig. 41, A-F). The number of esg$^+$ cells was decreased in GF esg>GFP flies subjected to DR or PEM compared to GF esg>GFP flies fed a CD (Fig. 41, B, D and F). The quantitative analysis of esg$^+$ cells in the anterior midgut of the fly's intestines further support these observations (Fig. 41, G).

4.3.5 Amino acid-restricted diets and microbes affect the number of EECs

The number of EECs were revealed by an anti-prospero staining to examine the effect of a long-term intervention of amino acid-restriction on the cellular composition of the anterior midgut. The number of EECs in the anterior midgut was decreased in RC flies subjected to DR or PEM in comparison to RC flies fed a CD (Fig. 42, A, C and E). Interestingly, DR or PEM treated GF flies showed an increased number of EECs compared to RC flies fed a DR diet or PEM diet (Fig. 42, A-B and C-D). RC flies fed a PEM diet and PEM subjected GF flies revealed a comparable number of EECs (Fig. 42, E-F). The number of EECs was increased in GF flies fed a CD compared to GF flies subjected to DR and PEM (Fig. 42, B, D and F). These observations

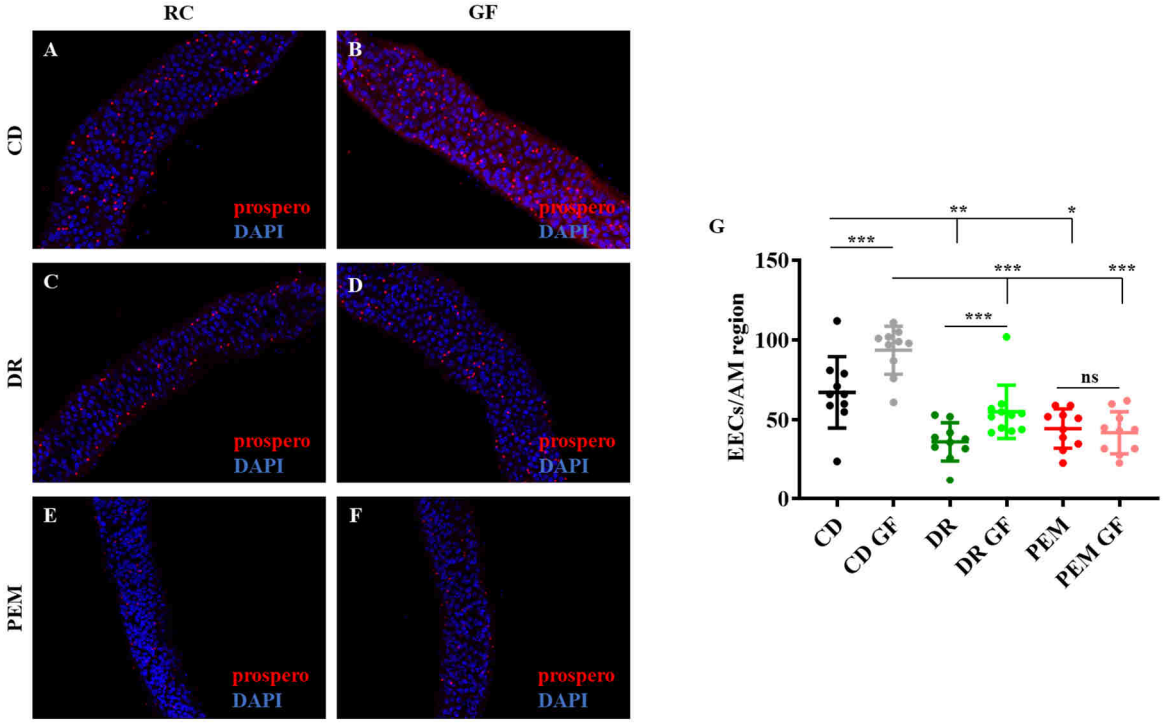

Fig. 42: The number of EEC of RC and GF flies fed a CD, DR diet or PEM diet. (A-F) Representative images of anterior midgut regions of RC and GF flies fed a CD, a DR diet or a PEM diet. The intestines were stained with an anti-prospero antibody to detect EECs. (G) Quantitative analysis of the number of EECs in the anterior midgut region of CD, DR or PEM treated RC and GF flies (n = 10-12). RC: reconstituted, GF: germ-free, CD: control diet, DR: dietary restriction, PEM: protein-energy malnutrition, EEC: enteroendocrine cell, AM: anterior midgut, ns: not significant, *p < 0.05, **p < 0.01, ***p < 0.001.

were further supported by a quantitative analysis of the number of EECs in the anterioir midgut of RC and GF flies fed a CD, DR diet or PEM diet (Fig. 42, G).

4.3.6 Amino acid-restricted diets and the microbiota alters EC size

Next, I investigated the influence of the microbiota as well as of the amino acid-restricted diets on the EC distance and EC size. The EC distance was calculated by measuring the nearest neighbor distance of the nuclei centroids of ECs via ImageJ (Fig. 43, A). The EC distance of RC flies fed a CD was significantly decreased in comparison to RC flies fed a PEM diet. No significant differences were observed between RC flies fed a CD and DR treated RC flies. GF flies fed a CD or a DR diet revealed a decreased EC distance in comparison to RC flies fed the respective diet. The EC distance of RC flies and GF flies subjected to PEM was comparable. No differences in the EC distance were observed between GF flies fed either a CD, DR diet or a PEM diet (Fig. 43, B). The EC size was evaluated by measuring the EC area surrounded by the cell membrane. Therefore, the intestines were stained with an anti-coracle antibody, which marks septate junctions within the cell membrane. Interestingly, the EC area was increased in RC flies fed a CD in comparison to RC flies subjected to DR or PEM (Fig. 43, C-E). The

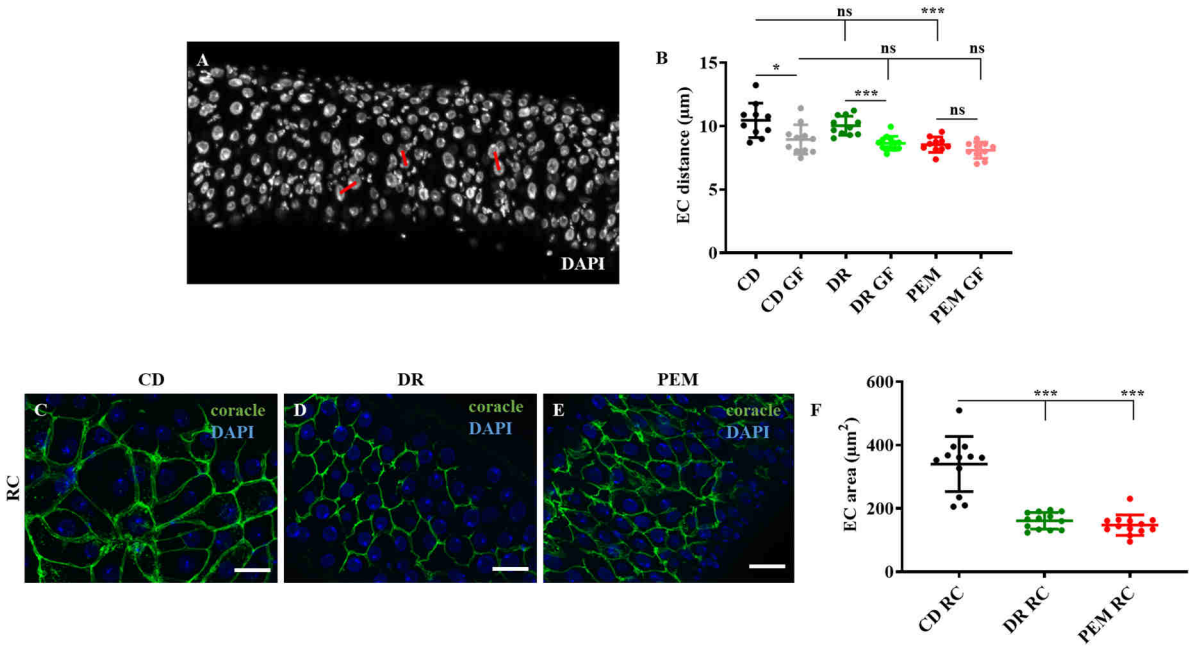

Fig. 43: EC distance and EC area of flies fed a CD, DR diet or PEM diet. (A) Representative image of an intestine stained with DAPI. The nearest neighbor distance of nuclei centroids (indicated by red lines) of ECs were analyzed via ImageJ. (B) Quantitative analysis of the EC distance of RC and GF flies fed either a CD, DR diet or PEM diet (n = 10-13). (C) Representative images of intestines of RC flies fed with the indicated diets. The intestines were stained with an anti-coracle antibody to mark the cell membranes (scale bar = 20 µm). (F) Quantitative analysis of the EC area of RC flies a CD, DR diet or PEM diet (n = 12-13). RC: reconstituted, GF: germ-free, CD: control diet, DR: dietary restriction, PEM: protein-energy malnutrition, EC: enterocyte, ns: not significant, *p < 0.05, ***p < 0.001.

quantitative analysis revealed a significantly increased EC area in RC flies fed a CD compared to RC flies fed a DR diet or PEM diet (Fig. 43, F).

4.3.7 Intestinal transcriptomic analysis of DR and PEM subjected RC flies

I performed an RNA-seq analysis, in order to examine the coding transcriptomic profile of midguts of RC flies fed a CD, DR diet or PEM diet for 14 days. For each dietary treatment, 50 – 70 midguts were collected in 4 replicates each. The PCoA of differential regulated genes (DEGs) showed 3 main clusters between RC flies fed a CD, a DR diet or a PEM diet. Each data point represents a single biological replicate (Fig. 44, A). Differential expression analysis resulted in 76 genes that are specifically regulated in intestines of RC flies subjected to DR in comparison to RC flies fed a CD. Moreover, 6362 DEGs were detected in intestines of PEM treated RC flies compared to CD fed RC flies. The analysis also elucidated an overlap of 773 genes that were differentially regulated in intestines of DR and PEM treated RC flies compared to RC flies upon control dieting (Fig. 44, B). Gene ontology (GO) category enrichment analyses

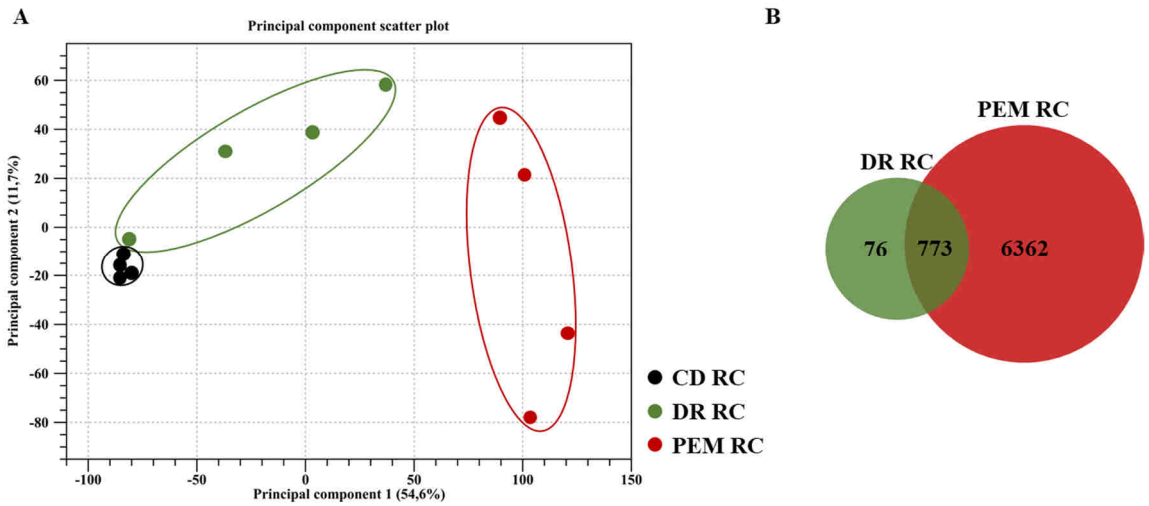

Fig. 44: DR and PEM transcriptomic signatures of intestines of RC flies. (A) PCoA plot for DEGs of intestines of RC flies fed either a DR diet or a PEM diet compared to RC flies fed a CD. Each datapoint represents a single biological replicate. (B) Venn Diagram of DEGs of DR or PEM specific signatures in the intestines of RC flies. The following comparisons are illustrated: DR RC vs. CD RC and PEM RC vs. CD RC. RC: reconstituted, CD: control diet, DR: dietary restriction, PEM: protein-energy malnutrition, DEG: differentially expressed gene, FDR = 0.05.

were performed for each comparison (DR RC vs. CD RC and PEM RC vs. CD RC). In the intestine of RC flies fed a DR diet were significantly upregulated DEGs, belong to biological processes (BPs) like translation, response to bacterium, innate immune response, glucose import or transmembrane transport (Fig. 45, A). On the other hand, DR-specific downregulated DEGs belong to BPs such as determination of life span, regulation of JAK-STAT cascade, lipid homeostasis, carbohydrate metabolism or mannose metabolic metabolism (Fig. 45, B).

Processes like proteolysis, cytoplasmic translation, RNA methylation, mitochondrial translation or ATP (adenosine triphosphate) metabolic process were significantly upregulated in RC flies subjected to PEM (Fig. 45, C). In RC flies fed a PEM, processes such as regulation of glucose metabolism, regulation of cell shape, regulation of cell proliferation, positive regulation of innate immune response, response to starvation, JNK cascade or transcription were downregulated (Fig. 45, D). All DEGs and BPs related to Fig. 44 and Fig. 45 are presented in Appendix A.

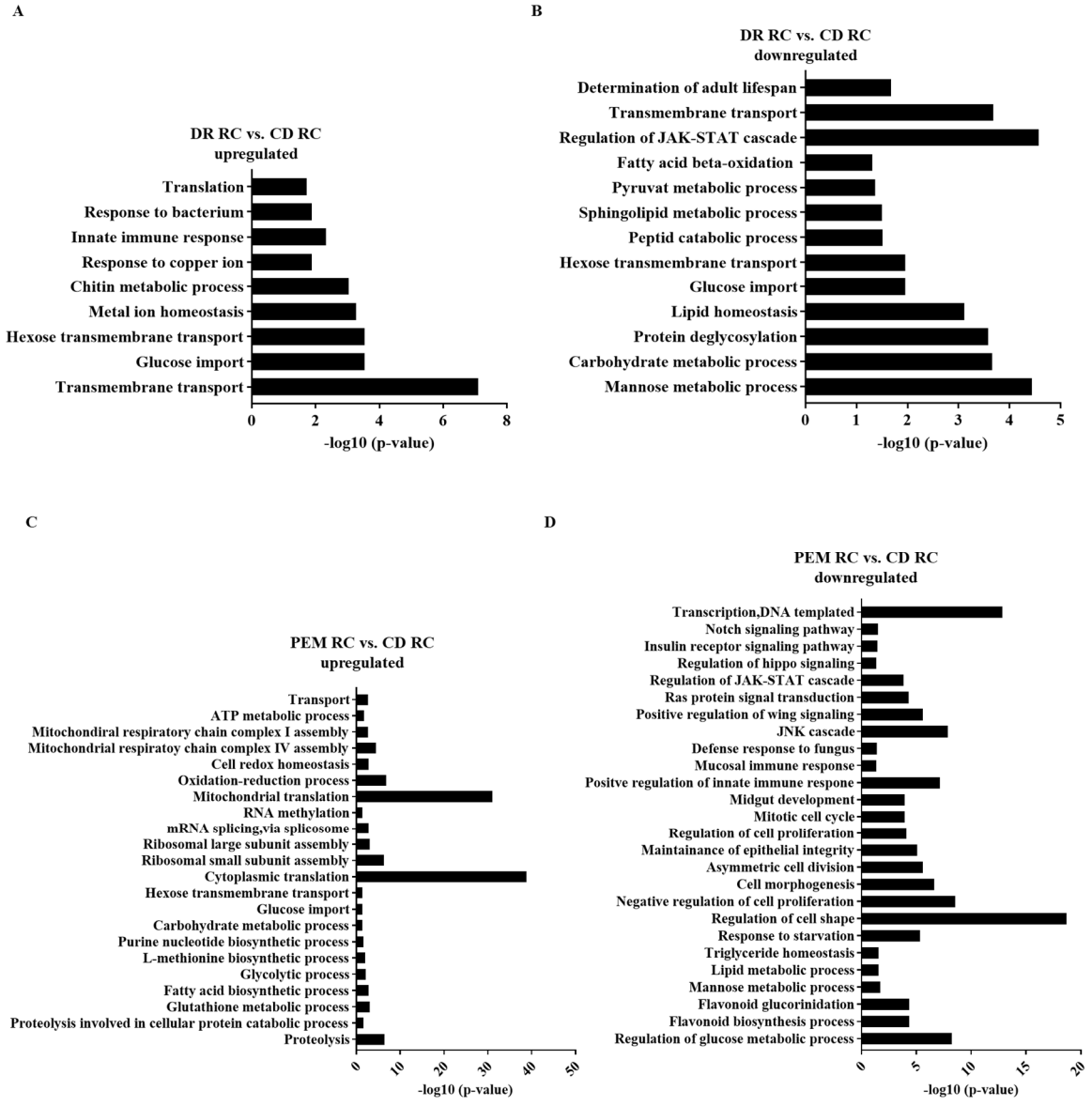

Fig. 45: Selected GO terms of DEGs in intestines of RC flies subjected to DR or PEM. (A-B) Selected GO terms (category: biological process) of significantly up- and downregulated DEGs in intestines of RC flies fed a DR diet (n = 4). (C-D) Selected GO terms (category: biological process) of up- and downregulated DEGs in intestines of PEM treated RC flies (n = 4). RC: reconstituted, CD: control diet, DR: dietary restriction, PEM: protein-energy malnutrition, DEG: differentially expressed gene.

4.3.8 Effect of amino acid restriction on the intestinal transcriptional landscape in GF flies

I performed RNA-Seq analysis in order to reveal exclusive effects of amino acid restriction on the transcriptional landscape of the intestine. Therefore, I compared GF flies subjected to DR or PEM with GF flies fed a CD to remove microbial signatures in the analysis. The PCoA of DEGs revealed 3 separated main clusters between GF flies fed either a CD, DR or PEM diet (Fig. 46, A). Differential expression analysis resulted in 257 DEGs that are specifically regulated in GF flies subjected to DR in comparison to GF CD fed flies. Moreover, 5883 DEGs were expressed in the intestine of GF flies fed a PEM diet compared to GF flies upon control dieting. The analysis revealed an overlap of 427 DEGs that are regulated in GF flies subjected to DR and PEM in comparison to GF flies fed a CD (Fig. 46, B).

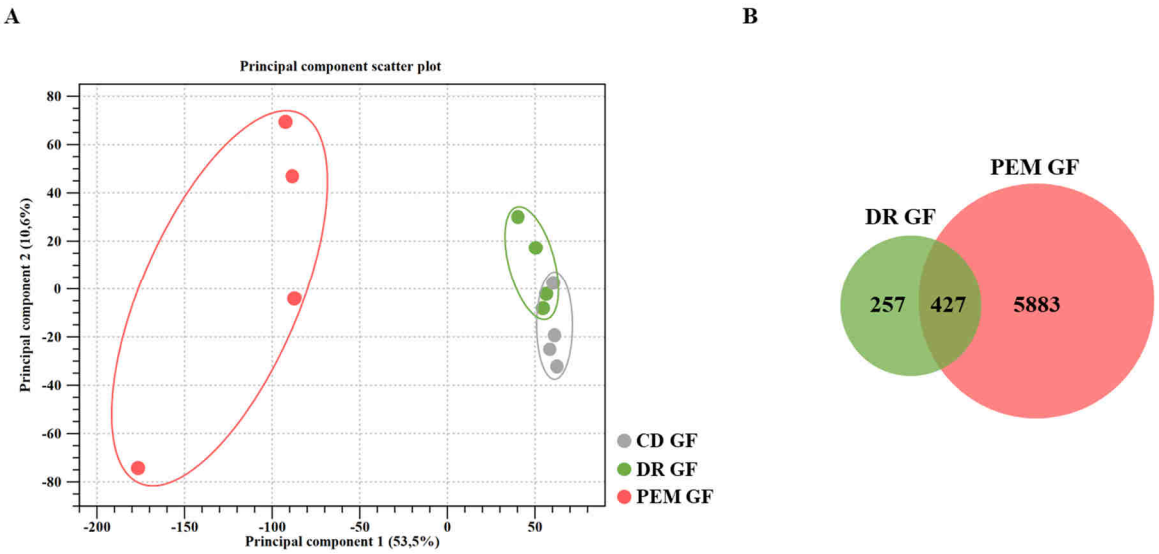

Fig. 46: DR and PEM transcriptomic signatures of intestines of GF flies. (A) PCoA plot for DEGs of intestines of GF flies fed either a DR diet or a PEM diet compared to GF flies fed a CD. Each datapoint represents a single biological replicate. (B) Venn Diagram of DEGs of DR or PEM specific signatures in the intestines of GF flies. The following comparisons are illustrated: DR GF vs. CD GF and PEM GF vs. CD GF. GF: germ-free, CD: control diet, DR: dietary restriction, PEM: protein-energy malnutrition, DEG: differentially expressed gene, FDR = 0.05.

GO category enrichment analysis were performed for each comparison (DR GF vs. CD GF and PEM GF vs. CD GF). Processes such as response to unfolded protein, lipid metabolic process or glutathione metabolic process were significantly upregulated in GF flies subjected to DR in comparison to GF flied fed a CD (Fig. 47, A). In intestines of GF flies BPs like carbohydrate metabolic process, Toll signaling pathway, proteolysis or lipid catabolic process were downregulated in comparison CD fed GF flies (Fig. 47, B). Processes such as mitochondrial translation, cytoplasmic translation, apoptotic process or cellular response to starvation were significantly upregulated in intestines of GF flies subjected to PEM compared to GF flies fed a CD (Fig. 47, C). On the other hand, processes like regulation of cell shape, transcription, protein

phosphorylation, regulation of JAK/Stat cascade, JNK cascade, carbohydrate metabolic process or immune response were significantly downregulated in intestine of GF flies fed a PEM diet in comparison to GF flies upon control dieting (Fig. 47, D). All DEGs and BPs related to Fig. 46 and Fig. 47 are presented in Appendix B.

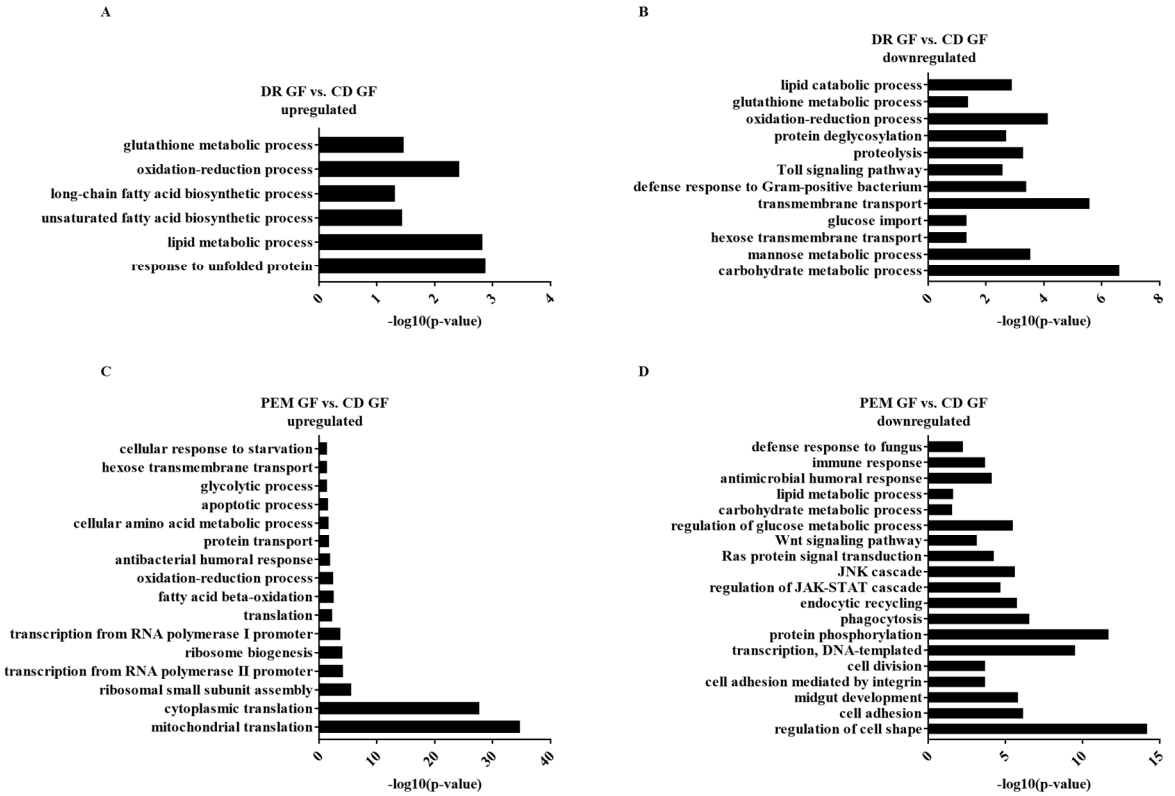

Fig. 47: Selected GO terms of DEGs in intestines of GF flies subjected to DR or PEM. (A-B) Selected GO terms (category: biological process) of significantly up- and downregulated DEGs in intestines of GF flies fed a DR (n = 4). (C-D) Selected GO terms (category: biological process) of up- and downregulated DEGs in intestines of PEM treated GF flies (n = 4). GF: germ-free, CD: control diet, DR: dietary restriction, PEM: protein-energy malnutrition, DEG: differentially expressed gene.

4.3.9 Influence of the microbiota on the intestinal transcriptional landscape

Furthermore, I used RNA-seq analysis to reveal the impact of the microbiota on the intestinal transcriptional regulation of genes upon interventions of amino acid-restriction. The PCoA of DEGs unveiled 6 main clusters between RC and GF flies fed a CD, DR diet or PEM diet. Interestingly, the dissimilarities between the clusters of RC flies and GF flies became larger the lower the protein content in the diet (Fig. 48, A). This is supported by the number of significantly DEGs, which are specifically regulated by the microbiota on the respective diet. 120 genes were differentially expressed in intestines of GF flies fed a CD in comparison to RC flies upon control dieting. In the intestines of GF flies subjected to DR, 303 genes were

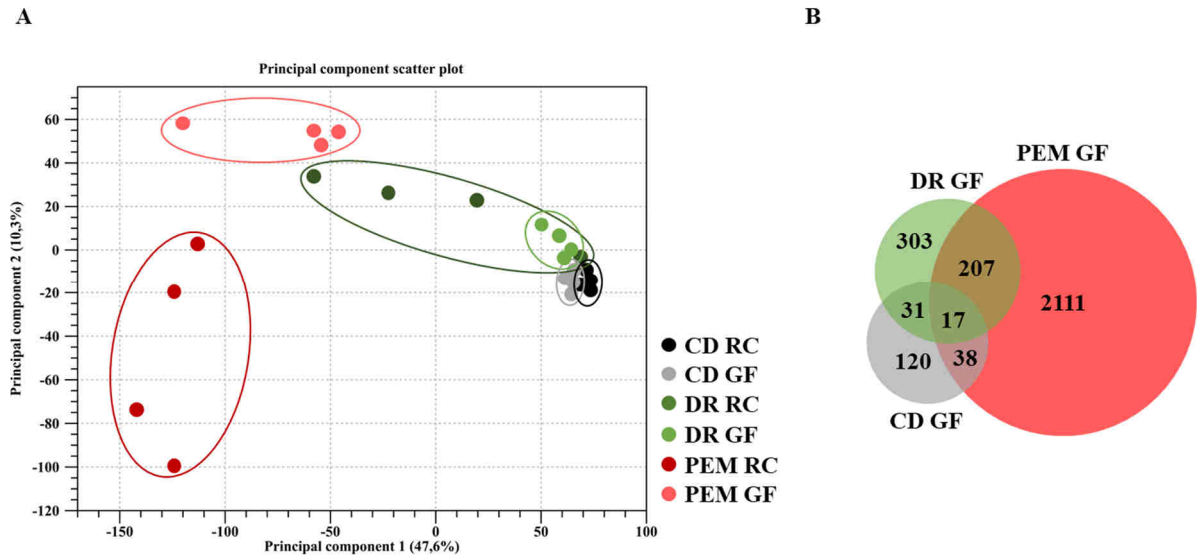

Fig. 48: Microbiota-associated intestinal transcriptional signatures of flies fed a CD, DR or PEM diet. (A) PCoA plot for DEGs of intestines of GF flies fed either a CD, DR diet or PEM diet compared to flies fed an equivalent diet. Each datapoint represents a single biological replicate. (B) Venn Diagram of DEGs of GF specific signatures upon control dieting, DR dieting or PEM dieting in the intestines of flies. The following comparisons are illustrated: CD GF vs. CD RC, DR GF vs. DR RC and PEM GF vs. PEM RC. RC: reconstituted, GF: germ-free, CD: control diet, DR: dietary restriction, PEM: protein-energy malnutrition, DEG: differentially expressed gene, FDR = 0.05.

differentially expressed compared to RC flies fed a DR diet. 2111 genes were specifically regulated in intestines of GF flies fed a PEM diet in comparison to RC flies subjected to PEM. Noteworthy, GF flies fed a CD, DR diet or PEM diet revealed an overlap of only 17 genes (Fig. 48, B). GO category enrichment analysis were performed for each comparison (CD GF vs. CD RC, DR GF vs. DR RC, PEM GF vs. PEM RC). BPs such as mannose metabolic process, lipid catabolic process, transmembrane transport or protein deglycosylation were significantly upregulated in intestines of GF flies fed a CD compared to RC flies upon control dieting (Fig. 49, A). On the other hand, BPs like carbohydrate metabolic process, determination of life span, cellular response to unfolded protein and negative regulation of cell growth are downregulated in GF flies fed a CD in comparison to CD fed RC flies (Fig. 49, B). In intestines of GF flies

subjected to DR BPs such as mannose metabolic process, lipid catabolic process, transmembrane transport or amino acid transport were significantly upregulated compared to

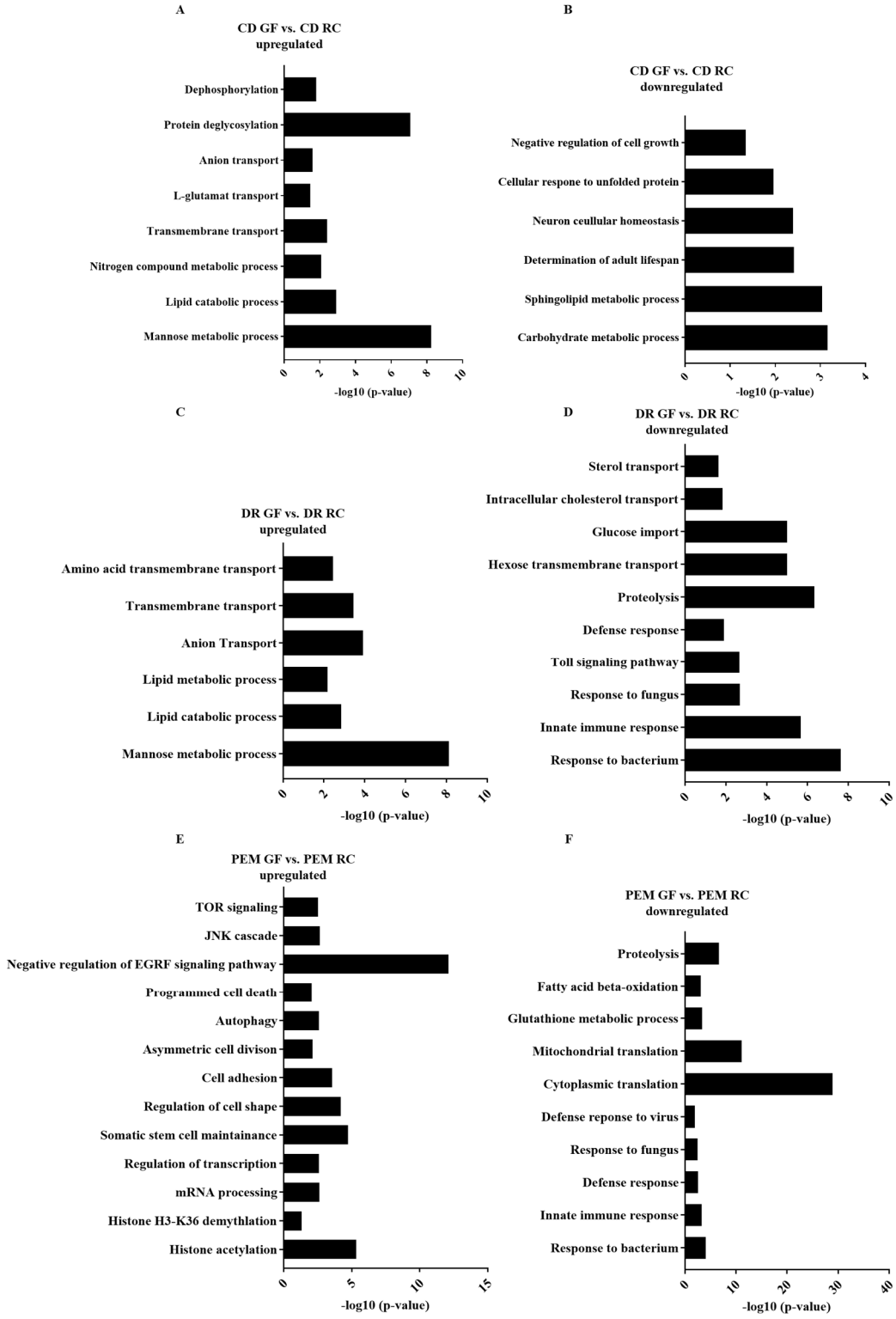

Fig. 49: Selected GO terms of microbiota associated DEGs in intestines of flies fed a CD, DR or PEM diet. (A-B) Selected GO terms (category: biological process) of significantly up- and downregulated DEGs in intestines of GF flies fed a CD (n = 4). (C-D) Selected GO terms (category: biological process) of up- and downregulated DEGs in intestines of DR treated GF flies (n = 4). (E-F) Selected GO terms (category: biological process) of up- and downregulated DEGs in intestines of PEM treated GF flies (n = 4). RC: reconstituted, GF: germ-free, CD: control diet, DR: dietary restriction, PEM: protein-energy malnutrition, DEG: differentially expressed gene.

RC flies fed a DR diet (Fig. 49, C). BPs like response to bacterium, innate immune response, proteolysis, glucose import or intracellular cholesterol transport were upregulated in DR treated GF flies in comparison to RC flies fed a DR diet (Fig. 49, D). In intestines of GF flies fed a PEM diet BPs such as histone acetylation, histone H3-K36 demethylation, regulation of transcription, somatic stem cell maintenance, asymmetric cell division, programmed cell death, JNK cascade or Tor signaling were significantly upregulated compared to RC flies subjected to PEM (Fig. 49, E). In PEM treated GF flies BPs like response to bacterium, innate immune response, cytoplasmic translation, mitochondrial translation, glutathione metabolic process and proteolysis are downregulated in comparison to RC flies fed a PEM diet (Fig. 49, F). All DEGs and BPs related to Fig. 48 and Fig. 49 are presented in Appendix C. A comparison of the RNA concentration of intestines, it was noticeable that amino acid-restriction led to a significantly decreased RNA amount in RC flies subjected to DR or PEM compared to RC flies fed a CD. The amount of RNA per intestine was increased in GF flies fed a DR diet compared to DR treated RC flies. No significant differences in the RNA amount were observed in GF flies fed a CD or DR diet in comparison to RC flies fed the equivalent diet. GF flies fed a CD revealed an increased RNA amount in comparison to GF flies subjected to DR or PEM (Fig. 50, A). To further validate these findings, I analyzed the integrated fluorescence intensity of DAPI stained ECs as an indicator for ploidy, whereas it is suggested that higher polyploidy coincidences with an increased transcription rate (270). Indeed, the DAPI intensity was significantly reduced in RC flies subjected to PEM in comparison to RC flies fed a PEM diet. GF flies fed a CD or a

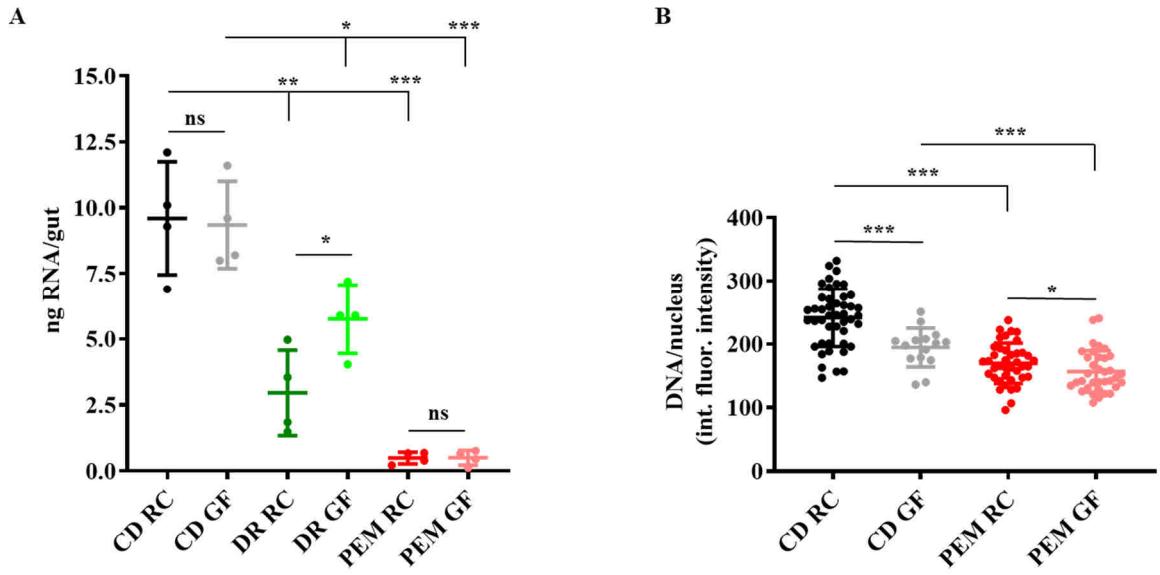

Fig. 50: RNA amount per intestine and EC DAPI intensity. (A) Measured RNA amount per intestine of RC flies and GF flies fed either a CD, DR diet or PEM diet (n = 4). (B) Integrated DAPI fluorescence intensity of ECs of RC flies and GF flies subjected to a CD, DR or PEM (n = 15-45). RC: reconstituted, GF: germ-free, CD: control diet, DR: dietary restriction, PEM: protein-energy malnutrition, ns: not significant, *p < 0.05, **p < 0.01, ***p < 0.001.

PEM diet revealed a decreased DAPI intensity compared to RC flies fed the equivalent diet. Likewise, GF flies upon control dieting exhibited a higher DAPI intensity than GF flies subjected to PEM (Fig. 50, B).

4.3.10 **Amino acid-restricted diets and microbes affect the nitrogen excretion**

An excess of amino acid intake leads to an increased amount of ammonia due to deamination processes. *Drosophila* is an uricothelic organism, which convert ammonia to uric acid. Therefore, the uric acid content is an indicator for consumed amino acids. RC flies fed a CD revealed an increased uric acid content in comparison to RC flies subjected to DR or PEM. Interestingly, GF flies fed either a CD, DR diet or PEM diet had a significantly decreased uric acid content compared to RC flies fed the equivalent diet. GF flies upon control dieting showed a higher uric acid content than GF flies subjected to DR or PEM (Fig. 51, A). I measured the uricase activity, to further proof if the diet and the microbiota also affect the enzymatic process of uric acid degradation. Indeed, RC flies subjected to DR or PEM revealed a significant decreased uricase activity in comparison to RC flies fed a CD. The uricase activity was also decreased in GF flies fed a CD compared to RC flies upon control dieting. However, the uricase activity was comparable between GF flies fed a DR diet or PEM diet and RC flies fed the respective diet. No differences in uricase activity were detected in GF flies subjected to DR or PEM compared to GF flies fed a CD (Fig. 51, B).

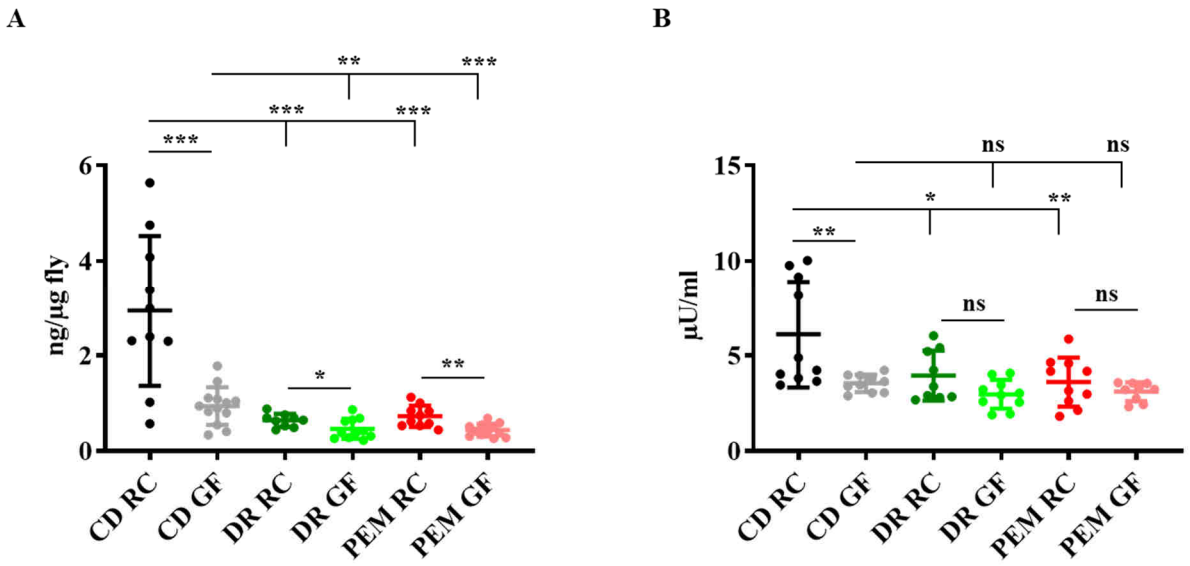

Fig. 51: Uric acid content and uricase activity of RC and GF flies fed amino acid-restricted diets. (A) Uric acid content of RC flies or GF flies fed either a CD, DR diet or PEM diet (n = 9-13). (B) Uricase activity of whole fly lysates subjected to a CD, DR or PEM (n = 9-10). RC: reconstituted, GF: germ-free, CD: control diet, DR: dietary restriction, PEM: protein-energy malnutrition, ns: not significant, **p < 0.01, **p < 0.01***p < 0.001.

4.3.11 Amino acid-restricted diets affect infection susceptibility and intestinal barrier function

The RNA-seq analysis revealed that the immune response is diminished in flies fed an amino acid-restricted diets (chapter 4.3.6). I performed an infection assay to check if this diminished transcription of immune genes manifest in a phenotype. Therefore, RC flies were fed for 1 week with either a CD, DR diet or PEM diet. Afterwards, the flies got a daily oral infection with *S. marcescens* (OD_{600} = 1) until they deceased. The survival rate of RC flies fed a CD was significantly higher compared to RC flies subjected to DR or PEM (Fig. 52, A). I performed a smurf assay to examine if this increased infection susceptibility was also due to a disturbed intestinal integrity. Therefore, 70-100 flies were fed with either a CD, DR diet or PEM diet for 2 weeks. Surprisingly, RC flies subjected to DR revealed an increased intestinal integrity compared to RC flies fed a CD. However, PEM treated RC flies had a significantly decreased intestinal integrity in comparison to RC flies upon control dieting. No significant differences in intestinal integrity could be observed between RC flies and GF flies fed either a CD, DR diet or PEM diet. Moreover, the intestinal integrity was not altered between GF flies subjected to a CD, DR or PEM (Fig. 52, B).

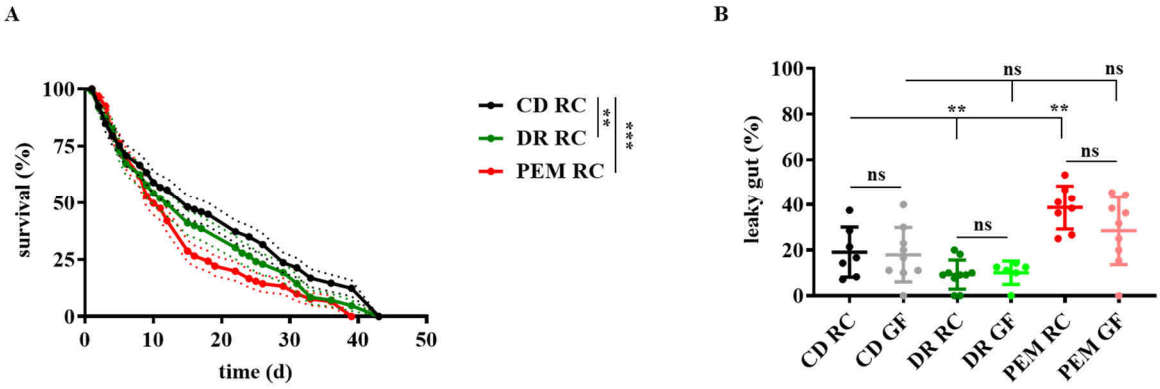

Fig. 52: Infection susceptibility and gut integrity of flies subjected to a CD, DR or PEM. (A) Infection assay of flies that were fed for 1 week with either a CD, DR diet or PEM diet. Flies got an daily oral infection with *S. marcescens* (OD_{600} = 1, ~$x_{CD\ RC}$ = 15 days, ~$x_{DR\ RC}$ = 12 days, ~$x_{PEM\ RC}$ = 10 days, n = 100). (B) Intestinal integrity of RC flies and GF flies subjected to a CD, DR or PEM for 2 weeks (N = 7-10). RC: reconstituted, GF: germ-free, CD: control diet, DR: dietary restriction, PEM: protein-energy malnutrition, ns: not significant, **p < 0.01, **p < 0.01, ***p < 0.001.

4.3.12 **PEM dieting affect the intestinal microbial composition**

To examine the effect of PEM dieting on the intestinal microbiota, I compared the microbial composition between flies fed a CD and those subjected to PEM. The most abundant phylum of CD fed flies were *Firmicutes*, whereas PEM dieting led to an increased abundance of *Proteobacteria* (**Fig. 53**, A). The altered microbial community was also illustrated by the separation in beta diversity, which was evaluated by a PcoA based on unweighted UNIFRAC (**Fig. 53**, B). However, flies subjected to PEM did not reveal an increased intestinal bacterial load in comparison to CD fed flies (**Fig. 53**, C).

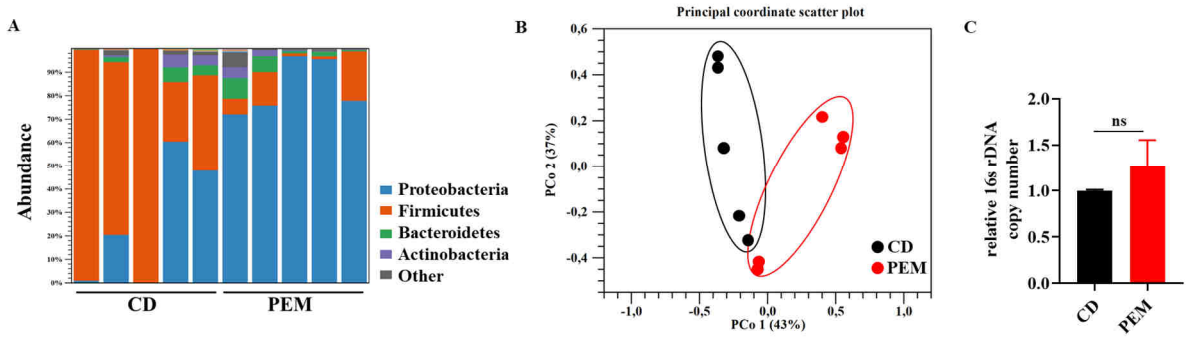

Fig. 53: Effect of PEM dieting on the microbial community and bacterial abundance. (A) Abundance table of the microbial composition of flies fed a CD or PEM diet (n = 5). (B) Principal coordinate analysis revealed a significant shift in the microbial community upon PEM dieting compared to flies fed a CD (n = 5). (C) Bacterial load of PEM subjected flies in comparison to CD fed flies (n = 5). CD: control diet, PEM: protein-energy malnutrition, PCoA: principal coordinate analysis.

4.3.13 **Effect of amino acid-restriction in a DSS-based experimental model**

The irritant dextran sulfate sodium (DSS) is known to trigger proliferation and damage the basement membrane (271). 100 conventionally reared flies were fed with either a CD, DR diet or PEM diet for 2 weeks. Afterwards, these flies were fed daily with a 5 % DSS solution until they deceased. CD fed flies revealed a significantly increased survival rate upon DSS treatment in comparison to flies subjected to DR or PEM (Fig. 54, A). Next, I checked the influence of DSS on the basement membrane in the intestine. For that, I used viking-GFP reporter flies to visualize the basement membrane. The dissected intestines were co-stained with an anti-spectrin antibody, which visualizes the plasma membrane. The basement membrane appeared thinner in DSS flies fed either a CD, DR diet or PEM diet in comparison to the proper sugar control (Fig. 54, B-G). The quantification of the basement membrane thickness further confirmed these observations. Interestingly, CD fed flies showed a significantly thinner basement membrane compared to flies subjected to DR and PEM (Fig. 54, H). The influence

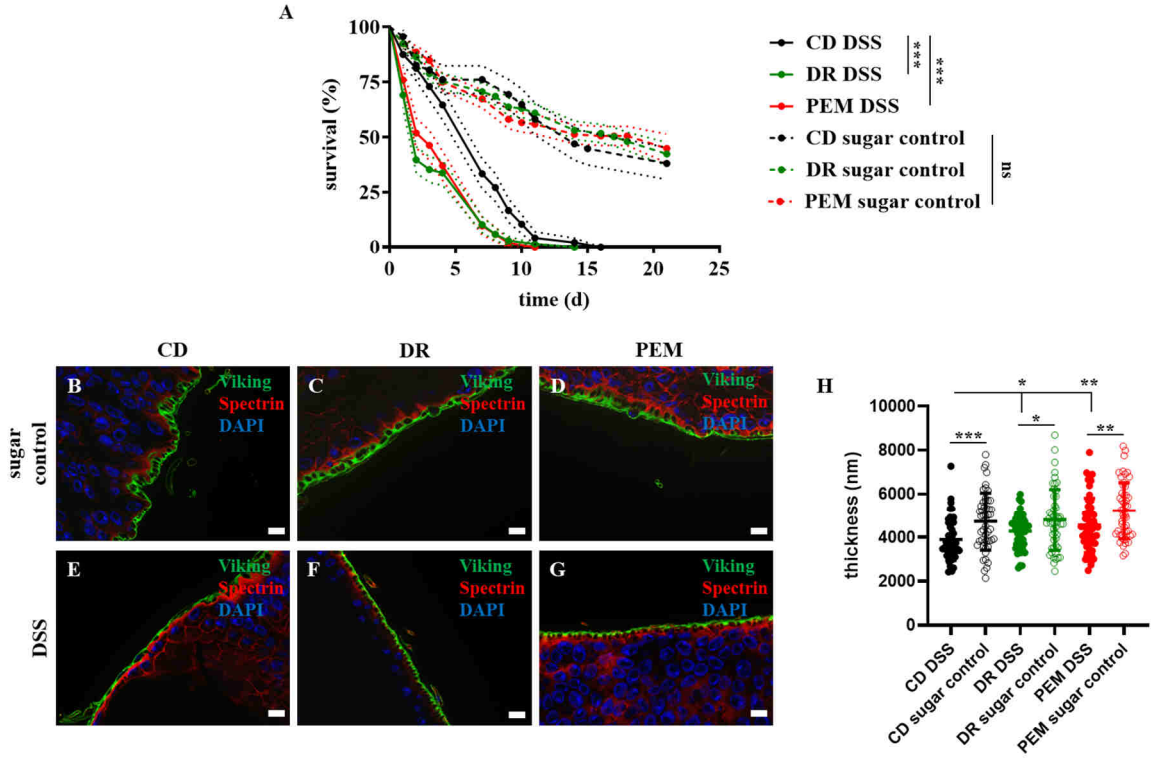

Fig. 54: Survival assay and basement membrane of DSS treated flies subjected to a CD, DR or PEM. (A) Flies were fed with either a CD, DR or PEM diet for 2 weeks. Afterwards, the flies were treated with a 5 % DSS solution or a 5 % sugar solution as a control (n = 100). (B-G) Representative images of intestines of viking-GFP flies treated either with a 5 % DSS solution or 5 % sugar solution after subjected to a CD, DR or PEM for 2 weeks. The intestines were co-stained with an anti-spectrin antibody to visualize the plasma membrane. (H) Quantification of the basement membrane thickness (n = 48-50). CD: control diet, DR: dietary restriction, PEM: protein-energy malnutrition, DSS: dextran sodium sulfate, ns: not significant, *p < 0.01, **p < 0.01, ***p < 0.001.

on the intestinal proliferation was examined by using esg>GFP flies. DSS treated esg>GFP flies fed a CD, DR diet or PEM diet revealed an increased number of esg$^+$ cells in comparison to the equivalent sugar control (Fig. 55, A-F). These observations were validated by a quantification of the number of esg$^+$ cells in the anterior midgut region. Surprisingly, no significant different counts of esg$^+$ cells were detected between CD fed flies and flies subjected to DR or PEM (Fig. 55, G). The number of pH3$^+$ cells were highly increased in DSS treated flies fed a CD or a DR diet in comparison to the proper sugar control. However, the number of pH3$^+$ cells in DSS treated flies subjected to PEM was comparable to sugar treated flies fed a PEM diet (Fig. 55, H-M). Flies fed a CD revealed an increased number of pH3$^+$ cells in comparison to flies subjected to DR or PEM (Fig. 55, N).

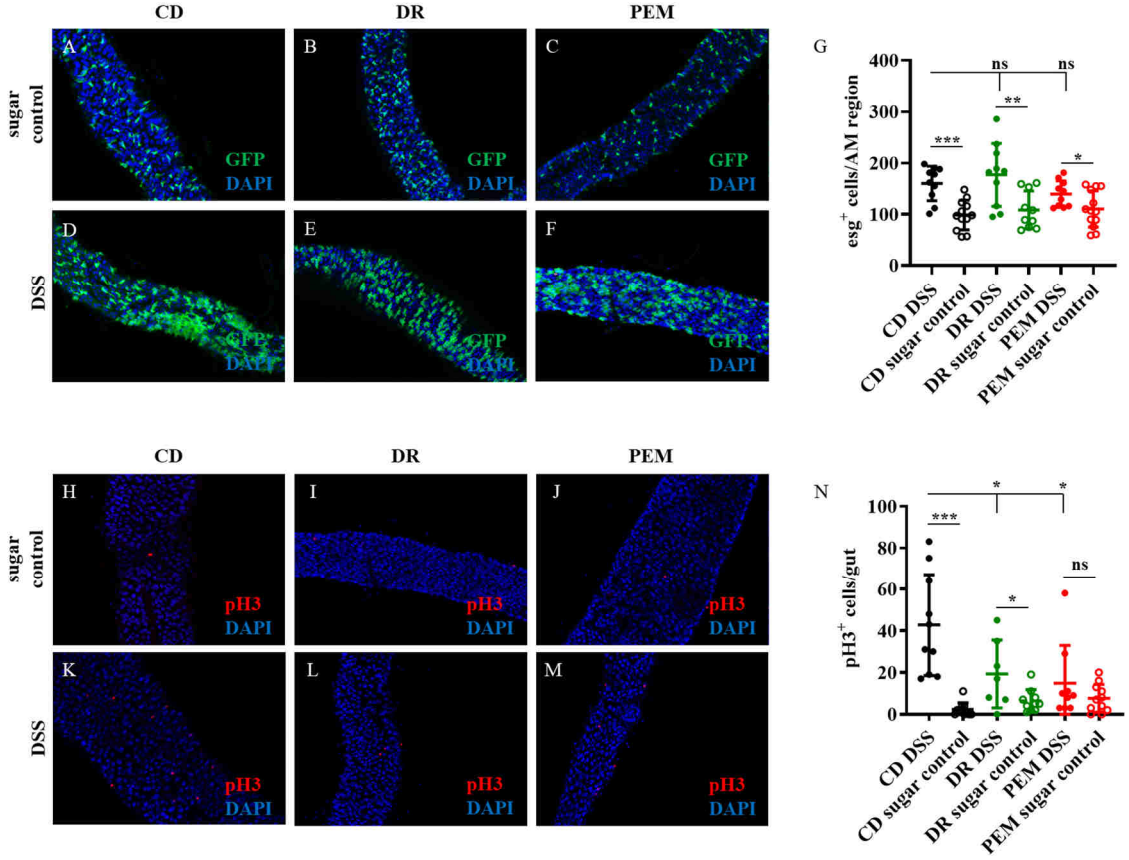

Fig. 55*:* **DSS induced proliferation in flies fed a CD, DR diet or PEM diet.** (A-F) Representative images of the anterior midgut region of esg>GFP flies subjected to a CD, DR or PEM. Esg>GFP flies were treated with a 5 % DSS solution or a 5 % sugar solution. DSS treatment led to an increased number of esg$^+$ cells (GFP) compared to the sugar control. (G) Quantification of the number of esg$^+$ cells in the anterior midgut region (n = 10-13). (H-M) Representative images of intestines of esg>GFP flies stained with an anti-pH3 antibody to visualize mitotically active cells. (N) Quantification pH3$^+$ cells in the intestines of esg>GFP flies (n = 8-11). CD: control diet, DR: dietary restriction, PEM: protein-energy malnutrition, DSS: dextran sodium sulfate, AM: anterior midgut, esg: escargot, GFP: green fluorescent protein, pH3: phospho-histone 3, ns: not significant, *p < 0.05, **p < 0.01, ***p < 0.001.

4.3.14 **4EBP and ATG8 signaling in response to amino acid-restriction**

The Tor pathway senses energy levels as well as amino acids and regulates for example cell growth, proliferation, translation and autophagy (272,273). Tor pathway activation leads to phosphorylation of 4EBP to promote mRNA translation and to a repression of the autophagy-related gene 8 (ATG8) expression to suppress autophagy (160,274). I used 4EBP::RFP reporter lines to confirm 4EBP activation due to attenuated Tor pathway activity on amino acid-restricted diets. Indeed, flies subjected to DR (Fig. 56, B,B' and B'') or PEM (Fig. 56, C,C' and C'') revealed an increased the 4EBP signal in comparison to CD fed flies (Fig. 56, A,A' and A''). The 4EBP signal of flies fed a DR or PEM diet was detectable in the cytoplasm and in the nuclei, whereas 4EBP signaling in CD fed flies was restricted to the cytoplasm. I used NP1>GFP-mcherry-atg8a flies to visualize ATG8-related autophagy in ECs. In these flies, the GFP fluorescence signal is quenched by acidic hydrolases when autophagosomes fuse with lysosomes to form autolysosomes and the resulting autolysosomes will fluoresce red, whereas only autolysosomes are displayed in the following experiment (275). Flies subjected to DR and

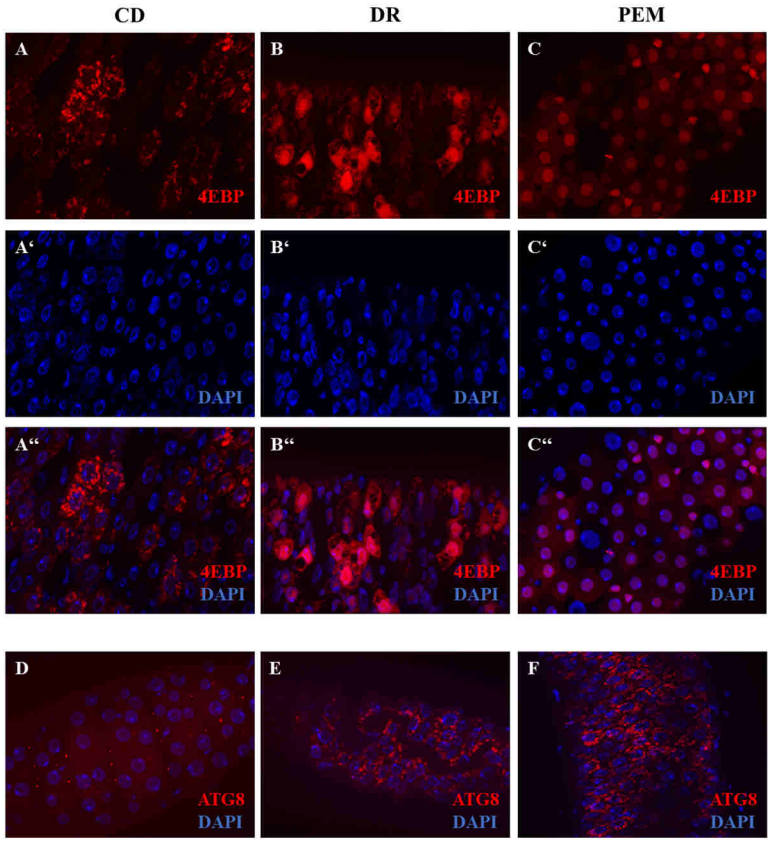

Fig. 56: 4EBP and ATG8 signaling in intestines of flies subjected to DR or PEM. (A-C) Representative images of the anterior midgut region of 4EBP::RFP reporter fly lines fed either a CD, DR or PEM diet. Flies fed a DR or PEM diet revealed a stronger RFP signal in the cytoplasm and in the nuclei in comparison to CD fed flies (D-F) Representative images of the anterior midgut region of NP1>GFP-mcherry-atg8a flies, which express GFP-mcherry-atg8a in ECs. Only the fluorescence signal from mcherry is shown as it indicates autolysosome formation. CD: control diet, DR: dietary restriction, PEM: protein-energy malnutrition, 4EBP: eIF4E binding protein, ATG8: autophagy-related gene 8.

PEM showed a higher mcherry-atg8a fluorescence signal, and therefore an increased formation of autolysosomes in comparison to CD fed flies (Fig. 56, D-F).

4.3.15 **Impact of protein-restriction on gut structure in Tor-deficient flies**

I used flies with a hypomorphic Tor^{k17004} allele to reveal the impact of amino acid-restricted diets on the cellular homeostasis and structure of the intestine in the absence of the Tor pathway. RC Tor^{k17004} flies fed a CD revealed a significant longer intestine in comparison to RC Tor^{k17004} flies subjected to DR or PEM. Interestingly, no significant differences in intestinal length were observed between RC Tor^{k17004} flies and GF Tor^{k17004} flies fed either a CD, DR diet or PEM diet. The length of the intestines were comparable between GF Tor^{k17004} flies subjected to a CD, DR or PEM (Fig. 57, A). RC Tor^{k17004} flies fed a CD revealed a significantly shorter intestine compared to the RC CD fed genetic control flies. Also, RC Tor^{k17004} flies subjected either to DR or PEM showed a shorter intestine in comparison to RC genetic control flies fed the equivalent diet (Fig. 57, B). No significant differences were observed between GF Tor^{k17004} flies fed either a CD or DR diet and RC genetic control flies fed the respective diet. GF genetic control flies subjected to DR revealed a longer intestine than DR treated GF Tor^{k17004} flies (Fig. 57, C). The number of EECs in the anterior midgut region was comparable between RC Tor^{k17004} flies fed a CD and RC Tor^{k17004} flies subjected to DR or PEM. No differences were observed in the number of EECs between GF Tor^{k17004} flies fed a CD and DR or PEM treated GF Tor^{k17004} flies. Surprisingly, the number of EECs in GF Tor^{k17004} flies subjected to either a CD, DR or PEM was significantly higher compared to RC Tor^{k17004} flies fed the respective diet (Fig. 58, A). RC Tor^{k17004} flies fed a CD or PEM diet revealed a significant decreased number of EECs in comparison to RC genetic control flies fed the equivalent diet. However, no

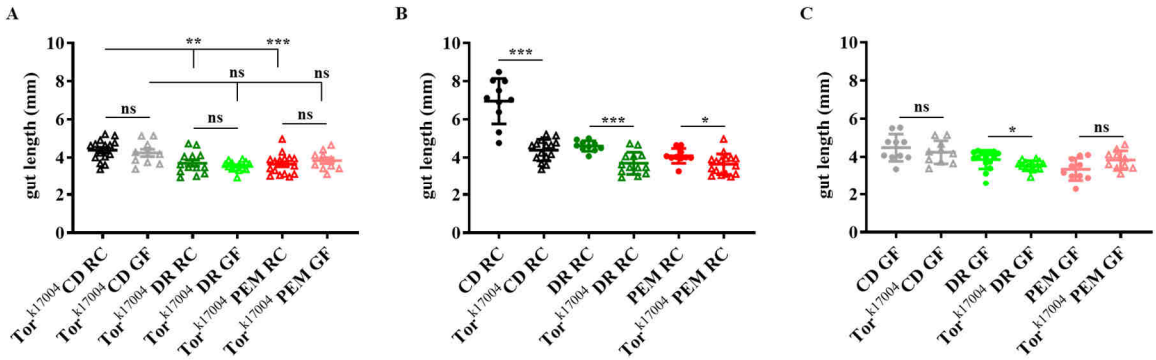

Fig. 57: Intestinal length of RC and GF Tor^{k17004} flies fed amino acid-restricted diets. (A) Length of the intestines of RC and GF Tor^{k17004} fed either a CD, DR diet or PEM diet (n = 10-15). (B-C) Length of the intestines of RC and GF *Tor*^{k17004} flies in comparison to genetic control flies (n = 10-15). CD: control diet, DR: dietary restriction, PEM: protein-energy malnutrition, RC: recolonized, GF: germ-free ns: not significant, *p < 0.05, **p < 0.01, ***p < 0.001.

differences in the number of EECs were detectable between RC Tor^{k17004} flies and RC genetic control flies subjected to DR (Fig. 58, B). DR treated GF Tor^{k17004} flies showed fewer EECs in the anterior midgut region in comparison to GF genetic control flies. The number of EECs was comparable between GF Tor^{k17004} flies subjected to DR or PEM compared to GF genetic control flies fed the respective diet (Fig. 58, C). Interestingly, no differences in the EC distance was detectable in RC and GF flies fed either a CD, DR diet or PEM diet for each comparison (Fig. 58, D). The EC distance was significantly increased in RC genetic control flies subjected to a CD or DR in comparison to RC Tor^{k17004} flies fed the equivalent diet. However, the EC distance was comparable in RC genetic control flies and RC Tor^{k17004} flies fed a PEM diet (Fig. 58, E). GF Tor^{k17004} flies fed a CD or DR diet revealed a decreased EC distance compared to GF genetic control flies subjected to the respective diet. No differences in the EC distance were observed between PEM treated GF Tor^{k17004} flies and GF control flies (Fig. 58, F).

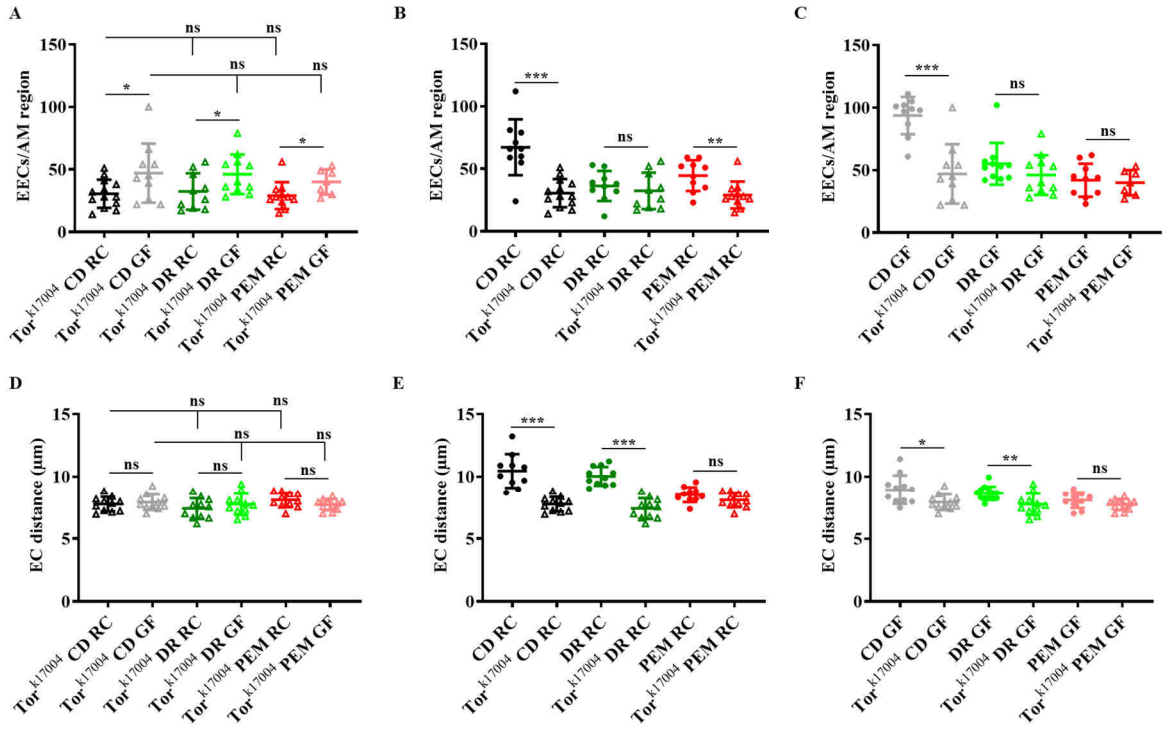

Fig. 58: EECs number and EC distance of Tor^{k17004} flies subjected to a CD, DR or PEM. (A) The number of EECs in RC and GF Tor^{k17004} flies fed either a CD, DR diet or PEM diet (n = 6-13). (B-C) EECs number of Tor^{k17004} flies in comparison to RC and GF genetic control flies (n = 6-13). (E) EC distance of RC and GF Tor^{k17004} flies subjected to a CD, DR or PEM (n = 11). EC distance of RC and GF Tor^{k17004} flies compared to RC and GF genetic control flies (n = 10-11). CD: control diet, DR: dietary restriction, PEM: protein-energy malnutrition, RC: recolonized, GF: germ-free, EEC: enteroendocrine cell, EC: enterocyte AM: anterior midgut, ns: not significant, *p < 0.05, **p < 0.01, ***p < 0.001.

4.3.16 **Tor-deficient flies exhibit a decreased infection susceptibility**

As the Tor pathway affects the cellular homeostasis as well as the intestinal structure, I investigated the impact Tor-deficiency on the immune homeostasis. Therefore, I fed Tor^{k17004} flies and genetic control flies for 2 weeks with a CD. Afterwards, these flies were orally infected with *S. marcescens* every day until they deceased. Tor^{k17004} fed a CD revealed a significant increased survival rate upon daily infection in comparison to genetic control flies (Fig. 59, A). Interestingly, a qRT-PCR analysis revealed a significant increase of diptericin and drosomycin transcripts already in non-infected Tor^{k17004} flies fed a CD in comparison to genetic control flies subjected to a CD (Fig. 59, B).

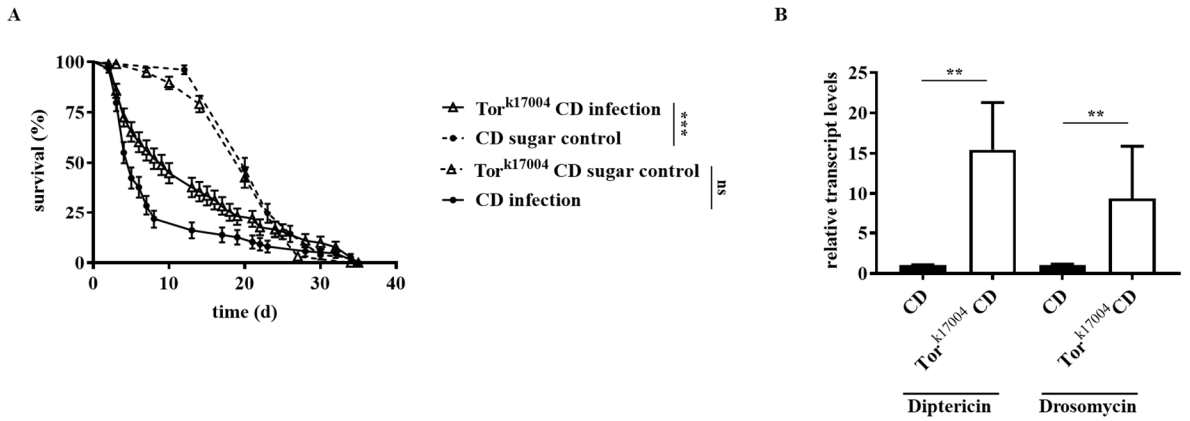

Fig. 59: Infection susceptibility and AMP expression of Tor^{k17004} flies. (A) Survival assay of Tor^{k17004} flies fed a CD for 2 weeks before infected with *S. marcescens* orally (OD_{600} = 1) in comparison to genetic control flies (n = 100). (B) qRT-PCR analysis of the AMPs diptericin and drosomycin in non-infected Tor^{k17004} flies and genetic control flies (n = 5). CD: control diet, ns: not significant, **p < 0.01, ***p < 0.001.

4.3.17 **L-tryptophan and BCA restriction affects AMP-production and bacterial abundance**

As the Tor pathway affects the transcriptional regulation of diptericin and drosomycin, the question arises if the depletion of single amino acids in the diet also leads to a regulation of AMPs. Therefore, I created a L-tryptophan (trp) restricted diet and a branched-chained amino acid (BCA, L- valin, L-leucin and L-isoleucin) restricted diet based on the CD. Conventional flies fed a trp-restricted diet revealed reduced intestinal transcript level of drosomycin (Drsm), metchnikowin (Mtk), drosocin (Dros) and diptericin (Dip) in comparison to CD fed flies. However, defensin (Def) was upregulated in flies fed a trp-restricted diet compared to flies fed a CD (Fig. 60, A). Flies subjected to a BCA-restricted diet showed a downregulation of Drsm, Mtk, Dros, Dip, and Def in the intestine compared to CD fed flies (Fig. 60, B). Interestingly,

the intestinal bacterial load was significantly decreased in flies subjected to a trp-restricted diet or BCA-restricted diet in comparison to CD fed flies (Fig. 60, C).

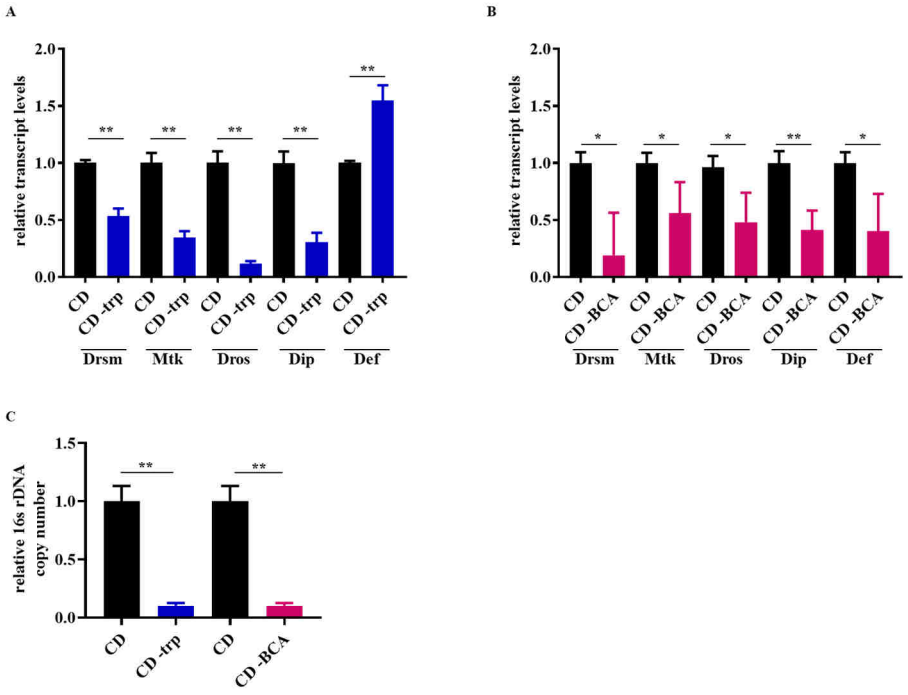

Fig. 60: Intestinal AMP expression upon dietary amino acid restriction. (A) qRT-PCR analysis of Drsm, Mtk, Dros, Dip and Def transcript levels in intestines of flies fed a trp-restricted diet (n = 5). (B) qRT-PCR analysis of Drsm, Mtk, Dros, Dip and Def transcript levels in intestines of flies fed a BCA-restricted diet (n = 5). (C) qRT-PCR analysis of the relative 16s rDNA copy number of flies fed a trp- or BCA-restricted diet (n = 5). CD: control diet, trp = L-tryptophan, BCA: branched-chained amino acids (L-valin, L-leucin, L-isoleucin), Drsm: Drosomycin, Mtk: Metchnikowin, Dros: Drosocin, Dip: Diptericin, Def: Defensin, *p < 0.05, **p < 0.01.

4.3.18 **Effect of the Tor pathway on the microbial community and abundance**

I performed 16s analysis with intestines of Tor^{k17004} flies fed a CD or PEM diet, to investigate if the Tor pathway affects the intestinal microbial composition. No differences in the microbial community were observed between Tor^{k17004} flies subjected to PEM or to a CD (**Fig. 61**, A). This was also illustrated by the separation in beta diversity, which was evaluated by a PCoA based on unweighted UNIFRAC (**Fig. 61**, B). The intestinal bacterial load was significantly decreased in Tor^{k17004} flies subjected to PEM in comparison to Tor^{k17004} flies fed a CD (**Fig. 61**, C). A Principal component analysis revealed dissimilarities in the microbial composition between genetic control flies and Tor^{k17004} flies fed a CD. Interestingly, evaluation of the PCoA also unveiled a high similarity in the intestinal microbial community between genetic control flies subjected to PEM and Tor^{k17004} flies (**Fig. 61**, D).

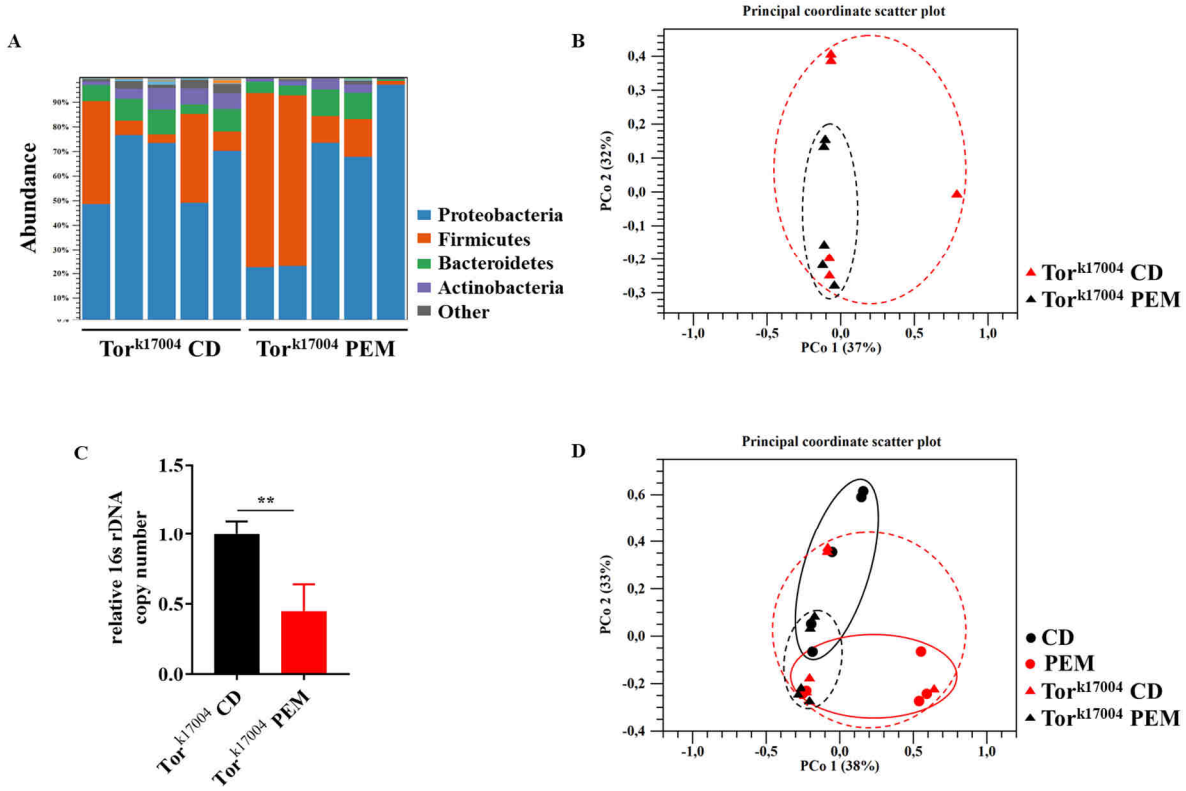

Fig. 61: Influence of the Tor pathway on the microbial composition and abundance. (A) Abundance table of the microbial composition of Tor^{k17004} flies fed a CD or PEM diet (n = 5). (B) Principal coordinate analysis of the microbial community in Tor^{k17004} flies upon PEM dieting compared to Tor^{k17004} flies fed a CD (n = 5). (C) Bacterial load of PEM subjected Tor^{k17004} flies in comparison to CD fed Tor^{k17004} flies (n = 5). (D) Principal coordinate analysis of the microbial community in Tor^{k17004} flies and genetic control flies fed a CD or PEM diet. CD: control diet, PEM: protein-energy malnutrition, PCoA: principal coordinate analysis.

4.3.19 **PEM induce long-lasting changes in the transcriptional profile**

It is established that severe PEM at an early life stage predispose an individual to non-communicable diseases in later life (276). However, it is not known which factors contribute to this long-lasting PEM-induced effect. Therefore, I investigated if a short-term intervention of PEM in early life stages of adult *Drosophila* leads to long-lasting changes in the transcriptional profile of the intestine. Flies were transferred for 3 days on CD, afterwards one group of flies were switched to a PEM diet for 7 days while the other group of flies remained on CD. After 7 days, flies of the PEM group were switched back to CD for 14 days (Fig. 62, A). I compared the transcriptional profile of flies fed for 7 days a PEM diet with flies fed a CD for 8 days and flies recovered from PEM dieting for 14 days with flies fed a CD for 21 day to uncover memory signatures. Differential expression analysis revealed 3566 genes that were differentially expressed in intestines of flies subjected to PEM in comparison to CD fed flies. 345 genes were differentially expressed in intestines of flies recovered for 14 days after a 7 days period of PEM

dieting compared to flies fed a CD for 21 days. I identified 1326 genes that were differentially expressed in both, in intestines of flies subjected to PEM for 7 days and in flies that recovered from an period of PEM dieting (Fig. 62, B). Interestingly, some DEGs of flies recovered from a period of PEM dieting showed a memory phenotype, means that their transcriptional profile remained at the level of the PEM group subjected 7 days to PEM. Many of the downregulated

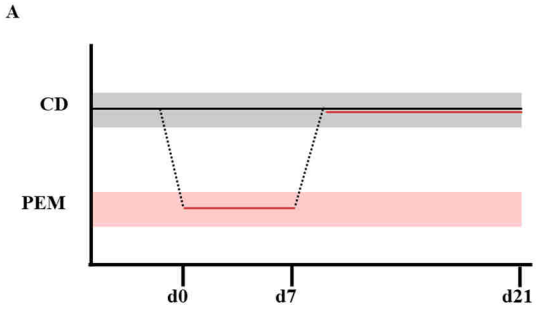

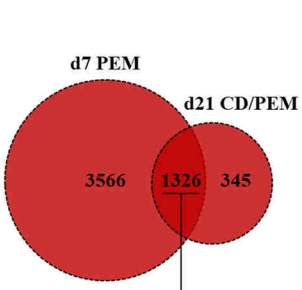

C

Biological process	Gene	Molecular function	d7 Fold change	d24 Foldchange
carbohydrate metabolic process	tobi	alpha-galactosidase	-3.503	-3.877
	alpha-Man-Ib	alpha-mannosidase	-5.598	-3.111
	beta-Man	beta-mannosidase	-3.668	-2.619
	LManIII	alpha-mannosidase	-43.86	-7.55
	LManIV	alpha-mannosidase	-66.39	-4.533
	LManV	alpha-mannosidase	-42.99	-5.704
	LManVI	alpha-mannosidase	-32.56	-6.977
	Gk2	glycerol kinase	-1.875	-2.708
	Gal	beta-galactosidase	-1.636	-3.689
	Amyrel	alpha-amylase	-26.79	-3.127
	Mal-A1	alpha-glucosidase	-4.079	-2.779
	Mal-A2	alpha-glucosidase	-1.555	-2.02
	Mal-A3	alpha-glucosidase	-4.842	-3.422
	Mal-A6	alpha-glucosidase	-4.145	-5.04
	Men-b	malat dehydrogenase	-11.26	-5.142
glucose transmembrane transport	CG1208	glucose transmembrane transporter	-2.22	-2.592
	CG10960	glucose transmembrane transporter	-5.5	-2.993
lipid catabolic process	CG31091	triglyceride lipase	-22,34	-20,53
	CG31089	triglyceride lipase	-45,97	-29,98
	CG8009	phosphatidate phosphatase activity	-3.788	-2.172
	CG17928	fatty acid desaturase	-4.245	-3.413
	ATPCL	fatty acid synthesis	-2.286	-2.669
	CG8093	lipase activity	-2.99	-2.341
	sws	lipase activity	-3.376	-2.087

D

Biological process	Gene	Molecular function	d7 Fold change	d24 Foldchange
proteolysis	Jon99Fii	serine-endopeptidase activity	3.6441	3.0252
	Jon99Fi	serine-endopeptidase activity	2.3101	4.644
	Jon66Ci	serine-endopeptidase activity	4.0173	15.579
	Jon65Aii	serine-endopeptidase activity	2.1954	2.3678
	Jon65Ai	serine-endopeptidase activity	2.4868	2.0899
	kappaTry	serine-endopeptidase activity	2.4194	2.35
	alphaTry	serine-endopeptidase activity	2.2979	2.3946
	epsilonTry	serine-endopeptidase activity	2.6826	3.4784
	CG30025	serine-endopeptidase activity	2.2819	2.4555
proteasome-mediated protein catabolic process	Prosalpha7	threonine-endopeptidase activity	1.8807	2.1372
	Prosbeta5	threonine-endopeptidase activity	2.4638	2.363
	Prosbeta1	threonine-endopeptidase activity	2.6624	3.0383
	Prosalpha5	threonine-endopeptidase activity	2.057	2.9012
	Prosbeta7	threonine-endopeptidase activity	1.8621	2.254

Fig. 62: Short-term intervention of PEM dieting induces long-lasting changes in the intestinal transcriptional landscape. (A) Schematic of the experimental design. (B) Venn Diagram of DEGs of flies subjected for 7 days to PEM and flies recovered from a short-term intervention of PEM dieting. The following comparisons are illustrated: d7 PEM vs. d8 CD and d21 PEM (recovered) vs. d21 CD. 1326 genes were differentially regulated in both comparisons (n = 4). (C) Selected DEGs that were downregulated in both comparisons. (D) Selected genes that were upregulated in bot comparisons. CD: control diet, PEM: protein-energy malnutrition, DEG: differentially expressed gene, FDR = 0.05.

DEGs were associated with carbohydrate metabolic process including mannosidases, galactosidases or amylases. Furthermore, several DEGs involved in glucose transport or lipase activity were repressed (Fig. 62, C). On the other hand, upregulated DEGs were associated with proteolysis or proteasome-mediated protein catabolic processes including serine- and threonine-endopeptidases (Fig. 62, D). All DEGs and BPs related to Fig. 62 are presented in Appendix D.

4.3.20 Effect of short-term interventions of PEM on the intestinal cellular homeostasis

I was interested, if a short-term intervention of PEM dieting leads to long-lasting changes in the intestinal cellular homeostasis. Therefore, I used the same experimental design as described in chapter 4.3.17 and examined the effect on ISC activity by using esg>GFP flies. Flies subjected to PEM for 7 days revealed fewer esg$^+$ cells (Fig. 63, D) in comparison to flies fed a

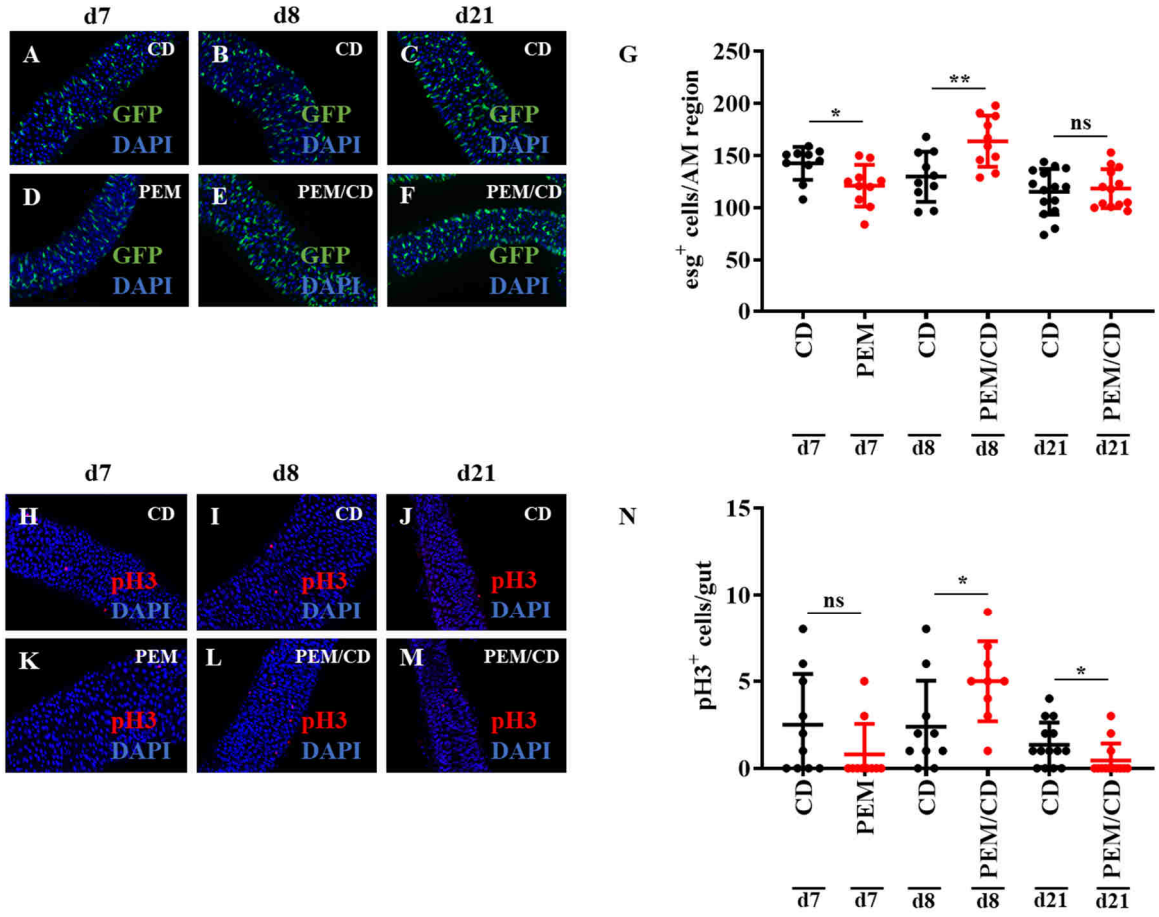

Fig. 63:Effect of short-term interventions of PEM dieting on the ISC activity. (A-F) Representative images of anterior midgut regions of esg>GFP flies subjected to PEM for 7 days, flies recovered from PEM (PEM/CD) and flies constantly fed a CD. (G) Quantification of the number of esg$^+$ cells in the anterior midgut region (n = 10). (H-M) Representative images of midgut regions with pH3$^+$ cells. (N) Quantification of the number of pH3$^+$ cells (n = 10).CD: control diet, PEM: protein-energy malnutrition, esg: escargot, AM, anterior midgut, GFP: green fluorescent protein, pH3: phospho-histone 3, ns: not significant, *p < 0.05, **p < 0.01.

CD for 7 days (Fig. 63, A). Interestingly, the dietary switch from PEM to the CD on day 8 led an elevated number of esg$^+$ cells (Fig. 63, E) compared to flies fed a CD constantly for 8 days (Fig. 63, B). The number of esg$^+$ cells was comparable between flies recovered from an PEM intervention (Fig. 63, F) and flies fed a CD for 21 days (Fig. 63, C). The quantification of the number of esg$^+$ cells further supported these observations (Fig. 63, G). No differences in the number of mitotically active cells were detected between flies subjected to PEM for 7 days (Fig. 63, K) and flies fed a CD for 7 days (Fig. 63, H), which was revealed by an anti-pH3$^+$ antibody staining. The switch from a PEM diet to a CD on day 8 led to increased number of pH3$^+$ cells (Fig. 63, L) compared to flies fed a CD for 8 days (Fig. 63, I). The number of pH3$^+$ cells was decreased in flies recovered from a short-term PEM intervention on day 21 (Fig. 63, M) in comparison to flies fed a CD for 21 days (Fig. 63, J). These observations were further supported by a quantification of pH3$^+$ cells in the intestines (Fig. 63, N).

4.3.21 **Effect of short-term interventions of DR and PEM on DSS-induced stem cell activity**

Next, I investigated the effect of DSS on the intestinal epithelial after a short-term intervention of DR or PEM. Therefore, I fed flies with a DR diet or PEM diet for 7 days, afterwards they were switched to the CD for 14 days. Control flies were fed a CD for 21 days continuously. Subsequently, these flies were fed daily with a 5 % DSS solution until they deceased. No significant differences were observed in the survival rate were observed between flies, which were subjected to DR or PEM for a short-term period in comparison to flies fed a CD constantly (Fig. 64, A). Next, I checked the influence of DSS on the basement membrane in the intestine by using viking-GFP reporter flies. The intestines were co-stained with an anti-spectrin antibody to visualize the plasma membrane. The DSS treatment led to an thinner basement membrane of flies fed a DR (Fig. 64, F) or PEM diet (Fig. 64, G) for a short period of time and of flies fed a CD (Fig. 64, E) in comparison to the sugar control fed the same diet (Fig. 64, A-C). The quantification of the basement thickness further confirmed these observations. Interestingly, flies recovered from a short-term period of PEM dieting revealed a significantly thinner basement membrane compared to flies fed a CD continuously (Fig. 64, H). The influence on the intestinal proliferation was examined by using esg>GFP flies. DSS treated esg>GFP flies recovered from a short-term intervention of DR (Fig. 65, E) or PEM (Fig. 65, F) revealed an increased number of esg$^+$ cells in comparison to the equivalent sugar control (Fig. 65, B and C). The same phenotype was observed in flies fed a CD (Fig. 65, D)

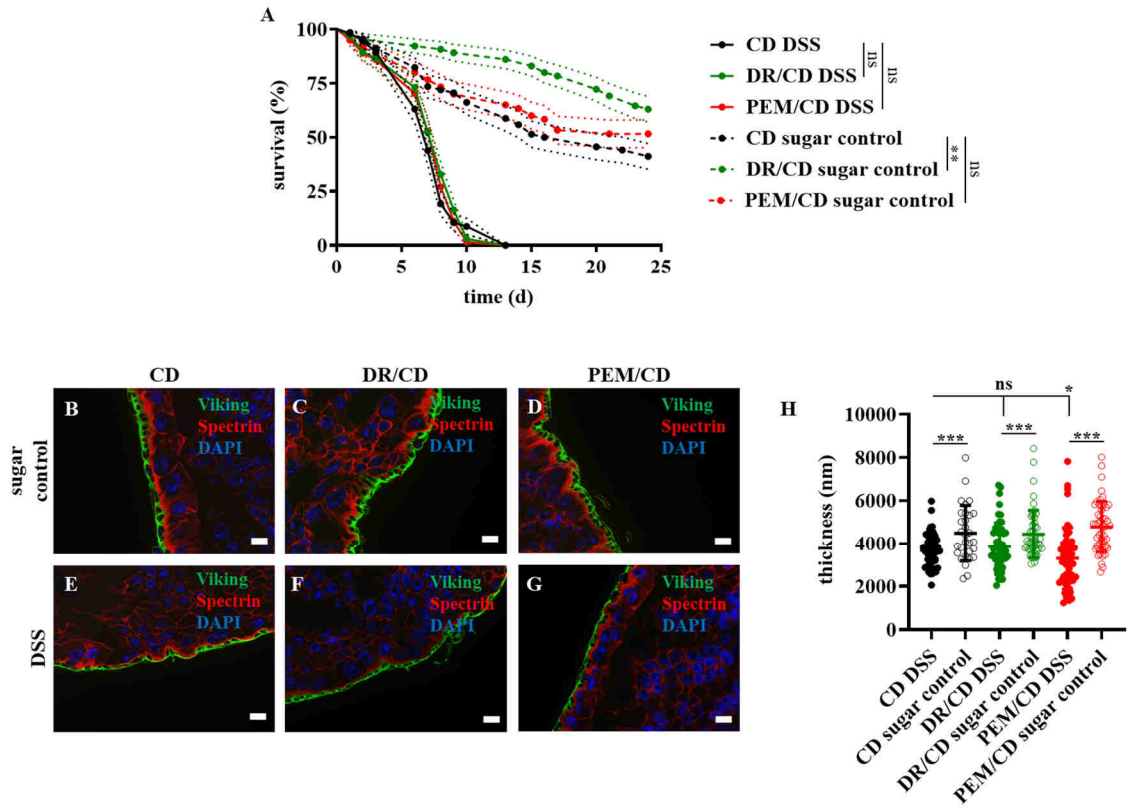

Fig. 64: Effect of DSS on the survival rate and intestinal basement membrane in flies recovered from a short-term period of DR or PEM. (A) Flies were fed with either a DR or PEM diet for 7 days, subsequently they were transferred to a CD for 14 days. Control flies were fed a CD for 21 days. Afterwards, these flies were treated with a 5 % DSS solution or a 5 % sugar solution as a control (n = 100). (B-G) Representative images of intestines of viking-GFP flies treated either with a 5 % DSS solution or 5 % sugar solution. The intestines were co-stained with an anti-spectrin antibody to visualize the plasma membrane. (H) Quantification of the basement membrane thickness (n = 30-50). CD: control diet, DR: dietary restriction, PEM: protein-energy malnutrition, DSS: dextran sodium sulfate, ns: not significant, *p < 0.05, **p < 0.01, ***p < 0.001.

constantly in comparison to the sugar control (Fig. 65, A). These observations were further supported by a quantification of esg$^+$ cells in the anterior midgut. No significant differences in the number of esg$^+$ cells were detected between flies recovered from an DR or PEM diet compared to flies fed a CD continuously (Fig. 65, G). The number of pH3$^+$ cells was elevated in flies recovered from a short-term intervention of DR (Fig. 65, L) or PEM (Fig. 65, M) and in flies continuously fed a CD (Fig. 65, K) compared to the equivalent sugar control (Fig. 65, H-J). No significant differences in the number of pH3$^+$ cells were observed between flies fed a CD and flies recovered from a DR or PEM diet intervention (Fig. 65, N).

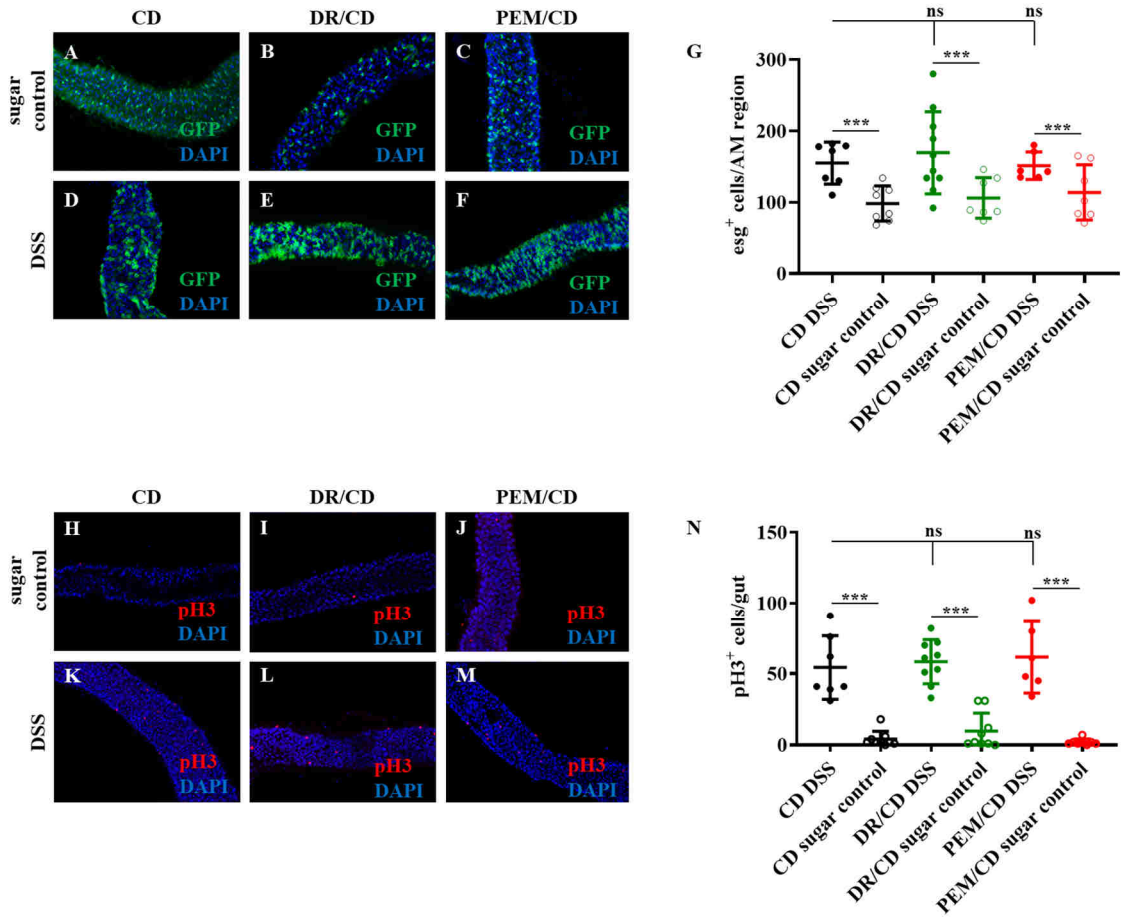

Fig. 65: Effect of DSS on the ISC activity in flies recovered from a short-term period of DR or PEM. (A-F) Representative images of the anterior midgut region of esg>GFP flies that lived for 14 days on a CD after a 7 days period of DR or PEM and flies that fed continuously a CD. Esg>GFP flies were treated with a 5 % DSS solution or a 5 % sugar solution. DSS treatment led to an increased number of esg$^+$ cells (GFP) compared to the sugar control. (G) Quantification of the number of esg$^+$ cells in the anterior midgut region (n = 7-11). (H-M) Representative images of intestines of esg>GFP flies stained with an anti-pH3 antibody to visualize mitotically active cells. (N) Quantification pH3$^+$ cells in the intestines of esg>GFP flies (n = 6-9). CD: control diet, DR: dietary restriction, PEM: protein-energy malnutrition, DSS: dextran sodium sulfate, AM: anterior midgut, esg: escargot, GFP: green fluorescent protein, pH3: phospho-histone 3, ns: not significant, ***p < 0.001.

5 Discussion

5.1 High fat dieting induces microbiota-dependent increase of stem cell proliferation

Overweight and obesity are defined as an excessive fat accumulation that can lead to a plethora of health-impairing consequences. The intestinal epithelium plays an important role in nutrient absorption, barrier function and hormone secretion. The intestine retains its epithelial homeostasis by undergoing cell renewal driven by ISCs proliferation. It is known that the intestine responds to dietary factors such a dietary lipids. Excessive intake of dietary lipids is associated with colorectal cancer (277,278). These findings imply that high fat dieting affects intestinal signaling pathways, which promote cell proliferation. In this study, I used the model organism *Drosophila melanogaster* to investigate the effect of a 20 % coconut-fat based diet on the intestinal epithelial homeostasis and to reveal the underlying signaling pathways. I found that a 3 days short-term intervention is sufficient to induce an increased mitotic activity of ISCs. The HFD-induced mitotic activity was accompanied by a marked hyperproliferation of esg^+ cells, namely ISCs and EBs, in the anterior as well as posterior midgut. The number of ISCs and EBs did not remain elevated after 7 days. However, a continuous HFD-treatment led to an altered cellular composition as the number of EECs was significantly increased, whereas the number of ECs was not affected. Most interestingly, the HFD-induced hyperproliferation completely relied on the presence of the intestinal microbiota since the HFD-induced activation of ISC proliferation was absent in GF flies. Furthermore, I suggest that the observed effect depends on JNK signaling in ECs, which in turn activates JAK/Stat signaling in ISCs and EBs.

An increased number of ISCs and transient cells upon high fat dieting was also shown in several mouse and rat models (279,280). In mice, a HFD also leads to structural changes of the intestine. Mice subjected to a HFD have shorter intestines and increased villus heights (281,282). High fat dieting does not affect the number of EECs in mice, but reduces the number of bactericidal-producing Paneth cells and mucus-producing goblet cells (278,281,282). In mammals, ISCs are located in a niche at the bottom of crypts. Paneth cells are interspersed throughout these crypts and are essential for maintaining the ISC niche (283). It is suggested that the reduced number of Paneth cells within the crypts leads to an uncoupling of ISCs from their niche and therefore a Paneth cell-independent growth. On the other hand, CR increases the number of Paneth cells and the interaction of ISCs with their niche (284). In *Drosophila* it was shown that bacterial infection or a treatment with genotoxic chemicals leads to an extended cell-cell contact between

ISCs and EBs. The extended cell-cell contact between ISCs and EBs did not occur under homeostatic conditions, suggesting that the extended cell-cell contact is related to increased epithelial renewal. The increased cell-cell contact as well as proliferation and differentiation were associated with JAK/Stat signaling in ISCs and EBs (285). In fact, the observed HFD-induced elevated number of esg^+ cells in *Drosophila* could be due to either increased proliferation or developmental arrest. However, by using the REDDM linage tracing method I showed that the differentiation of EBs is not blocked. In contrast to the effect of high fat dieting on the abundance of EECs in mice, a diet containing high concentrations of cholesterol increases the number of EECs in *Drosophila*. A diet with low concentrations of cholesterol decreases the number of EECs and prevents the formation of EEC tumors. The increase of EECs is associated with decreased Delta levels in ISCs and reduced Notch signaling in EBs, whereas it is known that attenuated Notch signaling in EBs directs to a differentiation of EECs (214). The cholesterol-induced effect is mediated through the *Drosophila* dHR96 nuclear receptor, which binds cholesterol and affects Delta-Notch signaling (286,287). However, in the aforementioned study they used high concentrations of cholesterol, whereas I used a HFD containing triglycerides with mainly medium-chained saturated fatty acids such as lauric acid, myristic acid, caprylic acid and palmitic acid (255). I showed that even the supplementation of the diet with specific triglycerides such as tripalmitin, tristearin or tricaprin induces hyperproliferation of ISCs. Considering that the HFD-induced effect on proliferation is dependent on the intestinal microbiota, I suggest an indirect mechanism that causes induction of stemness and differentiation.

The JNK signaling pathway in *Drosophila* responds to a variety of external stressors and mediates protective mechanism to increase the stress tolerance (224,288,227). The JNK signaling pathway in *Drosophila* consist of one of several JNKKKs, a JNKK Hep and the JNK Bsk. Bsk regulates cell responses by phosphorylating effector molecules. Negative feedback mechanisms, regulated by the MAP kinase phosphatase Puckered (Puc), tightly control the duration and extent of JNK signaling (289). In my *Drosophila* HFD model, the level of phosphorylated JNK was significantly increased in cells throughout the whole intestine. One downstream target of the JNK signaling pathway is the cytokine Upd3, whereas the molecular mechanism to induce its expression is not known (224,290,291). The observed increase of the Upd3 level in HFD fed flies originates from stressed ECs, which could be shown by EC-targeted RNAi experiments. Our lab could also show that the HFD-induced expression of Upd3 was dependent on the activation of the JNK pathway in ECs (292). Furthermore, the HFD triggered hyperproliferation was absent in flies with a negatively modulated JAK/Stat pathway in ISC

and EBs. These data indicate that the JNK and JAK/Stat pathways synergize to promote ISC proliferation and cell renewal in response to stressed ECs caused by dietary lipids. A JNK pathway dependent release of Upd3 in stressed or damaged ECs and subsequent activation of the JAK/Stat pathway in ISCs and EBs was also observed in *Drosophila* model treated with pathogens or genotoxic chemicals (218,229,293). In *Drosophila* it is not known how the JNK signaling cascade is activated upon high fat stress. *In vitro* studies demonstrated that the saturated fatty acid palmitate can bind to the toll-like receptor 4 (TLR4), which in turn activates JNK and increases the expression of the proinflammatory cytokine interleukin-6 (IL-6), which is homologous to Upd3 in *Drosophila* (294,295). Mice lacking a TLR4 do not show a palmitate-induced IL-6 expression suggesting TLR4 as an important mediator of the effects of palmitate (296). An increased activation of the Toll receptor upon high fat dieting could not be shown in *Drosophila* (290). Interestingly, high fat dieting does not solely lead to local intestinal responses in *Drosophila*. Flies subjected to a HFD revealed a systemic JAK/Stat activation mediated by plasmatocytes, which releases Upd3 in a JNK-dependent manner (290). Excessive intake of dietary lipids leads to a local release of IL-6 in the intestine, the bone marrow, adipocytes and the brain as well as to increased systemic IL-6 levels in mice. (297,298,299,300,301,302). It is known that disruption of the STAT inhibitor suppressor of cytokine signaling 3 (SOCS3) in intestinal epithelial cells of mammals increases the proliferative response to damaged or stressed tissue (303). IL-6 is able to promote colon cancer cell growth by activating STAT3 (304,305). However, *in vitro* wound healing assays showed that the cytokine IL-6 had no positive effect on the epithelial regeneration. Moreover, IL-6 deficient mice are not susceptible to DSS-induced colitis and display regular epithelial regeneration suggesting that IL-6 is not an essential growth signal for epithelial regeneration in mammals (306). Nevertheless, it is likely that the mitogenic role of IL-6-like cytokines and JAK/Stat signaling is conserved in vertebrates and invertebrates.

Besides the JNK and JAK/Stat signaling pathways, Beyaz and colleagues reported that some fatty acids directly activate the signaling cascade that involves the nuclear peroxisome proliferator-activated receptor δ (PPAR-δ) in ISCs and transient cells (278). PPARs are molecular sensors of fatty acids and play a role in lipid metabolism, proliferation, differentiation and inflammation (307). PPAR-δ is associated with the Wnt pathway, which is required for ISC maintenance and the development of intestinal tumors (308,309). Mice fed a HFD revealed an increased expression of PPAR-δ and many of its target genes such as Wnt/ß-catenin (278). It has been suggested that *Drosophila* do not have a homolog of PPAR. However, it is speculated that the ecdysone-induced protein E75 (E75) is a putative divergent functional homolog of

PPAR-γ (310). In addition to the effect of HFD on the stem cell activity in the intestine, I also found out that this dietary intervention leads to changes in the composition of the microbial community. *Caulobacteriales* and *Enterobacteriales* were significantly enriched in flies fed a HFD, whereas the abundance of *Lactobacillacea* was reduced. A HFD-induced dysbiosis in the microbial composition could also be shown in other organisms (311,312,313,314). It has been reported that high fat dieting lead to a decrease of *Bacteroidetes* and an increase in *Firmicutes* and *Proteobacteria* in mice and human (315,316). However, a meta-analysis revealed an inconsistent data situation regarding the HFD-associated microbial composition as well as the alpha-diversity richness (317). It suggested that the HFD alters the microbial community directly and not the obese state of the individual (315). Intake of HFD stimulates the secretion of bile acids, which have a selective antimicrobial activity (318). Thus, the selective antimicrobial activity of bile acids could mediate alterations in the microbial composition (319). However, it was also reported that high fat dieting affects the regulation of PPAR-γ in the intestine of mice, which in turn led to a dysregulation of AMPs. A disturbed AMP-production could influence the composition of the microbial community. Furthermore, HFD fed mice revealed an altered viscosity of the mucus layer due to an accumulation of Mucin2 (MUC2) on the apical side of the goblet cells and is known that an altered mucus layer affects the microbial composition as well as the intestinal structure (320,321). In mice, it was reported that the HFD-associated microbiota has an increased capacity to harvest energy from the diet. This trait was transmissible as recolonization of the HFD-associated microbiota in GF mice resulted in an increase in body fat in comparison to GF mice recolonized with a microbiota harvested from lean mice (322). Interestingly, the concentration of SCFA, the main fermentation products of dietary fiber mediated by the microbiota, is increased in stool samples of obese individuals (323). The fact that SCFA are absorbed by the intestine and contribute to the host's energy metabolism could explain the transmissible obese phenotype. However, the observed microbiota-dependent hyperproliferation of ISCs in HFD fed flies described in my study was not transmitted as the fecal transplantation experiment failed to recapitulate the stemness phenotype. I showed that the HFD-triggered proliferation of ISCs is absent in GF flies suggesting that the presence of the bacteria alone seems to have more impact on the intestinal cellular homeostasis than the composition of the microbial community. The absence of the microbiota also attenuates Upd3 signaling in the intestine, which could be an explanation for the non-existent HFD-induced hyperproliferation of ISCs. In *Drosophila* it was already demonstrated that GF flies exhibit lower basal proliferation activity of ISCs and a highly reduced expression of JAK/Stat and JNK pathway components in the intestine (224). The data

suggests that the indigenous microbiota maintain a basal level of intestinal epithelial renewal. GF mice and rats also show an reduced cell proliferation rate and an altered intestinal architecture compared to conventionally reared animals (324,325). Moreover, the recolonization with bacteria is able to restore the aforementioned observations (326). The molecular mechanism how the indigenous bacteria affect the intestinal homeostasis is not well understood. The microbiota in the intestine of mammals is recognized by TLRs via microbe-associated molecular patterns (MAMPs, 327). It was shown the activation of TLRs is crucial to protect the intestine against injury and associated mortality (328). On the other hand, an overactivation of TLRs cause increased epithelial proliferation and neoplasia in an Wnt signaling dependent manner (329). There are also other studies using mice or zebra fish showing that the intestinal microbiota promote proliferation through Wnt signaling (330,331). Furthermore, the incidence rate of colorectal cancer is much higher than small intestine cancer as the bacterial density in the small intestine is lower (332,333). Therefore, one can consider that a higher density of intestinal bacteria leads to an increased proliferation. In my studies, I showed an increased bacterial load upon high fat dieting. The higher bacterial load is probably caused by the provision of high energy-dense food or by the increased intestinal transit time and reduced fecal output. The provision of high energy-dense food could facilitate bacterial growth in the intestine and in the flood. The increased intestinal transit time and the accompanied reduced fecal output could lead to a reduced loss of bacteria. This constipation phenotype as well as the increased bacterial burden also occurs in mice and humans upon high fat dieting (334,335,336). These data suggest that constipation and an increased bacterial load is a general concomitant of high fat dieting. *Drosophila* display a marked increase of the bacterial load during aging, which is associated with hyperproliferation of ISCs and a disturbed epithelial integrity of the intestine (227,228,337).The age-associated hyperproliferation is accompanied with increased JNK activity (227). Interestingly, immune-deficient flies also shows a higher burden of indigenous bacteria and an increased activity of the JNK and JAK/Stat pathways (224). These data support the idea that a higher bacterial load leads to an imbalanced intestinal epithelial turnover mediated by JNK and JAK/Stat signaling.

Furthermore, I showed that high fat dieting led to increased diameter of the intestine and therefore probably to an elevated luminal pressure. The intestine of flies fed with methylcellulose, an indigestible fiber and food thickener, display an increased luminal diameter. Interestingly, the increased diameter of the intestine leads to an elevated number of ISCs, EBs and EECs mediated by the activation of the stretch-activated ion channel Piezo. The Piezo channel is expressed in ISCs pre-EECs and triggers proliferation and EEC differentiation

through Ca^{2+} signaling (338). In a previous study it was shown that bacteria are able to induce Ca^{2+} signaling in IECs of mice (339). Therefore, the HFD-associated constipation phenotype could lead to an increased mechanical stress and subsequent initiation of ISCs activity and EEC differentiation. In my studies, the uptake of TAGs in ECs and the storage in the fat body was highly increased in GF flies in comparison to RC flies. In *Drosophila*, it is known that GF flies display a hyperlipidemia phenotype independent of high fat dieting (340). Strikingly, GF mice had 40 % less total body fat compared to the conventionally reared mice even though they consumed more food (341). This could be explained by the fact that the intestinal microbiota provides energy from otherwise indigestible fibers (342). Furthermore, the intestinal absorption of fatty acids is increased in conventionally raised mice and zebra fish compared to their GF counterparts and therefore contributes to overnutrition (343,344). GF flies show a reduced protein content probably due to the missing amino acid harvest promoted by the microbiota (340,345). Following the protein leverage hypothesis of obesity, GF flies would tend to overfeed to consume sufficient protein (346). However, GF flies seem to eat less and therefore the protein leverage hypothesis would not explain the hyperlipidemia observed in GF flies (340).

Increased uptake of fat is associated with a plethora of metabolic disorders including deleterious effects on neurological conditions (347). In this study, I revealed a microbiota-independent effect of high fat dieting on the physical activity and sleep of flies. HFD fed flies showed a decreased locomotor activity as well as an increased time of sleep. A HFD-induced decrease in physical activity and a disruption of the circadian rhythm was also shown in mouse models (348,349). An enhanced starvation-induced hyperactivity was observed in HFD-fed flies (350). This might explain that HFD-fed flies in my study did not show an increased starvation resistance as the increased energy expenditure compensate the increased energy resource in the form of TAGs. It is known that EECs are scattered throughout the intestinal epithelia and sense signals such as nutrients, microorganisms or mechanical stimuli with their cell surface receptors. EECs release hormones that can enter the circulation, whereas other EECs are directly innervated by afferent and efferent nerves which allows them to provide a bidirectional communication between the nervous system and the intestine (351,352). In *Drosophila*, EECs respond to a fed state by secreting the hormone Bursicon α, which is able to attenuate adipokinetic hormone (AKH) containing neurons (353). Since AKH is involved in locomotor activity one can assume that the observed HFD-associated decreased physical activity is also mediated by the endocrine system (354). Another hormone released by EECs in the intestine of flies is Allatostatin A (AstA), which is able to promote sleep (355). In mice, the glucagon-like

peptide 1 (GLP-1) is released by EECs after food consumption and is associated with an attenuation of locomotor activity (356). It was reported that high fat dieting in zebra fish converts EECs into a nutrient-insensitive state, with bacteria offsetting this effect (357). This data show that the microbiota plays a role in endocrine signaling. However, it is not clear whether altered locomotor activity is a consequence or a cause of HFD-induced obesity (358). Long sleep durations in mammals is associated with an increase of inflammation markers (359). Interestingly, I could show increased JNK signaling in the brain after long-term high fat dieting. Recent studies in *Drosophila* also demonstrated that many inflammatory pathways in the head are upregulated and that memory formation is impaired upon high fat dieting (360,360). It is also known from mice and humans that a HFD leads to several detrimental effects on the cognitive function as well as to neurodegenerative processes (361,362,363). All these described deleterious consequences of high fat dieting on intestinal homeostasis, inflammation, abnormal fat accumulation and altered physical activity can lead to lifespan shortening as reported in my study.

5.2 Importance and optimization of a holidc diet

Drosophila melanogaster has a long history as an experimental model to study human metabolic disorders. However, when designing experiments with model organisms, the importance of the diets is mostly overlooked. This happens for the most part if the diet is not the prime focus of the study. Dietary factors can profoundly influence the expression of phenotypes (251,364,365). *Drosophila melanogaster* is a cosmopolitan species and its distribution is highly associated with the presence of humans (366). As a commensal *Drosophila* was found in a variety of habitats, but mostly on rotten fruits (367). A recent study showed that ancestral *Drosophila* in Africa used the marula fruit as a food source. It is suggested that the usage of marula fruits by human drove *Drosophila melanogaster* into commensalism (368). As *Drosophila* is mainly found on fermenting fruits, they have a tolerance for low pH values and high alcohol contents (369). Nowadays, *Drosophila* is cultured on a huge scale in labs on complex diets containing mainly sucrose, yeast, agar and corn meal (260). However, there are also labs that use a variety of other ingredients such as bananas, molasses, apple juice, opuntia powder, malt extracts or soy (370). All these ingredients can be obtained from different resources, whereby the macro- and micronutrient composition can vary between studies even by using the same fly food recipe. Unfortunately, these fly food recipes are referred to as ‘standard media’ and without the method of preparation, which in turn can lead to inconsistent

outcomes between laboratories. Therefore, an increasing number of researcher highlights the importance of standardizing experimental diets (251,371,372). For the purpose of standardization, it is essential to develop a so-called holidic diet, which addresses the nutritional requirements of larvae and adults. The term holidic diet refers to a completely chemically defined diet, which differ from meridic or oligidic diets that contain one or more non-defined ingredients. One of the first efforts to develop a holidic diet for *Drosophila* was done in 1956, but until now only a few holidic diets have been reported (373,374,261,262,251,252). However, most of these diets do not support larval development as good as a complex diet. The first highly recognized holidic diet was developed by Piper *et al*. in 2014. They showed that *Drosophila* larvae were able to develop on the holidic diet although with an increased developmental time and a reduced eclosion rate. The holidic diet contains a total amount of amino acids of 21.4 g/l and 17.12 g/l sucrose, which corresponds to a P:C ratio of 1.25:1. Previous studies used the nutritional geometry to disentangle the complex effects of P:C ratios on life-history traits in *Drosophila*. The developmental time from larvae to pupae decreased on low P:C ratios with a minimized developmental time at P:C 1:2. Moreover, the egg-to-adult viability and adult size was maximized at P:C 1:2. Lower protein or carbohydrate concentrations than 20 g/l were not tested or had detrimental effect on various life-history traits (263,264,375,376). In my study, I raised the total carbohydrate amount to 75 g/l and the total amino acid amount to 42.8 g/l, which led to a P:C ratio of 1:1.75. The P:C ratio of 1:1.75 decreased the developmental time and increases the egg-to-adult viability, which coincidences with the previously mentioned studies. A further increase of the amino acids to 64.2 g/l (P:C 1:1.17) showed detrimental effects on the pupation and eclosion rate supporting the importance of a balanced nutritional geometry (377). The deleterious effects of 64.2 g/l amino acids in the diet on the viably is presumably caused by toxic effects, which can occur when amino acids are present in high concentrations (378,379,380). Furthermore, I showed in an oviposition choice assay that mated females laid more eggs in higher carbohydrate food, as the flies preferred P:C ratios of 1:1.75 over 1.25:1. This was also demonstrated in a previous study, were females preferred P:C ratios of 1:8 over 1:4 and 1:4 over 1:1. Interestingly, larva preferred moderate P:C rations of 1:2 over 1:16 or 1:1 over 1:8, which promotes their development (263). Thus, adult flies tend to lay their eggs in substratum suboptimal for the larval development. It is known that the amount of yeast populations, the primary protein source for *Drosophila*, increases with fruit decomposition (381). *Drosophila* prefer to lay their eggs near to yeast sources, rather than in yeast sources (382). This leads to the assumption that *Drosophila* prefer oviposition sites with low P:C ratios as they will provide optimal feeding sides for larval development in the future.

The supplementation of the holidic diet with cobalamin, cobalt, molybdenum and a cholesterol/ergosterol mixture further decreased the developmental time and yielded an increased pupation as well as eclosion rate. The positive effect of the ergosterol/cholesterol mix is surprising as yeast-based complex *Drosophila* diets mainly contain ergosterol and lanosterol. On the other hand, plant-based complex *Drosophila* diets contain sitosterol, campesterol and stigmasterol. Both, yeast-based as well as plant-based diets contain only traces of cholesterol (267,268). Ergosterol and lanosterol are both fungi-derived sterols, whereas sitosterol, campesterol and stigmasterol are derived from plants (383,384). Cholesterol is mainly is from animal sources (385). In contrast to mammals, arthropods are sterol auxotroph and require exogenous dietary sterols. As *Drosophila* in the wild feed on yeast and plant material, there is no apparent source of cholesterol in this environment. The ancestral food habitat of *Drosophila*, the marula fruit, mainly contains ß-sitosterol, avenasterol and stigmasterol, but only traces of cholesterol (386). However, *Drosophila* can convert plant-derived sterols to cholesterol in their intestines, therefore cholesterol is detectable in wild-living flies even when they do not have a dietary cholesterol source (387,267). Furthermore, it is known that some bacteria contain cholesterol in their membranes (388). Sterols are important components for the ecdysteroid synthesis in arthropods that triggers molting and regulates growth, whereby titers of ecdysteroids peak in every critical developmental transition of the larva (389,390). Cholesterol seems to be essential for the *Drosophila* larval development as larvae on a low cholesterol diet do not reach the pupal stage (391). It was reported that ergosterol alone is not able to support larval growth. However, adding trace amounts of cholesterol to the ergosterol containing diet could rescue larvae to adulthood (391). Strikingly, mine and other studies showed that ergosterol alone is sufficient to support larval development to adulthood (392). It was shown that flies reared on a cholesterol supplemented diet produces ecdysone (E) and 20-hydroxyecdysone (20E), whereas flies reared on stigmasterol supplemented food only contain makisterone A (MaA). Flies fed with ergosterol contained 24(28)-dehydromakisterone (dhMaA) and 24-epi-makisterone (24-epi-MaA). 20E, MaA and dhMaA fully support development until adulthood and function interchangeably. Interestingly, flies fed with an equal mixture of cholesterol and stigmasterol contained exclusively 20E. Flies began to produce MaA when the ratio of stigmasterol:cholesterol reached 10.000:1, suggesting that cholesterol is used preferentially for the production of 20E. However, flies fed with cholesterol alone formed smaller pupae and adults compared to those fed with plant sterols (392). Nevertheless, it is not known what drives the selective use of cholesterol for the ecdysteroid production.

Surprisingly, Piper *et al*. denoted RNA extracts as non-defined ingredients and excluded them from their initial holidic diet (251). One of the first developed holidic diets for *Drosophila* already showed that RNA extracts improve the larval development (393). RNA extracts contain nucleotides, which are linked to ribose and an organic base such as adenine, guanine, cytosine and uracil. Nucleotides can be synthesized endogenously and are not essential nutrients (394). However, the supplementation of dietary nucleotides can promote the early growth and development of rats (265). It was shown that dietary nucleotides have positive effects on the intestinal growth of rats in the weanling, a time of rapid growth (395). Intra-uterine growth restriction in piglets, which received dietary nucleotide supplemented milk revealed improved growth performance, development and immune response (396). In fed infants, dietary nucleotide supplementation does not influence growth, but leads to an improved immune function (397). These data suggest, that dietary nucleotides can become essential for growth in periods of reduced nutrient intake or rapid growth.

Molybdenum is an essential micronutrient for a variety of organisms. Molybdenum itself is catalytically inactive but gains catalytic activity when it binds to pterin to form the molybdenum cofactor (Moco). Moco is the catalytic site of all molybdenum-containing enzymes in organisms (398). In *Drosophila*, 4 enzymes are known that use Moco: aldehyde oxidases 1-4 (Aox1-4), mitochondrial amidoxime reducing component (mArc), xanthine dehydrogenase (rosy) and sulfite oxidase (Suox,399). Defects in rosy lead to hypersensitivity of oxygen stress, disturbed cuticle development and to the inability to generate uric acid. Furthermore, rosy mutant show changes in metabolism pathways such as an accumulation of xanthine, which in turn can lead to conglomerates in malpighian tubules (400,401,402,403). Suox mutants show elevated sulfite level affecting the glutamate homeostasis, which is important for normal neuronal excitation (404). Moreover, low-dose supplementation of molybdenum leads to an enhanced antioxidant capacity in *Drosophila* (405). Doses over 0.05 mM can be toxic and lead to an disturbed larval development or reduced viability (406). However, I supplemented 0.5 µM molybdenum, which is in a range not negatively affecting the development. Cobalamin and its central atom cobalt are important for cell proliferation, hematopoiesis and proper function of the nervous system (407). Cobalamin is produced by certain bacteria and is concentrated in bodies of predators positioned higher in the food chain (407). Cobalamin is absent in plant-derived food sources, the only exceptions are some edible mushrooms and algae (408). Nothing is known about the cobalamin requirements of *Drosophila*. A previous study demonstrated that *Drosophila melanogaster* contained no detectable cobalamin levels, whereas other insects or arthropods did (409,410). Nonetheless, I could show that molybdenum, cobalamin and cobalt

have positive effects on the larval development, even when cobalamin and/or cobalt did not improve the development of GF larvae significantly. Other studies could show that a vitamin mixture, containing also cobalamin, decreases the developmental time and increases the egg-to-adult viability of GF African cotton stainer's (411). However, as they used a mixture of different vitamins, this is not a proof that cobalamin alone is able to improve larval development. It was also demonstrated that the supplementation of single B vitamins, but not cobalamin, promote the survival of GF *Drosophila* larvae to pupation (250). Therefore, B vitamins seem to be essential for the development of GF insects.

In 2017, Piper *et al*. presented a new interesting approach for the development of a holidic diet for *Drosophila* and mice (252). They hypothesized that the amino acid requirements of an animal is encoded in its genome. Thus, they calculated the proportional representation of each amino acid in each of the 19.736 predicted protein-coding genes. Without changing the total amount of amino acids of 21.4 g/l, the exom-matched holidic diet improves the development of *Drosophila* substantially. They showed that the fecundity of adult flies is affected by the most limiting amino acid in the diet. The most limiting amino acid in their initial holidic diet from 2014 was arginine. Increasing the amount of arginine caused egg production to increase in the same extent as when all amino acids were altered by the same amount. An additional supplementation of arginine in my studies did not improve the development suggesting this led to an imbalanced diet, which in turn can have adverse effects on fly's growth. Piper *et al*. demonstrated that increasing total amount of amino acids up to 21.4 g/l led to a decreased developmental time but also to a decreased life span of adult flies. However, further increasing the total amino acid content could still promote the developmental time without affecting the healthy lifespan as I showed in my study. Even though the exom-matched holidic diet from Piper *et al*. (2017) is superior to the holidic diet from Piper *et al.* (2014), the supplementation of ergosterol, cholesterol, cobalamin, cobalt and molybdenum still improved the development of larvae and fitness parameters of adult flies. I showed that increasing amount of carbohydrates, independent of the carbohydrate source, led to adverse effects on the development of larvae and partially on adult size parameters. It was already reported that high concentrations of glucose, sucrose or fructose lead to a developmental delay in *Drosophila* larvae (412). Interestingly, high sugar concentrations inversely correlates with larval feeding as hyperglycemic larvae have an aversion to feed (413,414). Thus, I suggest that the food aversion on high sugar diets leads to a scarcity of other ingredients which support growth. High sugar diets cause insulin resistance in larvae (415). Reduced insulin signaling in the prothoracic gland during larval stages leads to delayed pupation and reduced larval growth rate mediated by the

ecdysteroid 20E (416,417). On the other hand, less intake of amino acids due to high sugar concentrations could lead to a attenuated Tor signaling in the prothoracic gland, which in turn also causes developmental delays (418). Interestingly, intake of glucose as a carbohydrate source led to a reduced pupation rate in my study compared to a sucrose containing diet. This was also reported elsewhere (412). That is surprising as glucose, besides trehalose, is the main circulating sugar in the hemolymph of *Drosophila* (419). On the contrary, larvae show a stronger preference to fructose and sucrose while glucose elicits only weak preference responses (413). For adult *Drosophila*, it was showed that sucrose fed flies revealed a decreased lifespan when compared to fructose or glucose fed flies (420). Thus, nutritional requirements of adult flies are most likely not the same as those of larvae. In my study, I tried to find a dietary formulation that is primary optimized for larval development and which is probably not optimal for fitness parameters of adult flies. Moreover, nutritional requirements for adult *Drosophila* optimal for lifespan can have adverse effects on fecundity (252). The required nutrient composition can vary between genotypes, environment and organism age, which enhance the complexity of the development of a holidic diet.

5.3 Morphological and physiological adjustments of the intestine are mediated by amino acid availability and microbes

DR is associated with a plethora of health promoting effects, whereas PEM is linked several pathophysiological conditions. In this study, I used the OHD to create a DR and PEM diet with P:C ratios of 1:16 or PEM diet a P:C ratio of 0:1, respectively. In *Drosophila*, it is known that a low P:C ratio of 1:16 maximizes the lifespan, whereas a P:C ratio of 0:1 leads to an increased mortality (101,102). I confirmed these results as DR increased the lifespan compared to the CD and a PEM diet led to an elevated mortality rate. DR and PEM were both associated with a reduced protein content. Reduced expression of the *Drosophila* IR or the IR substrate Chico extends lifespan, which implies that reduced insulin signaling may induce a DR-like state (421,422). *Drosophila melanogaster* is known to have 8 *Drosophila* insulin-like peptides (dILP), which all have impacts on development and on lifespan (423,424). The expression rate of the several dILPs highly depends on the protein and carbohydrate concentration. Notably, the expression rate of dILP2, dILP3 and dILP6 is greatest on low protein diets (425). Strikingly, reduced dILP2 activity, achieved by genetic manipulations, is associated with lifespan extension (423,426). As dFoxO is negatively regulated by insulin signaling and therefore overexpression of dFoxO mimics reduced insulin signaling, overexpression of dFoxO in adult

fat bodies increases lifespan and reduces dILP2 expression (427). However, dFoxO mutants are able to respond normally to DR suggesting that dFoxO is not required to mediate the DR-associated lifespan effect and that other mechanisms can compensate the loss of dFoxO (428). This is consistent with studies in *C. elegans*, where it was shown that DR increases the lifespan independently from daf-16, the *C. elegans* FoxO ortholog (429). Contrarily, DR cannot further increase the lifespan in insulin signaling mice mutants (430). The facts that 4EBP reacts to DR (425, this study) and that dFoxO mutants respond to DR but with an overall decreased lifespan implicates that dFoxO activity is affected by DR. The Tor pathway modulates cellular responses to amino acids and energy levels, furthermore it is known that rapamycin is able to increase the lifespan of *Drosophila* through inhibition of TorC1 (431). Emran *et al*. found that adding back essential amino acids to a DR diet decreases lifespan, but not in rapamycin treated flies. Moreover, flies with deletions for *dILP2*, *dILP3*, and *dILP5* showed the same responses as wild type flies to the addition of essential amino acids to the DR diet(432). These data suggest that the Tor pathway mediates the effect of DR and not insulin signaling. On the other hand, it was reported that the lifespan is not decreased in flies carrying a dominant-negative form of the IR by the addition of essential amino acids to a DR diet (93). The restriction of the essential amino acid methionine can extend the lifespan in *Drosophila*. However, this lifespan extension is abolished in flies overexpressing TSC2 or a dominant negative form of the IR (90). It was also shown that DR and rapamycin act additively to extent lifespan suggesting that Tor pathway independent mechanism exists, which mediate the DR effects (431).

The exact nutritional and molecular mediators of the DR response are not resolved nowadays, and the interpretation can be challenging (433). Nonetheless, the response of the insulin and Tor pathway to DR imply that they are involved in the DR-mediated effects. A recent study demonstrated that intermitting fasting, another type of DR, led to a Tor pathway independent lifespan extension in *Drosophila*. They proposed that the intermitting fasting-mediated extended lifespan is partially explained by an improved intestinal health (434). In my study, I showed that a dietary long-term intervention of DR or PEM led to substantial changes in the intestinal morphology as well as in stemness, cell morphology and cell composition. Flies subjected to DR or PEM revealed a decreased proliferation of ISCs, a reduced number of EECs and smaller ECs. As ECs are the most abundant cells in the intestine, the reduced size of ECs caused probably the overall intestinal morphology as DR or PEM subjected flies exhibited significantly shorter and thinner intestines. It was demonstrated that CR subjected mice revealed an altered intestinal morphology as they had a decreased villi length, a decreased mass of the intestine and an increased crypt expansion, whereas the length of the intestine was not

affected. Furthermore, CR reduced the frequency of EECs, ECs, goblet cells and transient cells. Interestingly, CR led to an increased number of ISCs and Paneth cells (284,435). Yilmaz *et al*., showed that CR attenuates the mTorC1 pathway in Paneth cells, which in turn elevates Bst1 levels (284). Bst1 converts NAD^+ to the paracrine effector cyclic ADP ribose (cADPR) and is able to activate responder cells via nucleoside transporters to activate Ca^{2+} signaling and promote proliferation (436). It was shown that cADPR from Paneth cells entered ISCs and increased Ca^{2+} and AMPK phosphorylation, whereas the AMPK phosphorylation in turn activated sirtuin-1 (SIRT1). SIRT1 led to an activation of mTorC1 and S6K1 in ISCs (435). Therefore, CR in mice leads to an increased number of ISCs through non-autonomous mechanism mediated by mTorC1 signaling in Paneth cells. As the number of transient cells and differentiated cells is reduced in CR subjected mice suggests that CR favors ISC self-renewal at the expense of differentiation. However, the mice in these studies were subjected to CR, which means an overall reduced intake of calories, and not to a specific restriction of amino acids as in my studies. Thus, the effect of DR and PEM are possibly regulated through other mechanism. Nonetheless, it was reported that even fasted flies show a reduction of ISCs and EBs as well as a smaller intestine. These flies showed a decreased dILP3 secretion from intestinal muscle cells, which is thought to act on ISCs and EBs through the IR pathway (221,222). It is suggested that symmetric versus asymmetric division is partially mediated by the IR pathway. IR pathway activity in EBs during asymmetric division probably contributes to the separation of the EB daughter cell from the ISC, which is required to allow continuous ISC proliferation (221). Another study showed that the IR pathway acts through nutritionally regulated microRNA-305 expression, which controls Notch pathway activity (437). Overexpression of the IR in ISCs in *Drosophila* leads to an increased proliferation of ISCs and to an increased EC size. Conversely, overexpressing a dominant-negative form of the IR or Chico reduces ISC proliferation and EC size (438). Thus, reduced insulin signaling due to protein-restriction could partially explain the reduced number of EECs and the attenuated ISC proliferation in my studies.

Another possible nutritional-regulated pathway, which could additionally mediate the DR and PEM induced intestinal epithelial phenotype, is the Tor pathway. Flies treated with rapamycin, which represses Tor activity, attenuates the proliferation of ISCs (439). These results were also confirmed in mice (435). In *Drosophila*, Kapuria *et al*. showed that TSC2 is highly expressed in ISCs but not in EBs, which led to lower Tor activity in ISCs compared to EBs. Loss of Tor pathway activity in ISCs reduced the ISC proliferation capacity and EC size. ISCs with increased Tor activity did not revealed significant differences in cell number, however, the

increased Tor activity led to larger ECs. Furthermore, Notch pathway mediated repression of TSC2 in EBs was required to promote the commitment of EBs into ECs or EECs (438). Two studies reported that the ISC activity was increased in yeast-fed flies compared to starved flies, providing evidence for a strong response of ISC to proteins (222,221). Interestingly, the ISC proliferation is also reduced in high yeast diets and this phenotype is more severe in TSC1 mutant flies suggesting that TSC1 activity isolates the Tor pathway from dietary stimuli in ISCs to maintain stemness and that even high protein concentrations are able to negatively regulate Tor pathway activity (438). Therefore, the IR pathway as well as the Tor pathway are possible mediators of ISC proliferation, cell differentiation and cell growth in DR or PEM subjected flies. Notably, the observed phenotypes on the intestinal epithelial homeostasis in flies fed a DR or PEM were highly influenced by the presence of the intestinal microbiota. The length and the width of the intestine were significantly reduced in GF flies fed a CD or DR diet compared to their equivalent RC counterpart. No differences were observed between GF flies and RC flies fed a PEM diet as well as between GF flies subjected to CD, DR or PEM. This is consistent with the reduced EC distance, which is an indicator for the EC size as reduced distance implies smaller ECs. The addition of amino acids to the diet did not compensate for the loss of the microbiota. This means that amino acids foster growth of the intestine but only in the presence of the microbiota and that the microbiota potentially provide growth-stimulating effects to the cell through amino acid assimilation. However, amino acid restriction attenuated the proliferation of ISCs in RC as well as in GF flies suggesting that amino acids, even in the absence of the microbiota, promote ISC activity. As the amino acids have no influence on organ growth but on ISC proliferation in GF flies, I suggest that the minimal size of the intestine is limited and therefore no differences between GF flies on the different diets were detectable. In mice, the depletion of the intestinal microbiota do not affect the length of the whole intestine but leads to morphological changes as the villus width is reduced (440,441). GF mice reveal an overall reduction of cells in the villus and the small intestine as well as an attenuated ISC proliferation (441,442). I showed elevated levels of 4EBP and ATG8 in intestines of flies subjected to DR or PEM suggesting that the Tor pathway is inhibited due to amino acid restriction. RC Tor deficient flies fed a CD revealed a significantly longer intestine in comparison to RC Tor deficient flie fed a DR or PEM diet. However, no differences in intestinal lengths were observed between RC Tor deficient and GF Tor deficient flies fed on the same diet. Moreover, RC Tor deficient flies had a shorter intestine as the equivalent RC genetic control, whereas no differences were observed between GF Tor deficient flies and GF genetic controls. The data suggest that the Tor pathway is an essential regulator for the intestinal

development and a potential gateway for the microbiota to promote organ growth in *Drosophila*. It may also be that Tor deficient flies already reflect the minimal size of the intestine and therefore no effects of the microbiota are detectable.

Even when the number of EECs was lower in Tor deficient flies in comparison to the genetic control, the number of EECs was significantly higher in GF Tor deficient than in RC Tor deficient flies. This phenotype was also detectable between RC and GF genetic control flies. Thus, the microbiota seems to depress the differentiation of progenitor cells into EECs. The increased number of EECs was already shown in GF *Drosophila* and it is supposed that the microbiota affects the Notch pathway, which is implicated in cell fate decision of progenitor cells (225). Tor deficient flies revealed an increased susceptibly towards *S. marcescens* infection compared to the genetic control, which was accompanied with higher basal expression levels of the AMPs Diptericin and Drosomycin. It was shown that decreased Tor signaling due to protein-restriction activates the transcription factor Myc, which in turn induces AMP generation and promote infection susceptibility (443). Protein-restriction in mice is also associated with an decreased mortality upon infection (444). The intestinal epithelial barrier prevents uptake of harmful environmental toxins and microbial contamination into the circulation. Thus, an increased infection susceptibility is normally linked to a disturbed intestinal barrier integrity (445). I revealed a microbiota-independent effect of amino acid-restriction on the intestinal epithelial barrier function, in which DR improved the barrier function and PEM led to a disturbed integrity. These results are consistent with findings of other studies (446,447). However, I showed that DR as well as PEM led to a decreased infection susceptibility in *Drosophila*. Interestingly, the AMP production of Drosomycin, Metchnikowin, Drosocin, Diptericin and Defensin was significantly reduced in flies fed a L-tryptophane- or BCA-restricted diet, which could partially explain the reduced survival of flies subjected to DR or PEM. The reduced ISC proliferation could be an additional explanation for the increased mortality rate upon infection in DR and PEM diet fed flies as reduced ISC pool potentially reduce the regenerative capacity of the intestinal epithelium. In mice it was shown that CR enhanced intestinal epithelial regeneration following radiation injury suggesting that CR induced ISC activity leads to an preservation of an injury-resistant reserve of ISC function (284,448). DSS increases the intestinal permeability and leads to induced ISC activity in mice and *Drosophila* (449,219). In my studies, flies fed a CD showed a decreased mortality rate in comparison to flies subjected to DR or PEM. Interestingly, the number of esg^+ cells was comparable between the diets upon DSS-treatment, whereas significantly more $pH3^+$ cells were detectable in CD fed flies. In *Drosophila*, it was demonstrated that a DSS-treatment led to an

accumulation of EBs, which do not further differentiate to ECs (219). The absence of EC maturation potentially increases the effect of DSS on the intestinal permeability. This block of differentiation could be more severe in DR or PEM diet fed flies as reduced Tor signaling in EBs represses EC growth (438).

In *Drosophila* and mice, it was shown that single amino acids such as methionine or glutamine promote ISC activity (450,451,223,452). There is an increasing evidence that the metabolites of the intestinal microbiota like SCFA or amino acids are important modulators of the host intestinal physiology. Furthermore, some metabolic functions such as lipopolysaccharide biosynthesis or BCA biosynthesis seems to be dominated by the intestinal bacteria (453). GF mice have an altered distribution of free amino acids along the intestine in comparison to their conventionally reared counterparts suggesting that the microbiota plays an important role in the amino acid homeostasis of the host (454). The favored amino acid substrates of intestinal bacteria are glycine, arginine, serine, glutamine, lysine and BCA, which leads to a generation of SCFA, branched-chain fatty acids (BCFA), ammonia and biogenic amines (455). SCFAs and BCFAs affect immunomodulation, intestinal integrity, intestinal energy homeostasis as well as lipid, glucose and cholesterol homeostasis in a variety of tissues (456,457). Biogenic amines such as agmatine or tryptamine are able to mimic CR-associated metabolic functions or to stimulate the intestinal motility, respectively (458,459). Intestinal bacteria are also able to synthesize amino acids *de novo* from nitrogen sources such as ammonia and urea (150). It was shown that bacteria generated lysine from ammonia is absorbed in the intestine and contribute for the most part of the host lysine pool (149,150). Therefore, endogenous ammonia or urea sources that enters the intestinal lumen can be used by bacteria for the *de novo* synthesis of amino acids, which in turn can be incorporated in microbial protein. This process could be considered a nitrogen recycling as the microbial-derived amino acids and proteins can be absorbed and therefore contribute to the amino acid supply of the organism. I showed that the uric acid content in is significantly reduced in DR or PEM subjected flies, which is likely caused due to the reduced nitrogen intake in form of amino acids. Interestingly, the uric acid content is further reduced in GF flies suggesting that the intestinal microbiota provide relevant nitrogen sources to the host. Thus, the effects of the microbiota on the intestinal homeostasis is described by a complex interaction network of nutrient allocation and direct stimulation of proliferation-associated signaling pathways such as the JNK and JAK/Stat signaling cascade (described in chapter 5.1).

Moreover, I demonstrated that amino acid-restricted diets as well as the indigenous microbiota have pronounced effects on the intestinal transcriptional landscape. RC flies fed a DR diet

revealed 76 DEGs in comparison to RC flies fed a CD, whereas 6362 DEGs were detected in RC flies subjected to PEM. Considering the fact that the *Drosophila* genome encodes approximately 13.600 genes means that 46 % of the genes in the intestine are differentially regulated upon PEM dieting. Many of the DEGs are pathway components that are involved in cell proliferation and differentiation such as the JNK, Wg, Notch or JAK/Stat pathway, which are likely a part of the phenotypic expression of the intestinal cell homeostasis of flies fed a DR or PEM diet. The immune response was induced on DR diets, where a PEM led to a repressed immune response. However, an induced immune response alone may not be enough to gain fitness benefits upon a continuous oral infection of *S. marcescens*. My study also showed that when amino acid content is low a cascade of metabolic adaptions is brought into play to face the decrease of amino acid availability. Proteolytic processes are upregulated in RC flies subjected to PEM in comparison to RC flies fed a CD, whereas genes involved in lipid metabolism or glucose metabolism are downregulated. These data probably indicate an increase in amino acid utilization at the expense of lipid and carbohydrate utilization. Lipid and glucose homeostasis is often disrupted in children with severe PEM including hypoglycaemia, impaired glucose clearance and increased lipolysis (460,461,55). Interestingly, biological processes such as mitochondrial translation and mitochondrial respiratory chain complex assembly are highly upregulated in RC flies fed a PEM diet. Intestinal cells must respond to changes in amino acid availability in order to survive times of amino acid restriction. This response includes inhibition of anabolic processes and activation of autophagy and proteasomal degradation in order to recycle proteins. Mitochondria generate cellular ATP through oxidative phosphorylation and therefore have a central function in energy production within a cell. It is reported that mitochondria fuse in response to amino acid restriction to protect them from autophagosomal degradation (462). Furthermore, amino acid restriction increases mitochondrial protein synthesis and the capacity of mitochondria to catabolize amino acids (463). These data suggest that the cell channels the protein turnover to mitochondria to achieve mitochondrial protein biosynthesis. This seems not be driven by energy demand, because an alternative energy source in form of glucose is present in the diet. Therefore, the increased mitochondrial biosynthesis is a mechanism to limit cellular anabolism. This is in contrast to the detected upregulated DEGs that are involved in cytoplasmic translation or ribosomal subunit assembly in flies fed a PEM diet as these processes are anabolic. Protein synthesis depends on mRNA transcript abundance and accessibility, and consumes the highest fraction of nutrients and energy in cells (464). However, the biological process transcription was highly downregulated which was also confirmed by RNA concentration measurements. The RNA concentration per intestine was

approximately 20-fold lower in PEM subjected RC flies in comparison to CD fed RC flies. This was further confirmed as EC revealed decreased ploidy in absence of amino acids, which is an indicator for a decreased transcription rate within the EC. Amino acid restriction is normally associated with ribosome pausing and suppressed polysome formation, which results in a subsequent decrease in protein expression (465). Based on these data and the finding that the RNA abundance is reduced upon PEM dieting, I suggest that the protein synthesis is restricted even when ribosomal genes are upregulated. The comparison of GF flies subjected to DR or PEM with GF flies fed a CD revealed that genes involved in cell proliferation are downregulated suggesting that the amino acid status can influence proliferation pathways even when the indigenous microbiota is absent. Interestingly, processes that are associated with an induced immune response are downregulated in GF flies fed a DR diet in comparison to GF flies fed a CD. This means that the intestinal microbiota has a positive influence on the immune response when amino acids are present, whereas the microbiota does not stimulate the immune reaction when amino acids are absent. Surprisingly, the comparison between GF flies and RC flies fed the same diet revealed that the impact of the indigenous microbiota on the transcriptional landscape of the intestine increased with lower amino acid content. Therefore, the presence of the intestinal microbiota as well as the microbiota-mediated nutrient allocation is all the more important for the transcriptional regulation in times of amino acid scarcity. For sure, processes that are involved in immune responses are downregulated in GF flies as the microbiota is the main inducer of the immune system (225). Interestingly, the biological processes mitochondrial translation and proteolysis, which are upregulated upon PEM dieting in RC flies, are downregulated in GF flies subjected to DR or PEM in comparison to RC flies fed the same diet. These data suggest that the microbiota provide factors to the host for maintaining energy homeostasis and protein catabolic processes in the cell under amino acid scarcity, which is crucial for the cell viability. Thus, the constant association of the intestine with the microbiota have important roles in intestinal development and physiology, ranging from intestinal epithelial homeostasis to immunity and metabolic processes.

Furthermore, I identified memory signatures in the intestinal transcriptome of that flies subjected to a CD for 14 days after a 7 days period of PEM exhibited. The transcriptional profile of several genes on day 21 remained completely at the level of flies fed a PEM for 7 days. Genes belong to processes such as carbohydrate metabolic process, glucose transmembrane transport and lipid catabolic process were downregulated. These processes comprised galactosidases, mannosidases, amylases, glucosidases, glucose transmembrane transporter and genes with lipase activity. On the other hand, genes belong to processes such as proteolysis and

proteasome-mediated protein catabolic process were upregulated including several serine-endopeptidases and threonine-endopeptidases. Thus, the metabolic shift observed in long-term PEM diet fed flies is also detectable in flies recovered for 14 days from a short-term intervention of PEM suggesting that even short periods of nutritional stress can lead to long alterations of the metabolic status in the intestine. In *Drosopila*, it was shown that interventions of nutritional stress in early life can lead long-lasting changes in the metabolic homeostasis, which can sustain over several generations (466,467). These long-lasting alterations are partially explained by epigenetic reprogramming of metabolic genes (468). PEM in early childhood often favor later obesity, type 2 diabetes and impaired glucose tolerance, which is referred to as the dual burden paradox (469,470,471). However, the critical time window or etiology of childhood PEM for the establishment of these effects is still unclear. I showed that short-term PEM dieting in early life did not affect the intestinal homeostasis in later life. Nonetheless, comparable mortality rates were observed upon DSS-treatment between flies fed a CD continuously and flies subjected to DR or PEM for a short period of time in early life. These data suggest that imprinting of nutritional stressor events on the transcriptional profile can also lead to long-term consequences on the individual fitness.

6 Curriculum Vitae

Name:	Jakob von Frieling
Date of birth:	13.10.1986
Place of birth:	Göttingen, Germany
Nationality:	German

Education

2016 – 2020	PhD candidate - Department of Molecular Physiology, University of Kiel, Germany Thesis: Effects of malnutrition on epithelia-microbe interactions in the intestinal tract of *Drosophila melanogaster*.
2015 – 2016	Research assistant - Department of Molecular Physiology, University of Kiel, Germany
2012 - 2015	Master of Science, Biology – Department of Molecular Physiology, University of Kiel, Germany Thesis: Dopamine receptors in the *Drosophila* nervous system: physiological and behavioral aspects.
2008 – 2012	Bachelor of Science, Biology – Department of Cellular Neurobiology, University of Göttingen, Germany Thesis: Regulation der Corpora allata von *Locusta migratoria* durch die Neuropeptide Proctolin und FMRFamid.

7 Publications

Von Frieling J, Roeder T (2020)
Factors that affect the translation of dietary restriction into a longer life.
IUBMB Life, doi: 10.1002/iub.2224

Von Frieling J, Faisal NM, Sporn F, Pfefferkorn R, Nolte SS, Sommer F, Rosenstiel P, Roeder T (2019)
A high fat diet induces a microbiota dependent increase in stem cell activity in the *Drosophila* intestine.
BioRxiv, doi: 10.1101/604744

Rausch P, Rühlemann M, Hermes B, Doms S, Dagan T, Dierking K, Domin H, Fraune S, **von Frieling J**, (…), Roeder T, Schmitz RA, Schulenburg H, Soluch R, Sommer F, Stuckenbrock E, Weiland-Bräuer N, Rosenstiel P, Franke A, Bosch T, Baines JF (2019)
Comparative analysis of amplicon and metagenomic sequencing methods reveals key features in the evolution of animal metaorganisms.
Microbiome, 7(133), doi: 10.1186/s40168-019-0743-1

Von Frieling J, Fink C, Hamm J, Klischies K, Forster M, Bosch TC, Roeder T, Rosenstiel P, Sommer F (2018)
Grow with the challenge – microbial effects on epithelial proliferation, carcinogenesis and cancer therapy.
Frontiers in Microbiology, 9(2020), doi: 10.3389/fmicb.2018.02020

Stephano F, Nolte S, Hoffmann J, El-Kholy S, **von Frieling J**, Bruchhaus I, Fink C, Roeder T (2018)
Impaired Wnt signaling in dopamine containing neurons is associated with pathogenesis in a rotenone triggered *Drosophila* Parkinsons's disease model.
Scientific Reports, 8(1), doi: 10.1038/s41598-018-20836-w

Romey-Glüsing R*, Li Y*, Hoffmann J, **von Frieling J**, Knop M, Pfefferkorn R, Bruchhaus I, Fink C, Roeder T (2017)
Nutritional regimes with periodically recurring phases of dietary restriction extend lifespan in *Drosophila*.
FASEB Journal, 32, doi: 10.1096/fj.201700934R

Fink C, **von Frieling J**, Knop M, Roeder T (2017)
Drosophila fecal sampling.
Bio-protocols, 7(18), doi: 10.21769/BioProtoc.2547

Li Y, Tiedemann L, **von Frieling J**, Nolte S, El-Kholy S, Stephano F, Gelhaus C, Bruchaus I, Fink C, Roeder T (2017)
The role of monoaminergic neurotransmission for metabolic control in the fruit fly *Drosophila* melanogaster.
Frontiers in Systems Neuroscience, 1(50), doi: 10.3389/fnsys.2017.00060

Fink C, Schukies S, **von Frieling J**, Roeder R (2014)
Molekulare Analyse aminerger Signalwege im ZNS der Taufliege.
Biospektrum, 20(6): 636-639

8 Acknowledgements

In the beginning, I would like to express my sincere gratitude to my supervisor Thomas Roeder for the support and guidance throughout my PhD study. His guidance, motivation and expertise were a vital part to the success of this work. His calm manner and care helped me in all the time of research.

Besides my supervisor, I would like to thank my thesis committee. I gratefully acknowledge Dr. Kai Lüersen for the support and encouragement in the development of the holidic diet. I also thank Dr. Felix Sommer who was very helpful and provided me his assistance with 16s sequencing.

Many thanks to Ruben Prange for the fruitful discussions and for all the fun we have had in the last 4 years. I would also like to thank Dr. Stella Nolte, Dr. Roxana Pfefferkorn, Dr. Benedikt Mortzfeld and Dr. Judith Bossen who all helped me in numerous ways during various stages of my PhD. Special thanks go out to Britta Laubenstein and Christiane Sandberg for their technical support and ensuring laboratory routine.

I would like to say heartful thank to my mum, dad, Helmut, Stephan, Hannah, Timo and Janina for helping in whatever way they could during the sometimes stressful and challenging times.

Finally, I thank the CRC 1182 “Origin and function of Metaorganisms” for funding my research.

9 Declaration

I declare that the dissertation titled “Effects of malnutrition on epithelia-microbe interactions in the intestinal tract of *Drosophila melanogaster”* apart from my supervisor´s guidance and the listed references, is my own literary property and represents my own work. This dissertation has not been submitted elsewhere in order to obtain an academic degree and was prepared according to the *Rules of Good Scientific Practice* of the German research Foundation. An academic degree never was not withdrawn.

Hiermit erkläre ich, dass die vorliegende Dissertation mit dem Titel “ Effects of malnutrition on epithelia-microbe interactions in the intestinal tract of *Drosophila melanogaster*”, die ich unter der Betreuung durch meinen Supervisor Prof. Dr. Thomas Roeder und unter Zuhilfenahme der angegebenen Referenzen angefertigt habe, mein eigenes geistiges Eigentum ist und meine eigene Arbeit widerspiegelt. Die Arbeit wurde unter Berücksichtigung der *Regeln guter wissenschaftlicher Praxis* der Deutschen Forschungsgesellschaft angefertigt und an keiner weiteren Stelle im Rahmen eines Promotionsvorhabens eingereicht. Ein akademischer Grad wurde mir nicht entzogen.

Kiel, den

_____

Jakob von Frieling

10 References

1. Obesity and overweight [Internet]. [cited 2020 Jan 23]. Available from: https://www.who.int/news-room/fact-sheets/detail/obesity-and-overweight

2. Templin T, Cravo Oliveira Hashiguchi T, Thomson B, Dieleman J, Bendavid E. The overweight and obesity transition from the wealthy to the poor in low- and middle-income countries: A survey of household data from 103 countries. Popkin BM, editor. PLOS Med [Internet]. 2019 Nov 27 [cited 2020 Jan 23];16(11):e1002968. Available from: https://dx.plos.org/10.1371/journal.pmed.1002968

3. Blüher M. Obesity: global epidemiology and pathogenesis. Vol. 15, Nature Reviews Endocrinology. Nature Publishing Group; 2019. p. 288–98.

4. Obesity Update - OECD [Internet]. [cited 2020 Jan 23]. Available from: https://www.oecd.org/health/obesity-update.htm

5. Ladabaum U, Mannalithara A, Myer PA, Singh G. Obesity, abdominal obesity, physical activity, and caloric intake in US adults: 1988 to 2010. Am J Med. 2014;127(8).

6. Swinburn BA, Sacks G, Hall KD, McPherson K, Finegood DT, Moodie ML, et al. The global obesity pandemic: Shaped by global drivers and local environments. Vol. 378, The Lancet. Lancet Publishing Group; 2011. p. 804–14.

7. Christ A, Lauterbach M, Latz E. Western Diet and the Immune System: An Inflammatory Connection. Immunity [Internet]. 2019 Nov [cited 2020 Jan 24];51(5):794–811. Available from: https://linkinghub.elsevier.com/retrieve/pii/S1074761319304169

8. Singh GM, Danaei G, Farzadfar F, Stevens GA, Woodward M, Wormser D, et al. The Age-Specific Quantitative Effects of Metabolic Risk Factors on Cardiovascular Diseases and Diabetes: A Pooled Analysis. Wang G, editor. PLoS One [Internet]. 2013 Jul 30 [cited 2020 Jan 23];8(7):e65174. Available from: https://dx.plos.org/10.1371/journal.pone.0065174

9. Lauby-Secretan B, Scoccianti C, Loomis D, Grosse Y, Bianchini F, Straif K. Body fatness and cancer - Viewpoint of the IARC working group. Vol. 375, New England Journal of Medicine. Massachussetts Medical Society; 2016. p. 794–8.

10. Fabbrini E, Sullivan S, Klein S. Obesity and nonalcoholic fatty liver disease:

Biochemical, metabolic, and clinical implications. Hepatology [Internet]. 2010 Feb [cited 2020 Feb 2];51(2):679–89. Available from: http://doi.wiley.com/10.1002/hep.23280

11. Czernichow S, Kengne AP, Stamatakis E, Hamer M, Batty GD. Body mass index, waist circumference and waist-hip ratio: Which is the better discriminator of cardiovascular disease mortality risk? Evidence from an individual-participant meta-analysis of 82864 participants from nine cohort studies. Obes Rev. 2011 Sep;12(9):680–7.

12. Anandacoomarasamy A, Caterson I, Sambrook P, Fransen M, March L. The impact of obesity on the musculoskeletal system. Vol. 32, International Journal of Obesity. 2008. p. 211–22.

13. Anstey KJ, Cherbuin N, Budge M, Young J. Body mass index in midlife and late-life as a risk factor for dementia: A meta-analysis of prospective studies. Obes Rev. 2011 May;12(501).

14. Alberti KGMM, Eckel RH, Grundy SM, Zimmet PZ, Cleeman JI, Donato KA, et al. Harmonizing the metabolic syndrome: A joint interim statement of the international diabetes federation task force on epidemiology and prevention; National heart, lung, and blood institute; American heart association; World heart federation; International atherosclerosis society; And international association for the study of obesity. Vol. 120, Circulation. 2009. p. 1640–5.

15. Fontaine KR, Redden DT, Wang C, Westfall AO, Allison DB. Years of life lost due to obesity. J Am Med Assoc. 2003 Jan 8;289(2):187–93.

16. Flegal KM, Kit BK, Orpana H, Graubard BI. Association of all-cause mortality with overweight and obesity using standard body mass index categories a systematic review and meta-analysis. Vol. 309, JAMA - Journal of the American Medical Association. 2013. p. 71–82.

17. Reaven GM, Hollenbeck C, Jeng CY, Wu MS, Chen YDI. Measurement of plasma glucose, free fatty acid, lactate, and insulin for 24 h in patients with NIDDM. Diabetes. 1988;37(8):1020–4.

18. Björntorp P, Bergman H, Varnauskas E. PLASMA FREE FATTY ACID TURNOVER RATE IN OBESITY. Acta Med Scand. 1969;185(1–6):351–6.

19. Medina-Urrutia A, Posadas-Romero C, Posadas-Sánchez R, Jorge-Galarza E, Villarreal-

Molina T, González-Salazar M del C, et al. Role of adiponectin and free fatty acids on the association between abdominal visceral fat and insulin resistance. Cardiovasc Diabetol. 2015 Feb 10;14(1).

20. Boden G, Cheung P, Peter Stein T, Kresge K, Mozzoli M. FFA cause hepatic insulin resistance by inhibiting insulin suppression of glycogenolysis. Am J Physiol - Endocrinol Metab. 2002;283(1 46-1).

21. Boden G, Chen X, Ruiz J, White J V., Rossetti L. Mechanisms of fatty acid-induced inhibition of glucose uptake. J Clin Invest. 1994;93(6):2438–46.

22. Santomauro ATMG, Boden G, Silva MER, Rocha DM, Santos RF, Ursich MJM, et al. Overnight lowering of free fatty acids with acipimox improves insulin resistance and glucose tolerance in obese diabetic and nondiabetic subjects. Diabetes. 1999;48(9):1836–41.

23. Cusi K, Kashyap S, Gastaldelli A, Bajaj M, Cersosimo E. Effects on insulin secretion and insulin action of a 48-h reduction of plasma free fatty acids with acipimox in nondiabetic subjects genetically predisposed to type 2 diabetes. Am J Physiol Metab [Internet]. 2007 Jun [cited 2020 Feb 2];292(6):E1775–81. Available from: https://www.physiology.org/doi/10.1152/ajpendo.00624.2006

24. KURIOKA S, MURAKAMI Y, NISHIKI M, SOHMIYA M, KOSHIMURA K, KATO Y. Relationship between Visceral Fat Accumulation and Anti-Lipolytic Action of Insulin in Patients with Type 2 Diabetes Mellitus. Endocr J [Internet]. 2002 [cited 2020 Feb 2];49(4):459–64. Available from: http://joi.jlc.jst.go.jp/JST.JSTAGE/endocrj/49.459?from=CrossRef

25. Boden G, Lebed B, Schatz M, Homko C, Lemieux S. Effects of Acute Changes of Plasma Free Fatty Acids on Intramyocellular Fat Content and Insulin Resistance in Healthy Subjects. Diabetes. 2001;50(7):1612–7.

26. Mundi MS, Koutsari C, Jensen MD. Effects of Increased Free Fatty Acid Availability on Adipose Tissue Fatty Acid Storage in Men. J Clin Endocrinol Metab [Internet]. 2014 Dec [cited 2020 Feb 2];99(12):E2635–42. Available from: https://academic.oup.com/jcem/article-lookup/doi/10.1210/jc.2014-2690

27. Tripathy D, Mohanty P, Dhindsa S, Syed T, Ghanim H, Aliada A, et al. Elevation of Free Fatty Acids Induces Inflammation and Impairs Vascular Reactivity in Healthy Subjects.

Diabetes. 2003 Dec;52(12):2882–7.

28. Esposito K, Pontillo A, Di Palo C, Giugliano G, Masella M, Marfella R, et al. Effect of Weight Loss and Lifestyle Changes on Vascular Inflammatory Markers in Obese Women: A Randomized Trial. J Am Med Assoc. 2003 Apr 9;289(14):1799–804.

29. Bradley RL, Fisher FM, Maratos-Flier E. Dietary fatty acids differentially regulate production of TNF-α and IL-10 by murine 3T3-L1 adipocytes. Obesity. 2008 May;16(5):938–44.

30. Kris-Etherton PM, Yu S. Individual fatty acid effects on plasma lipids and lipoproteins: Human studies. In: American Journal of Clinical Nutrition. American Society for Nutrition; 1997.

31. James MJ, Gibson RA, Cleland LG. Dietary polyunsaturated fatty acids and inflammatory mediator production. In: American Journal of Clinical Nutrition. 2000.

32. Cranmer-Byng MM, Liddle DM, De Boer AA, Monk JM, Robinson LE. Proinflammatory effects of arachidonic acid in a lipopolysaccharide-induced inflammatory microenvironment in 3T3-L1 adipocytes in vitro. Appl Physiol Nutr Metab [Internet]. 2015 Feb [cited 2020 Feb 2];40(2):142–54. Available from: http://www.nrcresearchpress.com/doi/10.1139/apnm-2014-0022

33. Albracht-Schulte K, Gonzalez S, Jackson A, Wilson S, Ramalingam L, Kalupahana NS, et al. Eicosapentaenoic acid improves hepatic metabolism and reduces inflammation independent of obesity in high-fat-fed mice and in HepG2 cells. Nutrients. 2019 Mar 1;11(3).

34. Stunkard AJ, Harris JR, Pedersen NL, McClearn GE. The Body-Mass Index of Twins Who Have Been Reared Apart. N Engl J Med. 1990 May 24;322(21):1483–7.

35. Wardle J, Carnell S, Haworth CMA, Plomin R. Evidence for a strong genetic influence on childhood adiposity despite the force of the obesogenic environment. Am J Clin Nutr. 2008 Jan 2;87(2):398–404.

36. Clément K, Vaisse C, Lahlou N, Cabrol S, Pelloux V, Cassuto D, et al. A mutation in the human leptin receptor gene causes obesity and pituitary dysfunction. Nature. 1998 Mar 26;392(6674):398–401.

37. Montague CT, Farooqi IS, Whitehead JP, Soos MA, Rau H, Wareham NJ, et al.

Congenital leptin deficiency is associated with severe early-onset obesity in humans. Nature. 1997 Jun 26;387(6636):903–8.

38. Krude H, Biebermann H, Luck W, Horn R, Brabant G, Grüters A. Severe early-onset obesity, adrenal insufficiency and red hair pigmentation caused by POMC mutations in humans. Nat Genet. 1998;19(2):155–7.

39. Dubern B, Clément K, Pelloux V, Froguel P, Girardet JP, Guy-Grand B, et al. Mutational analysis of melanocortin-4 receptor, agouti-related protein, and α-melanocyte-stimulating hormone genes in severely obese children. J Pediatr. 2001;139(2):204–9.

40. Kublaoui BM, Holder JL, Tolson KP, Gemelli T, Zinn AR. SIM1 overexpression partially rescues agouti yellow and diet-induced obesity by normalizing food intake. Endocrinology. 2006;147(10):4542–9.

41. Boisvert JA, Harrell WA, Garcia-Estan J, Santonja-Medina F, García-Sanz MP, Martínez F, et al. Exploring the developmental overnutrition hypothesis using parental-offspring associations and FTO as an instrumental variable. PLoS Med [Internet]. 2015 [cited 2020 Jan 25];5(11):0484–93. Available from: https://www.dovepress.com/articles.php?article_id=25574%5Cnhttp://search.ebscohost.com/login.aspx?direct=true&db=cin20&AN=103760273&site=ehost-live

42. Malomo K, Ntlholang O. The evolution of obesity: from evolutionary advantage to a disease. Biomed Res Clin Pract. 2018;3(2).

43. Pijl H. Obesity: evolution of a symptom of affluence. Neth J Med [Internet]. 2011 Apr [cited 2020 Jan 25];69(4):159–66. Available from: http://www.ncbi.nlm.nih.gov/pubmed/21527802

44. Grover Z, Ee LC. Protein Energy Malnutrition. Vol. 56, Pediatric Clinics of North America. 2009. p. 1055–68.

45. The state of food security and nutrition in the world 2019 | UNICEF [Internet]. [cited 2020 Jan 23]. Available from: https://www.unicef.org/reports/state-of-food-security-and-nutrition-2019

46. Black RE, Victora CG, Walker SP, Bhutta ZA, Christian P, De Onis M, et al. Maternal and child undernutrition and overweight in low-income and middle-income countries. Vol. 382, The Lancet. Lancet Publishing Group; 2013. p. 427–51.

47. Kelly P. Undernutrition. In: Nutrition and Metabolism: Second Edition. Wiley-Blackwell; 2011. p. 378–86.

48. Saunders J, Smith T. Malnutrition: Causes and consequences. Vol. 10, Clinical Medicine, Journal of the Royal College of Physicians of London. Royal College of Physicians; 2010. p. 624–7.

49. Batool R, Butt MS, Sultan MT, Saeed F, Naz R. Protein-Energy Malnutrition: A Risk Factor for Various Ailments. Vol. 55, Critical Reviews in Food Science and Nutrition. Taylor and Francis Inc.; 2015. p. 242–53.

50. Schofield C, Ashworth A. Why have mortality rates for severe malnutrition remained so high? Bull World Health Organ. 1996;74(2):223–9.

51. Jackson AA. Blood glutathione in severe malnutrition in childhood. Trans R Soc Trop Med Hyg [Internet]. 1986 Jan [cited 2020 Jan 25];80(6):911–3. Available from: https://academic.oup.com/trstmh/article-lookup/doi/10.1016/0035-9203(86)90256-7

52. Ahmed HM, Laryea MD, El-Karib AO, El-Amin EO, Biggemann B, Leichsenring M, et al. Vitamin E status in Sudanese children with protein-energy malnutrition. Z Ernahrungswiss. 1990 Mar;29(1):47–53.

53. Hosni Barakat S, Latif Hatem N, Ahmed Barghash N, El-Sayed Ibrahim H. Antioxidants in Children with Protein Energy Malnutrition. Vol. 13, Alexandria Journal of Pediatrics. 1999.

54. Manary MJ, Broadhead RL, Yarasheski KE. Whole-body protein kinetics in marasmus and kwashiorkor during acute infection. Am J Clin Nutr [Internet]. 1998 Jun 1 [cited 2020 Jan 25];67(6):1205–9. Available from: https://academic.oup.com/ajcn/article/67/6/1205-1209/4666079

55. Badaloo A V, Forrester T, Reid M, Jahoor F. Lipid kinetic differences between children with kwashiorkor and those with marasmus. Am J Clin Nutr [Internet]. 2006 Jun 1 [cited 2020 Jan 25];83(6):1283–8. Available from: https://academic.oup.com/ajcn/article/83/6/1283/4633057

56. Rice AL, Sacco L, Hyder A, Black RE. Malnutrition as an underlying cause of childhood deaths associated with infectious diseases in developing countries. Bull World Health Organ. 2000;78(10):1207–21.

57. Nassar MF, Younis NT, Tohamy AG, Dalam DM, El Badawy MA. T-lymphocyte subsets and thymic size in malnourished infants in Egypt: A hospital-based study. East Mediterr Heal J. 2007 Sep;13(5):1031–42.

58. Cunha MCR, Lima F da S, Vinolo MAR, Hastreiter A, Curi R, Borelli P, et al. Protein Malnutrition Induces Bone Marrow Mesenchymal Stem Cells Commitment to Adipogenic Differentiation Leading to Hematopoietic Failure. Shi X-M, editor. PLoS One [Internet]. 2013 Mar 14 [cited 2020 Jan 25];8(3):e58872. Available from: http://dx.plos.org/10.1371/journal.pone.0058872

59. Reid M, Badaloo A, Forrester T, Morlese JF, Heird WC, Jahoor F. The acute-phase protein response to infection in edematous and. Am J Physiol. 2002;1(5).

60. Rikimaru T, Taniguchi K, Yartey JE, Kennedy DO, Nkrumah FK. Humoral and cell-mediated immunity in malnourished children in Ghana. Eur J Clin Nutr. 1998;52(5):344–50.

61. Malavé I, Vethencourt MA, Pirela M, Cordero R. Serum levels of thyroxine-binding prealbumin, C-reactive protein and interleukin-6 in protein-energy undernourished children and normal controls without or with associated clinical infections. J Trop Pediatr. 1998;44(5):256–62.

62. Hassanein ESA, Assem HM, Rezk MM, El-Maghraby RM. Study of plasma albumin, transferrin, and fibronectin in children with mild to moderate protein-energy malnutrition. J Trop Pediatr. 1998;44(6):362–5.

63. Thavaraj V, Sesikeran B. Histopathological changes in skin of children with clinical protein energy malnutrition before and after recovery. J Trop Pediatr. 1989 Jun;35(3):105–8.

64. Shiner M, Redmond AOB, Hansen JDL. The jejunal mucosa in protein-energy malnutrition. A clinical, histological, and ultrastructural study. Exp Mol Pathol. 1973;19(1):61–78.

65. Schneider RE, Viteri FE. Morphological aspects of the duodenojejunal mucosa in protein--calorie malnourished children and during recovery. Am J Clin Nutr. 1972 Oct;25(10):1092–102.

66. Keet MP, Moodie AD, Wittmann W, Hansen JD. Kwashiorkor: a prospective ten-year follow-up study. S Afr Med J [Internet]. 1971 Dec 25 [cited 2020 Jan 25];45(49):1427–

49. Available from: http://www.ncbi.nlm.nih.gov/pubmed/4334564

67. Hoorweg J, Stanfield JP. The Effects of Protein Energy Malnutrition in Early Childhood on Intellectual and Motor Abilities in Later Childhood and Adolescence. Dev Med Child Neurol [Internet]. 2008 Nov 12 [cited 2020 Jan 25];18(3):330–50. Available from: http://doi.wiley.com/10.1111/j.1469-8749.1976.tb03656.x

68. Kar BR, Rao SL, Chandramouli BA. Cognitive development in children with chronic protein energy malnutrition. Behav Brain Funct [Internet]. 2008 [cited 2020 Jan 25];4(1):31. Available from: http://behavioralandbrainfunctions.biomedcentral.com/articles/10.1186/1744-9081-4-31

69. Constans T, Bacq Y, Bréchot J -F, Guilmot J -L, Choutet P, Lamisse F. Protein-Energy Malnutrition in Elderly Medical Patients. J Am Geriatr Soc. 1992;40(3):263–8.

70. Thorslund S, Toss G, Nilsson I, v Schenck H, Symreng T, Zetterqvist H. Prevalence of protein-energy malnutrition in a large population of elderly people at home. Scand J Prim Health Care. 1990;8(4):243–8.

71. Cederholm T, Jägren C, Hellström K. Outcome of protein-energy malnutrition in elderly medical patients. Am J Med. 1995;98(1):67–74.

72. Fontana L, Partridge L. Promoting health and longevity through diet: From model organisms to humans. Vol. 161, Cell. Cell Press; 2015. p. 106–18.

73. Lee C, Longo V. Dietary restriction with and without caloric restriction for healthy aging. Vol. 5, F1000Research. Faculty of 1000 Ltd; 2016.

74. Mirzaei H, Suarez JA, Longo VD. Protein and amino acid restriction, aging and disease: From yeast to humans. Vol. 25, Trends in Endocrinology and Metabolism. Elsevier Inc.; 2014. p. 558–66.

75. Hoedjes KM, Rodrigues MA, Flatt T. Amino acid modulation of lifespan and reproduction in Drosophila. Vol. 23, Current Opinion in Insect Science. Elsevier Inc.; 2017. p. 118–22.

76. Yoshida S, Yamahara K, Kume S, Koya D, Yasuda-Yamahara M, Takeda N, et al. Role of dietary amino acid balance in diet restriction-mediated lifespan extension, renoprotection, and muscle weakness in aged mice. Aging Cell. 2018 Aug 1;17(4).

77. Mirisola MG, Taormina G, Fabrizio P, Wei M, Hu J, Longo VD. Serine- and Threonine/Valine-Dependent Activation of PDK and Tor Orthologs Converge on Sch9 to Promote Aging. PLoS Genet. 2014 Feb;10(2).

78. Laeger T, Castaño-Martinez T, Werno MW, Japtok L, Baumeier C, Jonas W, et al. Dietary carbohydrates impair the protective effect of protein restriction against diabetes in NZO mice used as a model of type 2 diabetes. Diabetologia. 2018 Jun 1;61(6):1459–69.

79. Weindruch R, Walford RL, Fligiel S, Guthrie D. The retardation of aging in mice by dietary restriction: Longevity, cancer, immunity and lifetime energy intake. J Nutr. 1986;116(4):641–54.

80. Hennig M, Ewering L, Pyschny S, Shimoyama S, Olecka M, Ewald D, et al. Dietary protein restriction throughout intrauterine and postnatal life results in potentially beneficial myocardial tissue remodeling in the adult mouse heart. Sci Rep. 2019 Dec 1;9(1).

81. Colman RJ, Beasley TM, Kemnitz JW, Johnson SC, Weindruch R, Anderson RM. Caloric restriction reduces age-related and all-cause mortality in rhesus monkeys. Nat Commun. 2014 Apr 1;5.

82. Mattison JA, Roth GS, Mark Beasley T, Tilmont EM, Handy AM, Herbert RL, et al. Impact of caloric restriction on health and survival in rhesus monkeys from the NIA study. Nature. 2012 Sep 13;489(7415):318–21.

83. von Frieling J, Roeder T. Factors that affect the translation of dietary restriction into a longer life. IUBMB Life. Blackwell Publishing Ltd; 2019.

84. Hwangbo DS, Garsham B, Tu MP, Palmer M, Tatar M. Drosophila dFOXO controls lifespan and regulates insulin signalling in brain and fat body. Nature. 2004 Jun 3;429(6991):562–6.

85. Selman C, Lingard S, Choudhury AI, Batterham RL, Claret M, Clements M, et al. Evidence for lifespan extension and delayed age-related biomarkers in insulin receptor substrate 1 null mice. FASEB J. 2008 Mar;22(3):807–18.

86. Lin K, Dorman JB, Rodan A, Kenyon C. daf-16: An HNF-3/forkhead family member that can function to double the life-span of Caenorhabditis elegans. Science (80-). 1997 Nov 14;278(5341):1319–22.

87. Papadopoli D, Boulay K, Kazak L, Pollak M, Mallette FA, Topisirovic I, et al. Mtor as a central regulator of lifespan and aging. F1000Research. 2019;8.

88. Wu Z, Song L, Liu SQ, Huang D. Independent and additive effects of glutamic acid and methionine on yeast longevity. PLoS One. 2013 Nov 7;8(11).

89. de Marte ML, Enesco HE. Influence of low tryptophan diet on survival and organ growth in mice. Mech Ageing Dev. 1986;36(2):161–71.

90. Lee BC, Kaya A, Ma S, Kim G, Gerashchenko M V., Yim SH, et al. Methionine restriction extends lifespan of Drosophila melanogaster under conditions of low amino-acid status. Nat Commun. 2014 Apr 7;5.

91. Shanley DP, Kirkwood TBL. CALORIE RESTRICTION AND AGING: A LIFE-HISTORY ANALYSIS. Evolution (N Y). 2000;54(3):740.

92. Moatt JP, Nakagawa S, Lagisz M, Walling CA. The effect of dietary restriction on reproduction: a meta-analytic perspective. BMC Evol Biol. 2016 Oct 7;16(1):1–9.

93. Grandison RC, Piper MDW, Partridge L. Amino-acid imbalance explains extension of lifespan by dietary restriction in Drosophila. Nature. 2009 Dec 24;462(7276):1061–4.

94. McCarty MF, Barroso-Aranda J, Contreras F. The low-methionine content of vegan diets may make methionine restriction feasible as a life extension strategy. Med Hypotheses. 2009 Feb;72(2):125–8.

95. Melnik BC, John SM, Schmitz G. Milk is not just food but most likely a genetic transfection system activating mTORC1 signaling for postnatal growth. Vol. 12, Nutrition Journal. 2013.

96. Coker RH, Miller S, Schutzler S, Deutz N, Wolfe RR. Whey protein and essential amino acids promote the reduction of adipose tissue and increased muscle protein synthesis during caloric restriction-induced weight loss in elderly, obese individuals. Nutr J. 2012;11(1).

97. Noguchi T. Protein nutrition and insulin-like growth factor system. Br J Nutr. 2000;84(S2):S241–4.

98. Levine ME, Suarez JA, Brandhorst S, Balasubramanian P, Cheng CW, Madia F, et al. Low protein intake is associated with a major reduction in IGF-1, cancer, and overall mortality in the 65 and younger but not older population. Cell Metab. 2014 Mar

4;19(3):407–17.

99. Solon-Biet SM, McMahon AC, Ballard JWO, Ruohonen K, Wu LE, Cogger VC, et al. The ratio of macronutrients, not caloric intake, dictates cardiometabolic health, aging, and longevity in ad libitum-fed mice. Cell Metab. 2014 Mar 4;19(3):418–30.

100. Solon-Biet SM, Mitchell SJ, Coogan SCP, Cogger VC, Gokarn R, McMahon AC, et al. Dietary Protein to Carbohydrate Ratio and Caloric Restriction: Comparing Metabolic Outcomes in Mice. Cell Rep. 2015 Jun 16;11(10):1529–34.

101. Bruce KD, Hoxha S, Carvalho GB, Yamada R, Wang HD, Karayan P, et al. High carbohydrate-low protein consumption maximizes Drosophila lifespan. Exp Gerontol. 2013;48(10):1129–35.

102. Lee KP. Dietary protein: Carbohydrate balance is a critical modulator of lifespan and reproduction in Drosophila melanogaster: A test using a chemically defined diet. J Insect Physiol. 2015 Apr 1;75:12–9.

103. Chaix A, Zarrinpar A, Miu P, Panda S. Time-restricted feeding is a preventative and therapeutic intervention against diverse nutritional challenges. Cell Metab. 2014 Dec 2;20(6):991–1005.

104. Gabel K, Hoddy KK, Haggerty N, Song J, Kroeger CM, Trepanowski JF, et al. Effects of 8-hour time restricted feeding on body weight and metabolic disease risk factors in obese adults: A pilot study. Nutr Heal Aging. 2018;4(4):345–53.

105. Moro T, Tinsley G, Bianco A, Marcolin G, Pacelli QF, Battaglia G, et al. Effects of eight weeks of time-restricted feeding (16/8) on basal metabolism, maximal strength, body composition, inflammation, and cardiovascular risk factors in resistance-trained males. J Transl Med [Internet]. 2016 Dec 13 [cited 2020 Feb 1];14(1):290. Available from: http://translational-medicine.biomedcentral.com/articles/10.1186/s12967-016-1044-0

106. Mitchell SJ, Bernier M, Mattison JA, Aon MA, Kaiser TA, Anson RM, et al. Daily Fasting Improves Health and Survival in Male Mice Independent of Diet Composition and Calories. Cell Metab. 2019 Jan 8;29(1):221-228.e3.

107. Xie K, Neff F, Markert A, Rozman J, Aguilar-Pimentel JA, Amarie OV, et al. Every-other-day feeding extends lifespan but fails to delay many symptoms of aging in mice. Nat Commun. 2017 Dec 1;8(1).

108. Goodrick CL, Ingram DK, Reynolds MA, Freeman JR, Cider N. Effects of intermittent feeding upon body weight and lifespan in inbred mice: interaction of genotype and age. Mech Ageing Dev. 1990;55(1):69–87.

109. Whitaker R, Pilar Gil M, Ding F, Tatar M, Helfand SL, Neretti N. Dietary switch reveals fast coordinated gene expression changes in Drosophila melanogaster. Aging (Albany NY). 2014;6(5):355–68.

110. Romey-Glüsing R, Li Y, Hoffmann J, Von Frieling J, Knop M, Pfefferkorn R, et al. Nutritional regimens with periodically recurring phases of dietary restriction extend lifespan in Drosophila. FASEB J. 2018 Apr 1;32(4):1993–2003.

111. Sender R, Fuchs S, Milo R. Are We Really Vastly Outnumbered? Revisiting the Ratio of Bacterial to Host Cells in Humans. Vol. 164, Cell. Cell Press; 2016. p. 337–40.

112. Walter J, Ley R. The Human Gut Microbiome: Ecology and Recent Evolutionary Changes. Annu Rev Microbiol. 2011 Oct 13;65(1):411–29.

113. Turnbaugh PJ, Hamady M, Yatsunenko T, Cantarel BL, Duncan A, Ley RE, et al. A core gut microbiome in obese and lean twins. Nature. 2009 Jan 22;457(7228):480–4.

114. Lee S, Sung J, Lee JE, Ko GP. Comparison of the gut microbiotas of healthy adult twins living in South Korea and the United States. Appl Environ Microbiol. 2011 Oct;77(20):7433–7.

115. Goodrich JK, Waters JL, Poole AC, Sutter JL, Koren O, Blekhman R, et al. Human genetics shape the gut microbiome. Cell. 2014 Nov 6;159(4):789–99.

116. Rothschild D, Weissbrod O, Barkan E, Kurilshikov A, Korem T, Zeevi D, et al. Environment dominates over host genetics in shaping human gut microbiota. Nature. 2018 Mar 8;555(7695):210–5.

117. Korem T, Zeevi D, Suez J, Weinberger A, Avnit-Sagi T, Pompan-Lotan M, et al. Growth dynamics of gut microbiota in health and disease inferred from single metagenomic samples. Science (80-). 2015 Sep 4;349(6252):1101–6.

118. Smits SA, Leach J, Sonnenburg ED, Gonzalez CG, Lichtman JS, Reid G, et al. Seasonal cycling in the gut microbiome of the Hadza hunter-gatherers of Tanzania. Science (80-). 2017 Aug 25;357(6353):802–5.

119. Singh RK, Chang HW, Yan D, Lee KM, Ucmak D, Wong K, et al. Influence of diet on

the gut microbiome and implications for human health. Vol. 15, Journal of Translational Medicine. BioMed Central Ltd.; 2017.

120. Yatsunenko T, Rey FE, Manary MJ, Trehan I, Dominguez-Bello MG, Contreras M, et al. Human gut microbiome viewed across age and geography. Vol. 486, Nature. 2012. p. 222–7.

121. Obregon-Tito AJ, Tito RY, Metcalf J, Sankaranarayanan K, Clemente JC, Ursell LK, et al. Subsistence strategies in traditional societies distinguish gut microbiomes. Nat Commun. 2015;6.

122. Manichanh C, Rigottier-Gois L, Bonnaud E, Gloux K, Pelletier E, Frangeul L, et al. Reduced diversity of faecal microbiota in Crohn's disease revealed by a metagenomic approach. Gut. 2006 Feb;55(2):205–11.

123. De Goffau MC, Luopajärvi K, Knip M, Ilonen J, Ruohtula T, Härkönen T, et al. Fecal microbiota composition differs between children with β-cell autoimmunity and those without. Diabetes. 2013 Apr;62(4):1238–44.

124. Shah V, Lambeth SM, Carson T, Lowe J, Ramaraj T, Leff JW, et al. Composition Diversity and Abundance of Gut Microbiome in Prediabetes and Type 2 Diabetes. J Diabetes Obes. 2015 Dec 26;2(2):108–14.

125. Dao MC, Everard A, Aron-Wisnewsky J, Sokolovska N, Prifti E, Verger EO, et al. Akkermansia muciniphila and improved metabolic health during a dietary intervention in obesity: Relationship with gut microbiome richness and ecology. Gut. 2016 Mar 1;65(3):426–36.

126. Le Chatelier E, Nielsen T, Qin J, Prifti E, Hildebrand F, Falony G, et al. Richness of human gut microbiome correlates with metabolic markers. Nature. 2013;500(7464):541–6.

127. Cantarel BL, Lombard V, Henrissat B. Complex carbohydrate utilization by the healthy human microbiome. PLoS One. 2012 Jun 13;7(6).

128. Wong JMW, De Souza R, Kendall CWC, Emam A, Jenkins DJA. Colonic health: Fermentation and short chain fatty acids. In: Journal of Clinical Gastroenterology. 2006. p. 235–43.

129. Singh N, Gurav A, Sivaprakasam S, Brady E, Padia R, Shi H, et al. Activation of

Gpr109a, receptor for niacin and the commensal metabolite butyrate, suppresses colonic inflammation and carcinogenesis. Immunity. 2014 Jan 16;40(1):128–39.

130. Maslowski KM, Vieira AT, Ng A, Kranich J, Sierro F, Di Yu, et al. Regulation of inflammatory responses by gut microbiota and chemoattractant receptor GPR43. Nature. 2009 Oct 29;461(7268):1282–6.

131. Byndloss MX, Olsan EE, Rivera-Chávez F, Tiffany CR, Cevallos SA, Lokken KL, et al. Microbiota-activated PPAR-γ signaling inhibits dysbiotic Enterobacteriaceae expansion. Science (80-). 2017 Aug 11;357(6351):570–5.

132. De Vadder F, Kovatcheva-Datchary P, Goncalves D, Vinera J, Zitoun C, Duchampt A, et al. Microbiota-generated metabolites promote metabolic benefits via gut-brain neural circuits. Cell. 2014;156(1–2):84–96.

133. Lin H V., Frassetto A, Kowalik Jr EJ, Nawrocki AR, Lu MM, Kosinski JR, et al. Butyrate and Propionate Protect against Diet-Induced Obesity and Regulate Gut Hormones via Free Fatty Acid Receptor 3-Independent Mechanisms. Brennan L, editor. PLoS One [Internet]. 2012 Apr 10 [cited 2020 Jan 28];7(4):e35240. Available from: https://dx.plos.org/10.1371/journal.pone.0035240

134. Kirkpatrick C, Maurer LM, Oyelakin NE, Yoncheva YN, Maurer R, Slonczewski JL. Acetate and formate stress: Opposite responses in the proteome of Escherichia coli. J Bacteriol. 2001;183(21):6466–77.

135. Pinhal S, Ropers D, Geiselmann J, De Jong H. Acetate metabolism and the inhibition of bacterial growth by acetate. J Bacteriol. 2019;201(13).

136. LeBlanc JG, Milani C, de Giori GS, Sesma F, van Sinderen D, Ventura M. Bacteria as vitamin suppliers to their host: A gut microbiota perspective. Vol. 24, Current Opinion in Biotechnology. 2013. p. 160–8.

137. Macfarlane GT, Macfarlane S. Bacteria, colonic fermentation, and gastrointestinal health. J AOAC Int. 2012;95(1):50–60.

138. Meijers BKI, Evenepoel P. The gut-kidney axis: Indoxyl sulfate, p-cresyl sulfate and CKD progression. Vol. 26, Nephrology Dialysis Transplantation. 2011. p. 759–61.

139. Kushkevych I, Dordević D, Kollar P, Vítězová M, Drago L. Hydrogen Sulfide as a Toxic Product in the Small–Large Intestine Axis and its Role in IBD Development. J Clin Med.

2019 Jul 19;8(7):1054.

140. Andriamihaja M, Lan A, Beaumont M, Audebert M, Wong X, Yamada K, et al. The deleterious metabolic and genotoxic effects of the bacterial metabolite p-cresol on colonic epithelial cells. Free Radic Biol Med. 2015 Jun 20;85:219–27.

141. Nowak A, Libudzisz Z. Ability of intestinal lactic bacteria to bind or/and metabolise phenol and p-cresol. Ann Microbiol. 2007;57(3):329–35.

142. Cremin JD, Fitch MD, Fleming SE. Glucose alleviates ammonia-induced inhibition of short-chain fatty acid metabolism in rat colonic epithelial cells. Am J Physiol - Gastrointest Liver Physiol. 2003 Jul 1;285(1 48-1).

143. Chen J, Rao JN, Zou T, Liu L, Marasa BS, Xiao L, et al. Polyamines are required for expression of Toll-like receptor 2 modulating intestinal epithelial barrier integrity. Am J Physiol Liver Physiol [Internet]. 2007 Sep [cited 2020 Jan 28];293(3):G568–76. Available from: https://www.physiology.org/doi/10.1152/ajpgi.00201.2007

144. Rao JN, Rathor N, Zhuang R, Zou T, Liu L, Xiao L, et al. Polyamines regulate intestinal epithelial restitution through TRPC1-mediated Ca2+ signaling by differentially modulating STIM1 and STIM2. Am J Physiol - Cell Physiol. 2012 Aug 1;303(3).

145. Kibe R, Kurihara S, Sakai Y, Suzuki H, Ooga T, Sawaki E, et al. Upregulation of colonic luminal polyamines produced by intestinal microbiota delays senescence in mice. Sci Rep. 2014 Apr 1;4.

146. Reitzer L. Nitrogen Assimilation and Global Regulation in *Escherichia coli*. Annu Rev Microbiol [Internet]. 2003 Oct [cited 2020 Jan 28];57(1):155–76. Available from: http://www.annualreviews.org/doi/10.1146/annurev.micro.57.030502.090820

147. Gill SR, Pop M, DeBoy RT, Eckburg PB, Turnbaugh PJ, Samuel BS, et al. Metagenomic analysis of the human distal gut microbiome. Science (80-). 2006 Jun 2;312(5778):1355–9.

148. Metges CC, Petzke KJ. Utilization of essential amino acids synthesized in the intestinal microbiota of monogastric mammals. Br J Nutr. 2005 Nov;94(5):621–2.

149. Torrallardona D, Harris CI, Fuller MF. Pigs' Gastrointestinal Microflora Provide Them with Essential Amino Acids. J Nutr [Internet]. 2003 Apr 1 [cited 2020 Jan 28];133(4):1127–31. Available from:

https://academic.oup.com/jn/article/133/4/1127/4688139

150. Metges CC, El-Khoury AE, Henneman L, Petzke KJ, Grant I, Bedri S, et al. Availability of intestinal microbial lysine for whole body lysine homeostasis in human subjects. Am J Physiol - Endocrinol Metab. 1999 Oct;277(4 40-4).

151. Fraune S, Bosch TCG. Why bacteria matter in animal development and evolution. BioEssays [Internet]. 2010 Jul [cited 2020 Jan 22];32(7):571–80. Available from: http://doi.wiley.com/10.1002/bies.200900192

152. Zilber-Rosenberg I, Rosenberg E. Role of microorganisms in the evolution of animals and plants: The hologenome theory of evolution. Vol. 32, FEMS Microbiology Reviews. 2008. p. 723–35.

153. Link W, Fernandez-Marcos PJ. FOXO transcription factors at the interface of metabolism and cancer. Int J Cancer [Internet]. 2017 Dec 15 [cited 2020 Feb 1];141(12):2379–91. Available from: http://doi.wiley.com/10.1002/ijc.30840

154. Saxton RA, Sabatini DM. mTOR Signaling in Growth, Metabolism, and Disease. Vol. 168, Cell. Cell Press; 2017. p. 960–76.

155. Loewith R, Hall MN. Target of rapamycin (TOR) in nutrient signaling and growth control. Vol. 189, Genetics. 2011. p. 1177–201.

156. Laplante M, Sabatini DM. mTOR signaling at a glance. J Cell Sci. 2009 Oct 15;122(20):3589–94.

157. Jacinto E, Loewith R, Schmidt A, Lin S, Rüegg MA, Hall A, et al. Mammalian TOR complex 2 controls the actin cytoskeleton and is rapamycin insensitive. Nat Cell Biol. 2004 Nov;6(11):1122–8.

158. Ma XM, Yoon SO, Richardson CJ, Jülich K, Blenis J. SKAR Links Pre-mRNA Splicing to mTOR/S6K1-Mediated Enhanced Translation Efficiency of Spliced mRNAs. Cell. 2008 Apr 18;133(2):303–13.

159. Holz MK, Ballif BA, Gygi SP, Blenis J. mTOR and S6K1 mediate assembly of the translation preinitiation complex through dynamic protein interchange and ordered phosphorylation events. Cell. 2005 Nov 18;123(4):569–80.

160. Gingras AC, Gygi SP, Raught B, Polakiewicz RD, Abraham RT, Hoekstra MF, et al. Regulation of 4E-BP1 phosphorylation: A novel two step mechanism. Genes Dev. 1999

Jun 1;13(11):1422–37.

161. Hosokawa N, Hara T, Kaizuka T, Kishi C, Takamura A, Miura Y, et al. Nutrient-dependent mTORCl association with the ULK1-Atg13-FIP200 complex required for autophagy. Mol Biol Cell. 2009 Apr 1;20(7):1981–91.

162. Porstmann T, Santos CR, Griffiths B, Cully M, Wu M, Leevers S, et al. SREBP Activity Is Regulated by mTORC1 and Contributes to Akt-Dependent Cell Growth. Cell Metab. 2008 Sep 3;8(3):224–36.

163. Ben-Sahra I, Howell JJ, Asara JM, Manning BD. Stimulation of de novo pyrimidine synthesis by growth signaling through mTOR and S6K1. Science (80-). 2013 Mar 15;339(6125):1323–8.

164. Hara K, Yonezawa K, Weng QP, Kozlowski MT, Belham C, Avruch J. Amino acid sufficiency and mTOR regulate p70 S6 kinase and eIF-4E BP1 through a common effector mechanism. J Biol Chem. 1998 Jun 5;273(23):14484–94.

165. Nicklin P, Bergman P, Zhang B, Triantafellow E, Wang H, Nyfeler B, et al. Bidirectional Transport of Amino Acids Regulates mTOR and Autophagy. Cell. 2009 Feb 6;136(3):521–34.

166. Sancak Y, Peterson TR, Shaul YD, Lindquist RA, Thoreen CC, Bar-Peled L, et al. The rag GTPases bind raptor and mediate amino acid signaling to mTORC1. Science (80-). 2008 Jun 13;320(5882):1496–501.

167. Zoncu R, Bar-Peled L, Efeyan A, Wang S, Sancak Y, Sabatini DM. mTORC1 senses lysosomal amino acids through an inside-out mechanism that requires the vacuolar H(+)-ATPase. Science [Internet]. 2011 Nov 4 [cited 2020 Feb 1];334(6056):678–83. Available from: http://www.ncbi.nlm.nih.gov/pubmed/22053050

168. Gwinn DM, Shackelford DB, Egan DF, Mihaylova MM, Mery A, Vasquez DS, et al. AMPK Phosphorylation of Raptor Mediates a Metabolic Checkpoint. Mol Cell. 2008 Apr 25;30(2):214–26.

169. Inoki K, Zhu T, Guan KL. TSC2 Mediates Cellular Energy Response to Control Cell Growth and Survival. Cell. 2003 Nov 26;115(5):577–90.

170. Tee AR, Manning BD, Roux PP, Cantley LC, Blenis J. Tuberous Sclerosis Complex gene products, Tuberin and Hamartin, control mTOR signaling by acting as a GTPase-

activating protein complex toward Rheb. Curr Biol. 2003 Aug 5;13(15):1259–68.

171. Ma L, Chen Z, Erdjument-Bromage H, Tempst P, Pandolfi PP. Phosphorylation and functional inactivation of TSC2 by Erk: Implications for tuberous sclerosis and cancer pathogenesis. Cell. 2005 Apr 22;121(2):179–93.

172. Boucher J, Kleinridders A, Ronald Kahn C. Insulin receptor signaling in normal and insulin-resistant states. Cold Spring Harb Perspect Biol. 2014 Jan;6(1).

173. Sarbassov DD, Guertin DA, Ali SM, Sabatini DM. Phosphorylation and regulation of Akt/PKB by the rictor-mTOR complex. Science (80-). 2005 Feb 18;307(5712):1098–101.

174. Arden KC. FOXO animal models reveal a variety of diverse roles for FOXO transcription factors. Vol. 27, Oncogene. 2008. p. 2345–50.

175. Wang M, Zhang X, Zhao H, Wang Q, Pan Y. FoxO gene family evolution in vertebrates. BMC Evol Biol. 2009;9(1).

176. Kramer JM, Davidge JT, Lockyer JM, Staveley BE. Expression of Drosophila FOXO regulates growth and can phenocopy starvation. BMC Dev Biol. 2003 Jul 5;3:1–14.

177. Ogg S, Paradis S, Gottlieb S, Patterson GI, Lee L, Tissenbaum HA, et al. The fork head transcription factor DAF-16 transduces insulin-like metabolic and longevity signals in C. elegans. Nature. 1997;389(6654):994–9.

178. Shimokawa I, Komatsu T, Hayashi N, Kim SE, Kawata T, Park S, et al. The life-extending effect of dietary restriction requires Foxo3 in mice. Aging Cell. 2015 Aug 1;14(4):707–9.

179. Seoane J, Le H Van, Shen L, Anderson SA, Massagué J. Integration of smad and forkhead pathways in the control of neuroepithelial and glioblastoma cell proliferation. Cell. 2004 Apr 16;117(2):211–23.

180. Allen DL, Unterman TG. Regulation of myostatin expression and myoblast differentiation by FoxO and SMAD transcription factors. Am J Physiol - Cell Physiol. 2007 Jan;292(1).

181. Tang TTL, Dowbenko D, Jackson A, Toney L, Lewin DA, Dent AL, et al. The forkhead transcription factor AFX activates apoptosis by induction of the BCL-6 transcriptional repressor. J Biol Chem. 2002 Apr 19;277(16):14255–65.

182. Sengupta A, Molkentin JD, Yutzey KE. FoxO transcription factors promote autophagy in cardiomyocytes. J Biol Chem. 2009 Oct 9;284(41):28319–31.

183. Tran H, Brunet A, Grenier JM, Datta SR, Fornace AJ, DiStefano PS, et al. DNA repair pathway stimulated by the forkhead transcription factor FOXO3a through the Gadd45 protein. Science (80-). 2002 Apr 19;296(5567):530–4.

184. Kerdiles YM, Beisner DR, Tinoco R, Dejean AS, Castrillon DH, DePinho RA, et al. Foxo1 links homing and survival of naive T cells by regulating L-selectin, CCR7 and interleukin 7 receptor. Nat Immunol. 2009;10(2):176–84.

185. Puig O, Marr MT, Ruhf ML, Tjian R. Control of cell number by Drosophila FOXO: Downstream and feedback regulation of the insulin receptor pathway. Genes Dev. 2003 Aug 15;17(16):2006–20.

186. Lee JH, Budanov A V., Park EJ, Birse R, Kim TE, Perkins GA, et al. Sestrin as a feedback inhibitor of TOR that prevents age-related pathologies. Science (80-). 2010 Mar 5;327(5970):1223–8.

187. Marr MT, D'Alessio JA, Puig O, Tjian R. IRES-mediated functional coupling of transcription and translation amplifies insulin receptor feedback. Genes Dev. 2007 Jan 15;21(2):175–83.

188. Guo S, Dunn SL, White MF. The reciprocal stability of FoxO1 and Irs2 creates a regulatory circuit that controls insulin signaling. Mol Endocrinol. 2006 Dec;20(12):3389–99.

189. Chandarlapaty S, Sawai A, Scaltriti M, Rodrik-Outmezguine V, Grbovic-Huezo O, Serra V, et al. AKT inhibition relieves feedback suppression of receptor tyrosine kinase expression and activity. Cancer Cell. 2011 Jan 18;19(1):58–71.

190. Chen CC, Jeon SM, Bhaskar PT, Nogueira V, Sundararajan D, Tonic I, et al. FoxOs Inhibit mTORC1 and Activate Akt by Inducing the Expression of Sestrin3 and Rictor. Dev Cell. 2010 Apr;18(4):592–604.

191. Adams MD, Celniker SE, Holt RA, Evans CA, Gocayne JD, Amanatides PG, et al. The genome sequence of Drosophila melanogaster. Vol. 287, Science. American Association for the Advancement of Science; 2000. p. 2185–95.

192. Reiter LT, Potocki L, Chien S, Gribskov M, Bier E. A systematic analysis of human

disease-associated gene sequences in Drosophila melanogaster. Genome Res. 2001;11(6):1114–25.

193. Brand AH, Perrimon N. Targeted gene expression as a means of altering cell fates and generating dominant phenotypes. Development. 1993;118(2):401–15.

194. Abot A, Cani PD, Knauf C. Impact of intestinal peptides on the enteric nervous system: Novel approaches to control glucose metabolism and food intake. Vol. 9, Frontiers in Endocrinology. Frontiers Media S.A.; 2018.

195. Raz E. Mucosal immunity: Aliment and ailments. Vol. 3, Mucosal Immunology. 2010. p. 4–7.

196. Capo F, Wilson A, Di Cara F. The intestine of Drosophila melanogaster: An emerging versatile model system to study intestinal epithelial homeostasis and host-microbial interactions in humans. Vol. 7, Microorganisms. MDPI AG; 2019.

197. Miguel-Aliaga I, Jasper H, Lemaitre B. Anatomy and physiology of the digestive tract of drosophila melanogaster. Genetics. 2018 Oct 1;210(2):357–96.

198. Buchon N, Osman D, David FPA, Yu Fang H, Boquete JP, Deplancke B, et al. Morphological and Molecular Characterization of Adult Midgut Compartmentalization in Drosophila. Cell Rep. 2013 May 30;3(5):1725–38.

199. Marianes A, Spradling AC. Physiological and stem cell compartmentalization within the Drosophila midgut. Elife. 2013 Aug 27;2013(2).

200. Thompson DG, Malagelada JR. Guts and their motions (gastrointestinal motility in health and disease). J Clin Gastroenterol. 1981;3:81–7.

201. Stoffolano JG, Haselton AT. The Adult Dipteran Crop: A Unique and Overlooked Organ. Annu Rev Entomol [Internet]. 2013 Jan 7 [cited 2020 Jan 24];58(1):205–25. Available from: http://www.annualreviews.org/doi/10.1146/annurev-ento-120811-153653

202. Edgecomb RS, Harth CE, Schneiderman AM. Regulation of feeding behavior in adult Drosophila melanogaster varies with feeding regime and nutritional state. J Exp Biol. 1994 Dec;197:215–35.

203. Chapman RF, Simpson SJ, Douglas AE. The Insects - Structure and Function (5th Ed). 2013. 961 p.

204. Demerec M (Milislav). Biology of Drosophila. Cold Spring Harbor Laboratory Press; 1994. 632 p.

205. Gartner LP. The fine structural morphology of the midgut of adult Drosophila: A morphometric analysis. Tissue Cell [Internet]. 1985 [cited 2020 Jan 22];17(6):883–8. Available from: http://www.ncbi.nlm.nih.gov/pubmed/18620152

206. Shanbhag S, Tripathi S. Epithelial ultrastructure and cellular mechanisms of acid and base transport in the Drosophila midgut. J Exp Biol [Internet]. 2009 Jun [cited 2020 Jan 22];212(Pt 11):1731–44. Available from: http://www.ncbi.nlm.nih.gov/pubmed/19448082

207. Hegan PS, Mermall V, Tilney LG, Mooseker MS. Roles for Drosophila melanogaster myosin IB in maintenance of enterocyte brush-border structure and resistance to the bacterial pathogen Pseudomonas entomophila. Mol Biol Cell. 2007 Nov;18(11):4625–36.

208. Crosnier C, Stamataki D, Lewis J. Organizing cell renewal in the intestine: Stem cells, signals and combinatorial control. Vol. 7, Nature Reviews Genetics. 2006. p. 349–59.

209. Kiger AA, Jones DL, Schulz C, Rogers MB, Fuller MT. Stem cell self-renewal specified by JAK-STAT activation in response to a support cell cue. Science (80-). 2001 Dec 21;294(5551):2542–5.

210. Ohlstein B, Spradling A. The adult Drosophila posterior midgut is maintained by pluripotent stem cells. Nature. 2006 Jan 26;439(7075):470–4.

211. Micchelli CA, Perrimon N. Evidence that stem cells reside in the adult Drosophila midgut epithelium. Nature. 2006 Jan 26;439(7075):475–9.

212. Umar S. Intestinal stem cells. Vol. 12, Current Gastroenterology Reports. 2010. p. 340–8.

213. Takashima S, Younossi-Hartenstein A, Ortiz PA, Hartenstein V. A novel tissue in an established model system: The Drosophila pupal midgut. Dev Genes Evol. 2011 Jun;221(2):69–81.

214. Ohlstein B, Spradling A. Multipotent Drosophila intestinal stem cells specify daughter cell fates by differential notch signaling. Science (80-). 2007 Feb 16;315(5814):988–92.

215. Zeng X, Chauhan C, Hou SX. Characterization of midgut stem cell- and enteroblast-

specific Gal4 lines in drosophila. Genesis. 2010 Oct 1;48(10):607–11.

216. Takashima S, Adams KL, Ortiz PA, Ying CT, Moridzadeh R, Younossi-Hartenstein A, et al. Development of the Drosophila entero-endocrine lineage and its specification by the Notch signaling pathway. Dev Biol. 2011;353(2):161–72.

217. Zeng X, Hou SX. Enteroendocrine cells are generated from stem cells through a distinct progenitor in the adult drosophila posterior midgut. Dev. 2015 Feb 15;142(4):644–53.

218. Buchon N, Broderick NA, Poidevin M, Pradervand S, Lemaitre B. Drosophila Intestinal Response to Bacterial Infection: Activation of Host Defense and Stem Cell Proliferation. Cell Host Microbe. 2009 Feb 19;5(2):200–11.

219. Amcheslavsky A, Jiang J, Ip YT. Tissue Damage-Induced Intestinal Stem Cell Division in Drosophila. Cell Stem Cell. 2009 Jan 9;4(1):49–61.

220. Antonello ZA, Reiff T, Ballesta-Illan E, Dominguez M. Robust intestinal homeostasis relies on cellular plasticity in enteroblasts mediated by miR-8–Escargot switch. EMBO J. 2015 Aug 4;34(15):2025–41.

221. Choi NH, Lucchetta E, Ohlstein B. Nonautonomous regulation of Drosophila midgut stem cell proliferation by the insulin-signaling pathway. Proc Natl Acad Sci U S A. 2011 Nov 15;108(46):18702–7.

222. O'Brien LE, Soliman SS, Li X, Bilder D. Altered modes of stem cell division drive adaptive intestinal growth. Cell. 2011 Oct 28;147(3):603–14.

223. Obata F, Tsuda-Sakurai K, Yamazaki T, Nishio R, Nishimura K, Kimura M, et al. Nutritional Control of Stem Cell Division through S-Adenosylmethionine in Drosophila Intestine. Dev Cell. 2018 Mar 26;44(6):741-751.e3.

224. Buchon N, Broderick NA, Chakrabarti S, Lemaitre B. Invasive and indigenous microbiota impact intestinal stem cell activity through multiple pathways in Drosophila. Genes Dev. 2009 Oct 1;23(19):2333–44.

225. Broderick NA, Buchon N, Lemaitre B. Microbiota-induced changes in Drosophila melanogaster host gene expression and gut morphology. MBio. 2014 May 27;5(3).

226. Choi N-H, Kim J-G, Yang D-J, Kim Y-S, Yoo M-A. Age-related changes in Drosophila midgut are associated with PVF2, a PDGF/VEGF-like growth factor. Aging Cell [Internet]. 2008 Jun [cited 2020 Jan 31];7(3):318–34. Available from:

http://doi.wiley.com/10.1111/j.1474-9726.2008.00380.x

227. Biteau B, Hochmuth CE, Jasper H. JNK Activity in Somatic Stem Cells Causes Loss of Tissue Homeostasis in the Aging Drosophila Gut. Cell Stem Cell. 2008 Oct 9;3(4):442–55.

228. Clark RI, Salazar A, Yamada R, Fitz-Gibbon S, Morselli M, Alcaraz J, et al. Distinct Shifts in Microbiota Composition during Drosophila Aging Impair Intestinal Function and Drive Mortality. Cell Rep. 2015 Sep 8;12(10):1656–67.

229. Jiang H, Patel PH, Kohlmaier A, Grenley MO, McEwen DG, Edgar BA. Cytokine/Jak/Stat Signaling Mediates Regeneration and Homeostasis in the Drosophila Midgut. Cell. 2009 Jun 26;137(7):1343–55.

230. Apidianakis Y, Pitsouli C, Perrimon N, Rahme L. Synergy between bacterial infection and genetic predisposition in intestinal dysplasia. Proc Natl Acad Sci U S A. 2009 Dec 8;106(49):20883–8.

231. Biteau B, Jasper H. EGF signaling regulates the proliferation of intestinal stem cells in Drosophila. Development. 2011 Mar;138(6):1045–55.

232. Shaw RL, Kohlmaier A, Polesello C, Veelken C, Edgar BA, Tapon N. The Hippo pathway regulates intestinal stem cell proliferation during Drosophila adult midgut regeneration. Development. 2010 Dec 15;137(24):4147–58.

233. Cordero JB, Stefanatos RK, Scopelliti A, Vidal M, Sansom OJ. Inducible progenitor-derived Wingless regulates adult midgut regeneration in *Drosophila*. EMBO J [Internet]. 2012 Oct 3 [cited 2020 Jan 31];31(19):3901–17. Available from: http://emboj.embopress.org/cgi/doi/10.1038/emboj.2012.248

234. Zhou F, Rasmussen A, Lee S, Agaisse H. The UPD3 cytokine couples environmental challenge and intestinal stem cell division through modulation of JAK/STAT signaling in the stem cell microenvironment. Dev Biol [Internet]. 2013 Jan 15 [cited 2020 Jan 31];373(2):383–93. Available from: http://www.ncbi.nlm.nih.gov/pubmed/23110761

235. Shilo BZ. Regulating the dynamics of EGF receptor signaling in space and time. Vol. 132, Development. 2005. p. 4017–27.

236. Buchon N, Broderick NA, Kuraishi T, Lemaitre B. DrosophilaEGFR pathway coordinates stem cell proliferation and gut remodeling following infection. BMC Biol

[Internet]. 2010 Dec 22 [cited 2020 Jan 31];8(1):152. Available from: https://bmcbiol.biomedcentral.com/articles/10.1186/1741-7007-8-152

237. Cordero JB, Stefanatos RK, Myant K, Vidal M, Sansom OJ. Non-autonomous crosstalk between the Jak/Stat and Egfr pathways mediates Apc1-driven intestinal stem cell hyperplasia in the Drosophila adult midgut. Dev. 2012 Dec 15;139(24):4524–35.

238. Chandler JA, Lang J, Bhatnagar S, Eisen JA, Kopp A. Bacterial communities of diverse Drosophila species: Ecological context of a host-microbe model system. PLoS Genet. 2011 Sep;7(9).

239. Wong ACN, Chaston JM, Douglas AE. The inconstant gut microbiota of Drosophila species revealed by 16S rRNA gene analysis. ISME J. 2013 Oct;7(10):1922–32.

240. Rausch P, Rühlemann M, Hermes BM, Doms S, Dagan T, Dierking K, et al. Comparative analysis of amplicon and metagenomic sequencing methods reveals key features in the evolution of animal metaorganisms. Microbiome [Internet]. 2019 Dec 14 [cited 2020 Jan 22];7(1):133. Available from: https://microbiomejournal.biomedcentral.com/articles/10.1186/s40168-019-0743-1

241. Weldon L, Abolins S, Lenzi L, Bourne C, Riley EM, Viney M. The gut microbiota of wild mice. PLoS One. 2015 Aug 10;10(8).

242. Pasolli E, Asnicar F, Manara S, Zolfo M, Karcher N, Armanini F, et al. Extensive Unexplored Human Microbiome Diversity Revealed by Over 150,000 Genomes from Metagenomes Spanning Age, Geography, and Lifestyle. Cell. 2019 Jan 24;176(3):649-662.e20.

243. Blum JE, Fischer CN, Miles J, Handelsman J. Frequent replenishment sustains the beneficial microbiome of Drosophila melanogaster. MBio [Internet]. 2013 Nov 5 [cited 2020 Jan 22];4(6):e00860-13. Available from: http://www.ncbi.nlm.nih.gov/pubmed/24194543

244. Pais IS, Valente RS, Sporniak M, Teixeira L. Drosophila melanogaster establishes a species-specific mutualistic interaction with stable gut-colonizing bacteria. PLoS Biol. 2018 Jul 5;16(7).

245. Bakula M. The persistence of a microbial flora during postembryogenesis of Drosophila melanogaster. J Invertebr Pathol. 1969;14(3):365–74.

246. Sharon G, Segal D, Ringo JM, Hefetz A, Zilber-Rosenberg I, Rosenberg E. Commensal bacteria play a role in mating preference of Drosophila melanogaster. Proc Natl Acad Sci U S A. 2010 Nov 16;107(46):20051–6.

247. Storelli G, Strigini M, Grenier T, Bozonnet L, Schwarzer M, Daniel C, et al. Drosophila Perpetuates Nutritional Mutualism by Promoting the Fitness of Its Intestinal Symbiont Lactobacillus plantarum. Cell Metab. 2018 Feb 6;27(2):362-377.e8.

248. Storelli G, Defaye A, Erkosar B, Hols P, Royet J, Leulier F. Lactobacillus plantarum promotes drosophila systemic growth by modulating hormonal signals through TOR-dependent nutrient sensing. Cell Metab. 2011;14(3):403–14.

249. Shin SC, Kim SH, You H, Kim B, Kim AC, Lee KA, et al. Drosophila microbiome modulates host developmental and metabolic homeostasis via insulin signaling. Science (80-). 2011;334(6056):670–4.

250. Wong AC-N, Dobson AJ, Douglas AE. Gut microbiota dictates the metabolic response of Drosophila to diet. J Exp Biol [Internet]. 2014;217(11):1894–901. Available from: http://jeb.biologists.org/cgi/doi/10.1242/jeb.101725

251. Piper MDW, Blanc E, Leitão-Gonçalves R, Yang M, He X, Linford NJ, et al. A holidic medium for Drosophila melanogaster. Nat Methods [Internet]. 2014 Jan [cited 2020 Jan 22];11(1):100–5. Available from: http://www.ncbi.nlm.nih.gov/pubmed/24240321

252. Piper MDW, Soultoukis GA, Blanc E, Mesaros A, Herbert SL, Juricic P, et al. Matching Dietary Amino Acid Balance to the In Silico-Translated Exome Optimizes Growth and Reproduction without Cost to Lifespan. Cell Metab. 2017 Mar 7;25(3):610–21.

253. Leitão-Gonçalves R, Carvalho-Santos Z, Francisco AP, Fioreze GT, Anjos M, Baltazar C, et al. Commensal bacteria and essential amino acids control food choice behavior and reproduction. Vosshall L, editor. PLOS Biol [Internet]. 2017 Apr 25 [cited 2020 Jan 22];15(4):e2000862. Available from: http://dx.plos.org/10.1371/journal.pbio.2000862

254. Markstein M, Dettorre S, Cho J, Neumüller RA, Craig-Müller S, Perrimon N. Systematic screen of chemotherapeutics in Drosophila stem cell tumors. Proc Natl Acad Sci U S A. 2014 Mar 25;111(12):4530–5.

255. Eyres L, Eyres MF, Chisholm A, Brown RC. Coconut oil consumption and cardiovascular risk factors in humans. Nutr Rev. 2016;74(4):267–80.

256. Biteau B, Karpac J, Hwangbo DS, Jasper H. Regulation of Drosophila lifespan by JNK signaling. Exp Gerontol. 2011 May;46(5):349–54.

257. Chatterjee N, Bohmann D. A Versatile ΦC31 Based Reporter System for Measuring AP-1 and Nrf2 Signaling in Drosophila and in Tissue Culture. Jennings B, editor. PLoS One [Internet]. 2012 Apr 11 [cited 2020 Jan 22];7(4):e34063. Available from: https://dx.plos.org/10.1371/journal.pone.0034063

258. Osman D, Buchon N, Chakrabarti S, Huang YT, Su WC, Poidevin M, et al. Autocrine and paracrine unpaired signaling regulate intestinal stem cell maintenance and division. J Cell Sci. 2012 Dec 15;125(24):5944–9.

259. Bach EA, Ekas LA, Ayala-Camargo A, Flaherty MS, Lee H, Perrimon N, et al. GFP reporters detect the activation of the Drosophila JAK/STAT pathway in vivo. Gene Expr Patterns. 2007 Jan 2;7(3):323–31.

260. Bloomington Drosophila Stock Center: Indiana University Bloomington [Internet]. [cited 2020 Feb 8]. Available from: https://bdsc.indiana.edu/information/recipes/index.html

261. Reis T. Effects of synthetic diets enriched in specific nutrients on drosophila development, body fat, and lifespan. PLoS One. 2016 Jan 7;11(1).

262. Lee W-C, Micchelli CA. Development and Characterization of a Chemically Defined Food for Drosophila. Hassan BA, editor. PLoS One [Internet]. 2013 Jul 2 [cited 2020 Jan 22];8(7):e67308. Available from: https://dx.plos.org/10.1371/journal.pone.0067308

263. Rodrigues MA, Martins NE, Balancé LF, Broom LN, Dias AJS, Fernandes ASD, et al. Drosophila melanogaster larvae make nutritional choices that minimize developmental time. J Insect Physiol [Internet]. 2015 Oct 1 [cited 2020 Feb 8];81:69–80. Available from: https://linkinghub.elsevier.com/retrieve/pii/S0022191015001377

264. Silva-Soares NF, Nogueira-Alves A, Beldade P, Mirth CK. Adaptation to new nutritional environments: Larval performance, foraging decisions, and adult oviposition choices in Drosophila suzukii. BMC Ecol. 2017 Jun 7;17(1):1–13.

265. Xu M, Ma Y, Xu L, Xu Y, Li Y. Developmental effects of dietary nucleotides in second-generation weaned rats. J Med Food. 2013 Dec 1;16(12):1146–52.

266. Watanabe F, Bito T. Vitamin B12 sources and microbial interaction. Exp Biol Med. 2018

Jan 1;243(2):148–58.

267. Knittelfelder O, Prince E, Sales S, Fritzsche E, Wöhner T, Brankatschk M, et al. Sterols as dietary markers for Drosophila melanogaster. [cited 2020 Feb 8]; Available from: http://dx.doi.org/10.1101/857664

268. Carvalho M, Sampaio JL, Palm W, Brankatschk M, Eaton S, Shevchenko A. Effects of diet and development on the *Drosophila* lipidome. Mol Syst Biol [Internet]. 2012 Jan 31 [cited 2020 Feb 8];8(1):600. Available from: https://onlinelibrary.wiley.com/doi/abs/10.1038/msb.2012.29

269. Kitada M, Ogura Y, Monno I, Koya D. The impact of dietary protein intake on longevity and metabolic health. Vol. 43, EBioMedicine. Elsevier B.V.; 2019. p. 632–40.

270. Claycomb JM, Benasutti M, Bosco G, Fenger DD, Orr-Weaver TL. Gene amplification as a developmental strategy: Isolation of two developmental amplicons in Drosophila. Dev Cell. 2004 Jan;6(1):145–55.

271. Howard AM, Lafever KS, Fenix AM, Scurrah CR, Lau KS, Burnette DT, et al. DSS-induced damage to basement membranes is repaired by matrix replacement and crosslinking. J Cell Sci. 2019 Apr 1;132(7).

272. Oldham S, Montagne J, Radimerski T, Thomas G, Hafen E. Genetic and biochemical characterization of dTOR, the Drosophila homolog of the target of rapamycin. Genes Dev. 2000 Nov 1;14(21):2689–94.

273. Zhang H, Stallock JP, Ng JC, Reinhard C, Neufeld TP. Regulation of cellular growth by the Drosophila target of rapamycin dTOR. Genes Dev. 2000 Nov 1;14(21):2712–24.

274. Kirisako T, Baba M, Ishihara N, Miyazawa K, Ohsumi M, Yoshimori T, et al. Formation process of autophagosome is traced with Apg8/Aut7p in yeast. J Cell Biol [Internet]. 1999 Oct 18 [cited 2020 Feb 13];147(2):435–46. Available from: http://www.ncbi.nlm.nih.gov/pubmed/10525546

275. Mauvezin C, Ayala C, Braden CR, Kim J, Neufeld TP. Assays to monitor autophagy in Drosophila. Methods. 2014 Jun 15;68(1):134–9.

276. Bhutta ZA, Berkley JA, Bandsma RHJ, Kerac M, Trehan I, Briend A. Severe childhood malnutrition. Vol. 3, Nature reviews. Disease primers. Nature Publishing Group; 2017. p. 17067.

277. Fu T, Coulter S, Yoshihara E, Oh TG, Fang S, Cayabyab F, et al. FXR Regulates Intestinal Cancer Stem Cell Proliferation. Cell. 2019 Feb 21;176(5):1098-1112.e18.

278. Beyaz S, Mana MD, Roper J, Kedrin D, Saadatpour A, Hong SJ, et al. High-fat diet enhances stemness and tumorigenicity of intestinal progenitors. Nature. 2016 Mar 2;531(7592):53–8.

279. Mah AT, Van Landeghem L, Gavin HE, Magness ST, Lund PK. Impact of Diet-Induced Obesity on Intestinal Stem Cells: Hyperproliferation but Impaired Intrinsic Function That Requires Insulin/IGF1. Endocrinology [Internet]. 2014 Sep [cited 2020 Feb 5];155(9):3302–14. Available from: https://academic.oup.com/endo/article-lookup/doi/10.1210/en.2014-1112

280. Liu Z, Uesaka T, Watanabe H, Kato N. High fat diet enhances colonic cell proliferation and carcinogenesis in rats by elevating serum leptin. Int J Oncol. 2001;19(5):1009–14.

281. Dinh CHL, Yu Y, Szabo A, Zhang Q, Zhang P, Huang XF. Bardoxolone Methyl Prevents High-Fat Diet-Induced Colon Inflammation in Mice. J Histochem Cytochem. 2016;64(4):237–55.

282. Zhou W, Davis EA, Dailey MJ. Obesity, independent of diet, drives lasting effects on intestinal epithelial stem cell proliferation in mice. Exp Biol Med. 2018 Jun 1;243(10):826–35.

283. Sato T, Van Es JH, Snippert HJ, Stange DE, Vries RG, Van Den Born M, et al. Paneth cells constitute the niche for Lgr5 stem cells in intestinal crypts. Nature. 2011 Jan 20;469(7330):415–8.

284. Yilmaz ÖH, Katajisto P, Lamming DW, Gültekin Y, Bauer-Rowe KE, Sengupta S, et al. MTORC1 in the Paneth cell niche couples intestinal stem-cell function to calorie intake. Nature. 2012 Jun 28;486(7404):490–5.

285. Zhai Z, Boquete J-P, Lemaitre B. A genetic framework controlling the differentiation of intestinal stem cells during regeneration in Drosophila. Barsh GS, editor. PLOS Genet [Internet]. 2017 Jun 29 [cited 2020 Feb 6];13(6):e1006854. Available from: https://dx.plos.org/10.1371/journal.pgen.1006854

286. Obniski R, Sieber M, Spradling AC. Dietary Lipids Modulate Notch Signaling and Influence Adult Intestinal Development and Metabolism in Drosophila. Dev Cell. 2018 Oct 8;47(1):98-111.e5.

287. Horner MA, Pardee K, Liu S, King-Jones K, Lajoie G, Edwards A, et al. The Drosophila DHR96 nuclear receptor binds cholesterol and regulates cholesterol homeostasis. Genes Dev. 2009 Dec 1;23(23):2711–6.

288. Wu H, Wang MC, Bohmann D. JNK protects Drosophila from oxidative stress by trancriptionally activating autophagy. Mech Dev. 2009 Aug;126(8–9):624–37.

289. Noselli S, Agnès F. Roles of the JNK signaling pathway in Drosophila morphogenesis. Curr Opin Genet Dev. 1999 Aug 4;9(4):466–72.

290. Woodcock KJ, Kierdorf K, Pouchelon CA, Vivancos V, Dionne MS, Geissmann F. Macrophage-Derived upd3 Cytokine Causes Impaired Glucose Homeostasis and Reduced Lifespan in Drosophila Fed a Lipid-Rich Diet. Immunity. 2015 Jan 20;42(1):133–44.

291. Santabárbara-Ruiz P, López-Santillán M, Martínez-Rodríguez I, Binagui-Casas A, Pérez L, Milán M, et al. ROS-Induced JNK and p38 Signaling Is Required for Unpaired Cytokine Activation during Drosophila Regeneration. Copenhaver GP, editor. PLOS Genet [Internet]. 2015 Oct 23 [cited 2020 Feb 6];11(10):e1005595. Available from: https://dx.plos.org/10.1371/journal.pgen.1005595

292. Frieling J von, Faisal MN, Sporn F, Pfefferkorn R, Nolte SS, Sommer F, et al. A high-fat diet induces a microbiota-dependent increase in stem cell activity in the Drosophila intestine. bioRxiv. 2019 May 15;604744.

293. Ren F, Shi Q, Chen Y, Jiang A, Ip YT, Jiang H, et al. Drosophila Myc integrates multiple signaling pathways to regulate intestinal stem cell proliferation during midgut regeneration. Cell Res. 2013 Sep;23(9):1133–46.

294. Huang S, Rutkowsky JM, Snodgrass RG, Ono-Moore KD, Schneider DA, Newman JW, et al. Saturated fatty acids activate TLR-mediated proinflammatory signaling pathways. J Lipid Res. 2012 Sep;53(9):2002–13.

295. Oldefest M, Nowinski J, Hung CW, Neelsen D, Trad A, Tholey A, et al. Upd3 - An ancestor of the four-helix bundle cytokines. Biochem Biophys Res Commun. 2013 Jun 21;436(1):66–72.

296. Kim F, Pham M, Luttrell I, Bannerman DD, Tupper J, Thaler J, et al. Toll-like receptor-4 mediates vascular inflammation and insulin resistance in diet-induced obesity. Circ Res. 2007 Jun;100(11):1589–96.

297. Guo X, Li J, Tang R, Zhang G, Zeng H, Wood RJ, et al. High Fat Diet Alters Gut Microbiota and the Expression of Paneth Cell-Antimicrobial Peptides Preceding Changes of Circulating Inflammatory Cytokines. Mediators Inflamm [Internet]. 2017 [cited 2020 Feb 6];2017:1–9. Available from: https://www.hindawi.com/journals/mi/2017/9474896/

298. Monteiro-Sepulveda M, Touch S, Mendes-Sá C, André S, Poitou C, Allatif O, et al. Jejunal T Cell Inflammation in Human Obesity Correlates with Decreased Enterocyte Insulin Signaling. Cell Metab. 2015 Jul 7;22(1):113–24.

299. Cortez M, Carmo LS, Rogero MM, Borelli P, Fock RA. A high-fat diet increases IL-1, IL-6, and TNF-α production by increasing NF-κb and attenuating PPAR-γ expression in bone marrow mesenchymal stem cells. Inflammation. 2013 Apr;36(2):379–86.

300. Wueest S, Laesser CI, Böni-Schnetzler M, Item F, Lucchini FC, Borsigova M, et al. IL-6-type cytokine signaling in adipocytes induces intestinal GLP-1 secretion. Diabetes. 2018 Jan 1;67(1):36–45.

301. Fernández-Gayol O, Sanchis P, Aguilar K, Navarro-Sempere A, Comes G, Molinero A, et al. Different Responses to a High-Fat Diet in IL-6 Conditional Knockout Mice Driven by Constitutive GFAP-Cre and Synapsin 1-Cre Expression. Neuroendocrinology [Internet]. 2019 [cited 2020 Feb 6];109(2):113–30. Available from: https://www.karger.com/Article/FullText/496845

302. Shi C, Li H, Qu X, Huang L, Kong C, Qin H, et al. High fat diet exacerbates intestinal barrier dysfunction and changes gut microbiota in intestinal-specific ACF7 knockout mice. Biomed Pharmacother. 2019 Feb 1;110:537–45.

303. Rigby RJ, Simmons JG, Greenhalgh CJ, Alexander WS, Lund PK. Suppressor of cytokine signaling 3 (SOCS3) limits damage-induced crypt hyper-proliferation and inflammation-associated tumorigenesis in the colon. Oncogene. 2007 Jul 19;26(33):4833–41.

304. Schneider MR, Hoeflich A, Fischer JR, Wolf E, Sordat B, Lahm H. Interleukin-6 stimulates clonogenic growth of primary and metastatic human colon carcinoma cells. Cancer Lett [Internet]. 2000 Apr 3 [cited 2020 Feb 6];151(1):31–8. Available from: http://www.ncbi.nlm.nih.gov/pubmed/10766420

305. Becker C, Fantini MC, Wirtz S, Nikolaev A, Lehr HA, Galle PR, et al. IL-6 signaling

promotes tumor growth in colorectal cancer. Cell Cycle. 2005;4(2):220–3.

306. Aden K, Breuer A, Rehman A, Geese H, Tran F, Sommer J, et al. Classic IL-6R signalling is dispensable for intestinal epithelial proliferation and repair. Oncogenesis. 2016 Nov;5(11):e270–e270.

307. Poulsen L la C, Siersbæk M, Mandrup S. PPARs: Fatty acid sensors controlling metabolism. Vol. 23, Seminars in Cell and Developmental Biology. Elsevier Ltd; 2012. p. 631–9.

308. Barker N, Van Es JH, Kuipers J, Kujala P, Van Den Born M, Cozijnsen M, et al. Identification of stem cells in small intestine and colon by marker gene Lgr5. Nature. 2007 Oct 25;449(7165):1003–7.

309. He TC, Chan TA, Vogelstein B, Kinzler KW. PPARδ is an APC-regulated target of nonsteroidal anti-inflammatory drugs. Cell. 1999 Oct 29;99(3):335–45.

310. Hong JW, Park KW. Further understanding of fat biology: Lessons from a fat fly. Vol. 42, Experimental and Molecular Medicine. Nature Publishing Group; 2010. p. 12–20.

311. Zhang C, Zhang M, Pang X, Zhao Y, Wang L, Zhao L. Structural resilience of the gut microbiota in adult mice under high-fat dietary perturbations. ISME J. 2012 Oct;6(10):1848–57.

312. Arias-Jayo N, Abecia L, Alonso-Sáez L, Ramirez-Garcia A, Rodriguez A, Pardo MA. High-Fat Diet Consumption Induces Microbiota Dysbiosis and Intestinal Inflammation in Zebrafish. Microb Ecol. 2018 Nov 1;76(4):1089–101.

313. Deshpande NG, Saxena J, Pesaresi TG, Carrell CD, Ashby GB, Liao MK, et al. High fat diet alters gut microbiota but not spatial working memory in early middle-aged Sprague Dawley rats. PLoS One. 2019 May 1;14(5).

314. Wu GD, Chen J, Hoffmann C, Bittinger K, Chen YY, Keilbaugh SA, et al. Linking long-term dietary patterns with gut microbial enterotypes. Science (80-). 2011 Oct 7;334(6052):105–8.

315. Hildebrandt MA, Hoffmann C, Sherrill-Mix SA, Keilbaugh SA, Hamady M, Chen YY, et al. High-Fat Diet Determines the Composition of the Murine Gut Microbiome Independently of Obesity. Gastroenterology. 2009;137(5).

316. Ley RE, Turnbaugh PJ, Klein S, Gordon JI. Microbial ecology: Human gut microbes

associated with obesity. Nature. 2006 Dec 21;444(7122):1022–3.

317. Castaner O, Goday A, Park YM, Lee SH, Magkos F, Shiow SATE, et al. The gut microbiome profile in obesity: A systematic review. Int J Endocrinol. 2018;2018.

318. Rafter JJ, Child P, Anderson AM, Alder R, Eng V, Bruce WR. Cellular toxicity of fecal water depends on diet. Am J Clin Nutr. 1987;45(3):559–63.

319. Islam KBMS, Fukiya S, Hagio M, Fujii N, Ishizuka S, Ooka T, et al. Bile acid is a host factor that regulates the composition of the cecal microbiota in rats. Gastroenterology. 2011;141(5):1773–81.

320. Tomas J, Mulet C, Saffarian A, Cavin JB, Ducroc R, Regnault B, et al. High-fat diet modifies the PPAR-γ pathway leading to disruption of microbial and physiological ecosystem in murine small intestine. Proc Natl Acad Sci U S A. 2016 Oct 4;113(40):E5934–43.

321. Sommer F, Adam N, Johansson MEV, Xia L, Hansson GC, Bäckhed F. Altered mucus glycosylation in core 1 O-glycan-deficient mice affects microbiota composition and intestinal architecture. PLoS One. 2014;9(1).

322. Turnbaugh PJ, Ley RE, Mahowald MA, Magrini V, Mardis ER, Gordon JI. An obesity-associated gut microbiome with increased capacity for energy harvest. Nature. 2006 Dec 21;444(7122):1027–31.

323. Schwiertz A, Taras D, Schäfer K, Beijer S, Bos NA, Donus C, et al. Microbiota and SCFA in Lean and Overweight Healthy Subjects. Obesity [Internet]. 2010 Jan [cited 2020 Feb 6];18(1):190–5. Available from: http://doi.wiley.com/10.1038/oby.2009.167

324. Reikvam DH, Erofeev A, Sandvik A, Grcic V, Jahnsen FL, Gaustad P, et al. Depletion of Murine Intestinal Microbiota: Effects on Gut Mucosa and Epithelial Gene Expression. Heimesaat M, editor. PLoS One [Internet]. 2011 Mar 21 [cited 2020 Feb 7];6(3):e17996. Available from: http://dx.plos.org/10.1371/journal.pone.0017996

325. Alam M, Midtvedt T, Uribe A. Differential cell kinetics in the ileum and colon of germfree rats. Scand J Gastroenterol. 1994;29(5):445–51.

326. Stappenbeck TS, Hooper L V., Gordon JI. Developmental regulation of intestinal angiogenesis by indigenous microbes via Paneth cells. Proc Natl Acad Sci U S A. 2002 Nov 26;99(24):15451–5.

327. Takeda K, Kaisho T, Akira S. T OLL -L IKE R ECEPTORS . Annu Rev Immunol. 2003 Apr;21(1):335–76.

328. Rakoff-Nahoum S, Paglino J, Eslami-Varzaneh F, Edberg S, Medzhitov R. Recognition of commensal microflora by toll-like receptors is required for intestinal homeostasis. Cell. 2004 Jul 23;118(2):229–41.

329. Santaolalla R, Sussman DA, Ruiz JR, Davies JM, Pastorini C, España CL, et al. TLR4 Activates the β-catenin Pathway to Cause Intestinal Neoplasia. Goel A, editor. PLoS One [Internet]. 2013 May 14 [cited 2020 Feb 7];8(5):e63298. Available from: http://dx.plos.org/10.1371/journal.pone.0063298

330. Cheesman SE, Neal JT, Mittge E, Seredick BM, Guillemin K. Epithelial cell proliferation in the developing zebrafish intestine is regulated by the Wnt pathway and microbial signaling via Myd88. Proc Natl Acad Sci U S A. 2011 Mar 15;108(SUPPL. 1):4570–7.

331. Neumann PA, Koch S, Hilgarth RS, Perez-Chanona E, Denning P, Jobin C, et al. Gut commensal bacteria and regional Wnt gene expression in the proximal versus distal colon. Am J Pathol. 2014 Mar;184(3):592–9.

332. Scheithauer TPM, Dallinga-Thie GM, de Vos WM, Nieuwdorp M, van Raalte DH. Causality of small and large intestinal microbiota in weight regulation and insulin resistance. Mol Metab. 2016 Sep 1;5(9):759–70.

333. Barsouk A, Rawla P, Barsouk A, Thandra KC. Epidemiology of Cancers of the Small Intestine: Trends, Risk Factors, and Prevention. Med Sci. 2019 Mar 17;7(3):46.

334. Anitha M, Reichardt F, Tabatabavakili S, Nezami BG, Chassaing B, Mwangi S, et al. Intestinal Dysbiosis Contributes to the Delayed Gastrointestinal Transit in High-Fat Diet Fed Mice. CMGH. 2016 May 1;2(3):328–39.

335. Vd Baan-Slootweg OH, Liem O, Bekkali N, Van Aalderen WMC, Rijcken THP, Di Lorenzo C, et al. Constipation and colonic transit times in children with morbid obesity. J Pediatr Gastroenterol Nutr. 2011 Apr;52(4):442–5.

336. Las Heras V, Clooney AG, Ryan FJ, Cabrera-Rubio R, Casey PG, Hueston CM, et al. Short-term consumption of a high-fat diet increases host susceptibility to Listeria monocytogenes infection. Microbiome [Internet]. 2019 Dec 18 [cited 2020 Feb 7];7(1):7. Available from: https://microbiomejournal.biomedcentral.com/articles/10.1186/s40168-

019-0621-x

337. Ren C, Webster P, Finkel SE, Tower J. Increased Internal and External Bacterial Load during Drosophila Aging without Life-Span Trade-Off. Cell Metab. 2007 Aug 8;6(2):144–52.

338. He L, Si G, Huang J, Samuel ADT, Perrimon N. Mechanical regulation of stem-cell differentiation by the stretch-activated Piezo channel. Nature. 2018 Mar 1;555(7694):103–6.

339. Adachi T, Kakuta S, Aihara Y, Kamiya T, Watanabe Y, Osakabe N, et al. Visualization of probiotic-mediated Ca2+ signaling in intestinal epithelial cells in vivo. Front Immunol. 2016;7(DEC).

340. Wong ACN, Dobson AJ, Douglas AE. Gut microbiota dictates the metabolic response of Drosophila to diet. J Exp Biol. 2014 Jun 1;217(11):1894–901.

341. Bäckhed F, Ding H, Wang T, Hooper L V., Gou YK, Nagy A, et al. The gut microbiota as an environmental factor that regulates fat storage. Proc Natl Acad Sci U S A. 2004 Nov 2;101(44):15718–23.

342. Yamanaka M, Nomura T, Kametaka M. Role of intestinal microbes in body composition in germ-free, gnotobiotic and conventional mice. J Nutr Sci Vitaminol (Tokyo) [Internet]. 1977 [cited 2020 Feb 7];23(3):211–20. Available from: http://joi.jlc.jst.go.jp/JST.Journalarchive/jnsv1973/23.211?from=CrossRef

343. Semova I, Carten JD, Stombaugh J, MacKey LC, Knight R, Farber SA, et al. Microbiota regulate intestinal absorption and metabolism of fatty acids in the zebrafish. Cell Host Microbe. 2012 Sep 13;12(3):277–88.

344. Martinez-Guryn K, Hubert N, Frazier K, Urlass S, Musch MW, Ojeda P, et al. Small Intestine Microbiota Regulate Host Digestive and Absorptive Adaptive Responses to Dietary Lipids. Cell Host Microbe. 2018 Apr 11;23(4):458-469.e5.

345. Yamada R, Deshpande SA, Bruce KD, Mak EM, Ja WW. Microbes Promote Amino Acid Harvest to Rescue Undernutrition in Drosophila. Cell Rep [Internet]. 2015 Feb 17 [cited 2020 Feb 7];10(6):865–72. Available from: http://www.ncbi.nlm.nih.gov/pubmed/25683709

346. Simpson SJ, Raubenheimer D. Obesity: The protein leverage hypothesis [Internet]. Vol.

6, Obesity Reviews. 2005 [cited 2020 Feb 7]. p. 133–42. Available from: http://doi.wiley.com/10.1111/j.1467-789X.2005.00178.x

347. González-Muniesa P, Mártinez-González MA, Hu FB, Després JP, Matsuzawa Y, Loos RJF, et al. Obesity. Nat Rev Dis Prim. 2017 Jun 15;3(1):1–18.

348. Kohsaka A, Laposky AD, Ramsey KM, Estrada C, Joshu C, Kobayashi Y, et al. High-Fat Diet Disrupts Behavioral and Molecular Circadian Rhythms in Mice. Cell Metab. 2007 Nov 7;6(5):414–21.

349. Wong CK, Botta A, Pither J, Dai C, Gibson WT, Ghosh S. A high-fat diet rich in corn oil reduces spontaneous locomotor activity and induces insulin resistance in mice. J Nutr Biochem. 2015 Apr 1;26(4):319–26.

350. Huang R, Song T, Su H, Wang L. High-fat diet enhances starvation-induced hyperactivity via sensitizing hunger-sensing neurons in Drosophila. bioRxiv [Internet]. 2019 Apr 18 [cited 2020 Feb 7];612234. Available from: https://www.biorxiv.org/content/10.1101/612234v1.abstract?%3Fcollection=

351. Ye L, Liddle RA. Gastrointestinal hormones and the gut connectome. Vol. 24, Current Opinion in Endocrinology, Diabetes and Obesity. Lippincott Williams and Wilkins; 2017. p. 9–14.

352. Latorre R, Sternini C, De Giorgio R, Greenwood-Van Meerveld B. Enteroendocrine cells: A review of their role in brain-gut communication. Vol. 28, Neurogastroenterology and Motility. Blackwell Publishing Ltd; 2016. p. 620–30.

353. Scopelliti A, Bauer C, Yu Y, Zhang T, Kruspig B, Murphy DJ, et al. A Neuronal Relay Mediates a Nutrient Responsive Gut/Fat Body Axis Regulating Energy Homeostasis in Adult Drosophila. Cell Metab [Internet]. 2019 Feb 5 [cited 2020 Feb 7];29(2):269-284.e10. Available from: http://www.ncbi.nlm.nih.gov/pubmed/30344016

354. Bednářová A, Tomčala A, Mochanová M, Kodrík D, Krishnan N. Disruption of adipokinetic hormone mediated energy homeostasis has subtle effects on physiology, behavior and lipid status during aging in Drosophila. Front Physiol. 2018 Jul 20;9(JUL).

355. Chen J, Reiher W, Hermann-Luibl C, Sellami A, Cognigni P, Kondo S, et al. Allatostatin A Signalling in Drosophila Regulates Feeding and Sleep and Is Modulated by PDF. PLoS Genet. 2016 Sep 1;12(9):e1006346.

356. Gault VA, Bhat VK, Irwin N, Flatt PR. A novel glucagon-like peptide-1 (GLP-1)/Glucagon hybrid peptide with triple-acting agonist activity at glucose-dependent insulinotropic polypeptide, GLP-1, and glucagon receptors and therapeutic potential in high fat-fed Mice. J Biol Chem. 2013 Dec 6;288(49):35581–91.

357. Ye L, Mueller O, Bagwell J, Bagnat M, Liddle RA, Rawls JF. High fat diet induces microbiota-dependent silencing of enteroendocrine cells. Elife. 2019 Dec 1;8.

358. Castañeda TR, Jürgens H, Wiedmer P, Pfluger P, Diano S, Horvath TL, et al. Obesity and the Neuroendocrine Control of Energy Homeostasis: The Role of Spontaneous Locomotor Activity. J Nutr [Internet]. 2005 May 1 [cited 2020 Feb 7];135(5):1314–9. Available from: https://academic.oup.com/jn/article/135/5/1314/4664069

359. Irwin MR, Olmstead R, Carroll JE. Sleep disturbance, sleep duration, and inflammation: A systematic review and meta-analysis of cohort studies and experimental sleep deprivation. Biol Psychiatry. 2016 Jul 1;80(1):40–52.

360. Hemphill W, Rivera O, Talbert M. RNA-sequencing of Drosophila melanogaster head tissue on high-sugar and high-fat diets. G3 Genes, Genomes, Genet. 2018 Jan 1;8(1):279–90.

361. Kalmijn S, Launer LJ, Ott A, Witteman JCM, Hofman A, Breteler MMB. Dietary fat intake and the risk of incident dementia in the Rotterdam study. Ann Neurol [Internet]. 1997 Nov [cited 2020 Feb 7];42(5):776–82. Available from: http://www.ncbi.nlm.nih.gov/pubmed/9392577

362. Thirumangalakudi L, Prakasam A, Zhang R, Bimonte-Nelson H, Sambamurti K, Kindy MS, et al. High cholesterol-induced neuroinflammation and amyloid precursor protein processing correlate with loss of working memory in mice. J Neurochem [Internet]. 2008 Jul [cited 2020 Feb 7];106(1):475–85. Available from: http://www.ncbi.nlm.nih.gov/pubmed/18410513

363. Janssen CIF, Jansen D, Mutsaers MPC, Dederen PJWC, Geenen B, Mulder MT, et al. The effect of a high-fat diet on brain plasticity, inflammation and cognition in female ApoE4-knockin and ApoE-knockout mice. PLoS One. 2016 May 1;11(5).

364. Lang P, Hasselwander S, Li H, Xia N. Effects of different diets used in diet-induced obesity models on insulin resistance and vascular dysfunction in C57BL/6 mice. Sci Rep. 2019 Dec 1;9(1):1–14.

365. Skorupa DA, Dervisefendic A, Zwiener J, Pletcher SD. Dietary composition specifies consumption, obesity, and lifespan in Drosophila melanogaster. Aging Cell. 2008 Aug;7(4):478–90.

366. Shorrocks B. An ecological classification of European Drosophila species. Oecologia [Internet]. 1977 Dec [cited 2020 Feb 8];26(4):335–45. Available from: http://www.ncbi.nlm.nih.gov/pubmed/28309499

367. Keller A. Drosophila melanogaster's history as a human commensal [Internet]. Vol. 17, Current Biology. 2007 [cited 2020 Feb 8]. p. R77-81. Available from: http://www.ncbi.nlm.nih.gov/pubmed/17276902

368. Mansourian S, Enjin A, Jirle E V., Ramesh V, Rehermann G, Becher PG, et al. Wild African Drosophila melanogaster Are Seasonal Specialists on Marula Fruit. Curr Biol. 2018 Dec 17;28(24):3960-3968.e3.

369. Th. Eisses K, Den Boer AA. Acetic acid tolerance in Drosophila is a prerequisite for ethanol tolerance. J Evol Biol [Internet]. 1995 Jul 1 [cited 2020 Feb 8];8(4):481–91. Available from: http://doi.wiley.com/10.1046/j.1420-9101.1995.8040481.x

370. Fly Food Service — Fly Facility [Internet]. [cited 2020 Feb 8]. Available from: https://www.flyfacility.gen.cam.ac.uk/Services/flyfoodservice

371. Staats S, Lüersen K, Wagner AE, Rimbach G. *Drosophila melanogaster* as a Versatile Model Organism in Food and Nutrition Research. J Agric Food Chem [Internet]. 2018 Apr 18 [cited 2020 Feb 8];66(15):3737–53. Available from: https://pubs.acs.org/doi/10.1021/acs.jafc.7b05900

372. Lüersen K, Röder T, Rimbach G. Drosophila melanogaster in nutrition research—the importance of standardizing experimental diets. Genes Nutr [Internet]. 2019 Dec 1 [cited 2020 Feb 8];14(1):3. Available from: https://genesandnutrition.biomedcentral.com/articles/10.1186/s12263-019-0627-9

373. SANG JH. The Quantitative Nutritional Requirements of Drosophila Melanogaster. J Exp Biol. 1956;33(1).

374. Rapport EW, Stanley-Samuelson D, Dadd RH. Ten generations ofDrosophila melanogaster reared axenically on a fatty acid-free holidic diet. Arch Insect Biochem Physiol [Internet]. 1983 Jan 1 [cited 2020 Feb 8];1(3):243–50. Available from: http://doi.wiley.com/10.1002/arch.940010307

375. Jang T, Lee KP. Comparing the impacts of macronutrients on life-history traits in larval and adult Drosophila melanogaster: The use of nutritional geometry and chemically defined diets. J Exp Biol. 2018 Nov 1;221(21).

376. Shingleton AW, Masandika JR, Thorsen LS, Zhu Y, Mirth CK. The sex-specific effects of diet quality versus quantity on morphology in Drosophila melanogaster. R Soc Open Sci. 2017;4(9).

377. Solon-Biet SM, Wahl D, Raubenheimer D, Cogger VC, Le Couteur DG, Simpson SJ. The geometric framework: An approach for studying the impact of nutrition on healthy aging. Vol. 27, Drug Discovery Today: Disease Models. Elsevier Ltd; 2018. p. 61–8.

378. Krall AS, Xu S, Graeber TG, Braas D, Christofk HR. Asparagine promotes cancer cell proliferation through use as an amino acid exchange factor. Nat Commun. 2016 Apr 29;7(1):1–13.

379. Watanabe D, Kikushima R, Aitoku M, Nishimura A, Ohtsu I, Nasuno R, et al. Exogenous addition of histidine reduces copper availability in the yeast Saccharomyces cerevisiae. Microb Cell. 2014 Jul 1;1(7):241–6.

380. Johnson CL, Vishniac W. Growth Inhibition in Thiobacillus neapolitanus by Histidine, Methionine, Phenylalanine, and Threonine. J Bacteriol [Internet]. 1970 Dec 1 [cited 2020 Feb 8];104(3):1145–50. Available from: http://www.ncbi.nlm.nih.gov/pubmed/16559087

381. Morais PB, Martins MB, Klaczko LB, Mendonca-Hagler LC, Hagler AN. Yeast succession in the amazon fruit Parahancornia amapa as resource partitioning among Drosophila spp. Appl Environ Microbiol. 1995 Dec 1;61(12):4251–7.

382. Miller PM, Saltz JB, Cochrane VA, Marcinkowski CM, Mobin R, Turner TL. Natural Variation in Decision-Making Behavior in Drosophila melanogaster. Kliebenstein DJ, editor. PLoS One [Internet]. 2011 Jan 20 [cited 2020 Feb 8];6(1):e16436. Available from: https://dx.plos.org/10.1371/journal.pone.0016436

383. Rodrigues ML. The multifunctional fungal ergosterol. Vol. 9, mBio. American Society for Microbiology; 2018.

384. Klingberg S, Andersson H, Mulligan A, Bhaniani A, Welch A, Bingham S, et al. Food sources of plant sterols in the EPIC Norfolk population. Eur J Clin Nutr. 2008 Jun 18;62(6):695–703.

385. Xu Z, McClure ST, Appel LJ. Dietary cholesterol intake and sources among U.S adults: Results from national health and nutrition examination surveys (NHANES), 2001–2014. Nutrients. 2018 Jun 14;10(6).

386. Mariod A, Matthäus B, Eichner K. Fatty acid, tocopherol and sterol composition as well as oxidative stability of three unusual sudanese oils. J Food Lipids [Internet]. 2004 Oct [cited 2020 Feb 9];11(3):179–89. Available from: http://doi.wiley.com/10.1111/j.1745-4522.2004.01131.x

387. CLARK AJ, BLOCK K. The absence of sterol synthesis in insects. J Biol Chem [Internet]. 1959 Oct [cited 2020 Feb 8];234:2578–82. Available from: http://www.ncbi.nlm.nih.gov/pubmed/13810427

388. Huang Z, London E. Cholesterol lipids and cholesterol-containing lipid rafts in bacteria. Chem Phys Lipids. 2016 Sep 1;199:11–6.

389. Lafont R, Dauphin-Villemant C, Warren JT, Rees H. Ecdysteroid Chemistry and Biochemistry. In: Insect Endocrinology. Elsevier; 2012. p. 106–76.

390. Kozlova T, Thummel CS. Steroid regulation of postembryonic development and reproduction in Drosophila. Trends Endocrinol Metab [Internet]. 2000 Sep [cited 2020 Feb 8];11(7):276–80. Available from: http://www.ncbi.nlm.nih.gov/pubmed/10920384

391. Carvalho M, Schwudke D, Sampaio JL, Palm W, Riezman I, Dey G, et al. Survival strategies of a sterol auxotroph. Development. 2010 Nov 1;137(21):3675–85.

392. Lavrynenko O, Rodenfels J, Carvalho M, Dye NA, Lafont R, Eaton S, et al. The ecdysteroidome of Drosophila: Influence of diet and development. Dev. 2015 Nov 1;142(21):3758–68.

393. Sang JH, King RC. NUTRITIONAL REQUIREMENTS OF AXENICALLY CULTURED DROSOPHILA MELANOGASTER ADULTS. Vol. 38, Exp. Biol. 1961.

394. Carver JD, Allan Walker W. The role of nucleotides in human nutrition [Internet]. Vol. 6, The Journal of Nutritional Biochemistry. 1995 [cited 2020 Feb 9]. p. 58–72. Available from: https://linkinghub.elsevier.com/retrieve/pii/095528639400019I

395. Uauy R, Stringel G, Thomas R, Quan R. Effect of dietary nucleosides on growth and maturation of the developing gut in the rat. J Pediatr Gastroenterol Nutr [Internet]. 1990 May [cited 2020 Feb 9];10(4):497–503. Available from:

https://insights.ovid.com/crossref?an=00005176-199005000-00014

396. Che L, Hu L, Liu Y, Yan C, Peng X, Xu Q, et al. Dietary nucleotides supplementation improves the intestinal development and immune function of neonates with intra-uterine growth restriction in a pig model. PLoS One. 2016 Jun 1;11(6).

397. Hawkes JS, Gibson RA, Roberton D, Makrides M. Effect of dietary nucleotide supplementation on growth and immune function in term infants: A randomized controlled trial. Eur J Clin Nutr [Internet]. 2006 Feb [cited 2020 Feb 9];60(2):254–64. Available from: http://www.ncbi.nlm.nih.gov/pubmed/16234834

398. Schwarz G, Mendel RR, Ribbe MW. Molybdenum cofactors, enzymes and pathways. Vol. 460, Nature. Nature Publishing Group; 2009. p. 839–47.

399. Marelja Z, Leimkühler S, Missirlis F. Iron sulfur and molybdenum cofactor enzymes regulate the Drosophila life cycle by controlling cell metabolism. Front Physiol. 2018 Feb 14;9(FEB).

400. Hilliker AJ, Duyf B, Evans D, Phillips JP. Urate-null rosy mutants of Drosophila melanogaster are hypersensitive to oxygen stress. Proc Natl Acad Sci U S A. 1992;89(10):4343–7.

401. Zhou X, Riddiford LM. rosy function is required for juvenile hormone effects in Drosophila melanogaster. Genetics [Internet]. 2008 Jan [cited 2020 Feb 9];178(1):273–81. Available from: http://www.ncbi.nlm.nih.gov/pubmed/18202373

402. Kamleh MA, Hobani Y, Dow JAT, Watson DG. Metabolomic profiling of Drosophila using liquid chromatography Fourier transform mass spectrometry. FEBS Lett [Internet]. 2008 Aug 20 [cited 2020 Feb 9];582(19):2916–22. Available from: http://doi.wiley.com/10.1016/j.febslet.2008.07.029

403. Bonse A. Untersuchungen über die chemische Natur und die Bildung der Harnkonglomerate in den Malpighischen Gefässen der Mutante rosy von Drosophila melanogaster. Z Naturforsch B. 1967 Oct 1;22(10):1027–9.

404. Otto N, Marelja Z, Schoofs A, Kranenburg H, Bittern J, Yildirim K, et al. The sulfite oxidase Shopper controls neuronal activity by regulating glutamate homeostasis in Drosophila ensheathing glia. Nat Commun. 2018 Dec 1;9(1):1–12.

405. Perkhulyn N V., Rovenko BM, Lushchak O V., Storey JM, Storey KB, Lushchak VI.

Exposure to sodium molybdate results in mild oxidative stress in Drosophila melanogaster. Redox Rep [Internet]. 2017 May 4 [cited 2020 Feb 9];22(3):137–46. Available from: http://www.ncbi.nlm.nih.gov/pubmed/28245708

406. Rovenko BM, Perkhulyn N V., Lushchak O V., Storey JM, Storey KB, Lushchak VI. Molybdate partly mimics insulin-promoted metabolic effects in Drosophila melanogaster. Comp Biochem Physiol Part - C Toxicol Pharmacol [Internet]. 2014 Sep [cited 2020 Feb 9];165:76–82. Available from: https://linkinghub.elsevier.com/retrieve/pii/S1532045614000817

407. O'Leary F, Samman S. Vitamin B12 in health and disease. Vol. 2, Nutrients. MDPI AG; 2010. p. 299–316.

408. Watanabe F, Yabuta Y, Bito T, Teng F. Vitamin B12-Containing Plant Food Sources for Vegetarians. Nutrients [Internet]. 2014 May 5 [cited 2020 Feb 9];6(5):1861–73. Available from: http://www.mdpi.com/2072-6643/6/5/1861

409. Wakayama EJ, Dillwith JW, Howard RW, Blomquist GJ. Vitamin B12 levels in selected insects. Insect Biochem [Internet]. 1984 Jan [cited 2020 Feb 9];14(2):175–9. Available from: https://linkinghub.elsevier.com/retrieve/pii/0020179084900271

410. Halarnkar PP, Chambers JD, Wakayama EJ, Blomquist GJ. Vitamin B12 levels and propionate metabolism in selected non-insect arthropods and other invertebrates. Comp Biochem Physiol -- Part B Biochem [Internet]. 1987 Jan [cited 2020 Feb 9];88(3):869–73. Available from: https://linkinghub.elsevier.com/retrieve/pii/0305049187902574

411. Salem H, Bauer E, Strauss AS, Vogel H, Marz M, Kaltenpoth M. Vitamin supplementation by gut symbionts ensures metabolic homeostasis in an insect host. Proc R Soc B Biol Sci. 2014 Oct 22;281(1796).

412. Musselman LP, Fink JL, Narzinski K, Ramachandran PV, Hathiramani SS, Cagan RL, et al. A high-sugar diet produces obesity and insulin resistance in wild-type Drosophila. DMM Dis Model Mech. 2011 Nov 1;4(6):842–9.

413. Schipanski A, Yarali A, Niewalda T, Gerber B. Behavioral analyses of sugar processing in choice, feeding, and learning in larval drosophila. Chem Senses. 2008;33(6):563–73.

414. Ugrankar R, Theodoropoulos P, Akdemir F, Henne WM, Graff JM. Circulating glucose levels inversely correlate with Drosophila larval feeding through insulin signaling and SLC5A11. Commun Biol. 2018 Dec 1;1(1):1–15.

415. Pasco MY, Léopold P. High sugar-induced insulin resistance in Drosophila relies on the Lipocalin Neural Lazarillo. PLoS One. 2012 May 2;7(5).

416. Caldwell PE, Walkiewicz M, Stern M. Ras activity in the Drosophila prothoracic gland regulates body size and developmental rate via ecdysone release. Curr Biol. 2005 Oct 25;15(20):1785–95.

417. Colombani J, Bianchini L, Layalle S, Pondeville E, Dauphin-Villemant C, Antoniewski C, et al. Antagonistic actions of ecdysone and insulins determine final size in Drosophila. Science (80-). 2005 Oct 28;310(5748):667–70.

418. Layalle S, Arquier N, Léopold P. The TOR Pathway Couples Nutrition and Developmental Timing in Drosophila. Dev Cell [Internet]. 2008 Oct 14 [cited 2020 Feb 9];15(4):568–77. Available from: http://www.ncbi.nlm.nih.gov/pubmed/18854141

419. Yamada T, Habara O, Kubo H, Nishimura T. Fat body glycogen serves as a metabolic safeguard for the maintenance of sugar levels in drosophila. Dev. 2018 Mar 1;145(6).

420. Lushchak O V., Gospodaryov D V., Rovenko BM, Yurkevych IS, Perkhulyn N V., Lushchak VI. Specific dietary carbohydrates differentially influence the life span and fecundity of Drosophila melanogaster. Journals Gerontol - Ser A Biol Sci Med Sci. 2014 Jan;69(1):3–12.

421. Tatar M, Kopelman A, Epstein D, Tu MP, Yin CM, Garofalo RS. A mutant Drosophila insulin receptor homolog that extends life-span and impairs neuroendocrine function. Science (80-) [Internet]. 2001 Apr 6 [cited 2020 Feb 10];292(5514):107–10. Available from: https://www.sciencemag.org/lookup/doi/10.1126/science.1057987

422. Clancy DJ, Gems D, Hafen E, Leevers SJ, Partridge L. Dietary restriction in long-lived dwarf flies [Internet]. Vol. 296, Science. 2002 [cited 2020 Feb 10]. p. 319. Available from: https://www.sciencemag.org/lookup/doi/10.1126/science.1069366

423. Grönke S, Clarke D-F, Broughton S, Andrews TD, Partridge L. Molecular Evolution and Functional Characterization of Drosophila Insulin-Like Peptides. Rulifson E, editor. PLoS Genet [Internet]. 2010 Feb 26 [cited 2020 Feb 10];6(2):e1000857. Available from: https://dx.plos.org/10.1371/journal.pgen.1000857

424. Colombani J, Andersen DS, Léopol P. Secreted peptide dilp8 coordinates Drosophila tissue growth with developmental timing. Science (80-) [Internet]. 2012 May 4 [cited 2020 Feb 10];336(6081):582–5. Available from:

https://www.sciencemag.org/lookup/doi/10.1126/science.1216689

425. Post S, Tatar M. Nutritional Geometric Profiles of Insulin/IGF Expression in Drosophila melanogaster. Min K-J, editor. PLoS One [Internet]. 2016 May 12 [cited 2020 Feb 10];11(5):e0155628. Available from: http://dx.plos.org/10.1371/journal.pone.0155628

426. Sato-Miyata Y, Muramatsu K, Funakoshi M, Tsuda M, Aigaki T. Overexpression of dilp2 causes nutrient-dependent semi-lethality in Drosophila. Front Physiol [Internet]. 2014 Apr 16 [cited 2020 Feb 10];5:147. Available from: http://journal.frontiersin.org/article/10.3389/fphys.2014.00147/abstract

427. Giannakou ME, Goss M, Jünger MA, Hafen E, Leevers SJ, Partridge L. Long-lived Drosophila with over-expressed dFOXO in adult fat body. Science (80-). 2004 Jul 16;305(5682):361.

428. Giannakou ME, Goss M, Partridge L. Role of dFOXO in lifespan extension by dietary restriction in Drosophila melanogaster: not required, but its activity modulates the response. Aging Cell [Internet]. 2008 Apr 1 [cited 2020 Feb 10];7(2):187–98. Available from: http://doi.wiley.com/10.1111/j.1474-9726.2007.00362.x

429. Houthoofd K, Braeckman BP, Johnson TE, Vanfleteren JR. Life extension via dietary restriction is independent of the Ins/IGF-1 signalling pathway in Caenorhabditis elegans. Exp Gerontol. 2003 Sep 1;38(9):947–54.

430. Bonkowski MS, Rocha JS, Masternak MM, Al Regaiey KA, Bartke A. Targeted disruption of growth hormone receptor interferes with the beneficial actions of calorie restriction. Proc Natl Acad Sci U S A. 2006 May 16;103(20):7901–5.

431. Bjedov I, Toivonen JM, Kerr F, Slack C, Jacobson J, Foley A, et al. Mechanisms of Life Span Extension by Rapamycin in the Fruit Fly Drosophila melanogaster. Cell Metab. 2010 Jan 6;11(1):35–46.

432. Emran S, Yang M, He X, Zandveld J, Piper MDW. Target of rapamycin signalling mediates the lifespan-extending effects of dietary restriction by essential amino acid alteration. Aging (Albany NY). 2014;6(5):390–8.

433. Gems D, Pletcher S, Partridge L. Interpreting interactions between treatments that slow aging. Aging Cell [Internet]. 2002 Oct 1 [cited 2020 Feb 10];1(1):1–9. Available from: http://doi.wiley.com/10.1046/j.1474-9728.2002.00003.x

434. Catterson JH, Khericha M, Dyson MC, Vincent AJ, Callard R, Haveron SM, et al. Short-Term, Intermittent Fasting Induces Long-Lasting Gut Health and TOR-Independent Lifespan Extension. Curr Biol [Internet]. 2018;28(11):1714-1724.e4. Available from: https://doi.org/10.1016/j.cub.2018.04.015

435. Igarashi M, Guarente L. mTORC1 and SIRT1 Cooperate to Foster Expansion of Gut Adult Stem Cells during Calorie Restriction. Cell [Internet]. 2016 Jul 14 [cited 2020 Feb 11];166(2):436–50. Available from: http://www.ncbi.nlm.nih.gov/pubmed/27345368

436. Podestà M, Benvenuto F, Pitto A, Figari O, Bacigalupo A, Bruzzone S, et al. Concentrative uptake of cyclic ADP-ribose generated by BST-1+ stroma stimulates proliferation of human hematopoietic progenitors. J Biol Chem. 2005 Feb 18;280(7):5343–9.

437. Foronda D, Weng R, Verma P, Chen YW, Cohen SM. Coordination of insulin and notch pathway activities by microRNA miR-305 mediates adaptive homeostasis in the intestinal stem cells of the Drosophila gut. Genes Dev. 2014 Nov 1;28(21):2421–31.

438. Kapuria S, Karpac J, Biteau B, Hwangbo DS, Jasper H. Notch-Mediated Suppression of TSC2 Expression Regulates Cell Differentiation in the Drosophila Intestinal Stem Cell Lineage. PLoS Genet. 2012 Nov;8(11).

439. Fan X, Liang Q, Lian T, Wu Q, Gaur U, Li D, et al. Rapamycin preserves gut homeostasis during Drosophila aging. Oncotarget. 2015;6(34):35274–83.

440. Grasa L, Abecia L, Forcén R, Castro M, de Jalón JAG, Latorre E, et al. Antibiotic-Induced Depletion of Murine Microbiota Induces Mild Inflammation and Changes in Toll-Like Receptor Patterns and Intestinal Motility. Microb Ecol. 2015 Oct 1;70(3):835–48.

441. Kernbauer E, Ding Y, Cadwell K. An enteric virus can replace the beneficial function of commensal bacteria. Nature. 2014 Dec 4;516(729):94–8.

442. Park J, Kotani T, Konno T, Setiawan J, Kitamura Y, Imada S, et al. Promotion of Intestinal Epithelial Cell Turnover by Commensal Bacteria: Role of Short-Chain Fatty Acids. Singh SR, editor. PLoS One [Internet]. 2016 May 27 [cited 2020 Feb 13];11(5):e0156334. Available from: https://dx.plos.org/10.1371/journal.pone.0156334

443. Lee JE, Rayyan M, Liao A, Edery I, Pletcher SD. Acute Dietary Restriction Acts via TOR, PP2A, and Myc Signaling to Boost Innate Immunity in Drosophila. Cell Rep. 2017

Jul 11;20(2):479–90.

444. Ariyasinghe A, Morshed SRM, Mannoor MK, Bakir HY, Kawamura H, Miyaji C, et al. Protection against malaria due to innate immunity enhanced by low-protein diet. J Parasitol [Internet]. 2006 Jun [cited 2020 Feb 15];92(3):531–8. Available from: http://www.ncbi.nlm.nih.gov/pubmed/16883996

445. Salazar AM, Resnik-Docampo M, Ulgherait M, Clark RI, Shirasu-Hiza M, Jones DL, et al. Intestinal Snakeskin Limits Microbial Dysbiosis during Aging and Promotes Longevity. 2018 [cited 2020 Feb 15]; Available from: https://doi.org/10.1016/j.isci.

446. Resnik-Docampo M, Koehler CL, Clark RI, Schinaman JM, Sauer V, Wong DM, et al. Tricellular junctions regulate intestinal stem cell behaviour to maintain homeostasis. Nat Cell Biol. 2017 Jan 1;19(1):52–9.

447. Akagi K, Wilson KA, Katewa SD, Ortega M, Simons J, Hilsabeck TA, et al. Dietary restriction improves intestinal cellular fitness to enhance gut barrier function and lifespan in D. melanogaster. Schneider DS, editor. PLOS Genet [Internet]. 2018 Nov 1 [cited 2020 Feb 15];14(11):e1007777. Available from: http://dx.plos.org/10.1371/journal.pgen.1007777

448. Yousefi M, Nakauka-Ddamba A, Berry CT, Li N, Schoenberger J, Simeonov KP, et al. Calorie Restriction Governs Intestinal Epithelial Regeneration through Cell-Autonomous Regulation of mTORC1 in Reserve Stem Cells. Stem Cell Reports. 2018 Mar 13;10(3):703–11.

449. Owen KA, Abshire MY, Tilghman RW, Casanova JE, Bouton AH. FAK regulates intestinal epithelial cell survival and proliferation during mucosal wound healing. PLoS One. 2011 Aug 24;6(8).

450. Deng H, Gerencser AA, Jasper H. Signal integration by Ca 2+ regulates intestinal stem-cell activity. Nature. 2015 Dec 10;528(7581):212–7.

451. Saito Y, Iwatsuki K, Hanyu H, Maruyama N, Aihara E, Tadaishi M, et al. Effect of essential amino acids on enteroids: Methionine deprivation suppresses proliferation and affects differentiation in enteroid stem cells. Biochem Biophys Res Commun. 2017 Jun 17;488(1):171–6.

452. Chen Y, Tseng S-H, Yao C-L, Li C, Tsai Y-H. Distinct Effects of Growth Hormone and Glutamine on Activation of Intestinal Stem Cells. J Parenter Enter Nutr [Internet]. 2017

May 16 [cited 2020 Feb 13];42(3):014860711770943. Available from: http://doi.wiley.com/10.1177/0148607117709435

453. Sridharan G V., Choi K, Klemashevich C, Wu C, Prabakaran D, Pan L Bin, et al. Prediction and quantification of bioactive microbiota metabolites in the mouse gut. Nat Commun. 2014 Nov 20;5(1):1–13.

454. Whitt DD, Demoss RD. Effect of Microflora on the Free Amino Acid Distribution in Various Regions of the Mouse Gastrointestinal Tract. Appl Microbiol. 1975;30(4):609–15.

455. Dai ZL, Wu G, Zhu WY. Amino acid metabolism in intestinal bacteria: Links between gut ecology and host health. Front Biosci. 2011 Jan 1;16(5):1768–86.

456. Den Besten G, Van Eunen K, Groen AK, Venema K, Reijngoud DJ, Bakker BM. The role of short-chain fatty acids in the interplay between diet, gut microbiota, and host energy metabolism. Vol. 54, Journal of Lipid Research. American Society for Biochemistry and Molecular Biology; 2013. p. 2325–40.

457. Ríos-Covián D, Ruas-Madiedo P, Margolles A, Gueimonde M, De los Reyes-Gavilán CG, Salazar N. Intestinal short chain fatty acids and their link with diet and human health. Vol. 7, Frontiers in Microbiology. Frontiers Media S.A.; 2016.

458. Nissim I, Horyn O, Daikhin Y, Chen P, Li C, Wehrli SL, et al. The molecular and metabolic influence of long term agmatine consumption. J Biol Chem. 2014 Apr 4;289(14):9710–29.

459. Mawe GM, Hoffman JM. Serotonin signalling in the gut-functions, dysfunctions and therapeutic targets. Vol. 10, Nature Reviews Gastroenterology and Hepatology. Nature Publishing Group; 2013. p. 473–86.

460. Kerpel-Fronius E, Kaiser E. Hypoglycaemia in infantile malnutrition. Acta Paediatr Scand. 1967;

461. Spoelstra MN, Mari A, Mendel M, Senga E, Van Rheenen P, Van Dijk TH, et al. Kwashiorkor and marasmus are both associated with impaired glucose clearance related to pancreatic β-cell dysfunction. Metabolism [Internet]. 2012 Sep [cited 2020 Feb 22];61(9):1224–30. Available from: http://www.ncbi.nlm.nih.gov/pubmed/22386944

462. Rambold AS, Kostelecky B, Elia N, Lippincott-Schwartz J. Tubular network formation

protects mitochondria from autophagosomal degradation during nutrient starvation. Proc Natl Acad Sci U S A [Internet]. 2011 Jun 21 [cited 2020 Feb 15];108(25):10190–5. Available from: http://www.pubmedcentral.nih.gov/articlerender.fcgi?artid=3121813&tool=pmcentrez&rendertype=abstract

463. Johnson MA, Vidoni S, Durigon R, Pearce SF, Rorbach J, He J, et al. Amino acid starvation has opposite effects on mitochondrial and cytosolic protein synthesis. PLoS One. 2014 Apr 9;9(4).

464. Buttgereit F, Brand MD. A hierarchy of ATP-consuming processes in mammalian cells. Biochem J. 1995;312(1):163–7.

465. Mazor KM, Dong L, Mao Y, Swanda R V., Qian SB, Stipanuk MH. Effects of single amino acid deficiency on mRNA translation are markedly different for methionine versus leucine. Sci Rep. 2018 Dec 1;8(1):1–13.

466. Stefana MI, Driscoll PC, Obata F, Pengelly AR, Newell CL, MacRae JI, et al. Developmental diet regulates Drosophila lifespan via lipid autotoxins. Nat Commun. 2017 Dec 1;8(1):1–13.

467. Guida MC, Birse RT, Dall'Agnese A, Toto PC, Diop SB, Mai A, et al. Intergenerational inheritance of high fat diet-induced cardiac lipotoxicity in Drosophila. Nat Commun. 2019 Dec 1;10(1):1–14.

468. Öst A, Lempradl A, Casas E, Weigert M, Tiko T, Deniz M, et al. Paternal diet defines offspring chromatin state and intergenerational obesity. Cell. 2014 Dec 4;159(6):1352–64.

469. Jehn M, Brewis A. Paradoxical malnutrition in mother-child pairs: Untangling the phenomenon of over- and under-nutrition in underdeveloped economies. Econ Hum Biol [Internet]. 2009 Mar [cited 2020 Feb 22];7(1):28–35. Available from: http://www.ncbi.nlm.nih.gov/pubmed/19246260

470. Doak CM, Adair LS, Bentley M, Monteiro C, Popkin BM. The dual burden household and the nutrition transition paradox [Internet]. Vol. 29, International Journal of Obesity. 2005 [cited 2020 Feb 22]. p. 129–36. Available from: http://www.ncbi.nlm.nih.gov/pubmed/15505634

471. Fall CHD, Sachdev HS, Osmond C, Lakshmy R, Biswas SD, Prabhakaran D, et al. Adult

metabolic syndrome and impaired glucose tolerance are associated with different patterns of BMI gain during infancy data from the New Delhi birth cohort. Diabetes Care. 2008 Dec;31(12):2349–56.

11 Appendix

The following appendices are contents of the attached CD:

CD\Appendix A	RNA-Seq data related to Fig. 44 and 45	• BiologicalProcess_DR RC vs. CD RC_downregulated • BiologicalProcess_DR RC vs. CD RC_upregulated • BiologicalProcess_PEM RC vs. PEM RC_downregulated • BiologicalProcess_PEM RC vs. EM RC_upregulated • DEGs_DR RC vs. CD RC_downregulated • DEGs_DR RC vs. CD RC_upregulated • DEGs_PEM RC vs. CD RC_downregulated • DEGs_PEM RC vs. CD RC_upregulated
CD\Appendix B	RNA-Seq data related to Fig. 46 and 47	• BiologicalProcess_DR GF vs. CD GF_downregulated • BiologicalProcess_DR GF vs. CD GF_upregulated • BiologicalProcess_PEM GF vs. PEM GF_downregulated • BiologicalProcess_PEM GF vs. EM GF_upregulated • DEGs_DR GF vs. CD GF_downregulated • DEGs_DR GF vs. CD GF_upregulated • DEGs_PEM GF vs. CD GF_downregulated • DEGs_PEM GF vs. CD GF_upregulated
CD\Appendix C	RNA-Seq data related to Fig. 48 and 49	• BiologicalProcess_CD GF vs. CD RC_downregulated • BiologicalProcess_CD GF vs. CD RC_upregulated • BiologicalProcess_DR GF vs. DR RC_downregulated • BiologicalProcess_DR GF vs. DR RC_upregulated • BiologicalProcess_PEM GF vs. PEM RC_downregulated • BiologicalProcess_PEM GF vs. PEM RC_upregulated • DEGs_CD GF vs. CD RC_downregulated • DEGs_CD GF vs. CD RC_upregulated • DEGs_DR GF vs. DR RC_downregulated • DEGs_DR GF vs. DR RC_upregulated • DEGs_PEM GF vs. PEM RC_downregulated • DEGs_PEM GF vs. PEM RC_upregulated
CD\Appendix D	RNA-Seq data related to Fig. 62	• BiologicalProcess_Memoryeffect_d24 PEM vs d7 PEM_downregulated • BiologicalProcess_Memoryeffect_d24 PEM vs d7 PEM_upregulated • DEGs_Memoryeffect_d24 PEM vs d7 PEM_downregulated • DEGs_Memoryeffect_d24 PEM vs d7 PEM_upregulated